BMR PUBLICATIONS COMPACTUS
(LENDING SECTION)

AUSTRALIA

Evaporites in Australia

078001

BUREAU OF MINERAL RESOURCES
LIBRARY
3
CANBERRA, A.C.T.

BMR Bulletin
198

A. T. Wells

BMR
555(94)
BUL.45
Copy 3

Central part of the Ringwood Dome, from the southwest. The lower deeply dissected part of the hill consists of white earthy weathered gypsum encrusting the underlying bedded gypsum; the upper part of the hill consists of limestone.

DEPARTMENT OF NATIONAL DEVELOPMENT & ENERGY
BUREAU OF MINERAL RESOURCES, GEOLOGY AND GEOPHYSICS

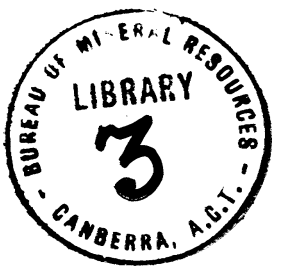

BULLETIN 198

Evaporites in Australia

A. T. WELLS

AUSTRALIAN GOVERNMENT PUBLISHING SERVICE
CANBERRA 1980

DEPARTMENT OF NATIONAL DEVELOPMENT AND ENERGY

MINISTER: SENATOR THE HON. J. L. CARRICK

SECRETARY: A. J. WOODS

BUREAU OF MINERAL RESOURCES, GEOLOGY AND GEOPHYSICS

DIRECTOR: R. W. R. RUTLAND

ASSISTANT DIRECTOR, GEOLOGICAL BRANCH: J. N. CASEY

This Bulletin was edited by I. M. Hodgson

Design assistance: P. J. Corrigan

ABSTRACT

Major evaporite basins have been discovered in Australia over the past two decades, chiefly as a result of exploratory drilling for petroleum. There are four major onshore deposits of bedded evaporites—in the Adavale, Amadeus, Canning, and Officer Basins—and one offshore sequence, in the Bonaparte Gulf Basin. Several other basins have indications of bedded evaporites, but their full extent and potential are unknown at present. The evaporites are Late Precambrian, Early Cambrian, possibly Silurian, and Devonian in age. The Canning Basin has the thickest known sequence: 740 m of halite was penetrated in McLarty No. 1 well. Most of the evaporites are in the Carribuddy Formation, which is probably Devonian. In the Amadeus Basin two formations contain evaporites. The less soluble evaporites of the Upper Precambrian Bitter Springs Formation crop out; evaporites of the Lower Cambrian Chandler Limestone do not, but have been intersected in drill holes. The evaporite deposits in the Middle Devonian Boree Salt Member of the Etonvale Formation in the Adavale Basin are the most interesting economically as they contain the only known occurrence of potash in Australia. Stratigraphic drilling in the eastern part of the Officer Basin in South Australia has indicated the presence of thick Lower Cambrian evaporite sequences in the Observatory Hill Beds. The most northerly occurrence comprises dolomite with abundant calcite pseudomorphs after trona and shortite, indicating non-marine evaporite deposition in saline or playa lakes. The southern evaporite occurrence in the Tallaringa Trough comprises halite, siltstone, and minor sandstone in the Observatory Hill Beds. Several diapirs with exposed cores of cap rock gypsum have been discovered in the northern part of the Officer Basin in Western Australia. Shallow drilling has shown that the cap rock is underlain by halite, and interpretation of seismic records has suggested that there are two levels of evaporites, ?Cambrian and Precambrian. The probable younger sequence is the Babbagoola Beds and the presumed older sequence, the Browne Beds. Many diapirs were detected on seismic sections in the offshore Bonaparte Gulf Basin and, subsequently, halite was intersected in Pelican Island No. 1 and Sandpiper No. 1 wells. The evaporites are Devonian, but not formally named. Evaporites are harvested in Australia by solar evaporation of sea water or brine, and by scraping the surfaces of natural salt lakes. There is obviously ample scope for further detailed investigations of evaporites in Australia. Stratigraphic drilling in some basins, funded by Government agencies, has led to the discovery of important deposits, but it is probable that most new information will, as in the past, accrue from petroleum exploration drilling.

Published for the Bureau of Mineral Resources, Geology and Geophysics by the Australian Government Publishing Service

ISSN 0084–7089

ISBN 0 642 05004 X

Printed by Graphic Services Pty Ltd, 516-581 Grand Junction Road, Northfield, S.A. 5085

CONTENTS

FIGURES

TABLES

PLATES

Page vii is blank.

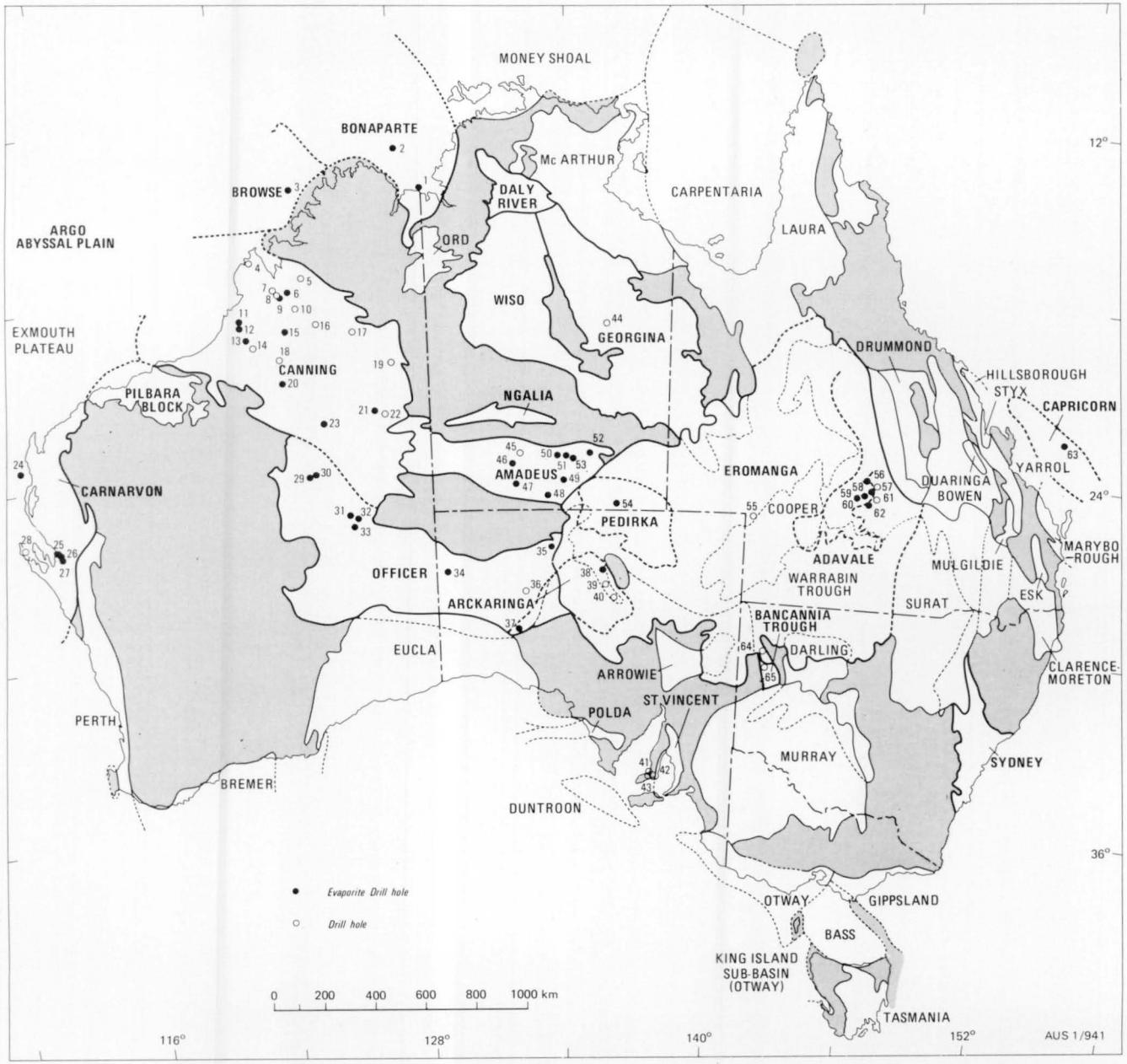

Fig. 1. Australian sedimentary basins and localities of drill holes referred to in text.

1. Pelican Island No. 1
2. Sandpiper No. 1
3. Rob Roy No. 1
4. Tappers Inlet No. 1
5. Blackstone No. 1
6. Grant Range No. 1
7. Logue No. 1
8. Doran No. 1
9. Frome Rocks No. 1
10. Matches Spring No. 1
11. Parda No. 1
12. Willara No. 1
13. Munda No. 1
14. Munro No. 1
15. McLarty No. 1
16. Barbwire No. 1
17. Lake Betty No. 1
18. Kemp Field No. 1
19. Point Moody No. 1
20. Sahara No. 1
21. Wilson Cliffs No. 1
22. Contention Heights No. 1
23. Kidson No. 1
24. Pendock I.D. No. 1
25. Hamelin Pool No. 1
26. Yaringa No. 1
27. Hamelin Pool No. 2
28. Dirk Hartog 17B
29. BMR Madley No. 1
30. BMR Warri No. 20
31. Browne No. 1
32. Browne No. 2
33. Yowalga No. 2
34. Birksgate No. 1
35. Byilkaoora No. 1
36. Emu No. 1
37. Wilkinson No. 1
38. Cootanoorina No. 1
39. Weedina No. 1
40. Boorthanna No. 1
41. Minlaton No. 1
42. Stansbury No. 1
43. Stansbury West No. 1
44. Frewina No. 1
45. BMR Hermannsberg No. 40
46. BMR Mount Liebig No. 1
47. BMR Lake Amadeus Nos. 3, 3A, 3B
48. Erldunda No. 1
49. Mount Charlotte No. 1
50. Orange No. 1
51. Alice No. 1
52. BMR Alice Springs No. 3
53. Ooraminna No. 1
54. McDills No. 1
55. Barrolka No. 1
56. Bonnie No. 1
57. Fairlea No. 1
58. Boree No. 1
59. Bury No. 1
60. Alva No. 1
61. Ravensbourne No. 1
62. Stafford No. 1
63. Aquarius No. 1
64. Bancannia North No. 1
65. Bancannia South No. 1

INTRODUCTION

Thin surface accumulations of salt in playa lakes have been known since the early exploration of Australia. However, surface occurrences of bedded evaporites, exposed in some sedimentary basins by erosion of the sedimentary sequence, have been discovered only recently, as a result of regional geological mapping, and it is only in the last two decades that substantial amounts of subsurface evaporites have been located. in the course of drilling for petroleum.

Forty-two petroleum and exploration wells have intersected evaporite beds (Fig. 1), but although evaporites can be important in some structures as cap rocks for hydrocarbon accumulations, there has been little incentive for the oil exploration companies to continuously core the evaporite sequences. In most well sections there are only one or two cores in any evaporite sequence, and in some wells no cores were attempted in what were undoubtedly thick evaporites. As a result, some of the more important details of depositional history are missing. It is, however, unlikely that significant beds of potassium-rich minerals have been overlooked, as they would be recorded on gamma-ray logs.

The known number of wells that have been drilled specifically to test or explore for evaporite deposits includes seven drilled by the Bureau of Mineral Resources, and seven by exploration companies and the South Australia Department of Mines and Energy.

In past geological time large tracts of what is now continental Australia were subjected to marine inundation. However, it is thought that for long periods these areas were not open sea, but large restricted basins, either narrowly connected to the open sea or separated from it by a shallow shelf or bar, and that evaporation of large quantities of sea water from these basins resulted in the formation of thick deposits of evaporites. This classical theory is generally called the Ochsenius bar theory of saline deposition (Ochsenius, 1877, 1888), and quantitative data in its support have been presented by Whelan (1972).

In Australia, evaporites formed chiefly in the late Precambrian, Silurian, and Devonian (Fig. 2), and are widespread in the subsurface of sedimentary basins. The largest deposits, volumetrically, are distributed between 18° and 20° south. The thickest known evaporites occur in this zone, and known evaporites outside it are relatively poorly developed. There does not appear to be any significance in this distribution, as the deposits are of several ages; their present distribution may have been partly controlled by the structural evolution of individual basins.

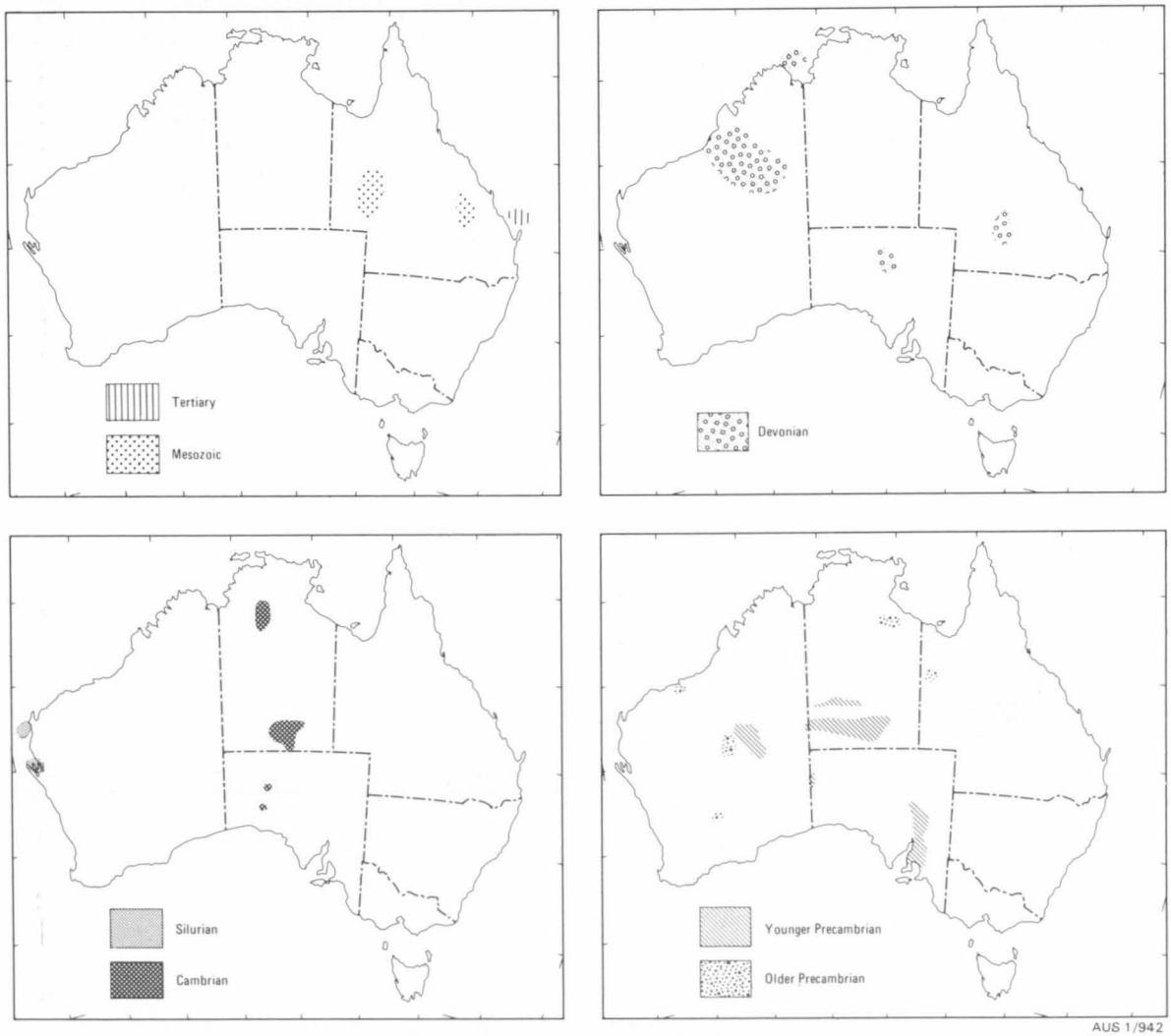

Fig. 2. Main distribution of evaporites in Australia.

TABLE 1. SUMMARY OF THE MAJOR EVAPORITE DEPOSITS IN AUSTRALIA

	ADAVALE BASIN	*AMADEUS BASIN*		*ARCKARINGA BASIN*
Basin area (km²)	28 500	150 000		100 000
Area of evaporites (km²)	8 000	83 000	41 000	
Maximum thickness of sediments (m)	about 5 000	9 000	9 000	about 1 200
Maximum thickness of evaporites (m)	about 900	215 (Mt Liebig No. 1)	225 (Mt Charlotte No. 1)	122 (Wilkinson No. 1)
Minimumum depth to evaporites (m)	900	Surface	Near-surface	?Mt Toodina structure
Formations	Boree Salt Member (Etonvale Formation)	Bitter Springs Formation	Chandler Limestone	Observatory Hill Beds, Cootanoorina Formation
Age	M. Devonian	Adelaidean ~900 m.y.	Early Cambrian	? Early Cambrian; Late Devonian
Minerals in evaporites	Anhydrite, halite, sylvinite	Halite, gypsum, anhydrite, dolomite	Halite, anhydrite	Anhydrite, halite
Wells penetrating significant evaporites	Boree No. 1 Bonnie No. 1 Bury No. 1 Stafford No. 1 Alva No. 1	Ooraminna No. 1 Erldunda No. 1 Mt Charlotte No. 1 BMR Alice Springs No. 1 BMR Mt Liebig No. 1 BMR Lake Amadeus No. 3	Alice No. 1 Mt Charlotte No. 1 Orange No. 1	Wilkinson No. 1 Cootanoorina No. 1
Diapirism and salt solution	Mobilised into pillows along faults	Johnstone Hill, ?Goyder Pass, Ringwood, and unnamed salt anticlines	Illmurta structure	Possible diapir of Mount Toondina structure
Deformation	Several periods of diastrophism, culminating in Carboniferous orogeny	Supratenuous folding	Incompetent folding	Minor Devonian movements. Basin established by faulting and graben formation in late Carboniferous-early Permian

There are no evaporites of significant extent and thickness known to be forming today in Australia, but surface deposits in modern playa lakes are common in areas of low rainfall, subdued topography, and internal drainage, such as are found in many parts of Western Australia, South Australia, and the Northern Territory.

The major deposits of evaporites in Australia are summarised in Table 1. Wells containing evaporites are listed by company or drilling authority in Table 2, and details of the wells and their evaporite intervals are given in Table 3.

TABLE 2. WELLS CONTAINING EVAPORITES, LISTED BY COMPANY OR DRILLING AUTHORITY

Company or drilling authority	*Well*	*Basin*
Amerada Petroleum	McDills No. 1	Pedirka
American Overseas Petroleum Ltd	Boree No. 1	Adavale
Arco Australia Ltd	Pelican Is. No. 1	Bonaparte Gulf (offshore)
	Sandpiper No. 1	Bonaparte Gulf (offshore)
Australian Aquitaine Petroleum Ltd	Wilson Cliffs No. 1	Canning
Australian Gulf Oil Co.	Aquarius No. 1	Capricorn Embayment
B.O.C. of Australia Ltd	Rob Roy No. 1	Browse
Bureau of Mineral Resources	Alice Springs No. 3	Amadeus
	Mount Liebig No. 1	Amadeus
	Lake Amadeus Nos. 3, 3A, 3B	Amadeus
	Madley No. 1	Officer
	Warri No. 20	Officer
Continental Oil Co. of Australia	Birksgate No. 1	Officer
	Yaringa No. 1	Carnarvon
Exoil N.L.	Alice No. 1	Amadeus
	Erldunda No. 1	Amadeus
	Ooraminna No. 1	Amadeus
Genoa Oil N.L.	Pendock I.D. No. 1	Carnarvon
Hartogen Explorations Pty Ltd	Alva No. 1	Adavale
Hunt Oil Co.	Browne No. 1	Officer

Tables 1 and 2 continue on next page.

BONAPARTE GULF BASIN	*CANNING BASIN*	*CARNARVON BASIN*	*OFFICER BASIN*
260 000	453 000	300 000	350 000
26 000	207 000	? 1 300	3 100
>12 000	about 10 000	7 000	12 000
190 (Pelican Is. No. 1)	740 (McLarty No. 1)	37 (Yaringa No. 1)	60+ (Woolnough Hills)
1 750 (Sandpiper No. 1)	688 (Frome Rocks No. 1)	1 130 Hamelin Pool No. 1	Surface
Depositional hiatus on shore	Carribuddy Formation, Tandalgoo/Poulton Formation	Yaringa Salt Member (Dirk Hartog Formation)	Babbagoola Beds, Browne Beds
Pre-Late Devonian	Devonian	Late Silurian	Early Cambrian, Adelaidean
Halite	Halite, dolomite, anhydrite, barite	Halite, anhydrite, dolomitic anhydrite, traces of sylvite	Gypsum, dolomitic gypsum, anhydrite, dolomitic anhydrite
Pelican Is. No. 1 Sandpiper No. 1	Kidson No. 1, Sahara No. 1, McLarty No. 1, Willara No. 1, Frome Rocks No. 1, Parda No. 1, Wilson Cliffs No. 1, Munda No. 1, Blackstone No. 1.	Dirk Hartog No. 17B, Yaringa No. 1, Pendock I.D. No. 1 Hamelin Pool Nos. 1 & 2	Byilkaoora No. 1, Yowalga No. 2, Browne Nos. 1 & 2; BMR Madley No. 1, BMR Warri No. 20
Salt domes, salt walls, stocks, peripheral sinks, pillows, turtle-back structures	Salt domes and salt solution structures	—	Salt domes: Woolnough Hills, Madley (6 domes), Browne
Diapirism U. Carboniferous-Tertiary; Permian-Triassic salt migration; Late Triassic salt walls; Late Jurassic-Early Cretaceous movements; 14 + diapirs	Moderate folding	Middle Mesozoic down-faulted sub-basins	

Acknowledgements

Geologists of State Geological Surveys and several petroleum and mineral exploration companies provided valuable information and made available data from unpublished sources.

The section on BMR Alice Springs No. 3 drill site is derived from a petrographic and geochemical study by A. J. Stewart of the Bureau of Mineral Resources.

The descriptions of the results of test drilling at the Woolnough Hills diapir in the Officer Basin, and in the Amadeus Basin at the Gardiner Range and Lake Amadeus are largely the work of P. J. Kenewell of the Bureau of Mineral Resources. S. K. Skwarko of BMR assisted as well-site geologist for part of the time at the Gardiner Range site.

The figures were drawn by J. Mifsud, BMR.

TABLE 2. WELLS CONTAINING EVAPORITES, LISTED BY COMPANY OR DRILLING AUTHORITY (cont.)

Company or drilling authority	*Well*	*Basin*
	Browne No. 2	Officer
Hunt-Placid Oil Co.	Yowalga No. 2	Officer
Magellan Petroleum (Australia) Ltd	Hamelin Pool No. 1	Carnarvon
	Hamelin Pool No. 2	Carnarvon
	Orange No. 1	Amadeus
Phillips Australian Oil Co.	Bonnie No. 1	Adavale
	Bury No. 1	Adavale
	Stafford No. 1	Adavale
South Australia Dept of Mines & Energy	Byilkaoora No. 1	Officer
	Cootanoorina No. 1	Arckaringa
	Wilkinson No. 1	Arckaringa
Total Exploration	McLarty No. 1	Canning
Transoil N.L.	Mount Charlotte No. 1	Amadeus
West Australian Petroleum Pty Ltd (WAPET)	Frome Rocks No. 1	Canning
	Grant Range No. 1	Canning
	Kidson No. 1	Canning
	Munda No. 1	Canning
	Parda No. 1	Canning
	Sahara No. 1	Canning
	Willara No. 1	Canning

TABLE 3. DETAILS OF EVAPORITE INTERVALS IN PETROLEUM AND MINERAL EXPLORATION WELLS

Abridged from well completion reports. All measurements in metres unless stated otherwise.

Well name, coordinates, total depth	*Company/ drilling authority*	*Formation thickness*	*Age*	*Interval*	*Brief description*	*Core*	*Cutings*
				ADAVALE BASIN			
Boree No. 1 24°45′32″S 145°34′36″E TD 2676.4	American Overseas Petroleum Ltd	Etonvale Formation 1358.5–2426.5 Boree Salt Member	Middle Devonian	1919.6–1954.6	White, finely crystalline *gypsum*, with dolomitic siltstone and shale. Traces of *anhydrite*.		
				1954.6–2426.5	*Rock salt*, with thin beds of shale and siltstone, rare *gypsum*.	No. 18, 1957.7–1960.7, rec. 2.5 m, analysis: 98.5% NaCl. No. 19, 2125.0–2131.4, rec. 6.2 m, analysis: 95.8% NaCl, 2.14% $CaSO_4$. No. 20, 2280.8–2286.9, rec. 6.0 m, analysis: 78.7% NaCl, 8.9% $CaSO_4$, 2.0% $CaCO_3$, 2.1% $MgCO_3$.	Available
Alva No. 1 25°11′47″S 145°23′02″E TD 3586.0	Hartogen Exploration Pty Ltd	Etonvale Formation 2626.8–3297.3 Boree Salt Member	Middle Devonian		*Halite* (200.2 net) with a few thin tough interbeds.	Nil	9.1-m intervals 0 to 1261.9 and 3.1 from 1264.9 to T.D. Colourless to pale brown, massive and very finely crystalline halite with minor shale.
				3097.1–3285.8	*Halite* with a few thin shale beds.		
				3285.8–3297.3	*Anhydrite*.		
Bonnie No. 1 25°00′43″S 145°22′01″E TD 2744.7	Phillips Australian Oil Co.	Etonvale Formation 1825.8–2326.2 Boree Salt Member	Middle Devonian	2225.6–2326.2	*Salt* assumed on drilling rate and Core No. 3 *rock salt* with rare clayey shale laminae.	No. 3, 2241.4–2244.5, rec. 2.7 m.	Available
Bury No. 1 25°02′40″S 145°36′20″E TD 2744.4	Phillips Australian Oil Co.	Etonvale Formation 1402.1–2358.6 Boree Salt Member	Middle Devonian	1774.5–2358.6			
				1774.5–1798.3	*Anhydrite*.	No. 8, 1809.9–1812.9, rec. 2.3 m.	Available
				1798.3–1805.0	Shale and limestone.	No. 9, 1969.0–1972.0, rec. 2.9 m.	
				1805.0–2358.6	*Rock salt* with traces of *anhydrite* and rare laminae and interbeds of shale.	No. 10, 2123.8–2127.0, rec. 3.7 m. No. 11, 2279.2–2282.3, rec. 2.8 m.	

TABLE 3 (cont.)

Stafford No. 1 15°17′33″S 145°26′03″E TD 3141.2	Phillips Australian Oil Co.	Etonvale 1996.4–2749.6 Boree Salt Member	Middle Devonian	2672.4–2749.6	Interpreted as predominantly *rock salt* with thin random sandstone and shale interbeds; some *anhydrite*.	No. 15, 2709.9–2713.0, rec. 1.2 m.	Available
				AMADEUS BASIN			
Alice No. 1 23°54′47″S 133°58′00″E TD 2291.4	Exoil N.L.	Giles Creek Dolomite 1568.8–2017.1	Middle Cambrian	1568.8–2017.1	Shale and minor dolomite in the upper part, dolomite and minor shale in the lower. Abundant 'felty' *anhydrite* occurs throughout, in beds, lenses and patches.	No. 17, 1574.2–1577.0, rec. 2.7 m. No. 18, 1660.8–1662.9, rec. 2.1 m. No. 19, 1744.3–1745.8, rec. 1.5 m. No. 20, 1847.6–1848.9, rec. 1.2 m. No. 21, 1858.0–1859.5, rec. 1.0 m. No. 22, 1864.1–1865.0, rec. 0.1 m. No. 23, 1865.0–1870.8, rec. 4.9 m. No. 24, 1963.8–1964.7, rec. 0.8 m.	Available
		Chandler Limestone 2017.1–2176.3	Early Cambrian	2017.1–2176.3	*Halite*, mudstone, dolomitic clay, shale. 'Felty' primary *anhydrite* is common.		
					Halite, 2064.7–2088.4	No. 25, 2059.8–2061.6, rec. 1.6 m.	
					Halite, 2094.5–2129.0	No. 26, 2095.8–2102.5, rec. 2.8 m.	
					Halite, 2148.4–2181.7		
BMR Alice Springs No. 3 23°53′S 134°53′E TD 259.7	Bureau of Mineral Resources	Bitter Springs Formation (Gillen Member) 0–TD	Proterozoic	0–133	Dolomite-gypsum breccia, friable dololutite, microcrystalline *anhydrite*, satin spar *gypsum* veins.	Continuous cores 16.8–253, 92% recovery.	0–259.7 at 1.5-m intervals
				133–TD	As above together with bituminous dolomite and coarse anhydrite.		
BMR Mount Liebig No. 1 23°52′30″S 131°56′00″E TD 305.9	Bureau of Mineral Resources	Bitter Springs Formation 0–TD	Proterozoic	0–92	Fragments of *gypsum*, *anhydrite* and dolomite in recrystallised evaporite breccia; veins of acicular gypsum.	Continuous cores 3-TD, 97% recovery.	0–75.6, & 89.9–305.9 at 3.1-m intervals
				92–TD	*Halite*, minor evaporite rock fragments composed of anhydrite, dolomite, quartz with minor halite, chlorite, hematite and limonite.		
BMR Lake Amadeus No. 3B 24°46′36″S 131°53′24″E TD 305.9	Bureau of Mineral Resources	Bitter Springs Formation 41–TD	Proterozoic	0–41	Tertiary siltstone	81 cores: 12.2–14.6, 31.4–33.5, and continuous cores 42.7-TD, 86% recovery.	Surface—42.7 & 90.2–98.5 at 3.1-m intervals
				41–149	*Gypsum*, laminae and beds of gypsiferous dolomite, grey friable dolomite, and rare black dolomite; contorted and brecciated acicular gypsum veins		
				149–165	Grey friable dolomite, some gypsum		
				165–251	*Gypsum* in grey friable dolomite matrix		
				251–TD	*Anhydrite* and dolomitic *anhydrite*		

TABLE 3 (cont.)

Well name, coordinates, total depth	*Company/ drilling authority*	*Formation thickness*	*Age*	*Interval*	*Brief description*	*Core*	*Cuttings*
Erldunda No. 1 25°18′36″S 133°11′48″E TD 1665.1	Exoil N.L.	Bitter Springs Formation 1310.6–1665.1 Loves Creek Member	Adelaidean	1310.6–1447.8	Dolomite with lenses and crystals of *anhydrite* and *gypsum;* sandstone and siltstone.	Nil	
		Gillen Member		1447.8–TD	Dolomite, *anhydrite* and minor *gypsum*, in beds, to 1618.4, 1618.4—TD, coarsely crystalline *halite.*	No. 10, 1460.3–1463.7, rec. 2.7 m. No. 12, 1661.1–1665.1, rec. 0.03 m.	Available
McDills No. 1 25°43′50″S 135°47′25″E TD 3205.0	Amerada	Todd River Dolomite (2750.5–3205.0)	Early Cambrian	2750.5–TD	Dolomite and limestone with *anhydrite* filling fractures, particularly in Core No. 31.	No. 29, 2851.0–2854.1, rec. 2.7 m. No. 30, 2935.8–2938.8, rec. 3.0 m. No. 31, 3065.6–3068.7, rec. 2.7 m.	
Mount Charlotte No. 1 24°53′41″S 133°59′11″E TD 2116.2	Transoil N.L.	Chandler Limestone 710.7–936.3	Early Cambrian	710.7–936.3	Coarsely crystalline *halite*, generally pure, but some interstitial clay; interbeds of calc. siltstone, 852.8–883.9.	No. 8, 795.2–801.3, rec. 1.2 m. No. 9, 885.4–891.5, rec. 1.8 m.	Available except for interval 1469.1–1481.3
		Bitter Springs Formation 1423.4–2116.2 Loves Creek Member	Adelaidean	1423.4–1554.4	Dolomite, with interbedded shale, siltstone, and sandstone. *Anhydrite* and *gypsum*, of secondary origin, are present as intrusive layers, in patches and as intergranular crystals.	No. 16, 1531.6–1539.2, rec. 7.8 m.	
		Gillen Member		1554.4–TD	Rhythmically laminated dolomite and *anhydrite* with *halite*, shale, siltstone and sandstone. *Halite* at 1862.9–1903.4 and streaks at 1924.8, 1938.5, 1961.3, 1999.4, 2036.0, 2048.2 and 2060.4.	No. 17, 1565.7–1568.8, rec. 3.3 m. No. 18, 1613.0–1619.4, rec. 3.7 m. No. 19, 1650.7–1654.7, rec. 4.0 m. No. 21, 1772.4–1776.0, rec. 3.7 m. No. 22, 1869.9–1873.9, rec. 3.7 m. No. 23, 1944.9–1947.3, rec. 2.0 m. No. 24, 2043.0–2046.4, rec. 3.5 m. No. 25, 2055.8–2060.1, rec. 4.4 m. No. 26, 2114.3–2116.2, rec. 1.5 m.	

TABLE 3 (cont.)

Ooraminna No. 1 24°00′06″S 134°09′50″E TD 1858.3	Exoil N.L.	Bitter Springs Formation 1299.9–1858.3 Loves Creek Member	Adelaidean	1299.9–1609.3	Limestone and claystone with three dolerite bands; *anhydrite* occurs in veins and cavities in limestone below 1338.0.	No. 15, 1351.1–1351.7, rec. 0.46 m. No. 17, 1505.4–1506.9, rec. 1.0 m. No. 18, 1591.9–1594.1, rec. 1.8 m. No. 19, 1690.4–1690.7, rec. 0.1 m. No. 20, 1792.5–1793.1, rec. 0.5 m. No. 21, 1854.7–1857.7, rec. 2.1 m (estimated)	Available Available
		Gillen Member		1609.3—TD	1609.3–1804.4 Dolomitic limestone, with coarse crystalline *anhydrite* and rare *gypsum* in patches and veins; below 1804.4, claystone, with very coarse *anhydrite* crystals mixed with transparent *halite*.		
Orange No. 1 24°02′34″S 133°46′32″E TD 2708.5	Magellan Petroleum (Australia) Ltd	Chandler Lime-2274.4–2502.4	Early Cambrian	2314.6–2502.4	Believed to be mainly *halite*, with interbedded impure carbonate, *anhydrite* and shale in the intervals 2336.2–2352.4, and 2401.8–2420.1; and thin shale and mudstone 2453.6–2502.4.	Nil recovery	Very small volume returns, no cuttings 2322.5–2325.6 2328.6–2331.7 2398.7–2405.7
				ARCKARINGA BASIN			
Boorthanna No. 1 28°56′04″S 135°45′18″E TD 1225.6	Occidental Minerals	—	—		*Evaporite* expected in Devonian, but Permian rests on Precambrian meta-volcanics		
Cootanoorina No. 1 28°00′30″S 135°20′00″E TD 948.2	South Australia Dept. of Mines	Stuart Range Formation 516.7–777.2	Early Permian	634.0–667.5	*Anhydritic* siltstone.		0–TD at 3-m intervals
		Cootanoorina Formation 897.5–948.2	Devonian	897.5–TD	Dolomite, dolomitic shale, *anhydrite*.	No. 9, 925.4–928.6, rec. 3.1 m. No. 10, 942.8–948.2, rec. 5.4 m.	
Wilkinson No. 1 29°52′02″S 132°33′55″E 710	South Australia Dept. of Mines & Energy	Observatory Hill Beds 594+	Cambrian	Unit III 573.6–710	*Halite*, siltstone and minor sandstone	109.7–111.05, rec. 25%. Continuous 210–710, rec. 95%.	Surface–107.9 111.05–210 97.3–97.8% NaCl 115–145 ppm Br 60–98 ppm K (average of five samples between 598.06 and 668.51).
				573.6–695.0	*Halite*, light brown, translucent, to dark red-brown, crystalline; *gypsiferous* light brown siltstone; very fine, *halite* throughout, showing poikiloblastic texture		
				695.0–TD	Siltstone and minor sandstone; minor *halite*		

TABLE 3 (cont.)

Well name, coordinates, total depth	*Company/ drilling authority*	*Formation thickness*	*Age*	*Interval*	*Brief description*	*Core*	*Cuttings*
				BONAPARTE GULF BASIN			
Pelican Island No. 1 14°46′19″S 128°46′27″E TD 1981.2	Arco Australia Ltd	Interbedded with, or older than, the Bonaparte Beds 1791.3–1981.2	? Middle to Late Devonian	1791.3–TD	*Halite.*	Sidewall cores: 1889.7, rec. 3.1 cm *halite*, light grey translucent, to transparent, fractured; 1965.9, rec. 1.9 cm *halite* as above.	3.0-m intervals.
Sandpiper No. 1 13°18′53″S 127°58′35″E TD 1891.6	Arco Australia Ltd	(Equivalent of Ningbing Limestone onshore) 944.0–1891.6	Late Devonian to Early Carboniferous cap rock ? Famennian halite	944.0–1752.9 1752.9–TD	Cap rock. *Halite* Transition zone from 1752.9–1793.7.	Sidewall cores of halite at 1789.1, 1798.3, 1801.3, 1813.5, 1815.3, 1821.1, 1828.8, 1840.9, 1848.3, 1854.4, 1859.2, 1868.4, 1874.5, 1882.1, and 1885.1.	No cuttings of *halite* recovered.
				BROWSE BASIN			
Rob Roy No. 1 13°58′15.6″S 124°11′57.1″E TD 2286.0	B.O.C. of Australia Ltd	Unnamed Unit 1572.4–2255.5	Early Permian (Sakmarian)	1572.4–2187.2	Interbedded sandstone and claystone with minor siltstone and occasional veins of *anhydrite.*	No. 2, 1888.2–1897.4, rec. 9.1 m. 1895.8–1897.4, fine to medium sandstone with siltstone laminae and patches and veins of *anhydrite* up to 15 cm wide.	405–TD at 3.1-m intervals
				CANNING BASIN			
Blackstone No. 1 17°35′14″S 124°21′01″ TD 3049.5	West Australian Petroleum Pty Ltd (Wapet)	Poulton Formation 1914.1–2220.5	Middle Devonian		Siltstone, minor shale, sandstone and trace dolomite. Probably contains *halite,* from evidence of 48 000 ppm NaCl in drilling fluid.	No. 12, 1975.1–1984.2, rec. 9.1 m, siltstone. No. 13, 2045.2–2052.2, rec. 6.2 m, siltstone. No. 14, 2128.7–2134.5, rec. 5.8 m, siltstone.	0–1219.2 at 9.1-m intervals 1219.2–TD at 3.1-m intervals
Frome Rocks No. 1 18°11′48″S 133°38′42″E TD 1220.1	Wapet		Pre-Mesozoic	687.6–TD	532.4 of *halite* with scattered small fragments of dolomite and occasionally *anhydrite,* several beds of dolomite breccia, some claystone. Analysis of core no. 5, 755.9–758.9, showed that the water-soluble part of the specimen consists essentially of *halite* with a little *gypsum.* Thin sections of cores nos. 5, 6, and 8 contain about 5% of *anhydrite.*	No. 5, 755.9–758.9, rec. 2.7 m. No. 6. 835.1–838.2, rec. 3.0 m. No. 7, 894.8–897.9, rec. 3.0 m. No. 8, 957.6–960.7, rec. 2.7 m. No. 9, 1021.0–1024.1, rec. 2.4 m. No. 10, 1085.0–1088.1, rec. 3.0 m No. 11, 1149.0–1152.1, rec. 3.0 m. No. 12, 1211.5–1214.6, rec. 2.4 m.	Available
Grant Range No. 1 18°01′00″S 124°00′30″E TD 3936.4	Wapet	Anderson Formation 1856.2–3936.5	Late Carboniferous	2950.4–3102.8	Interbedded limestone, shale and *anhydrite.*	Nos. 69–75.	

TABLE 3 (cont.)

Kidson No. 1 22°37′00″S 125°00′22″E TD 4431.4	Wapet	Mellinjerie Limestone 1570.6–1837.0	Middle to ?Late Devonian	1570.6–1667.2 (Unit 1)	Dolomite with some microcrystalline *anhydrite;* sandstone and dolomitic siltstone.	*Carribuddy Formation* No. 9, 2608.5–2611.5, rec. 3.0 m. *anhydritic sandy* dolomite. No. 10, 2768.8–2771.9, rec. 3.0 m. *anhydritic* dolomite and *anhydrite* veins. No. 11, 2929.4–2932.5, rec. 1.8 m, *anhydritic* dolomite. No. 12, nil rec. No. 13, 3095.2–3102.9, rec. 4.6 m, 55% *halite,* 35% quartz. No. 14, 3276.6–3282.7, rec. 0.4 m. *halite* and quartz. No. 15, 3543.0–3546.0, rec. 2.1 m, *anhydritic* calc. claystone. No. 16, nil rec. No. 17, 3742.0–3744.5, rec. 2.4 m, limestone. No. 18, 3864.3–3867.3, rec. 3.0 m, 50% clay, 23% quartz, 22% *halite* and *halite*-bearing limestone. No. 19, 4031.3–4034.3, rec. 3.0 m, 60% dolomite, 10% clay, 15% quartz, 5% halite. No. 20, 4191.6–4193.7, rec. 1.2 m, siltstone.	9.1-m intervals to 975.4, and 3.0-m intervals to T.D.
				1667.2–1837.0 (Unit 2)	Dolomite, dolomitic siltstone, some *anhydrite.*		
		Carribuddy Formation 2570.0–4279.3	? Siluro-Devonian	2570.0–2941.3 (Unit A)	Dolomite, siltstone, sandstone.		
				2941.3–3467.7 (Unit B)	Dominantly *halite;* coarse *anhydrite* in claystone.		
				3467.7–3905.5 (Unit C)	Claystone, with some microcrystalline *anhydrite* in sandstone; some *halite* in sandy limestone.		
				3905.0–4071.2 (Unit D)	Claystone, with dolomite and interbedded *halite.*		
				4071.2–4279.3 (Unit E)	Claystone and dolomite with rare thin beds and veins of *halite* and *anhydrite.*		
McLarty No. 1 19°23′45″S 123°39′30″E TD 2590.8	Total Exploration	Carribuddy Formation 452.0–1687.3	? Siluro-Devonian	452.0–675.4 (Unit A)	Dolomite with interbeds of shale, and shale and siltstone. *Halite* and *anhydrite* intercalations towards base.	No. 5, 463.2–466.3, rec. 2.4 m. No. 6, 577.5–580.6, rec. 1.9 m.	0–TD at 1.5-m intervals.
				675.4–1414.8 (Unit B)	*Halite,* minor mudstone and traces of *anhydrite.*	No. 7, 735.7–738.8, rec. 1.7 m. No. 8, 738.8–744.9, rec. nil	
				1414.8–1511.5 (Unit C)	Mudstone with some *halite* inclusions.	No. 9, 1288.3–1291.4, rec. 2.7 m. No. 10, 1495.9–1499.0, rec. 2.9 m.	
				1511.5–1577.9 (Unit D)	*Halite* and mudstone interbedded at top, overlying mudstone with *halite* and *anhydrite* inclusions.		
				1577.9–1687.3 (Unit E)	Mudstone, *anhydrite* and *anhydritic* dolomite in upper part (1577.9–1630.6), and limestone, minor shale and and *anhydrite* (1630.6–1687.3)	No. 11, 1663.9–1666.3, rec. 2.8 m.	

TABLE 3 (cont.)

Well name, coordinates, total depth	*Company/ drilling authority*	*Formation thickness*	*Age*	*Interval*	*Brief description*	*Core*	*Cuttings*
Parda No. 1 18°56'08"S 122°00'34"E TD 1906.8	Wapet	Carribuddy Formation 980.2–1183.8	? Siluro-Devonian				
				980.2–1152.1	Red-brown claystone, with *anhydrite* in fine-medium crystalline nodules and also as powder disseminated through the claystone.	Sidewall cores 20 (2)–7(2)	Available
				1152.1–1183.8	Green and grey-green claystone, moderately to very *anhydritic*, and limestone with *anhydrite* crystals.	Sidewall cores 5(2)–1(2)	Available
		Goldwyer Formation 1183.8–1495.3	Ordovician	1183.8–1269.4	Limestone, *anhydrite*, dolomitic and pyritic.	No. 1, 1184.7–1188.1; rec. 3.4 m.	
Munda No. 1 19°28'27"S 122°17'32"E TD 1066.8	Wapet	Carribuddy Formation 800.4–1066.8	? Siiuro-Devonian	800.4–1012.5 (Unit A) 1012.5–TD (Unit B)	1012.5–1021.9, *halite* common in claystone. 1021.9–1066.8, *halite*, massive rock salt, brown, pink and colourless, transparent to translucent, coarsely crystalline. Band and fragments of claystone similar to 961.9–1012.5 with minor siltstone and shale.	Sidewall core at 1036.3, rec. 2.5 cm of red-brown and grey claystone with white salt stringers. No. 1, 1060.7–1066.8, rec. 6.1 m. 1060.7–1063.4, *halite*, brown and white with minor (⁀10 mm) beds of limestone. 1063.4–1066.8, *halite* with increasing amounts of claystone towards base of core, brown-red and grey-green.	9.1-m intervals.
Sahara No. 1 21°04'40"S 123°23'30"E TD 2120.1	Wapet	Tandalgoo Red Beds 1127.8–1726.6 Unit B	Early Devonian				
				1199.3–1359.4	Red sandstone with minor siltstone; minor *anhydrite* below 1341.1.	Nil	Available
		Unit D		1417.3–1726.6	Red sandstone, with *?anhydrite* or ?kaolin.	No. 9, 1552.0–1555.6, rec. 2.4 m.	Available
		Carribuddy Formation (1726.7–2120.1)	? Siluro-Devonian	1726.6–2033.0 (Unit A)	Shale, with rare *anhydrite* and halite patches, spotted.	No. 12, 1999.7–2003.1, rec. 3.0 m.	Available according to well completion report, but none shown 1798.3–1889.7 on % lithology log.
				2033.0–TD (Unit B)	Shale and claystone, with *salt* and *anhydrite* as nodules and crystals, and rare crystalline veins up to 2.5 cm	No. 13, 2118.6–2120.1, rec. 12.7 cm.	Available

TABLE 3 (cont.)

Willara No. 1 19°10′48″S 122°04′14″E TD 3903.2	Wapet	Carribuddy Formation 1255.1–1873.9	? Siluro-Devonian	1255.1–1458.5 (Unit A) 1458.5–1736.4 (Unit B) 1736.4–1873.9 (Unit C)	24.4 m claystone, underlain by *rock salt* and *anhydrite*. Claystone, siltstone and sandstone; *rock salt* and *anhydrite* throughout interval. Dolomite with *anhydrite* to 1786.1; limestone below.	No. 2, 1284.7–1287.8, rec. 3.1 m. No. 3, 1459.1–1462.1, rec. 0.4 m. No. 4, 1602.0–1605.1 ,rec. 2.7 m. No. 5, 1739.2–1743.8, rec. 3.5 m.	0–1143 at 9.1-m intervals. 1143–TD at 3.1-m intervals. 1.5-m intervals during coring.
Wilson Cliffs No. 1 TD 3722.2	Australian Aquitaine Petroleum Ltd	Mellinjerie Limestone 966.8–1094.2	Middle to Late Devonian	1009.1–1094.2 (Member 2)	Dolomite with *anhydrite* in thin beds, vein fillings or kernel of oolites.	No. 2, 1010.7–1016.8. No. 8, 1814.7–1819.3, rec. 4.2 m.	0–TD at 3.1-m intervals.
		Carribuddy Formation 1778.5–2532.8	? Siluro-Devonian	2029.3–2368.2 (Unit C)	Grey calcareous shale, *anhydrite* nodules and veins in parts, trace *gypsum* throughout.	No. 9, 1992.4–1996.8, rec. 4.6 m. No. 10, 2211.6–2214.9, rec. 3.3 m. No. 11, 2434.1–2437.1, rec. 3.0 m.	
				2368.2–2496.3 (Unit D)	Mostly *halite*, traces *anhydrite*, some shale and sandstone.		
		Goldwyer Formation 2532.8–2847.4	Middle Ordovician (Llanvirnian-?Llandeilian)	2532.9–2847.4	Shale and limestone, traces *anhydrite* in shale.	No. 12, 2568.5–2572.2, rec. 3.7 m. No. 13, 2679.1–2683.7, rec. 4.6 m. No. 14, 2780.9–2784.0, rec. 3.0 m.	
CAPRICORN EMBAYMENT							
Aquarius No. 1 22°37′13″S 152°39′02″E TD 2650.2	Australian Gulf Oil	Unnamed Unit 1245.1–1702.3	Early Tertiary	1453.9–1472.2	Interbedded shale and *anhydrite*.	Sidewall No. 20 1411.2, rec. 40%, anhydrite and sandstone. No. 19, 1444.7, rec. 80%, anhydrite. No. 15, 1530.0, rec. 100%, anhydrite and sandstone.	Available, 3.0-m intervals.
		Unnamed Unit 1702.3–2642.6	? Pre-Tertiary Mesozoic	2079.0	*anhydrite*	No. 14, 2077.2–2083.3, 0.1 m. dense cryptocrystalline anhydrite.	
CARNARVON BASIN							
Dirk Hartog No. 17B 25°51′58″S 113°04′40.5″E TD 1523.4	Wapet	Dirk Hartog Formation 665–1404	Silurian		Limestone, shale, siltstone beds and veins of *anhydrite*.		
Hamelin Pool No. 1 26°01′31″S 114°12′17″E TD 1595.3	Magellan Petroleum (Australia) Ltd	Dirk Hartog Formation 209.4–1558.4	Late Silurian	1130.8–1131.4 1164.9–1165.5 1236.8–1243.5 1245.1–1247.5 1274.6–1277.7 1283.8–1288.6 1388.6–1391.7	Total of 22.9 m *halite* in seven beds.	No. 1, 1103.0–1104.5 No. 2, 1240.5–1244.8 No. 3, 1244.8–1262.1 No. 4, 1275.8–1282.2 (100% recovery in all cores)	3.0-m intervals to TD

TABLE 3 (cont.)

Well name, coordinates, total depth	*Company/ drilling authority*	*Formation thickness*	*Age*	*Interval*	*Brief description*	*Core*	*Cuttings*
Hamelin Pool No. 2 26°08′55″S 114°21′24″E TD 1219.2	Magellan Petroleum (Australia) Ltd	Dirk Hartog Formation 196.9–1219.2	Late Silurian	1138.7–1139.6 1174.1–1167.9 1174.1–1176.7	Total of 5.2 m *halite* in three beds.	No. 1, 1141.4–1150.6 No. 2, 1150.6–1168.9 No. 3, 1168.9–1187.1 No. 4, 1187.1–1205.4 (100% recovery in all cores)	3.0-m intervals to TD.
Pendock I.D. No. 1 23°17′02″S 113°20′10″E TD 2500.9	Wapet	Dirk Hartog Formation 1849.5–2500.9	Late Silurian	1901.9–1905.0 1929.3 2127.2 2136.6–2139.6	*Anhydrite* *Anhydrite* *Anhydrite* *Anhydrite*	Nil	Available 3.0-m intervals
Quail No. 1 23°57′04″S 114°29′57″E TD 3580.5	Wapet	Dirk Hartog Formation 3081.8–3549.1	Silurian	3081.8–3205.9 3205.9–3355.2 3355.2–3416.8 3416.8–3549.1	Sandstone Dolomite *Anhydrite,* dolomite, siltstone Dolomite, siltstone	No. 17, 3111.4–3112.0, rec. 0.05 m, siltstone No. 18, 3261.7–3262.3, rec. 0.3 m, dolomite No. 19, 3401.6–3403.7, rec. 1.8 m, 3401.6 *anhydrite*, 3402.2 dolomite, 3403.7 siltstone, 3403.7 *anhydrite*	Available
Wandagee No. 1 23°53′15″S 114°23′51″E TD 1073.2	Wapet	Dirk Hartog Formation 278–810.8	Silurian	278–398.7 398.7–626.4 626.4–685.2 685.2–810.8	Sandstone, minor lutites Oolitic dolomite, minor lutites, some *anhydrite* in lower 60 m. Dolomitic siltstone, minor claystone, dolomite, lenses of *anhydrite* *Anhydritic* dolomite, siltstone.	No. 2, 423.1–424.9, rec. 1.5 m, siltstone, claystone, dolomite. No. 3, 515.4–519.1, rec. 3.1 m, siltstone, dolomite. No. 4, 598.9–602.6, rec. 9 m, dolomite, anhydrite. No. 5, 704.1–707.7, rec. 3.6 m, dolomite. No. 6, 775.1–778.8, rec. 3.4 m, dolomite.	0–914.4 at 3.1-m intervals. 914.4–TD at 1.5-m intervals
Yaringa No. 1 26°03′58″S 114°21′35″E TD 2288.4	Continental Oil Co. of Australia	Dirk Hartog Formation 146.3–1526.4	Late Silurian	1204.5–1271.1 1342.6–1345.6	33.2 m of *halite* in seven beds. 3.0-m bed of *halite*. Total of 36.2 m of *halite* in eight beds.	No. 15, 1235.9–1239.0, rec. 2.6 m.	3.0-m intervals to TD.
				OFFICER BASIN			
Birksgate No. 1 27°56′20″S 129°48′10″E TD 1878.2	Continental Oil Co. of Australia	Unit 'B' 662.3–952.5	Proterozoic	777.2–798.5	Shale and limestone with up to 10% *anhydrite.*	Nil	Available
BMR Madley No. 1 24°13′40″S 124°20′50″E TD 207.6	Bureau of Mineral Resources	Unnamed formation 0–TD	Proterozoic	0– 46 46– 73 73–143 143–154 154–161 161–204	Dololutite, minor *gypsum* *Gypsum*, dololutite Dololutite, minor gypsum. N.R. Dololutite, *gypsum* breccia Dololutite, *anhydrite* breccia minor lithic arenite, tr. *halite.*	Cored 43–45, 154–208, 92% rec.	0–143 at 1.52-m intervals.

TABLE 3 (cont.)

BMR Warri No. 20 24°05′S 124°33′E TD 265.5	Bureau of Mineral Resources	Unnamed formation 0–TD	? Proterozoic	0–124 124–161 161–203 203–206 206–266	*Gypsum*, grey friable dolomite, gypsiferous dolomite, minor dolomitic *anhydrite* and *anhydrite*. Gypsum, grey friable dolomite, gypsiferous dolomite, dolomitic *anhydrite*, *anhydrite* *Anhydrite*, anhydritic dolomite, grey friable dolomite. *Anhydrite* with *halite* in *halite* matrix. *Halite*.	Continuous cores 3–206, 98% rec. 206–TD, 9% rec.	205–TD at 3-m intervals
Browne No. 1 25°51′15″S 125°48′58″E TD 386.7	Hunt Oil Co.	Browne Beds 132.6–386.8	Proterozoic	132.6–386.8	Interbedded calcareous shale, dolomitic limestone, *anhydrite*, *gypsum* and *halite*.	No. 2, 213.4–216.4, rec. 1.0 m. No. 3, 257.6–260.6, rec. 2.7 m. No. 4, 354.5–? rec. 0.1 m. No. 5, 354.5–357.3, rec. 2.3 m.	
Browne No. 2 25°56′00″S 125°57′45″E TD 292.6	Hunt Oil Co.	Browne Beds 262.1–292.6	Proterozoic	262.1–292.6	*Evaporites* occur in thin beds or as secondary fracture fillings. May be equivalent to Babbagoola Beds.	No. 2, 259.1–262.1, rec. 1.9 m. No. 3, 288.3–291.4, rec. 0.4 m.	0–228.6
Byilkaoora No. 1 27°17′00″S 133°30′30″E TD 496.7	South Australia Dept. of Mines & Energy	Observatory Hill Beds 155.8–379.4	Cambrian	Unit III 259.0–322.5 Unit II 322.5–376.0	Clayey and calcareous dolomite with *pseudomorphs after evaporite minerals.* Calcite pseudomorphs after *shortite* and *trona* as subspherical, 'feathery' rosette and cuneiform crystals and crystal aggregates embedded in clayey and cherty carbonate matrix. Very fine-grained sandy carbonate rock flecked with ?carbonate *pseudomorphs of evaporite mineral* of crystal morphology different to those in Unit III.	Continuous 13.1–TD, rec. 100%.	Surface–13.1
Yowalga No. 2 26°10′12″S 125°58′00″E TD 989.4	Hunt-Placid Oil Co.	Babbagoola Beds 845.9–989.4 Unit A 845.9–887.0 Unit B 887.0–893.0 Unit C 893.0–989.4		Proterozoic	851.3 m dolomitic to *anhydritic* sandstone (10% *anhydrite*). 893.0 m silicified dolomite *anhydrite*. 893.3 m *anhydrite* (70%)	No. 5, 851.0–854.0, rec. 1.9 m. No. 7, 891.8–894.8, rec. 1.9 m.	Available

ADAVALE BASIN

The Adavale Basin (Fig. 3) is entirely concealed beneath 1000-3000 m of Galilee Basin Permian and Carboniferous sediments and the practically flatlying sediments of the Eromanga Basin sequence (Jurassic-Cretaceous). Its lower Palaeozoic stratigraphy (after Galloway, 1970) is shown in Table 4.

Five petroleum exploration wells have penetrated rock salt along the eastern margin of the basin: Boree No. 1, Alva No. 1, Bonnie No. 1, Bury No. 1, and Stafford No. 1 (Fig. 4). The salt occurs in the Etonvale Formation, in the Boree Salt Member, whose extent has been outlined by seismic work.

The greatest thickness of salt is thought to be in an elongate northeast-trending body between the Warrego Fault and Stafford No. 1 well. In this well the salt occurs below 2670 m, and is about 75 m thick; close to the fault it has been estimated from seismic surveys to be up to 900 m thick, with its top only 900 m deep in places. The salt has not been drilled in the thickened zone, but the marked thickening along the Warrego Fault may be partly due to diapirism.

A probable salt diapir was detected by the Lake Dartmouth seismic survey in 1965 about 100 km south of Stafford No. 1 well (Tallis & Fjelstul, 1966). The seismic work also showed that the unconformity at the base of the Permian has a very uneven surface, which has been interpreted as hogbacks of Devonian sediments protruding into the Permian sequence; any evaporites present would be expected in the troughs between.

Keevers (personal communication) considers that the Adavale Basin was an intracratonic basin separated from the Cooper Basin to the west during deposition of the Cooladdi Dolomite, and barred to the east. The eastern part of the basin, where the classical evaporite sequence from carbonates through anhydrite and salt to potash salt occurs, would have been the deepest, and the thickest salt would be expected there. Strong correlation between geophysically identifiable units in the wells Bonnie No. 1, Boree No. 1, and Bury No. 1 suggests little disturbance of the sedimentary sequence as far east as Bury No. 1, which is only about 4 km west of the Warrego Fault. Interpretation of seismic records by Hartogen suggests the thickening was caused by thrusting rather than diapirism. Thrust faults are present in sediments on the west side of the Pleasant Creek Arch, and are particularly clearly defined in the Bury Limestone.

A salt pillow is evident on the seismic cross section, 10 km southwest of Stafford No. 1. The salt here is 640 m thick and only about 30 m deeper than at Stafford. At the western edge of the salt member the thickness of the interval from the base of the Permian to the top of the salt is 1500 m. The Devonian sequence pinches out towards the west, but the older beds (?Log Creek Formation) thin much more rapidly than those in the younger sequence (Etonvale Formation). In the area of salt deposition the Bury Limestone appears to thin rapidly towards the centre of the salt basin. Seismic reflections in the centre of the basin indicate, at the base of the salt section, the presence of a lenticular body which may possibly be anhydrite. The electric logs in Bonnie No. 1, Boree No. 1, and Bury No. 1 wells clearly indicate the presence of anhydrite.

Salt solution has been used to explain several unusual structures similar to those described in the Canning Basin. In the Adavale Basin salt solution could have occurred in the east towards the fault in D2 time, and in the west during the late Devonian, though in some places it is difficult to decide if the structures have been caused by removal of salt or if two different formations interfinger. Hartogen considers that the sequence in Leopardwood No. 1 indicates that salt was originally present. There is an anomaly on the seismic section east of Leopardwood No. 1 and west of the main salt zero line which is almost certainly a salt outlier and, therefore, indicative of solution between that point and the zero line. Clastic rocks predominate in Leopardwood No. 1 well, and the only evaporite minerals are traces of anhydrite and accessory dolomite. Keevers (personal communication) considers that this fact, the reduced thickness of the D3 horizon, and the position of the section in the basin make it unlikely that this part of the section ever contained more than traces of salt.

The evaporite sequence in the Adavale Basin is the only one in Australia known to include interbeds of potassium minerals. Sylvite occurs in Bonnie No. 1, Bury No. 1, and Boree No. 1 wells (Fig. 5). In Bonnie No. 1 coarse sylvite and halite occur in a bed 10 cm thick in core no. 3, at 2243.9 m (Fig. 6); in Bury No. 1

TABLE 4. LOWER PALAEOZOIC STRATIGRAPHY OF THE ADAVALE BASIN (AFTER GALLOWAY, 1970)

Lower Permian			Siltstone, shale
	MAJOR UNCONFORMITY		
Upper Devonian to Lower Carboniferous	Buckabie Formation	0–2 100 m	Sandstone, siltstone, shale
Middle Devonian	Etonvale Formation	0– 240 m	D1 Shale—siltstone member
		0– 500 m	D2 Sandstone member
		0– 40 m	D3 Cooladdi Dolomite Member
			Boree Salt Member
	UNCONFORMITY		
	Log Creek Formation	0– 600 m	D4 Gilmore Sandstone Member
		0– 450 m	Shale member
		0– 600 m	Bury Limestone Member
	Gumbardo Formation	0– 750 m	Volcanic rocks, tuffs and sediments
	MAJOR UNCONFORMITY		
Ordovician to Silurian			Igneous and metamorphic rocks

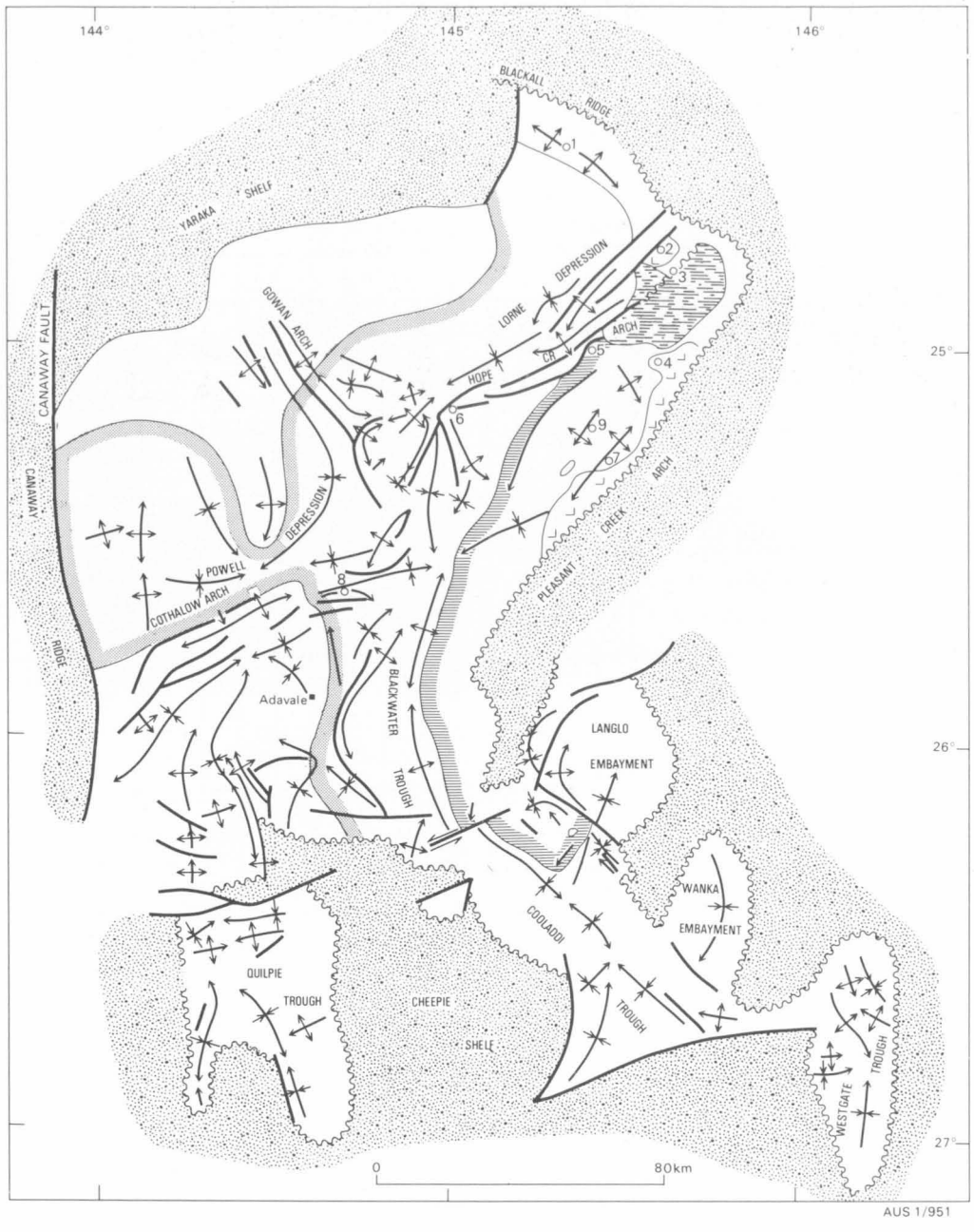

Salt bodies

Pre-Permian formation (Permian or Mesozoic on basement)

Area from which Buckabie and Etonvale Formations probably stripped

Probable westward extent of Cooladdi Dolomite

Westward extent of Boree Salt Member deposition

Faults cutting pre-Permian formations showing horizontal movement

Anticlinal axis showing direction of plunge and culmination

Synclinal axis showing direction of plunge and culmination

Truncated margins of pre-Permian formations

Drill hole

1 Fairlea

2 Boree

3 Ravensbourne

4 Bury

5 Bonnie

6 Etonvale

7 Stafford

8 Loepardwood

9 Alva

After Tanner (1968), Slanis and Netzel (1967), Marathon (1967), and Amoseas

Fig. 3. Adavale Basin; structure and distribution of Boree Salt Member.

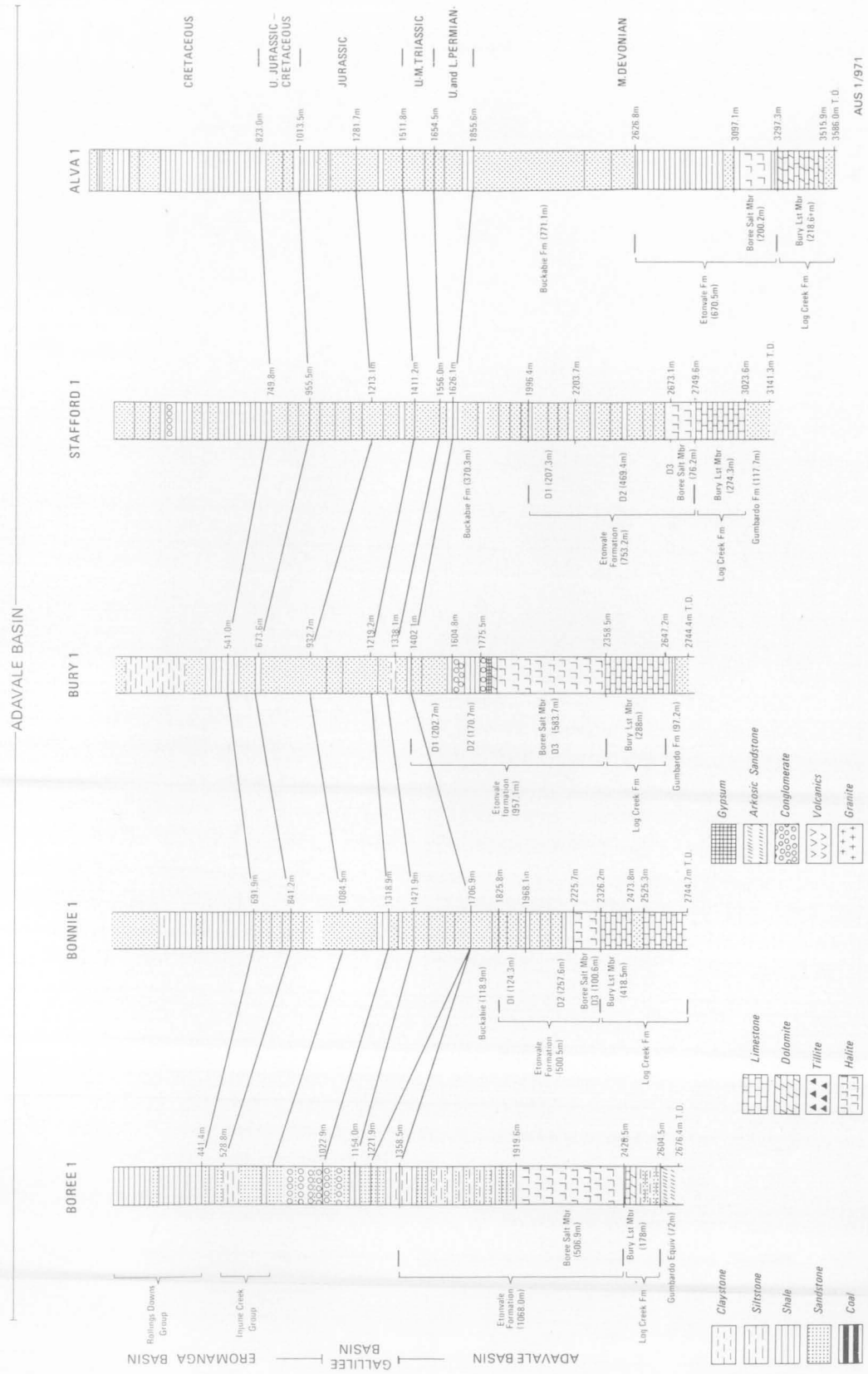

Fig. 4. Graphic sections of wells containing evaporites, Adavale Basin.

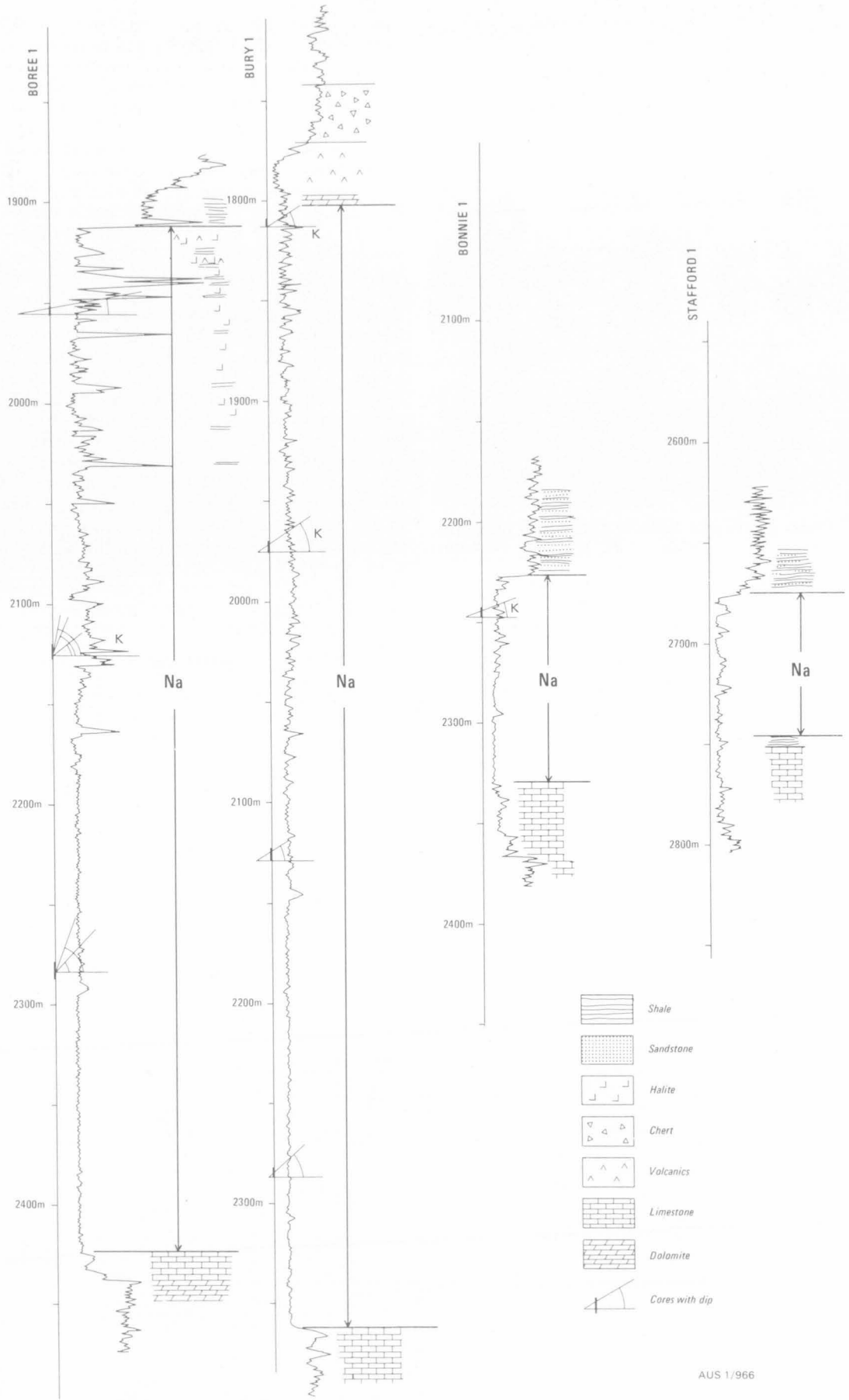

Fig. 5. Gamma-ray logs of the Boree Salt Member, Adavale Basin. The sylvite interbeds are indicated by K on the logs.

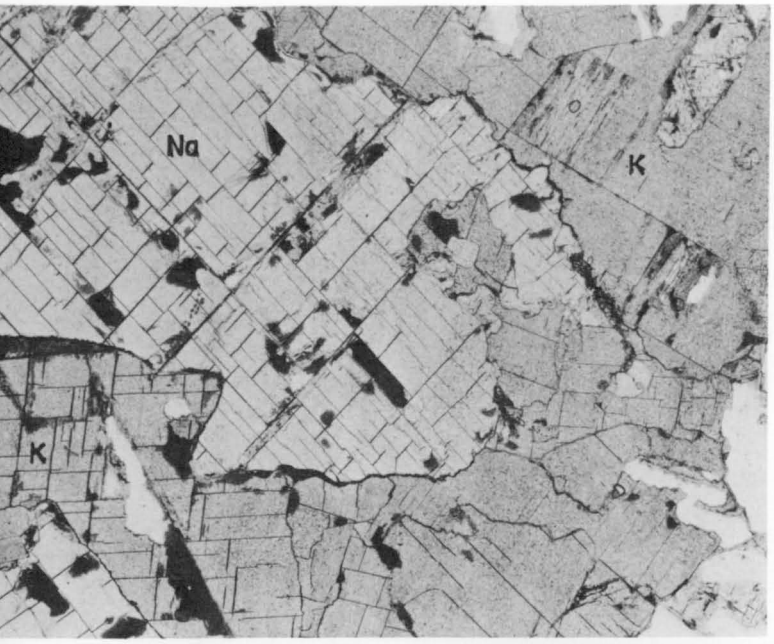

Fig. 6. Coarse sylvite and halite in core no. 3 (2244 m), Bonnie No. 1 well, Adavale Basin. K-sylvite, Na-halite. (GA/5495)

sylvite occurs in core no. 8 at 1810.5-1810.7 m and core no. 9 at 1970.4-1970.5 m; in Boree No. 1 core no. 19 contains a 2.5-cm bed and irregular pods of sylvite at 2125.7 m, and about 15 cm of interbedded sylvite and halite at 2129.3 m. Keevers (1968) suggested that in Bury No. 1 there is evidence of two evaporite cycles, with the second cycle only partly developed or, alternatively, partly removed by erosion or solution.

A reinterpretation of the stratigraphy of the basin has been made by Paten (1977) and is compared with that of Galloway in Fig. 7. Paten envisages a transgressive-regressive cycle of sedimentation to account for the facies changes, with a maximum transgression in the Middle Devonian. The sediments are predominantly red beds with the exception of the early fluviatile and adjacent marine beds. The history of the basin began with the deposition of the Lower to Middle Devonian Eastwood Beds in a southwards migrating delta system, originating from the Yaraka Shelf, deposited on a Lower Devonian basement of red beds and volcanics. The Eastwood Beds pass southwards into marine shale and limestone of the Log Creek Formation. The succeeding Middle Devonian carbonate phase shows a gradation from near-shore tidal-flat sediments of the Lissoy Sandstone, through thin, shallow-water, lagoonal, back-reef sediments of the Cooladdi Dolomite, to reefal and carbonate mounds of the Bury Limestone in the east. Reefal conditions existed in the limestone facies of the Bury Limestone along the area

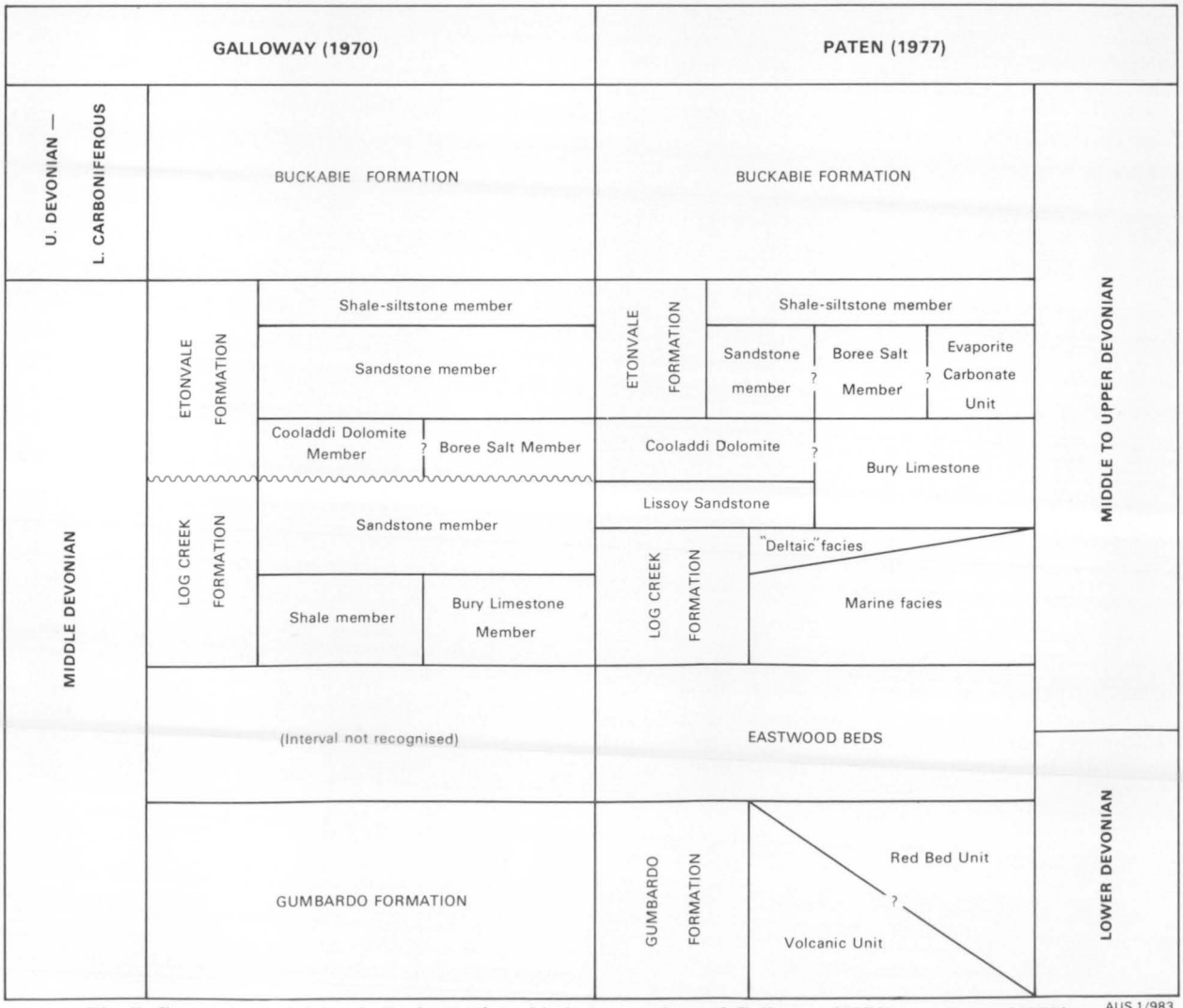

Fig. 7. Comparison of Adavale Basin stratigraphic interpretations of Galloway (1970) and Paten (1977).

subsequently occupied by the Pleasant Creek Arch, and carbonate mounds occur in the limestone/shale facies of the formation. Barring of the basin in the east by carbonate building up along the Quilberry Dartmouth trend, and a corresponding encroachment of desert conditions from the west resulted in the evaporitic phase of the Etonvale Formation, with the Boree Salt Member grading westwards into a nearshore sandstone member and eastwards into evaporitic carbonates. The post-evaporitic phase produced the red beds of the Etonvale and Buckabie Formations. The basin was cut by Late Carboniferous faulting, and salt solution and migration into salt pillows modified the structure and distribution of the evaporitic phase. Salt was mobilised into pillows along west-bounding faults.

The presence of potash in the Adavale Basin and the classical evaporite sequence from dolomite through anhydrite to salt make it one of the most prospective basins in Australia, the most prospective area being next to the Pleasant Creek Arch.

ADELAIDE GEOSYNCLINE

Numerous diapiric structures with cores of calcitic or dolomitic siltstone breccia occur in the Flinders Ranges of South Australia, and have been well documented (Webb, 1960, 1961; Coats, 1964, 1965, 1973; Dalgarno & Johnson, 1968; Binks, 1971).

During deposition of the early Sturtian (late Precambrian) and lower Cambrian sediments, which together exceed 15 000 m in thickness, an incompetent dolomite-siltstone sequence, the Callanna Beds, formed piercement structures, which influenced sedimentation. More than thirty diapiric structures are present along linear trends (Fig. 8), which are regarded as a basement fault system. The injected material is a carbonate-siltstone breccia with abundant exotic blocks including crystalline basement. There is no conclusive evidence of interbedded evaporites, but the grey siltstone in the core complex, contains abundant pseudomorphs after halite, and the red micaceous siltstone and well-bedded quartzite of unknown affinities both contain rare pseudomorphs after halite. The siltstone and quartzite are thought to be probably equivalent to the Willouran Series and part of the source beds for the diapirs. Alternatively, they are part of the overlying basal Burra Group, of Torrensian age (late Precambrian), in which similar sediments with halite pseudomorphs are found.

Many and varied mineral occurrences are known from the diapirs; some of the intrusions have been investigated in detail by the South Australian Mines Department (Barnes, 1969, 1970; Johns, 1969; Langsford, 1969).

Burns & others (1977), however, reject diapiric processes in the Flinders Ranges to account for the breccia masses. They suggest that the domes are not intrusive and do not have less dense core rocks. They suggest instead that much of the core breccia is formed by deformation of a stratigraphic unit composed of interbedded competent and incompetent beds at a décollement and results from folding during the Late Cambrian. They compare the Flinders Ranges structure to the Pyrenees or Jura, which are foreland terrains incorporating ductile basal formations.

The evidence for diapirism in the breccia masses is supported by that given in Coats (1973), namely: evidence for periodic movement over about 150 m.y.; 90° angular unconformities in the sequence adjacent to the diapirs; boulder trains of diapiric detritus in the rim sediments, indicating exposure of the core at various intervals; local uplift of sediments related to injection of the core complex; movements in the diapirs mainly preceded the Delamerian Orogeny. Many of the diapirs were initiated and localised in folds produced by the gentle warping and major faulting of the mild Sturtian Orogeny. The later Delamerian Orogeny probably mainly accentuated the earlier folds.

In the Adelaide Geosyncline a late Early Cambrian regression (Billy Creek Formation) was followed by

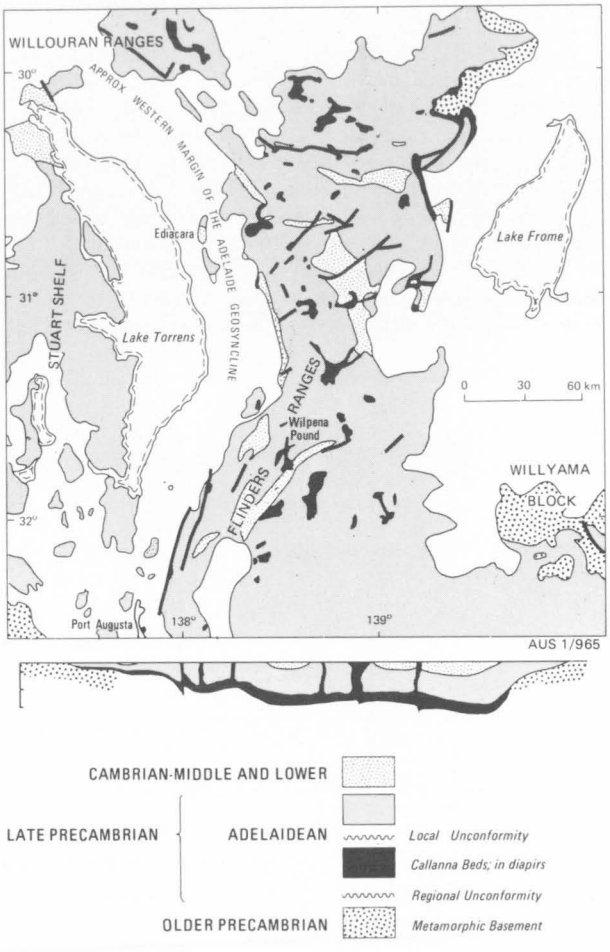

Fig. 8. Diapirs in the Adelaide Geosyncline.

a mildly evaporitic redbed environment, which characterised, though with increased clastic contribution, most of the Middle to Late Cambrian Lake Frome Group and its lithostratigraphic equivalents (Parkin, 1969). Watts & others (1966) described a sequence in Stansbury West No. 1 well, at the southern end of Yorke Peninsula, which reached a total depth of 1745 m. It penetrated an upper redbed sequence, of Cambrian age, at 335-579 m, unconformable beneath Permian rocks, and a lower redbed sequence at 828-925 m. Both sequences are clastic, but traces of gypsum were recorded in the top of the underlying Parara Limestone, which occurs at 925-1288 m.

Stansbury No. 1 stratigraphic well, 6 km east-southeast of Stansbury West No. 1, penetrated 140 m of Cambrian redbeds and was still in this sequence at total depth of 417 m.

Cambrian redbed sequences were also intersected 10.5 km north of Stansbury West No. 1, in the Minlaton No. 1 well, which reached a total depth of 994 m and intersected 750 m of Cambrian section, including redbed clastics.

AMADEUS BASIN

The Amadeus Basin (Fig. 9) is one of two sedimentary basins in Australia in which bedded evaporites are exposed in eroded diapirs and other structures (the Officer Basin is the other). Two levels of evaporites are present in the basin: the late Precambrian Bitter Springs Formation, and the Early Cambrian Chandler Limestone (Wells & others, 1970). Only the less soluble evaporites of the Bitter Springs Formation are exposed (Fig. 10).

Outcrops consist mostly of earthy weathered gypsum, which generally occurs with outcrops of dolomite and shale, of the Bitter Springs Formation. The unweathered form of the gypsum is distinct from that in modern gypsum deposits of playa lakes and soil profiles, in that it is crystalline, compact, and generally either strongly brecciated or tightly folded, and contains, in many places, erratic blocks of dolomite.

Gypsum of the Bitter Springs Formation crops out chiefly in a zone trending east-southeast from Johnstone Hill in the northwest to a few kilometres north of Curtin Springs. Exceptions are an occurrence near the Gardiner Fault in the Gardiner Range, and at the Ringwood Dome in the east of the basin.

In the Johnstone Hill-Curtin Springs zone the gypsum crops out in the cores of eroded anticlines, in isolated outcrops—which show no relation to the country rocks, and in structures that have been described as diapiric in origin. Three of the surface deposits, two of them outside the main zone, have been drilled: at the Ringwood Dome—BMR Alice Springs No. 3 (Stewart, 1974); in the Gardiner Range—BMR Mount Liebig No. 1 (Wells & Kennewell, 1972); and an outcrop north of Curtin Springs—BMR Lake Amadeus Nos. 3, 3A, and 3B (Wells & Kennewell, 1972). These holes are described later, as also is BMR Hermannsburg No. 40, a shallow exploratory hole drilled in the Goyder Pass structure.

The Ringwood and Curtin Springs holes produced similar sequences of strongly folded and partly brecciated gypsum, anhydrite, mixed evaporite rocks, and

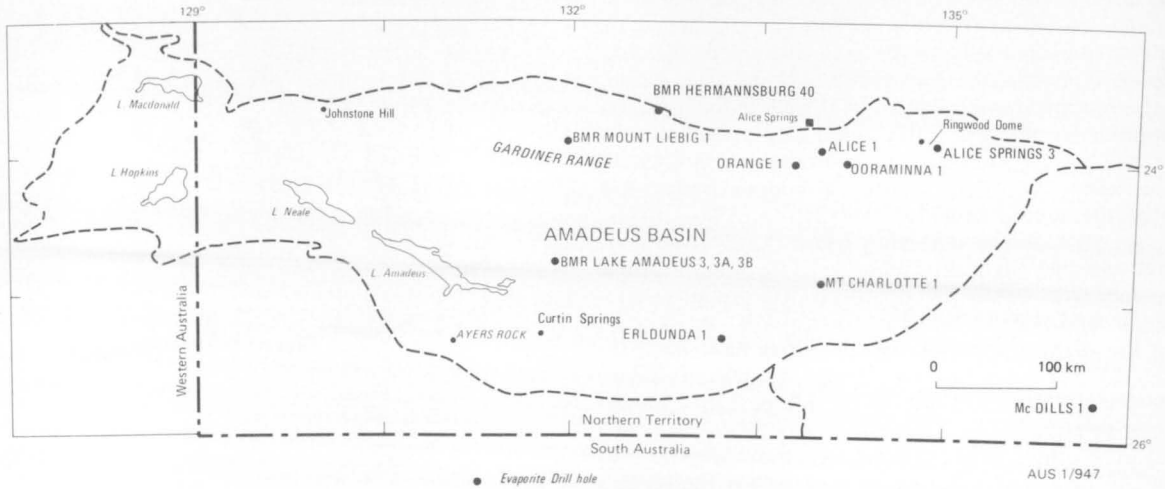

Fig. 9. Locality map, Amadeus Basin.

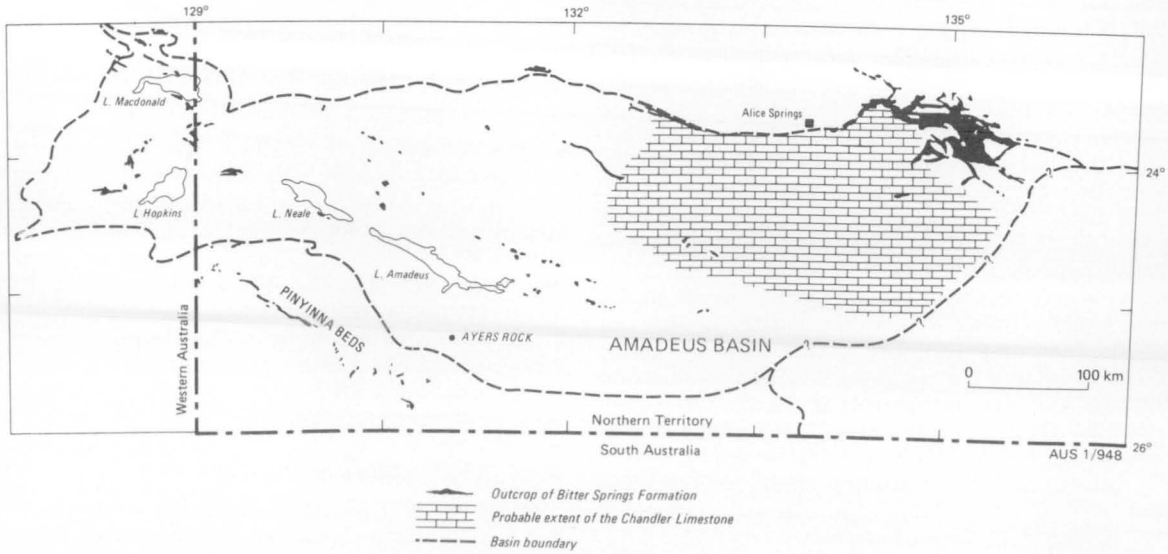

Fig. 10. Outcrop of the Bitter Springs Formation and probable extent of the Chandler Limestone, Amadeus Basin.

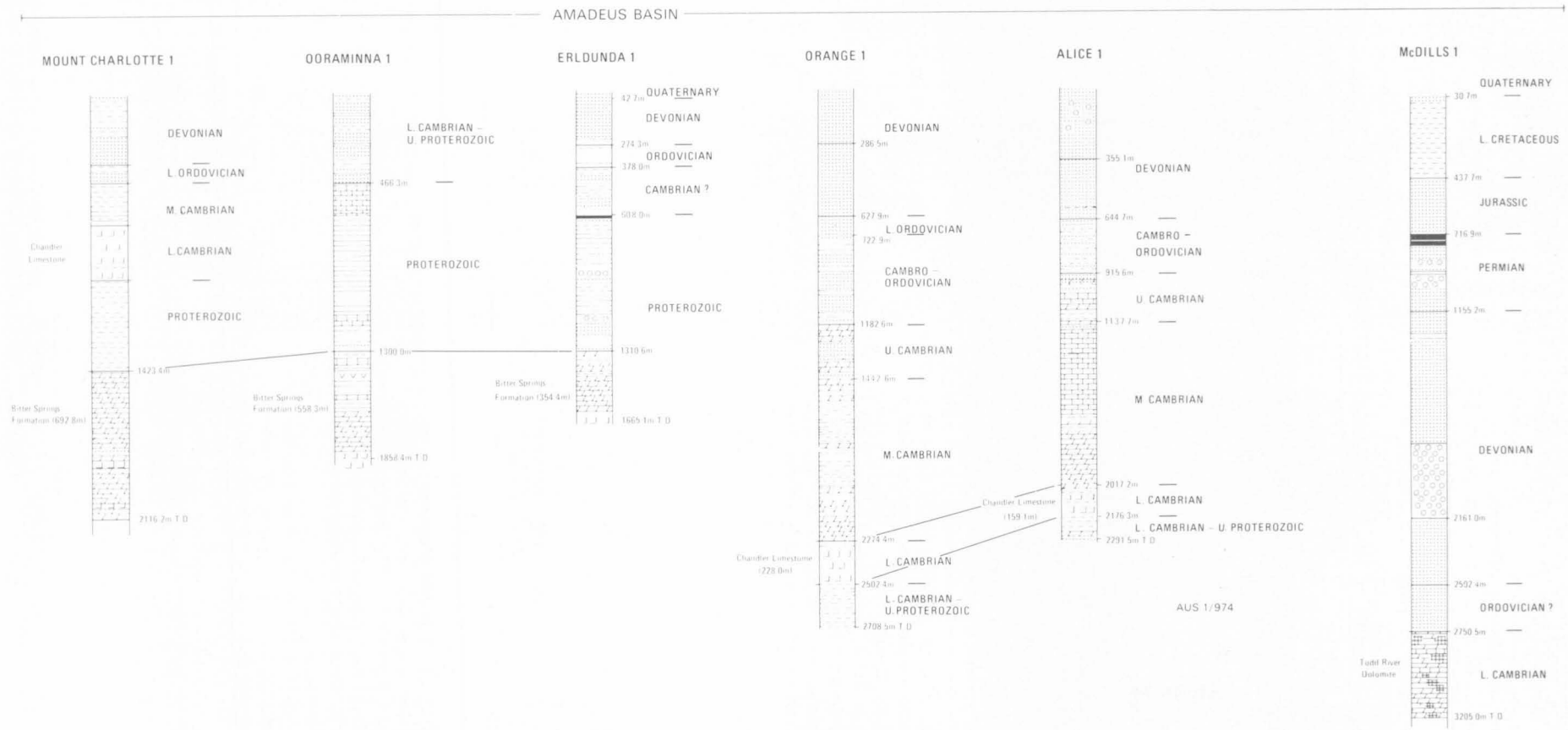

Fig. 11. Graphic sections of petroleum exploration wells containing evaporites, Amadeus Basin. For reference to symbols see Fig. 4.

dolomite. Anhydrite first appears at about 100 m in each hole and increases with depth. The mixed evaporite rocks consist of anhydrite, gypsum, dolomite, and euhedral quartz in various proportions.

The hole drilled in the Gardiner Range penetrated 90 m of brecciated mixed evaporite rocks and 210 m of pink and red halite, which contains minor impurities. The red, probably caused by ferric iron content, may indicate a shallow-water environment. The rocks of the top 90 m are very similar to those of subrosion zones in German salt domes (Richter-Bernburg, 1972). The salt in the lower part of the drill hole has a brecciated appearance, but no features of strong tectonic transport. A brecciated appearance can be caused by erosion of salt, owing to the influx of undersaturated salt water into a basin: the beds of anhydrite remain and a breccia is formed by their collapse and recementation. The evaporites here were probably emplaced by thrusting during the late Palaeozoic Alice Springs Orogeny. Décollement folding is the typical tectonic style in the Amadeus Basin, being facilitated by the evaporite sequences in both the Bitter Springs Formation and the Chandler Limestone.

The distribution of the gypsum outcrops in the Johnstone Hill-Curtin Springs zone is controlled by structure, but why the outcrops are, in the main, restricted to this zone is not certain. In the centre and east of the basin, the wells that intersected halite lie outside the zone. The distribution of evaporites may mean that the centre of the evaporite basin lies within the eastern part of the Amadeus Basin, with a halite zone surrounded by a gypsum 'halo'. The residual 'bitter' liquors with the most soluble salts would be expected in the palaeotopographic lows near the centre of this basin. During an investigation of the evaporites of the Bitter Springs Formation, Newmont drilled a hole at the eastern end of Lake Amadeus. The site was selected after consideration of the geophysical anomalies and structural framework of the basin. Sections, interpreted from magnetic profiles, were constructed across the basin, and an anomaly was found between the known thickness of sediments and the postulated depth of basement. This was explained by the presence of low-density halite in the sequence and Lake Amadeus being positioned where increased thickness of evaporites would be expected. Since both the northern and southern margins of the Amadeus Basin were formed by thrusting from the north and south, respectively, the salt-lake chain is postulated to be positioned over a salt anticlinorium. In the hole drilled by Newmont, about 60 m of Cainozoic clay and silt overlies about 60 m of limestone, dolomite, and sandstone of the Bitter Springs Formation. The postulated salt anticlinorium could probably be best outlined by detailed gravity surveys, which could distinguish salt from anhydrite/gypsum intercalations.

Petroleum exploration wells in the Amadeus Basin penetrated the Bitter Springs Formation in several structures, and thick salt sequences were intersected in Ooraminna No. 1, Mt Charlotte No. 1, and Erldunda No. 1 wells (Figs. 11, 12). In addition, a younger evaporitic sequence in the Lower Cambrian Chandler Limestone was penetrated in Alice No. 1, Orange No. 1, and Mount Charlotte No. 1 (Fig. 13). McDills No. 1 bottomed in Lower Cambrian Todd River Dolomite, which contains anhydrite-filled fractures, and for that reason it is included in this chapter, although it lies outside the Amadeus Basin boundary on Figure 9, and was, in fact, started in sediments of the Eromanga

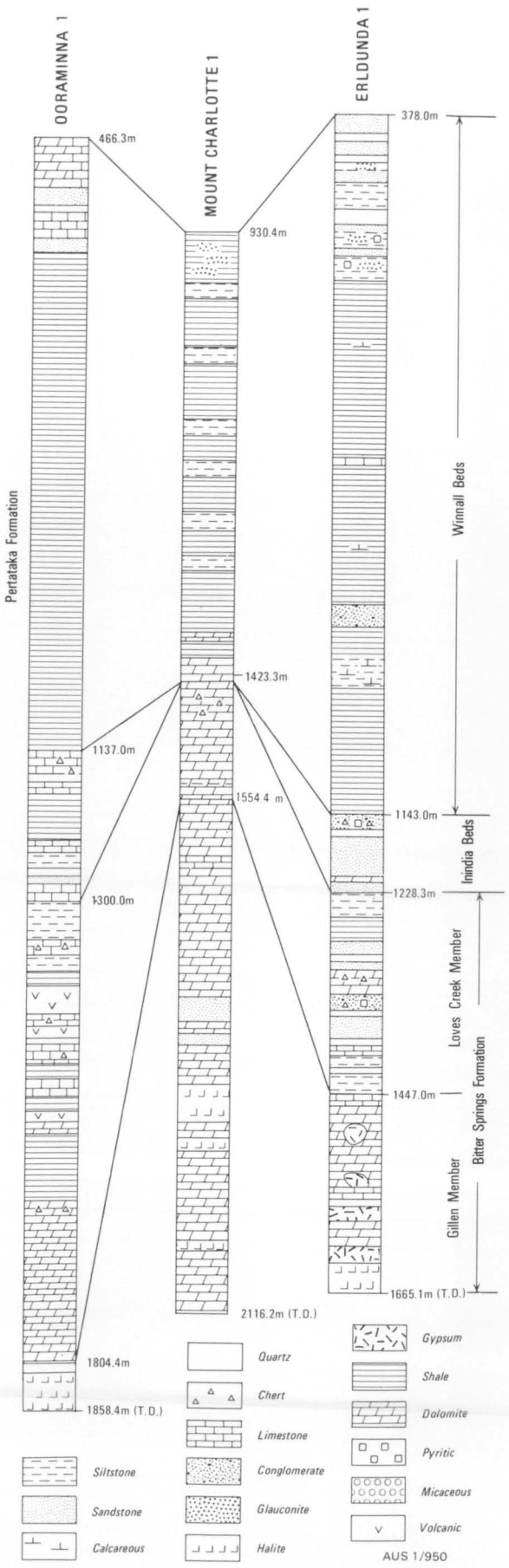

Fig. 12. Graphic sections of wells containing evaporites in the Bitter Springs Formation, Amadeus Basin.

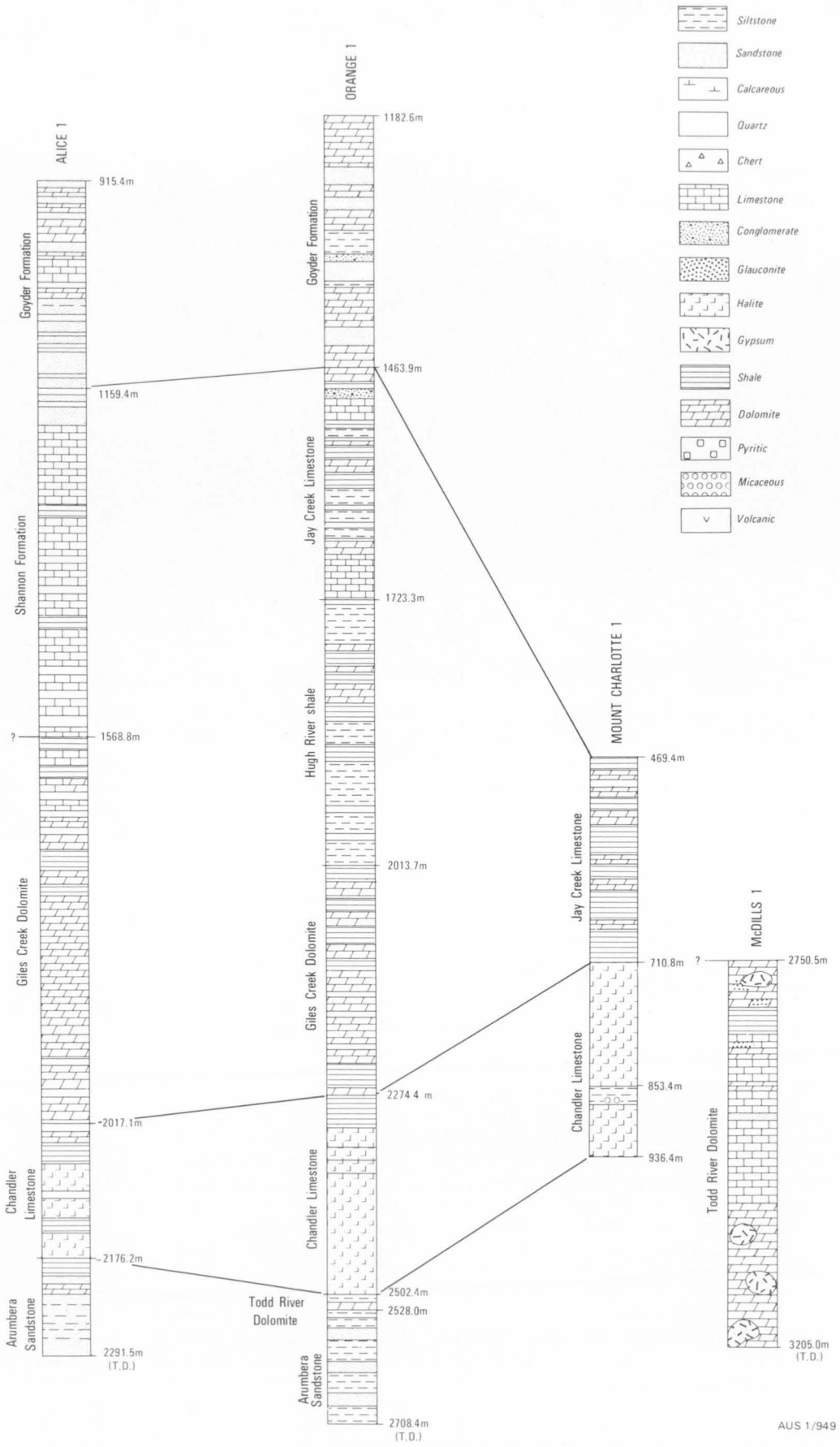

Fig. 13. Graphic sections of wells containing evaporites in the Chandler Limestone and Todd River Dolomite, Amadeus Basin.

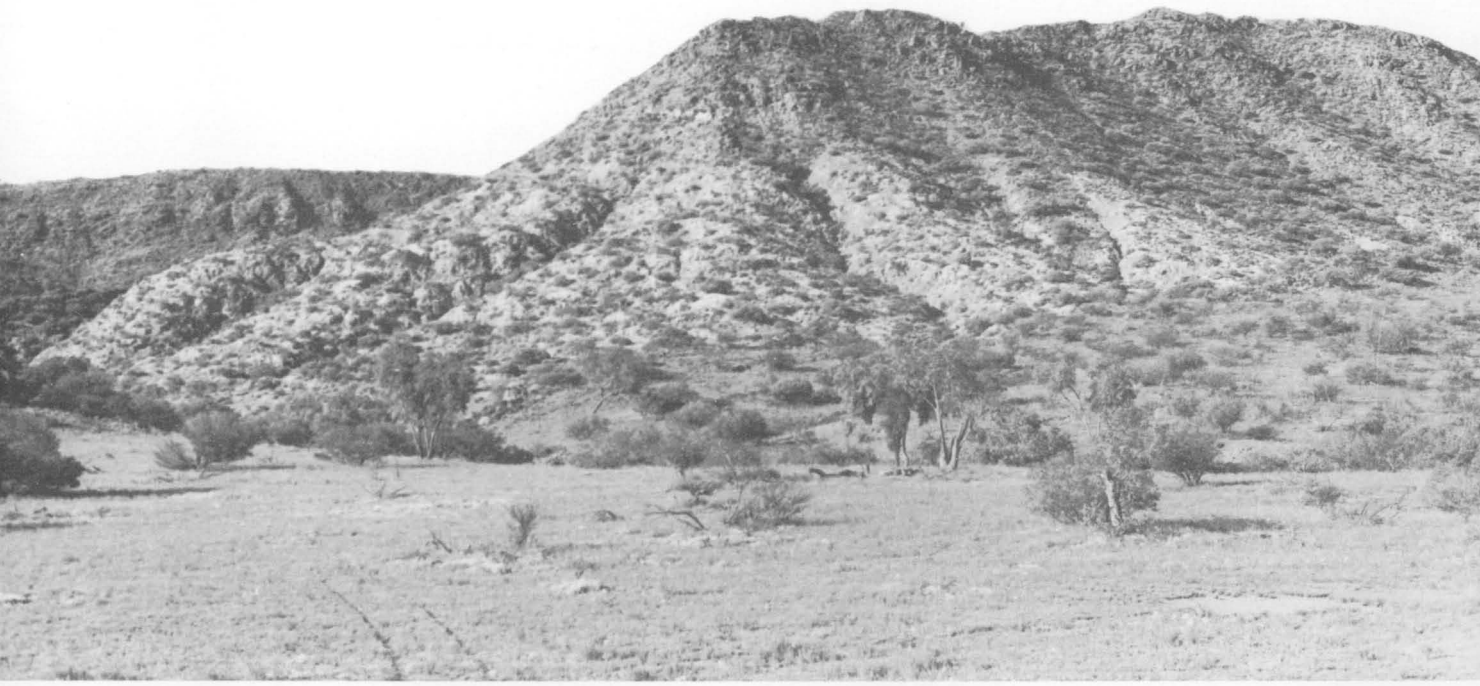

Fig. 14. Central part of the Ringwood Dome, from the southwest. The lower deeply dissected part of the hill consists of white earthy weathered gypsum encrusting the underlying bedded gypsum; the upper part of the hill consists of limestone. (GA/1405)

Basin. The Bitter Springs Formation is thought to underlie the whole basin, whereas the Chandler Limestone is restricted to the northeast and passes west into an arenitic facies without evaporites. No major facies changes have so far been described in the Bitter Springs Formation.

There are also indications of evaporitic environments in many of the younger formations in the Amadeus Basin. Halite pseudomorphs, probably slightly older than the Chandler Limestone, have been recorded in the northeast, from the youngest beds of the Arumbera Sandstone. Evidence of evaporitic conditions was also found in sandstone beds of the lower part of the Cambrian Goyder Formation in the western part of the Walker Creek Anticline, at many localities in siltstone of the Ordovician Stokes Siltstone and the Upper Ordovician Carmichael Sandstone of the Larapinta Group, and in the Upper Devonian Parke Siltstone of the Pertnjara Group. The ?Devonian Horseshoe Bend Shale of the Finke Group in the southeast contains halite pseudomorphs and is commonly gypsiferous.

BMR ALICE SPRINGS No. 3

(from Stewart, 1974)

Drill site geology

BMR Alice Springs No. 3 drill site (23°53′S, 134°53′E; TD 259.65 m) is about 10 km southwest of Ringwood homestead and 38.4 km east of Todd River homestead.

The Ringwood Dome is situated in the Eastern MacDonnell Ranges, a belt of long and narrow valleys and ridges curved in the folded and faulted sedimentary formations of the Amadeus Basin sequence. It consists of a core of gypsum, anhydrite, and several varieties of dolomite, surrounded by an envelope of outward-dipping carbonate and clastic rocks. Both the evaporite body and surrounding rocks are part of the Gillen Member of the Bitter Springs Formation. The gypsiferous mass forming the core of the Ringwood Dome has a hook-shaped outcrop in plan, elongated east-west, and measuring 1.6 km by 0.8 km. It forms a prominent steep-sided hill, whose lower half is covered with white, earthy, weathered gypsum with a hummocky surface (Fig. 14). The upper half of the hill is composed of limestone. Numerous steep-sided gullies radiate from the crest of the hill and reveal grey bedded gypsum beneath the crust of earthy gypsum. Small blocky fragments of grey, fine-grained dolomite can be found loose on the sides of the hill, but are not abundant.

Structurally, the Ringwood Dome is not a perfect dome, but an east-trending anticline that plunges gently westwards at its western end and has an isoclinal eastern end, where both limbs dip steeply south. No plunge is discernible here, owing to lack of outcrop, but the exposed gypsum tapers to a thin 'tail' only a few metres wide, suggesting that what plunge exists is probably eastwards. The gypsum almost certainly continues west along the anticline for some distance beyond its present area of exposure. The anticline is bounded on the north by a mass of Lower Cambrian carbonate rocks of the Pertaoorrta Group; these are in fault contact with the Bitter Springs sediments, and dip southwards beneath them. The continuity of beds of the Bitter Springs Formation on top of the anticline with those on its northern flank indicates that no diapiric

movement by the central salt body took place at the present level of exposure. This is probably to be expected in view of the closeness in specific gravities of the exposed rock-types of the area.

Description of rock-types

Dolomite-gypsum breccia

Dolomite-gypsum breccia is the most abundant rock-type in the Ringwood core. It comprises clasts and broken and contorted laminae of gypsiferous dolomite rock forming up to 50 percent of the total in a matrix of white crystalline gypsum. The clasts are composed of pale grey laminated dolomite, diffusely speckled and mottled with white gypsum. They range in size up to 10 cm across, are angular to sub-rounded, equant to tabular, and are commonly arranged in a subparallel orientation, so that the rock has both a partly bedded and a partly brecciated appearance. A few clasts are composed of dark grey soft friable dololutite.

In thin section, the breccia appears as a mixture of medium to coarse-grained granular gypsum and abundant rather ragged fragments of fine-grained gypsiferous dolomite rock, plus many partly dismembered laminae of dolomite, and isolated rhombs of recrystallised dolomite (Fig. 15). The dolomite laminae commonly extend without interruption through several gypsum crystals. In many places, the gypsum forms granular masses of fine-grained subhedral crystals, and in places these grade into laminae and small cross-cuttings veins and veinlets of acicular gypsum. Inclusions of other minerals are common in the gypsum, and, apart from the dolomite already mentioned, include anhydrite (Fig. 16), quartz, tourmaline, celestite, and pyrite; the anhydrite inclusions increase in size and abundance down the core, and many display a common optical orientation. Below 141.7 m anhydrite is sufficiently abundant in the rock to form laminae of pure crystalline anhydrite; in every case, these lamniae are separated from the rest of the dolomite-gypsum breccia by layers (or selvedges) of clear prismatic gypsum. Rare laminae of felted anhydrite plus granular dolomite are present below about 200 m.

The clasts of gypsiferous dolomite are composed of masses of very small anhedral grains of dolomite set in a subordinate patchy matrix of poikilitic gypsum. Small euhedra of quartz are the most abundant accessory, but there are also aggregates of anhedral angular silt-sized quartz grains, which grade into distinct silty laminae of dolomite, quartz, and gypsum. Other accessory minerals include irregular patches of chalcedonic silica, euhedral pyrite, tourmaline, and rutile, anhedral sphene, ragged porphyroblasts of chlorite (Fig. 17), and organic matter staining. Between 85.34 m and 86.87 m, the silty laminae contain abundant grains of microcline, plus increased amounts of tourmaline, rutile, and chlorite.

Chemical analyses of three bulk samples of the breccia are listed in Table 5.

Bituminous dolomite

Bituminous dolomite is the characteristic rock-type of the lower part of the core, and is dark grey, grey-brown, or black, very fine-grained, tough, commonly colour-laminated, and almost everywhere brecciated. The clasts are sharp-edged and blocky, and generally range up to 2 cm across; a few are up to 5 cm across. They are set in a cement of white, grey-blue, or blue

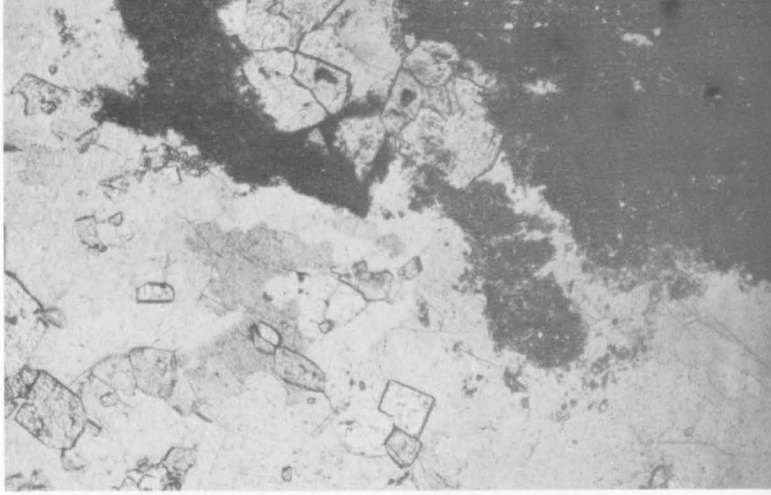

Fig. 15. Dolomite-gypsum breccia, showing ragged clasts of fine-grained gypsiferous dolomite and euhedral rhombs of recrystallised dolomite in coarse-grained granular gypsum; from 35.61 m. Plane polarised light, x 37. (M/1289)

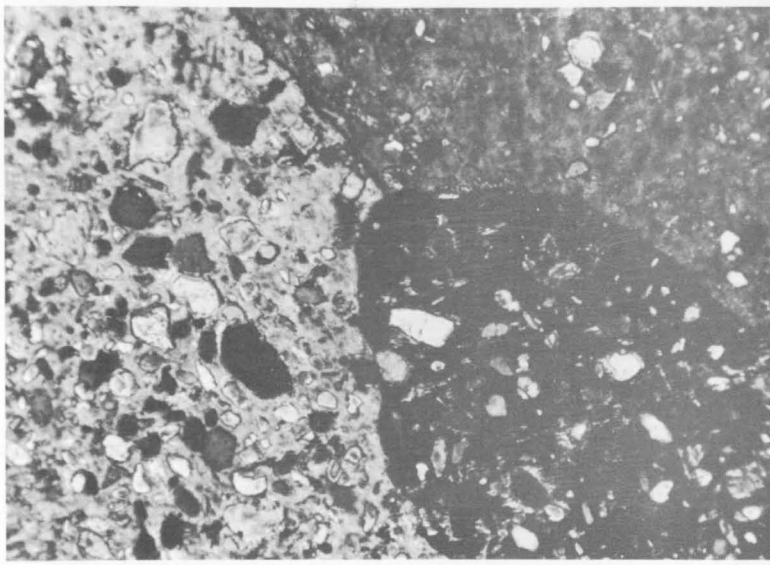

Fig. 16. Gypsum poikiliths (one in extinction position) containing inclusions of anhydrite; from 225.87 m. Crossed nicols, x 75. (M/1453)

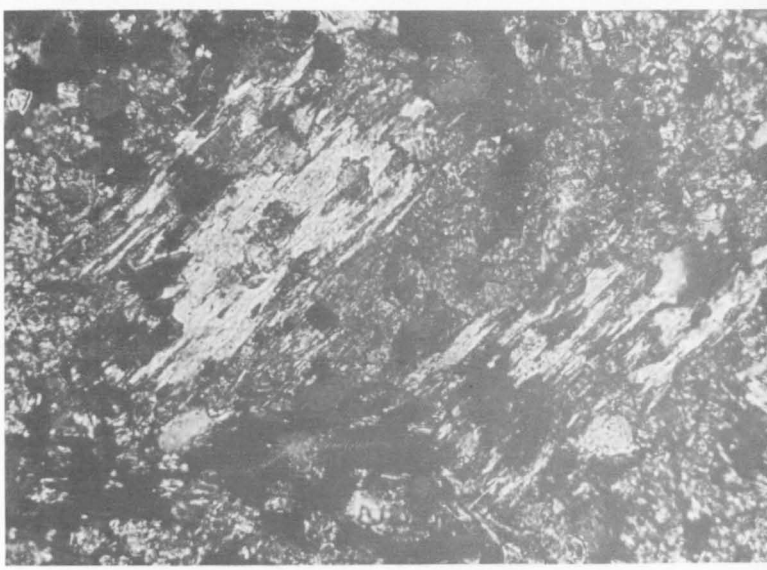

Fig. 17. Ragged porphyroblasts of chlorite in gypsiferous dolomite rock; from 86.28 m. Crossed nicols, x 300. (M/1453)

TABLE 5. CHEMICAL ANALYSES OF RINGWOOD EVAPORITES

*Sample No.**	*306*	*307*	*308*	*309*	*310*	*311*	*312*	*313*	*314*	*315*	*316*	*317*
Lithology	Bulk Samples			Dolomite-gypsum breccia				Dololutite		Bituminous dolomite		
Depth (m)	0–260	0–133	133–260	45.72 –47.24	120.39 –121.92	225.59 –227.11	43.80	155.11	250.20	171.35 & 171.71	207.03 & 207.16	244.33 & 245.65
Sample type	Cuttings	Cuttings	Cuttings	Cuttings	Cuttings	Cuttings	Core	Core	Core	Core	Core	Core
SiO_2	11.6	9.75	13.3	6.20	7.20	9.00	33.2	32.3	30.4	34.3	5.35	43.4
Al_2O_3	1.53	1.26	1.75	0.81	1.06	1.50	5.25	5.70	6.15	0.11	0.67	0.10
Fe_2O_3**	0.51	0.38	0.63	0.46	0.24	0.29	1.35	1.25	1.50	0.30	0.58	0.33
CaO	26.9	28.1	26.3	33.0	31.1	28.0	14.5	14.1	15.1	20.6	28.0	17.5
MgO	7.40	5.25	9.25	3.00	4.60	4.40	17.4	17.6	16.0	10.2	19.3	10.2
Na_2O	0.10	0.03	0.16	0.03	0.05	0.09	0.07	0.34	0.47	0.04	0.07	0.05
K_2O	0.17	0.19	0.14	0.16	0.12	0.09	0.38	0.34	0.36	0.02	0.06	0.02
MnO	0.01	0.01	0.01	0.01	0.01	0.01	0.01	0.01	0.01	0.01	0.02	0.01
H_2O^+	2.30	3.30	2.75	5.80	1.30	1.65	3.55	3.50	4.35	1.89	1.15	0.40
H_2O^-	9.75	11.0	6.45	11.2	6.95	8.9	0.49	0.40	0.75	1.31	0.60	1.01
P_2O_5	0.03	0.02	0.03	0.01	0.02	0.03	0.06	0.07	0.07	0.01	0.03	0.01
TiO_2	0.10	0.08	0.14	0.04	0.05	0.07	0.27	0.30	0.34	0.01	0.09	0.01
SrO	0.05	0.06	0.04	0.05	0.08	0.06	0.01	0.06	0.02	0.02	0.01	0.01
Cl	0.10	0.03	0.17	0.02	0.05	0.08	0.04	0.30	0.32	0.04	0.06	0.04
F	0.09	0.05	0.10	0.07	0.03	0.06	0.28	0.33	0.35	0.02	0.04	0.02
S***	0.1	0.1	0.6	1.0	0.1	0.1	1.2	1.5	1.5	0.1	0.1	0.1
SO_3	27.9	31.9	23.4	33.5	43.0	38.2	0.61	0.40	6.60	8.55	2.75	4.65
CO_2	11.8	8.7	14.8	5.3	4.70	7.00	21.4	21.3	15.8	22.6	40.4	22.3
Total	100.44	100.21	100.02	100.66	100.66	99.53	100.07	99.80	100.09	100.11	99.28	100.16
FeO****	0.46	0.34	0.56	0.42	0.22	0.26	1.22	1.12	1.34	0.26	0.52	0.30

Analyst: Australian Mineral Development Laboratories, Report AN3249/73, 16 February 1973
* Preceded by 71110 ** And total iron
*** Sulphide plus elemental sulphur
**** Calculated from Fe_2O_3

anhydrite which in many places is partly replaced by gypsum along the margins of the clasts. In some parts of the core, such as at 178 m, the anhydrite cement forms a single large skeletal crystal up to 10 cm across, poikilitically enclosing the dolomite fragments.

In thin section, the bituminous dolomite is seen to be composed of a mass of very small irregular dolomite grains tightly cemented together (Fig. 18); thin, linear, intersecting zones of coarser euhedral dolomite are present in places, and probably represent healed cracks in the rock. The colour lamination is found to be an effect of grainsize, the dark laminae being finer-grained than the pale laminae. Minor constituents in the dolomite clasts include isolated euhedra of quartz, small masses of chalcedonic silica, disseminated pyrite, dark brown organic matter, and tiny rounded grains of detrital material.

Fig. 18. Brecciated bituminous dolomite, showing angular dolomite clasts cemented by coarse gypsum containing remnants of clear anhydrite; from 170.66 m. Crossed nicols, x 68.

The cement between the dolomite fragments consists of medium to coarse-grained colourless anhydrite, generally accompanied by gypsum; in a few places, the cement is composed solely of anhydrite or gypsum. The anhydrite forms elongate prismatic crystals, which generally have a random orientation, but in some places are parallel or subparallel to the margins of the dolomite clasts. The gypsum (or where gypsum is absent, the anhydrite) forms large, skeletal, single crystals which enclose several dolomite clasts. Included anhydrite grains are abundant in the gypsum, and generally have a common optical orientation, indicating that they are remnants of larger anhydrite crystals which have been partly replaced by gypsum. Dolomite along the margins of the clasts next to gypsum is in places recrystallised to much coarser grains. In a few places, the cement between the dolomite fragments consists of subhedral to euhedral dolomite which is much coarser-grained than that of the fragments. In these areas pyrite is also coarser-grained than normal, and organic matter is concentrated at the junction of fine and coarse-grained dolomite (Fig. 19).

Impure varieties of the bituminous dolomite contain masses and laminae of pale brown very fine-grained chalcedonic silica, forming up to 50 percent of the rock in a few places. Under high power, blebs of bituminous organic matter are visible in the silica.

Table 5 lists chemical analyses of three composite samples of bituminous dolomite.

The single bed of bituminous dolomite in the upper part of the core, between 67.31 m and 68.25 m, is massive and non-brecciated, and has a finely spotted

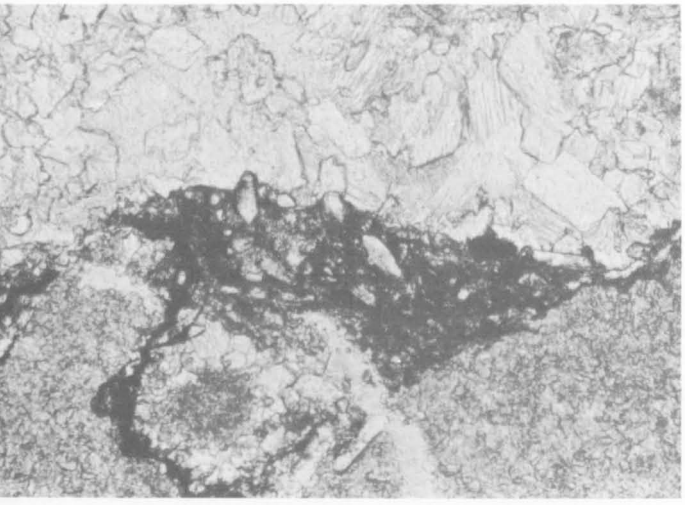

Fig. 19. Recrystallised bituminous dolomite, showing coarsened subhedral to euhedral dolomite and concentrations of opaque organic matter around clasts of fine-grained unrecrystallised dolomite from 161.21 m. Plane polarised light, x 125. (M/1449)

appearance. Each spot consists of a single anhedral gypsum crystal, which is generally accompanied by a single euhedral quartz crystal crowded with minute dusty inclusions; a dark ring of organic matter surrounds each gypsum spot.

Dololutite

The dololutite in the Ringwood core is pale to dark grey, soft and friable, very fine-grained, massive to poorly bedded rock which is easily crumbled by the fingers; it was originally identified as 'claystone' at the drill site (Stewart, 1974). It forms discrete beds, which are up to 1.3 m thick and generally cut by an anastomosing network of gypsum veins; rough, uneven masses of concretionary gypsum are also common in some beds. In thin section, the rock appears as a very fine-grained, faintly laminated, uncemented mass of tiny round grains of dolomite, many of which do not touch each other; they range in diameter from 0.0016 mm to 0.008 mm, and thus include both silt and clay-sized fractions. The rock is cut by a network of linear zones of coarse-grained dolomite, which, as in the bituminous dolomite, represent healed cracks, because streaky aggregates of pyrite are slightly offset where intersected by the coarser zones. Accessory minerals include abundant pyrite as isolated euhedra and elongate streaky aggregates, irregular streaks and regular veins of chalcedonic silica, rare needles of tourmaline, detrital grains of sphene, and dark laminar stains of organic matter, which is commonly concentrated in layers on each side of the veins of chalcedonic silica. Anhydrite is totally lacking in thin sections of dololutite, but some appears as a normative mineral in one of three analysed samples of the rock. The veins and masses of gypsum rock consist of coarse prismatic to equant anhedral gypsum accompanied by much coarse recrystallised dolomite at their margins. X-ray diffraction analysis of eight samples of dololutite indicated the presence of chlorite and muscovite in the rock, but these minerals were not observed in thin section; however, chlorite is abundant as a normative mineral. Table 5 lists chemical analyses of three composite samples of dololutite.

Anhydrite

Anhydrite rock is present only in the lower part of the core, below 141.73 m, and occurs as three varieties. The first is a speckled bluish-grey crystalline rock, medium-grained and lineated, forming discrete masses up to 0.69 m thick in the core; in places, the anhydrite is interlaminated with bituminous dolomite, and with disruption of the bedding this grades into the bituminous dolomite breccia with subordinate anhydrite matrix (described above). Crystalline anhydrite also forms contorted laminae in the dolomite-gypsum breccia in the lower part of the core. In thin section, the crystalline anhydrite is seen to consist of coarse colourless equant to prismatic anhedral crystals of anhydrite, which show the cleavage traces and polysynthetic twinning characteristic of the mineral (Fig. 20). Accessory minerals in the rock include numerous small euhedra of quartz (some of them broken), rare pyrite, and dark brown uneven laminae of organic matter; the anhydrite associated with the organic matter is very fine-grained and very anhedral.

Fig. 20. Medium to coarse-grained anhydrite, showing lamellar twinning and cleavage traces. Quartz euhedra also visible; from 169.62 m. Crossed nicols, x 41. (M/1289)

The second variety of anhydrite occurs only between 186.39 m and 186.54 m, where it forms a dark grey to black fine-grained rock which contains anhedral crystals of black dolomite up to 12 mm across; the rock has a prominent parting across the core. In thin section, the rock consists of disturbed laminae of fine-grained granular anhydrite with abundant organic matter, alternating with laminae of coarse-grained anhydrite, with a little euhedral dolomite, but without organic matter. The dolomite megacrysts comprise single crystals of dolomite crowded with anhedral inclusions of anhydrite and organic matter arranged in rows parallel to the lamination outside the megacryst. Surrounding the dolomite megacryst is a nearly complete shell of clear, coarse, poikilitic gypsum with included grains of anhydrite. Accessory minerals in the rock include euhedra of quartz, dark brown needles of rutile, colourless needles of tourmaline, and tiny euhedra of pyrite.

The third variety of anhydrite is a clear pale blue mineral which fills cross-cutting veins in the bituminous dolomite in the lower part of the core; the most prominent veins are situated between 186.54 m and

187.45 m and between 231.65 m and 232.71 m. As elsewhere, a layer of coarse gypsum separates the anhydrite from the dolomite wall-rock. The anhydrite is pure and coarse-grained and forms anhedral elongate prisms with a decussate arrangement.

Acicular gypsum

Acicular gypsum (or satin-spar) most commonly forms cross-cutting, parallel-sided veins up to 10 cm wide, but in places it also forms thin beds in the dolomite-gypsum breccia. It is more abundant in the upper part of the core, where 23 cross-cutting veins were noted, than in the lower part (12 veins). The needles of gypsum are oriented perpendicularly to the walls of veins, or nearly so. The margins of some veins are marked by thin laminar concentrations of other minerals, including friable uncemented dolomite (the most common), disseminated pyrite, chalcedonic silica, and organic matter. In thin section, the gypsum appears as long and narrow prismatic to acicular crystals, some slightly tapering. Inside the vein, parallel to its margins, but not generally at or even near its centre, is a narrow zone of randomly arranged stubby crystals of gypsum, and this presumably marks the junction where the encrusting needles met as they grew from the walls of the vein. Compositionally, the cross-cutting veins are almost pure gypsum, but the laminae and thin beds commonly contain small amounts of recrystallised dolomite and celestite, and small xenoliths of fine-grained dolomite rock.

Description of core

0-32.61 m

Cuttings from surface to 25.91 m consist of a mixture of colourless, broken prisms of gypsum, and fragments of grey to white, massive, fine-grained gypsum, plus a few small piecs of grey, calcareous friable dololutite. From 25.91 m to 32.61 m only fragments of massive gypsum and friable dololutite are present.

32.61-76.20 m

The core from 32.61 m to 76.20 m is composed of medium to coarse-grained gypsum, which almost everywhere carries films and laminae of calcareous friable dololutite. In the upper and lower thirds of this interval there are discrete fragments of gypsiferous dolomite in the gypsum, so that the rock is a breccia, and a 60-cm interval from 41.15 m to 41.76 m consists solely of brecciated dolomite with no gypsum. The middle third of this interval has a fair amount of massive gypsum which is almost free of dolomite. Throughout the whole interval are nineteen beds of calcareous friable dololutite with associated tabular masses of gypsum. Some friable dololutite beds also carry angular fragments of coarse-grained gypsum, and three of the friable dololutites are accompanied by abundant disseminated pyrite. Euhedral interpenetrating pyritohedral twins of pyrite up to 10 mm across occur in the dolomite at 33.53 m. The core is cut across at a number of places by veins of acicular gypsum.

76.20-132.89 m

From 76.20–132.89 m the core consists almost entirely of a mixture of colourless, medium to coarse-grained gypsum and grey laminated anhydrite, in approximately equal amounts. The dolomite forms large tabular fragments surrounded by the gypsum, and though disturbed to some extent, they still possess a subparallel orientation so that the rock has both a partly bedded and a partly brecciated appearance. Six beds of calcareous friable dololutite are present in this interval, all but one of them accompanied by uneven tabular masses of acicular gypsum. Pyrite occurs only in the uppermost of these six beds, and forms euhedral interpenetrating pyritohedral twins. About a dozen thick veins of coarse-grained, acicular gypsum cut the core; some of them, particularly those near 105.16 m, have layers of grey friable dololutite up to 6 mm thick along each contact with the enclosing host-rock.

132.89-259.69 m

From 132.89–259.69 m the core consists of intervals 6–9 m long composed of gypsum-dolomite breccia (as above) separated by somewhat shorter intervals of bituminous dolomite. Disseminated pyrite is an abundant accessory. Most of the bituminous dolomite is brecciated, and the fragments are enclosed in a subordinate matrix composed of clear, pale blue anhydrite, or less commonly of white to grey gypsum.

At several places in the core below 155.75 m, crystalline anhydrite is present, medium-grained, speckled bluish-grey, and with accessory pyrite. Locally, the core is composed wholly of this rock type, e.g. at 169.77 m, but usually it forms thin, contorted beds, lenses, or tongues up to 50 mm thick accompanied by fine-grained, gypsiferous dolomite and white, coarse-grained, massive to acicular gypsum, the three rock-types forming a contorted and interlayered mixture. A 6-mm layer of oriented prismatic gypsum usually separates the crystalline anhydrite from the two other rock types. At 214.27 m pyrite is concentrated along the margins of crystalline anhydrite layers. This mixed and contorted rock forms about eight sporadic but distinctive occurrences in the core.

Twenty-two beds of friable dololutite with fragments of coarse-grained gypsum are present below 132.89 m; only one contains pyrite, at 235.31 m. Cross-cutting veins of gypsum are present in the core, but are far less common below 132.89 m than above.

The interval from 252.98 to 259.69 m is represented only by cuttings. When one set of these cuttings was washed, a dark brown to black slime collected on the surface of the washing water. Presumably, this was organic matter. When the slime was skimmed off, small but clearly visible streaks of oil remained floating on the water.

Geochemistry

The full analyses of twelve samples are given in Table 5. One of the objectives of the Ringwood drilling was to look for potash, and, therefore, a set of cuttings was analysed for potassium by atomic absorption spectrophotometry. The cuttings were also analysed for fluorine, strontium, and manganese, as these three elements, particularly, show specific patterns of behaviour during the deposition of marine evaporites; fluorine and strontium are concentrated in the earlier products of deposition, particularly in the sulphate zone (Stewart, 1963), and strontium and manganese show significant differences in concentration in gypsum and anhydrite. The average contents of potassium, fluorine, strontium, and manganese are set out in Table 6.

Potassium

Potassium does not occur in economic quantities in the Ringwood cuttings, and the maximum value found was 0.603 percent between 85.34 m and 86.87 m. The content of potassium shows a slight and irregular increase up the hole, interrupted by a sudden increase

TABLE 6. AVERAGE CONTENTS (IN PERCENT) OF MINOR ELEMENTS IN RINGWOOD EVAPORITES

Element	*Average below 133 m*	*Average above 133 m*	*Average over entire hole*
K	0.102	0.138	0.123
F	0.10	0.05	0.07
Sr	0.04	0.06	0.05
Mn	0.0066	0.0064	0.0065

and decrease on each side of the maximum value. The maximum value appears anomalous when compared with the potassium analyses over the rest of the hole, and so 13 thin sections were cut from samples taken every few centimetres along the section of core between 85.34 m and 86.87 m. Microcline occurs in abundance in several of the thin sections, and its absence from elsewhere in the core indicates that it is the repository of the extra potassium.

Peaks in potassium content occur opposite dolomite or dololutite beds in the core (or opposite intervals of no recovery, which presumably correspond to dololutite beds), and the low points are opposite gypsum.

Fluorine

The distribution of fluorine in the Ringwood rocks is somewhat similar to that of potassium, especially in the lower part of the hole. Like potassium, fluorine is concentrated in dolomite as opposed to gypsum, particularly the dark bituminous dolomite in the lower part of the hole, and when deposition of this rock ceased, the concentration of fluorine in the rocks fell by half (Table 6). The maximum concentration of fluorine is 0.37 percent from 135.64 m to 137.16 m, i.e. at the top of the lower part of the hole. No specific fluorine-bearing mineral was identified in thin sections of the core.

Fluorine and potassium closely match one another in the lower part of the hole, but the match is poor in the upper part of the hole, particularly in the case of maximum potassium value, which has no corresponding fluorine peak at all.

Strontium

Unlike the other three elements determined, strontium is concentrated in the gypsum beds. The maximum concentration recorded is 0.135 percent at 25.91 m to 28.96 m. There is a perceptible change in strontium content at 132.89 m, and this is reflected in the averages for the lower and upper parts of the hole (Table 6).

Manganese

The concentration of manganese is very low in the Ringwood evaporites, and is only about one-tenth or less of those of the other elements determined. The maximum concentration recorded is 0.019 percent at 42.67 m to 44.20 m. The manganese is concentrated in dolomite, where it presumably substitutes for magnesium, and shows a reasonable match with potassium and fluorine in the lower part of the hole, but less so in the upper part.

Discussion

The abundances and changes in concentration with depth of the four minor elements determined in the Ringwood cuttings are typical of marine evaporites; potassium and strontium show slight increases in concentration upwards (though in different rock types), whereas fluorine and, to a lesser extent, manganese decrease in concentration upwards. The increase in potassium content reflects the increase in the concentration of potassium in the evaporating marine brine, whereas strontium follows calcium and reflects the greater content of this element in the upper part of the deposit.

The strontium and manganese analyses also provide evidence on the origin of the gypsum and anhydrite in the Ringwood evaporites, as these two elements show significant differences in concentration in the two sulphates. Kropachev (1960) found that manganese is low in anhydrite (0.012 percent Mn) and higher in gypsum (0.037 percent Mn), and therefore the low concentration (0.0065 percent Mn) in the Ringwood rocks is consistent with the deposition of primary anhydrite. With regard to strontium, analyses published in Deer & others (1962) show up to 0.60 percent Sr in anhydrite, but only 0.0008 percent Sr in gypsum, and Noll (1934) found up to 0.58 percent Sr in anhydrite rock, but only 0.11 percent Sr in gypsum rock. (However, Kropachev found the opposite situation in sulphates from the Perm Basin, viz. 0.06 percent Sr in anhydrite and 0.14 percent Sr in gypsum) (Stewart, 1963). Grahmann (1920) found that anhydrite can take up to 42 percent of $SrSO_4$ in solid solution at room temperature.

The proportion of gypsum increases up the hole, and if it is primary, then the analyses in Deer & others (1962) and Noll (1934) would lead one to expect that the concentration of strontium would correspondingly decrease, and that of manganese increase, upwards. However, the opposite is the case, indicating that the gypsum is not primary; and this agrees with the petrographic evidence. But, as the strontium is in fact concentrated in the gypsum beds, it was presumably deposited during precipitation of the calcium sulphate as anhydrite. The occurrence of celestite in the gypsum beds confirms the secondary origin of the gypsum, the celestite having formed from the strontium released from solid solution during hydration of anhydrite to gypsum.

The possibility remains that the anhydrite is secondary and formed by dehydration of primary evaporative gypsum during burial; but again the comparatively high content of strontium in the sulphate indicates that this is not the case.

Base metals

Two samples of the dark bituminous dolomite from the lower part of the core were analysed for base metals by atomic absorption spectrophotometry. No metal enrichment is apparent.

Boron

Fourteen core samples were analysed for boron by semi-quantitative methods (Table 7); the samples were chosen from the two intervals, both of friable dololutite, that had given the highest values for boron, viz.

TABLE 7. RESULTS OF SEMI-QUANTITATIVE ANALYSES FOR BORON IN RINGWOOD EVAPORITES

*Sample No.**	*Depth (m)*	*%B*
19	145.77–145.92	0.005
20	145.92–146.08	0.01
21	146.08–146.23	0.016
22	146.23–146.38	0.016
23	146.38–146.53	0.016
24	146.53–146.66	0.016
25	146.66–146.79	0.016
26	146.79–146.91	0.016
27	249.78–249.94	0.01
28	249.04–250.09	0.016
29	250.09–250.24	0.02
30	250.24–250.39	0.02
31	250.39–250.55	0.016
32	250.55–250.70	0.016

* All sample numbers are prefixed by 711100.

Analysts: C. W. Claxton & J. Weekes, BMR Laboratory Report No. 25.

0.21 percent at 146.38 m and 0.24 percent at 249.94m, during earlier analyses of the core by the Australian Mineral Development Laboratories, Adelaide.

Organic matter

Six core samples from the dolomite-gypsum breccia (three samples), bituminous dolomite (2), and dololutite (1) were analysed for organic carbon, extractable organic matter, and kerogen. Total organic carbon ranges from 0.04 to 0.84 percent; the other results are set out in McKirdy (1977).

Comparison of well logs with core lithology

Spontaneous potential

The spontaneous potential curve is fairly smooth throughout its length except for a sudden deflection of 100 millivolts between 128.02 m and 131.06 m. This is presumably caused by the abundant pyrite in the bituminous dolomite which forms so much of the core below 132.89 m. The 100 millivolt change between 25.60 m and 36.58 m is presumably caused by the steel casing, which extends from 0 to 25.91 m in the well.

Resistivity

The resistivity curve shows large and rapid variations throughout its length, and reflects quite faithfully the various lithologies in the core. In the upper part of the core, above 112.78 m, the gypsum-anhydrite rock has a resistivity between 4500 and 6500 ohms M^2/M, in sharp contrast to the friable dololutite beds, with have resistivities of only 100 to 200 ohms M^2/M. Between 112.78 m and 131.06 m the curve shows a steady decrease from 6000 to 3000 ohms M^2/M, which probably reflects the proximity of the mass of pyritic rocks in the lower part of the core. Below 131.06 m, the resistivities of the gypsum-anhydrite rock, the crystalline anhydrite and the non-pyrite-bearing bituminous dolomite average between 2000 and 3000 ohms M^2/M, whereas the pyrite-bearing bituminous dolomite and the friable dololutite have resistivities between 20 and 200 ohms M^2/M. As in the spontaneous potential log, the rise in the curve from 25.60 m to 36.58 m is presumably an effect of the steel casing, though in this case there are low values opposite friable dololutite beds super-imposed on the general rising trend.

Acoustic velocity

The travel time curve fluctuates regularly throughout most of its length, and there is good correlation with the lithology; low values (peaks to the right, corresponding to high velocity) occur opposite gypsum, anhydrite, and bituminous dolomite, and high values (low velocity) are given by the friable dololutite beds. From 76.2 m to 131.06 m there are only two friable dololutite beds of appreciable thickness, and accordingly the curve shows a constant low value interrupted by sharp peaks opposite these friable dololutites. Unlike the electrical curves, the travel time curve shows no fundamental change at the entry of the bituminous dolomite.

Gamma ray

The gamma ray curve also reflects faithfully the friable dololutite beds, with a high peak opposite each one, and correlates well with the travel time curve. The curve shows no fundamental change near 132.89 m, indicating that the clay content of the bituminous dolomite is close to that of the overlying gypsum and anhydrite.

Discussion and conclusions

Origin of gypsum and anhydrite

The petrographic textures visible in the Ringwood evaporites indicate that the gypsum originated by hydration of anhydrite; the evidence includes the selvedges of gypsum at the margins of anhydrite masses in the lower part of the core, and the numerous inclusions of anhydrite in the gypsum of the gypsiferous dolomite, many of them with a common optical orientation. Moreover, the gypsum is accompanied by celestite, which is consistent with the known ability of anhydrite to take up strontium in solid solution (up to 42 percent according to Grahmann, 1920), in contrast to gypsum, which can take up very little strontium (Noll, 1934; analyses in Deer & others, 1962); when the anhydrite hydrated to gypsum, the strontium was

unable to enter the gypsum lattices, and so precipitated as a separate mineral. If this is so, the high content of strontium in the parent anhydrite implies that it was primary anhydrite, not secondary anhydrite that had formed by dehydration of pre-existing gypsum.

Much of the gypsum in the Ringwood rocks occurs in gypsiferous dolomite, which was presumably anhydritic dolomite before it was hydrated, and the rare laminae of felted anhydrite plus granular dolomite below 200 m may be the remnants of the original evaporite rock.

The hydration of anhydrite to gypsum involves a volume increase by about half (Goldman, 1952; Pettijohn, 1957), and the consequent swelling of the whole rock mass probably caused the brecciation of the dolomite, the gaps between the clasts furnishing some of the extra space required by the new gypsum. The laminae and cross-cutting veins of acicular gypsum that are without marginal concentrations of dolomite, pyrite, silica, and organic matter are probably filled joints and channels through which water of hydration flowed into the anhydrite-bearing rocks, and out through which flowed solutions carrying excess calcium sulphate that was unable to precipitate in the body of the rock when the available space had been filled. In contrast, the laminae and veins of gypsum that do have marginal concentrations of the minerals presumably formed by recrystallisation of the rock along tight joint surfaces, allowing outward migration of the impurities until they came up against the adjoining unrecrystallised rock.

The almost complete absence of anhydrite from the friable dololutite is notable, and it is possible that the marked permeability of this rock facilitated the entry of water, and thus enabled hydration of anhydrite to go to completion. The permeability probably allowed the gypsum to aggregate into the anastomosing veins and concretions, rather than remaining dispersed through the rock.

Origin of dolomite, chalcedonic silica, and quartz

The dolomite rocks in the Ringwood evaporites consist of a very fine-grained aggregate of tiny anhedral dolomite grains generally cemented together, except in the beds of friable dololutite. The dolomite shows no evidence of a late diagenetic origin, such as replacement textures or relict biogenic structures, and, except where it forms a recrystallised cement between breccia clasts or next to gypsum veins, there are no lateral variations in grainsize or clusters of euhedral or subhedral crystals in the allotriomorphic groundmass. However, separate laminae are commonly of different grainsize, and there are rare instances of graded bedding. Thus it is very probable that the dolomite is a primary or early diagenetic mineral.

Friedman (1972) has shown that the bituminous calcilutite at the bottom of the Red Sea has probably formed by anaerobic bacterial oxidation of organic matter to carbonate, which then precipitates as calcium carbonate, concomitant with reduction of sulphate to sulphide, which precipitates as iron sulphide. The calcilutite is interbedded with layers of aragonite, which, by analogy with observed 'whitenings' in the Dead Sea, does appear to have formed by inorganic precipitation of carbonate ions from solution. The dolomite in the Ringwood core could be an early diagenetic mineral, and hence it may have started as a basinal calcilutite of the Red Sea type which then underwent early dolomitisation. However, an origin of limestone by bacterial activity means that all the carbon in the limestone is derived from organic matter, not from carbonate ions dissolved in seawater. Would there have been enough organic matter in Proterozoic time to form a dolomite in this way? Also, the lack of celestite in association with the Ringwood dolomite militates against the possibility that aragonite, which holds considerably more strontium in solid solution than does calcite (Deer & others, 1962), was the inorganic carbonate in the basinal deposit before dolomitisation. Moreover, Friedman's suggestion ignores the experimental fact that inorganic carbonate forms the first precipitate in the experimental evaporation of seawater. Thus it appears that the evidence in the Ringwood rocks indicates that the dolomite originated by precipitation of inorganic carbonate, either as calcite that was dolomitised shortly afterwards, or as primary dolomite.

A similar evaporitic origin is also possible for the masses of chalcedonic silica in the dolomite rocks; their laminar or shred-like form and nearly isotropic character suggest that the silica precipitated as an opaline deposit simultaneously with the deposition of the dolomite, as is happening at the present time in the lakes associated with the Coorong Lagoon in South Australia (Peterson & von der Borch, 1965). With burial and the passage of time, the opal became more or less recrystallised to chalcedonic quartz. The small euhedra of quartz present in all the evaporite rocks are probably recrystallised detrital grains.

Origin of chlorite

The occurrence of high-magnesium chlorite in the dolomitic rocks of the Ringwood core was unexpected, as neither Stewart (1963) nor Borchert & Muir (1964) include chlorite in their lists of evaporite rock constituents. Stewart (1949) recorded talc in the halite rocks (but not in the anhydrite-carbonate rocks) of the Magnesian Limestone of northern England, and its occurrence along cleavage cracks and grain boundaries of the halite led him to suggest that it had been precipitated from solution as a late secondary mineral. The porphyroblastic nature of the Ringwood chlorite, indicates that it is likewise of secondary origin. Normative chlorite in the Ringwood evaporites is most abundant in dololutite. Changes in the amounts of several other normative minerals in the dololutite are consistent with the rock having contained a significant amount of clay, and if this were the case the chlorite may have formed by the following reaction (suggested by Zen, 1959, p. 36):

dolomite + kaolinite + quartz + water
= calcite + chlorite + carbon dioxide

A similar reaction involving ankerite as well as dolomite was postulated by Muffler & White (1969) to account for the disappearance, with increasing depth, of dolomite, kaolinite, and ankerite and the simultaneous appearance of chlorite (containing slightly more iron than Ringwood chlorite) observed in the cuttings from wells in the Salton Sea geothermal field. The temperature in the wells where the transition occurs is about 200°C. The assemblage in the chlorite-bearing rocks at Ringwood, dolomite-chlorite-quartz, places them in the lowest subfacies, the muscovite-chlorite-dolomite-quartz subfacies proposed by McNamara (1965) as a threefold subdivision of the greenschist facies, with a hypothetical temperature of about 200°C corresponding to a depth of about 2 kb (bottom of the Amadeus Basin).

Calcite has not been recognised in the Ringwood rocks, but this may be because the two strongest peaks in its X-ray diffraction pattern very nearly coincide with prominent peaks in the patterns of gypsum and quartz.

Origin of pyrite and organic matter

Pyrite and organic matter are common in the lower parts of evaporite sequences. The pyrite is generally attributed to the action of sulphate-reducing bacteria, which oxidise the remains of organisms that sink down to the bottom of the evaporating basin after death (Friedman, 1972). Simultaneous reduction of sulphate during the bacterial decay produces hydrogen sulphide, which then reacts with dissolved iron and forms pyrite. Excess organic matter not decomposed by the bacteria is incorporated directly into the sediments.

Origin of microcline

The small angular grains of microcline show evidence of both detrital and authigenic origin. The elongate shapes of some grains (which suggests that they are cleavage fragments), the existence of such optical phenomena as undulatory extinction, rare lamellar twinning, and cross-hatched twinning, the absence of inclusions, and the association with increased amounts of quartz, tourmaline, and rutile, all indicate a detrital origin, whereas the highly angular shapes (including re-entrant angles), the general absence of twinning, and, when twins are found, their 'fourling' appearance indicate an authigenic origin (Kastner, 1971). The microcline is probably of detrital origin, and has been somewhat recrystallised during diagenesis or burial metamorphism.

Origin of detrital minerals

The Ringwood evaporites contain numerous tiny grains of quartz, tourmaline, rutile, sphene, and a few other minerals. These grains may have been brought into the basin by surface runoff from a nearby landmass, but their very small size and ubiquitous occurrence throughout the core rather suggest that the grains were blown into the basin as wind-borne dust, which was possibly a fairly common phenomenon during the Proterozoic, in a landscape devoid of vegetation. The increased amounts and larger size of these grains in the interval 85.34 m to 86.87 m, plus the presence of silt-sized grains of microcline, does suggest a local influx of water-borne terrigenous detritus.

Recrystallisation

There is abundant textural evidence of recrystallisation in the Ringwood evaporite rocks. The evidence includes:

- The large skeletal crystals of anhydrite and gypsum which form the cement in the bituminous dolomite breccia;
- The crusts of coarse dolomite and laminar concentrations of chalcedonic silica and pyrite at the margins of some veins and laminae of acicular gypsum;
- The existence of anastomosing veins and concretionary masses of gypsum in dololutite;
- The coarse grain and lineated texture of the anhydrite, with euhedral rhombs of dolomite in places;
- The coarse grain of the dolomite which forms the cement in parts of the bituminous dolomite breccia, with concentrations of organic matter at the margins of the coarse-grained masses; also, the coarse-grained dolomite in the intersecting cracks;
- The euhedral shapes of quartz crystals, tourmaline over-growths, and rutile needles;
- The enlargement of pyrite in some laminae, and the occurrence of large interpenetration twins of pyrite;
- The angular shapes, with re-entrant angles, of microcline grains.

The three major rock-forming minerals of the Ringwood evaporites show different degrees of recrystallisation, and different grainsizes. Gypsum is everywhere recrystallised, and forms the coarsest-grained rocks. Anhydrite is almost everywhere recrystallised to medium-sized grains, the only probable exception being the very fine-grained laminae of felted anhydrite laths and dolomite granules at 225.83 m. Dolomite is in general not recrystallised; recrystallisation is very local and occurs mostly where dolomite is associated with gypsum. Thus the three minerals can be arranged in the following order of decreasing ease of recrystallisation: gypsum, anhydrite, dolomite.

Much of the recrystallisation in the Ringwood rocks probably took place during diagenesis and burial metamorphism, e.g., the coarsening of anhydrite, the formation of euhedral quartz, tourmaline, and rutile, the enlargement of pyrite, the 'resculpturing' of microcline, and, after brecciation of the rocks, the local coarsening of dolomite and formation of large skeletal crystals of anhydrite as cement around the breccia clasts. The recrystallisation of gypsum into concretions and some of the laminae and cross-cutting veins occurred much later, after uplift of the rocks and hydration of the anhydrite to gypsum.

Origin of the Ringwood evaporite deposit

The rocks of the Ringwood evaporite deposit show all the criteria for formation in a classical barred basin, namely, a dark grey to black bituminous pyritic siliceous carbonate at the base, overlain by gypsum with inclusions of anhydrite, overlain in turn by limestone breccia and then by massive algal limestone. The evidence is consistent with diachronous deposition of carbonate and sulphate in a restricted basin behind a fringing algal reef. Celestite is not associated with dolomite, but it is associated with gypsum, and hence probably represents the strontium taken up in solid solution by primary anhydrite and then released during hydration to gypsum. The only terrigenous materials in the evaporite sequence are an influx of arkosic silt near the middle of the upper part of the core, and possible windblown clay in the dololutite interbeds.

The geological history of the Ringwood evaporite can be summarised thus:

1. Growth of an off-shore barrier reef, forming a lagoon with restricted access to the open ocean outside the reef. Stagnation ensued, followed by concentration of lagoon water by evaporation.

2. Deposition in the lagoon, of primary dolomite, primary opaline silica, organic matter, and pyrite.

3. Further concentration of lagoon water, leading to deposition of calcium sulphate, probably as primary anhydrite as discussed above. The interbeds within the lower part of the deposit indicate that conditions fluctuated between those of dolomite deposition and those necessary for sulphate deposition, but eventually conditions stabilised and sulphate became the dominant precipitate, forming the upper part of the deposit.

4. Dololutite formed at various times during the life of the lagoon, and represents additions of very fine-grained terrigenous material to the chemical deposits

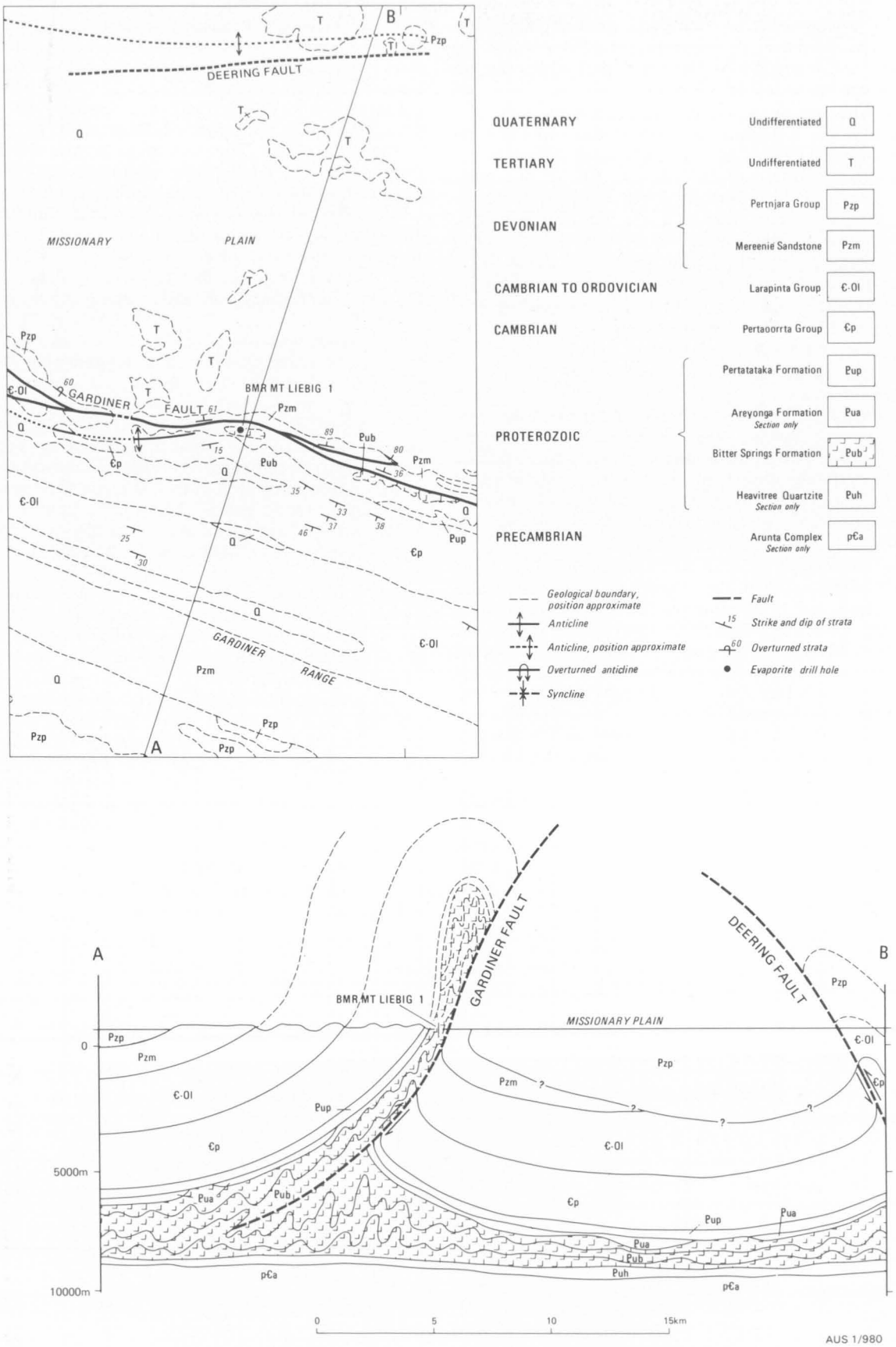

Fig. 21. Geology of the area around BMR Mount Liebig No. 1.

of the lagoon either as wind-borne dust or pluvial run-off. The presence of abundant silt-sized particles of quartz and microcline in the upper part of the deposit represents an influx of alluvium.

5. After the main period of sulphate deposition, conditions began a fluctuating return to those of the early part of the lagoon's history; carbonate formed an increasing proportion of the deposit, and at one stage bituminous pyritic dolomite precipitated. Evaporation was eventually terminated by a return to normal marine conditions, implying burial or collapse of the algal reef, or general subsidence of the entire area, or both.

6. The remainder of the Bitter Springs Formation was then deposited, followed by the succeeding formations of the Amadeus Basin sequence, burying the Ringwood evaporite to a depth of about 7 000 m.

7. Diagenesis, recrystallisation, and burial metamorphism affected the evaporite rocks, and resulted in such phenomena as: growth of chlorite porphyroblasts; crystallisation of opaline silica to chalcedonic silica and chert; growth of euhedral quartz crystals; formation of interpenetrating growth twins of pyrite; sculpturing of microcline grains; overgrowths of colourless tourmaline around detrital cores; conversion of any pre-existing gypsum to anhydrite.

8. The deposit was moved tectonically during the Carboniferous, when the evaporites were folded and brecciated, and tourmaline needles and quartz euhedra broken. Anhydrite was mobilised and formed the cement between breccia clasts, recrystallising to a blocky or bladed texture; anhydrite also formed contorted lenses and laminae where interbedded with anhydritic (now gypsiferous) dolomite. At this time dolomite also underwent local recrystallisation, mainly at the margins of breccia clasts, forming crusts of euhedral dolomite and concentrations of organic matter.

9. Erosion of landscape to present day; eventually the land surface was lowered sufficiently for meteoric water percolating down joints to reach the evaporites, and hydration of the anhydrite to gypsum ensued, accompanied by swelling and brecciation of the sulphate-bearing dolomite beds, resulting in the partly bedded, partly brecciated appearance of the dolomite-gypsum breccia. Strontium held in solid solution in the anhydrite was set free and precipitated as celestite. Joints in the evaporites were eventually filled with acicular gypsum.

BMR MOUNT LIEBIG No. 1

Drill site geology

BMR Mount Liebig No. 1 drill site (23°52′30″S, 131°56′00″E; TD 305.87) (Fig. 21) is situated on the north-east side of the Gardiner Range, a series of east-west ridges and valleys corresponding with hard and soft formations; relief is in the order of 300 m.

The Gardiner Fault, which crops out approximately 400 m north of the drill site, strikes east-west. It is a thrust fault with a hade of 15 to 20° (Moss, 1964) and a displacement of at least 6 000 m. It was formed during the late Devonian by compressional forces of the Alice Springs Orogeny acting from the north-north-east. Sediments of the northern side were thrust underneath those of the south.

Geophysical surveys indicate that the basement underneath the fault zone is flat lying; all movement during the faulting apparently took place by décollement in the evaporite sequence of the Bitter Springs Formation, the basement remaining undisturbed. The Bitter Springs Formation acted as a lubricant along the fault plane; it crops out immediately to the south of the fault along 50 km of its length.

Further south of the fault is a sequence of south-westerly dipping sediments of Proterozoic to ?Lower Carboniferous age. The Cambrian Eninta Sandstone crops out to the south of the drillsite as a prominent ridge of massive red sandstone dipping south at 35°.

To the north the Devonian Mereenie Sandstone is folded vertically against the fault plane, forming a prominent ridge; in places it is slightly overturned. North of the ridge is the Missionary Plain, where alluvium and Tertiary sediments conceal the underlying geology.

The gypsum outcrop (Fig. 22) occurs on a rise with relief in the order of 40 m. It is ellipsoidal in outline and 200 m across. The surface is covered with secondary gypsum, which in places is more than 0.5 m thick. A crust of coherent earthy gypsum up to 5 cm thick is underlain by white friable earthy gypsum. Within this surface deposit there are secondary gypsum crystals which have been corroded along their cleavage planes by meteoric waters. They occur both as single crystals up to 15 cm long and as large masses of smaller crystals up to 2 cm across. Gysum crops out as a coarsely crystalline, friable variety with an equigranular texture and brown and white mottling. Another variety is pink to brown and extremely coarsely crystalline, and has a granular texture. The gypsum becomes fluted when weathered, and in single crystals the fluting follows cleavage planes.

The gypsum outcrop is bordered on the south by a lenticular mass of breccia. This thins to the east, and the outcrop to the west is obscured by alluvium. The breccia contains white to grey laminated fragments up to 15 cm across of slightly calcareous dolomite, dolomitic chert and chert. The reddish brown matrix consists of calcite, dolomite, and quartz, with a trace of chlorite.

A sink hole occurs in the bed of the creek southwest of the drill site. It is 5 m across and has a small drainage hole 0.5 m across at its base. It probably

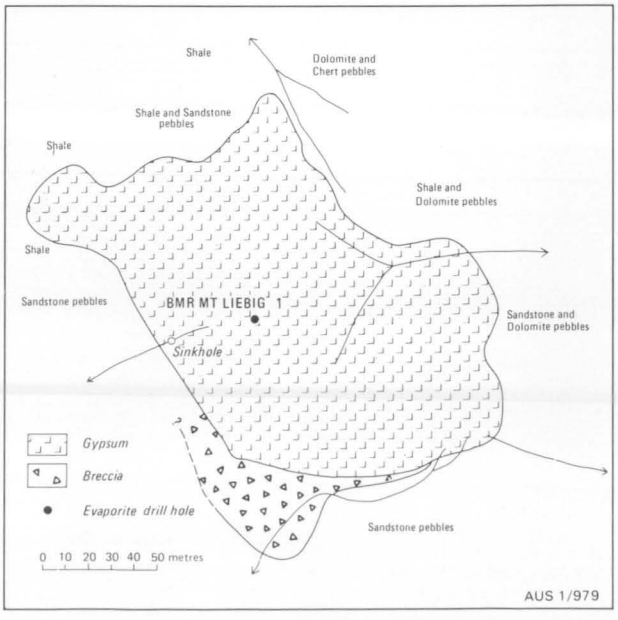

Fig. 22. Geological sketch of the Gardiner Range gypsum occurrence.

formed when a ridge of more resistant rock dammed the creek as it flowed off the soft gypsum outcrop. The rubble in the creek bed is composed of gypsiferous travertine for some distance downstream from the gypsum outcrop.

Outcrop around the gypsum is sparse and concealed by alluvium. The composition of pebbles on the surface may indicate the underlying lithology and has been recorded on the outcrop map. Shale is the dominant rock type on the western side, ferruginous sandstone on the south, and stromatolitic dolomite of the Bitter Springs Formation on the northeast.

Description of rock types

The classification of rock types shown on the composite log (Plate I) was devised after a study of sixteen thin sections of core. These were selected to cover the range of rock types and to yield as much information as possible on texture and mineralogy.

Difficulties were encountered in preparing the thin sections. Many of the rock types were friable and had to be impregnated with resin to prevent their disintegration while being sectioned. Because halite occurs in variable amounts in most of the rocks, it was necessary to make all thin sections in kerosene. Most were prepared with quartz grains mounted around the edge of the rock slice to ensure uniform and standard thickness throughout.

Identification of the minerals in twenty-one samples was carried out by X-ray diffraction analysis. Nineteen samples were selected from the core, and two samples from the breccia which crops out south of the drill site. Many of the samples were selected from the same rock specimen from which a thin section had been prepared. This enabled most of the minerals present in the thin section to be positively identified.

There are very few detrital minerals present and most minerals in the cores originated either as primary chemical precipitates or as products of recrystallisation: a crystal size classification for recrystallised carbonates suggested by Folk (1964) has been adopted: Extremely coarsely crystalline, >4.00 mm; very coarsely crystalline, 1.00–4.00 mm; coarsely crystalline, 0.25–1.00 mm; medium crystalline, 0.0625–0.25 mm; finely crystalline, 0.0156–0.0625 mm; very finely crystalline, 0.0039–0.0156 mm; aphanocrystalline, <0.0039 mm.

It is not known whether the dolomite and quartz in the core have an evaporitic origin or not. For the purposes of this report they are discussed with the evaporite minerals.

Following common practice, a rock composed dominantly of a single mineral has been referred to by the name of that mineral; 'rock' has been used after the mineral name when reference is made to an aggregate of crystals composed dominantly of one mineral.

Gypsum rock

Gypsum rock is present in the core from the surface to a depth of about 90 m. It is white, pink, and in places light grey. The texture is granular, even, and generally coarsely crystalline, but crystal size is variable, ranging from medium crystalline to extremely coarsely crystalline. The gypsum rock occurs both as massive beds up to 1 m thick and as elongated fragments with their long axes oriented subvertically in a matrix of recrystallised evaporite breccia.

Minor impurities are present throughout the gypsum rock. Dolomite is irregularly distributed as fine anhedral crystals enclosed in the coarse gypsum crystals, but concentrated near irregular fractures and cleavage traces.

Sparse, very fine to medium quartz crystals are scattered throughout the gypsum rock. They are anhedral to euhedral, and in places appear to be elongated with their long axes parallel to the gypsum cleavage planes. The mode of occurrence of both the quartz and dolomite suggests that they are of secondary origin. Recrystallisation has affected the gypsum in places. Aggregates of medium crystals with a granular texture and similar optical orientation replace very coarse gypsum crystals. Rarely, for example at 58 m, veins of acicular gypsum rock, satin spar, fill fractures.

Anhydrite rock

Anhydrite is rare above 76 m. From 76 m to 90 m it coexists with gypsum; the texture suggests that the gypsum formed by hydration of anhydrite. From 90 m to 92.03 m no gypsum is present and anhydrite rock is abundant. Below 92.03 m anhydrite is one of the constituents of evaporite rock.

Dolomite rock

Dolomite rock is common throughout the upper 92.03 m of the core, as elongated fragments in a matrix of recrystallised evaporative breccia and as massive beds up to 1 m thick. It grades from white to light grey, and has fine to very fine granular texture. Its hardness varies considerably as a result of both the fine crystal size and the presence of thin intergranular films of limonite and chlorite. Minor amounts of quartz and gypsum and/or anhydrite are present, with traces of limonite and chlorite. Dolomite rock resembles siltstone in hand specimen, and this term was used in field descriptions.

Recrystallised evaporite breccia

Recrystallised evaporite breccia forms a matrix for fragments of gypsum, dolomite, and anhydrite rock in the upper 92.03 m of the core (Fig. 23). It is light to dark brown, soft and friable, and is composed of finely crystalline dolomite and quartz with intergranular limonite, left after leaching of halite. It was further fragmented by later movement of the halite, and recrystallised by percolating meteoric waters. The

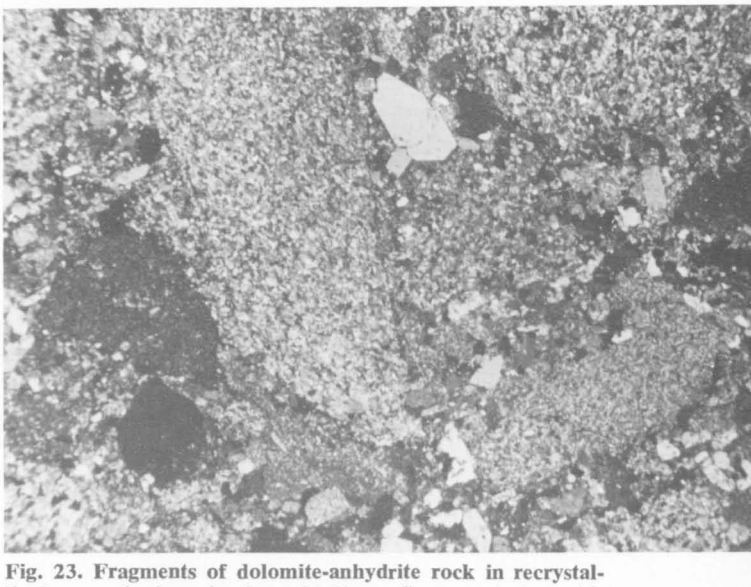

Fig. 23. Fragments of dolomite-anhydrite rock in recrystallised evaporite breccia; from 91.52 m. Crossed nicols, x 20. (M/1195-29)

breccia fragments range from 0.002 mm to 10 mm in diameter. The larger fragments are mostly composed of finely crystalline dolomite, gypsum, or anhydrite rock. The smaller fragments consist of single crystals of quartz, dolomite and some hematite; gypsum and anhydrite are rare.

The degree of recrystallisation ranges from slight to almost complete and the resulting texture is neoporphyritic; fine to coarse secondary crystals have formed at the expense of the original fine to very fine crystals and fragments. Gypsum is apparently the first mineral to recrystallise, as it is rare as fragmented crystals. Even where recrystallisation is slight, coarse to extremely coarse anhedral and subhedral secondary crystals of gypsum are present. These crystals occur in fractures between fragments and as inclusions in the fragments themselves. Secondary coarse euhedral crystals of dolomite, quartz, anhydrite, and sparse hematite are present throughout the rock.

Gypsum partly replaced by bassanite is common in most of the thin sections. This is probably caused by heating of the rock during either drilling or grinding of the thin sections.

Halite rock

From 92.03 m to total depth the core consists predominantly of halite rock. It is orange-brown, dark brown, pink, or, rarely, colourless, and compact, equigranular, and extremely coarsely crystalline. In thin section the crystals are anhedral and exhibit perfect cubic cleavage. Sparse medium euhedral to subhedral anhydrite crystals and very sparse medium anhedral dolomite crystals are scattered throughout the halite. Some halite crystals contain lines of aphanocrystalline anhydrite and ?quartz inclusions, approximately 0.02 mm wide, and 0.05 mm apart. The lines show no obvious relationship to the cleavage traces.

Rounded fragments of impure halite rock, 0.25 mm to 15 cm across, are scattered throughout parts of the halite rock. They contain generally 20 percent, and in places up to 80 percent, very finely to coarsely crystalline anhydrite and sparse fine euhedral crystals of hematite, which have partly stained the halite light reddish brown. The staining gives the fragments a deep brown colour in hand specimen and distinguishes them from the paler halite matrix. Lines of liquid inclusions, curved in parts, are present in some crystals. They bear no obvious relation to the cleavage planes and are not continuous across grain boundaries. The inclusions are less than 0.003 mm in diameter, and contain bubbles less than 0.001 mm in diameter, which vibrate because of Brownian movement.

The junction of the halite and the overlying recrystallised evaporative breccia at 92.03 m is horizontal, but serrated. At the contact, halite rock is replaced by anhydritic recrystallised evaporite breccia.

Throughout the core, halite rock is fractured into plates along horizontal planes; these have been referred to as fracture planes in the core descriptions. The spacing of fracture planes is variable and has been defined for the purposes of core description as follows: finely spaced, less than 2.5 cm; medium spaced, 2.5 cm to 8 cm; coarsely spaced, greater than 8 cm. The fractures possibly result from the release of vertical pressure, and their formation has been aided by halite crystals spliting along cleavage planes. The drilling may have relieved the confining pressure, or, alternatively, erosion may have relieved the pressure of overburden. The fractures have been accentuated by drilling, as the upper portion of each core is always finely fractured, while the lower portion is both finely and coarsely fractured.

Evaporite rock (medium crystalline)

The medium crystalline evaporite rocks occur as beds and fragments in a matrix of halite rock from 93.03 m to total depth. Beds are up to 0.7 m thick, and fragments, which are often elongated with long axes oriented near vertically, range from 1 cm to 8 cm long. The rocks vary from white to light grey, light grey-green and light brown, and the crystal size varies from 0.5 mm to 0.025 mm.

The rocks are extremely variable in mineralogy, and are composed of anhydrite, dolomite, and quartz with minor halite, chlorite, and hematite. In some specimens the minerals are present in equal quantities, while in others, dolomite, anhydrite, or quartz predominate, and the other minerals are subordinate. No gypsum has been found in these rocks.

Microscopic examination revealed that the field subdivision of these rocks, based on colour and hardness, bore no relation to mineralogy and little relation to grainsize. Colour depends on small amounts of hematite, limonite, and chlorite. Hardness is dependent not on the hardness of constituent minerals, but on the cohesion of the crystals, and this is affected by minor amounts of intergranular limonite and chlorite. Coarser crystalline varieties generally contain smaller amounts of these minerals and are harder, while fine crystalline varieties contain larger amounts and are softer. No further subdivision of the medium crystalline evaporite rocks is possible without examination of individual thin sections.

The degree of recrystallisation of these rocks varies considerably. Anhydrite and quartz appear to recrystallise most readily, and there is very little recrystallisation of dolomite.

Evaporite rock (finely crystalline)

Finely crystalline evaporite rocks vary from light grey to dark grey or chocolate brown. They are soft, and most specimens become plastic when wet. Their texture is even, and laminated specimens are rare. Crystal size is mostly fine and rarely medium. The physical characteristics of these rocks closely resemble those of claystone or mudstone, and these names were used in field descriptions. Their mode of occurrence is similar to that of their medium crystalline associates, and they occur as beds up to 0.3 m thick and fragments from 1 mm to 50 mm across. The fragments are commonly elongated and their long axes are subvertical.

The mineral content varies considerably, but consists dominantly of dolomite, quartz, and anhydrite, with minor halite, limonite, and chlorite (Fig. 24). A common composition is dolomite with subordinate quartz and anhydrite, and minor halite, limonite, and chlorite. The variation in composition is not as extreme as that of the medium crystalline rocks, and only rarely are rocks composed dominantly of one mineral.

As in the case of their medium crystalline associates, the physical characteristics of the rocks depend on minor amounts of hematite, limonite, and chlorite. Subdivisions based on colour and hardness were used in field descriptions, but, after microscopic examination of the specimens, were found to be unusable. No further subdivision of the finely crystalline evaporite

rocks is posible without examination of individual thin sections.

Compared with the medium crystalline evaporite rocks, the finely crystalline varieties are darker, softer, and mineralogically more uniform. They contain less anhydrite and more dolomite, hematite, limonite, and chlorite.

Description of core

0–92.03 m

The core from 0 to 92.03 m is brecciated, with fragments of gypsum, anhydrite, and dolomite rock in a brown matrix of recrystallised evaporite breccia. It is a cap rock overlying the more soluble halite rock. The matrix contains fragments of various rock types up to 10 mm across. Most fragments are rounded and lenticular in outline, with their long axes near-vertical; they are elongated along shear planes. The proportion of fragments varies greatly. In some places they make up the whole core, and in others they are absent. The proportion of gypsum or anhydrite rock fragments to dolomite rock fragments is extremely variable.

Anhydrite rock occurs only at the base of the interval, where little alteration of anhydrite to gypsum has taken place. Recrystallised evaporite breccia occurs as thin brown tracings between fragments, and as a matrix for the fragments. There are some zones in which the core is composed entirely of breccia.

The core contains cross-cutting veins of acicular gypsum rock in sparse zones throughout. At 57 m there is a zone in which slickensiding is present, possibly indicating minor faulting after the main deformation and brecciation. Small solution cavities are present between 25 m and 60 m.

92.03–305.87 m

From 92.03 m to total depth the core is composed dominantly of halite rock. It is generally orange-brown, but grades to light pink or colourless in several pure beds up to 5 m thick. These beds occur between 215 m and 253 m.

Fragments of fine and medium crystalline evaporite rock are scattered throughout the halite rock. As in the overlying interval, the fragments are rounded and lenticular in outline, with their long axes subvertical. They formed by brecciation of beds within the halite rock by shearing: the halite rock acted as matrix, being easily deformed by movement along cleavage planes.

Twelve intervals of evaporite rock were noted in the core descriptions; their thickness ranges from 10 to 50 cm. It is impossible to determine whether the evaporite rock occurs as beds or as large fragments or lenses which have the appearance of beds in the core. In some places the top and base of these inclusions are parallel, indicating that they are beds; in other instances top and base are at an angle, indicating that they are fragments. The contacts between the evaporite rock and halite rock dip at angles varying from horizontal to vertical.

Inclusions of evaporite rock rarely exceed 5% of the core; there are only two intervals, 252.88–258.61 m and 298.88–301.27 m, in which their percentage is large. These zones are probably remnants of beds of fine and medium crystalline evaporite rocks which were later deformed and brecciated. Throughout parts of the halite rock, particularly around 225 m, there are impure brown halite rock fragments. They are rounded and ellipsoidal with their long axes subvertical; in places they contain tracings and inclusions of brown, finely crystalline evaporative rock. The dark brown colouration is caused by hematite. These fragments are produced by brecciation of impure halite rock beds.

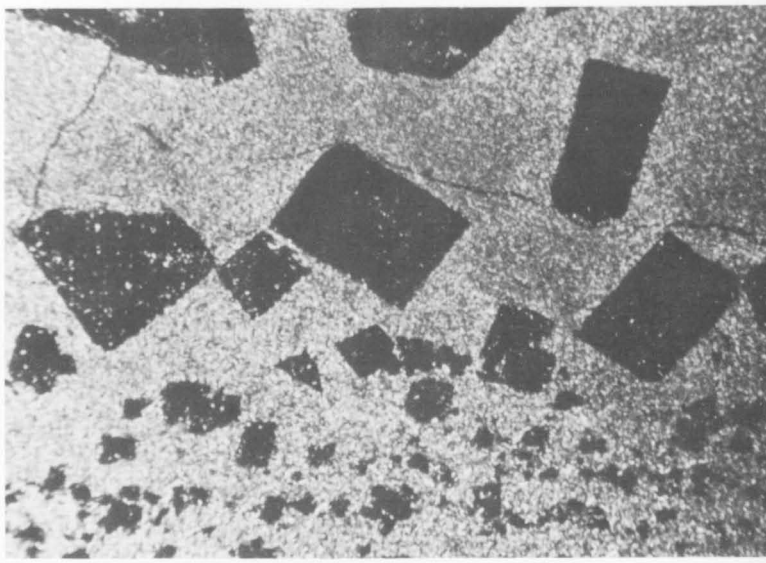

Fig. 24. Euhedral halite crystals in matrix of finely crystalline anhydrite, dolomite and quartz; from 137.31 m. Crossed nicols, x 20. (M/1195-27)

At 140.87 m a 10-cm fragment of hard black pyritic dolomite occurs which closely resembles the 'dolomitic siltstone' recorded throughout BMR Alice Springs No. 3 (Stewart, 1969). It is the only occurrence of this rock type in the core.

In a few places the evaporite rock fragments are surrounded by a layer of colourless, pure halite. This layer occurs mainly around the larger fragments, and can be up to 5 mm thick; it is the result of secondary recrystallisation of halite.

No vertical joints in the halite rock were noted anywhere in the core.

Geochemistry (Plate II)

Potassium

The potassium analyses show that no commercial quantities of this element are present. Up to 10 000 ppm (1%) is present in the gypsum-anhydrite-dolomite rock, but all results from the halite are less than 5000 ppm (0.5%). High potassium values seem to coincide with high iron concentrations. The analyses suggest that, at least in the small section sampled, deposition of evaporites did not reach the stage of precipitation of the more soluble potassium salts. The potassium in the mixed evaporite rocks may be derived from detrital minerals such as muscovite and feldspars.

Bromine

The amount of bromine present in the crystal lattice of chlorides is an indication of the salinity of the brine from which the minerals were deposited. Bromine concentration increases with salinity and high values indicate highly saline brines. Less than 5 ppm bromine is present in the gypsum-anhydrite-dolomite rock. The values recorded in the halite rock (140 to 200 ppm) are high, indicating that it formed at a late stage of halite deposition. No meaningful increase or decrease of bromine content with depth is apparent.

Boron

Boron content is average for evaporite deposits. Throughout the gypsum-anhydrite-dolomite rock quantities range from 3 to 100 ppm, but instrumental

difficulties limit detection in most of the halite to 100 ppm. At the top of the halite interval values range from 3 to 30 ppm.

Iron

Iron content of the core is high in sections which contain recrystallised evaporite breccia. This is due to the presence of brown limonite. Low values are recorded in beds composed dominantly of gypsum, dolomite, anhydrite, or halite, and also within the halite in zones in which it is colourless and pure.

Manganese

Manganese is present in very minor quantities throughout the halite, occurring only in samples with a high iron concentration. This suggests that both occur together as evaporite rock impurities. Throughout the gypsum-anhydrite-dolomite rock, values range from 10 to 150 ppm. Kropachev (1960) reported averages of 120 ppm in anhydrite rocks and 370 ppm in epigenetic gypsum rocks (*in* Stewart, 1963). The quantities detected in the core are typical for anhydrite rocks, and suggest that gypsum formed by hydration of the original anhydrite.

Barium

The lower limit of detection of barium was 100 ppm; the low values which are expected in evaporite minerals cannot be measured. Many analyses from the gypsum-anhydrite-dolomite rock and several from the halite record values in excess of 100 ppm. These are high for evaporite deposits. Barium replaces calcium in the crystal lattice of gypsum and anhydrite, and is much less abundant in halite (Stewart, 1963). High values recorded in the halite section could result from its presence in fragments of anhydritic evaporite rock.

Strontium

Strontium replaces calcium in sulphates and carbonates (Stewart, 1963). Throughout the halite it occurs in those samples with manganese, suggesting that they both occur in evaporite rock impurities. Results range up to 800 ppm, which is about average for anhydrite in evaporite rock.

Comparison of logs with core lithology (Plate I)
Spontaneous potential

The spontaneous potential curve shows irregular fluctuations throughout. Above 92.03 m several prominent deflections are present because of the permeability of the gypsum-dolomite-recrystallised evaporite breccia. Deflections are not sharp, because there are no large differences in permeability. Below this depth the curve has minor fluctuations superimposed on a drift, at first in a positive direction around 158 m, then in a negative direction with a maximum at 256 m. This depth corresponds to the zone of slight conductivity shown on the resistivity curve. Drift is irregular below this depth.

Below 92.03 m there is no relationship between the presence of minor amounts of evaporite rock and the variations in the SP curve. No deflection is present at the contact of the halite with the overlying bed. Drifting of the SP curve is expected in rocks in which there are no variations in permeability to give sharp deflections.

Resistivity

From the base of the casing at 43 m to the top of the anhydrite bed at 90 m, resistivity is low, with values between 5 and 10 ohm-metres. High values at 46 m and 51.5 m correspond with beds of recrystallised evaporite breccia, and a low value at 53 m correlates with a bed of gypsum. The curve is fairly smooth and variations reflect porosity differences; low resistivity is a result of interstitial water in the hole.

From 90 m to 92.03 m gypsum is absent; all calcium sulphate is present as anhydrite. There can be little interstitial water as this would be absorbed to hydrate the anhydrite. Resistivity in this bed increases from 12 ohms at the top to 100 ohms at the base.

A linear increase in resistivity is recorded over the next 36.6 m. This is a phenomenon caused by the upper bridle electrode being in highly conductive gypsum while the zero guard log was in highly resistive halite. Resistivity throughout most of the halite section of the core is 7500 ohm-metres. This is virtually an infinite resistance and indicates that the hole is dry. The curve shows marked deflections from 226 to 230 m and 249 to 257 m; they are very prominent, but only reflect a change from an infinite resistivity to a very high resistivity of 200 ohm-metres.

The deflections show little relationship to the lithology. The upper deflection coincides with a 40-m bed of evaporite rock, while the top of the lower one is 3.85 m above a 5.72-m bed of brecciated evaporite rock. A similar bed at 301.27 m does not give rise to irregularities in the curve, indicating that the presence of this rock type is not the reason for the deflection. The evaporite rock is dry and contains no conductive minerals such as pyrite.

The caliper log shows 20–25 mm of caving, possibly caused by zones of weakness in the halite over the less resistive intervals. Salty water could have seeped into the fractured rock associated with these zones, causing the formation to be slightly conductive.

The slight drift to the left throughout the graph may be a response to the increasing proximity of the conductive zones. Below 257 m the drift is to the right.

Gamma ray

The gamma-ray log shows radioactivity varying from 10 to 120 API units. Above 92.03 m the graph has values in excess of 70 API units with high values coresponding to beds of gypsum. Values are lower above the base of the casing at 43 m, owing to its shielding effect. Above 27 m the graph becomes smoother and values smaller, because cement behind the casing settled to this level before it set. In the halite, values are approximately 60 API units above 152 m and 20 API units below. A peak in excess of 100 API units occurs from 131 to 132.6 m. This was initially interpreted as a potassium-bearing zone, but chemical analyses have shown that only minor amounts of potassium are present. A series of regularly spaced peaks, 3 to 3.25 m apart, occurs from 119 to 169 m. These may reflect sedimentary cycles.

There is no correlation between radioactivity and proportion of evaporite rock fragments. Both impure halite at the top of the bed and pure halite from 213 to 253 m show radioactivity values higher than normal. The gamma-ray curve shows the highest deflection in zones of high potassium content. In some intervals it closely reflects variations in the potassium content revealed by chemical analyses.

Neutron

The neutron log from 0 to 43 m was recorded through steel casing, and recorded values are

anomalous. Below 18 m smoother fluctuations result from the presence of water in the hole.

From 43 to 89 m the log reflects the percentage of gypsum in the hole, and low counts at 49, 52, 61, 76, and 87 m result from gypsum beds. Gypsum gives low counts on the neutron log because hydrogen concentration is high, owing to water in the crystal lattice. Texture of the core from 61 to 75 m is even, but the log shows the proportion of gypsum to be variable.

From 88 to 90 m the curve shows a steep rise to a value of 870 cps, owing to the increasing amounts of unaltered anhydrite in the hole. Because neither halite nor anhydrite contain water of crystallisation, no deflection was recorded at their boundary.

Deflections in two zones, from 224 to 229 m and from 250 to 225 m correlate with the zones of lower resistivity. They may represent either zones of infiltration of salt water into fractures or beds of hydrous minerals. Core descriptions do not confirm the presence of any hydrous minerals; halite is the dominant mineral, with impurities of anhydrite, quartz, and dolomite.

Caliper

The caliper log shows a sharp decrease in hole diameter, corresponding to the base of the 20 cm casing at 41.5 m. This depth contrasts with the measured 43.0 m of casing run by the drillers. The hole was reamed to 158 mm diameter prior to electric logging. Throughout most of its length the hole is 158 to 165 mm diameter. Slight caving at 75.5 m is attributed to a bed of soft dolomite. Caving to a diameter greater than 178 mm is rare, but occurs at 228.5 m and from 250 to 255.5 m. It could be a result of either fractured zones or soft impurities in the halite.

Density

To a depth of 92.03 m the apparent density is 2.2 with fluctuations of up to 0.1. This figure is low, considering that the rock is composed of gypsum (density 2.3), dolomite (2.9) and quartz (2.7). Brecciation may have resulted in high porosity and low density. A sharp rise in recorded values occurs at the base of the casing. Peaks can be related to massive beds, but their composition appears unimportant.

From 90 to 92 m a bed containing anhydrite (density 2.9–3.0) occurs, but the expected increase in density is not recorded. This could be caused by the presence of halite (density 2.1–2.3), but the amounts involved would not be sufficient.

Below 92.03 m apparent densities are 2.0, with variations of 1.8–2.3. These values are low for halite and the log may be calibrated to give low values. Variations of density up to 0.2 occur over short intervals, and do not appear to be related to the presence of evaporite rock fragments in the core. Two large peaks correlate with sharp drops in resistivity. The cores showed little indication that the formation was denser across these intervals. A relation may exist between these deflections in the density log and caving recorded over the same interval by the caliper log. Slight caving at 290 m has an associated sharp density peak. Alternatively, an increase in formation density may have caused deflections in both the caliper and density logs.

The shape of the lower 213 m of the density curve is basically similar to that of the gamma ray, resistivity, and SP curves, with a decrease to 245 m, followed by a slight rise in values towards the bottom of the hole.

Discussion and conclusions

Origin of the Mount Liebig deposit

It is well established that evaporite rocks form in an aqueous environment in which evaporation exceeds precipitation. Water containing dissolved salts replaces that lost by evaporation, giving a mechanism for the formation of thick sequences of evaporite minerals. The setting in which these processes take place is uncertain. A shallow embayment or lagoon to which the sea has restricted access, because of a continuously rising bar, is the classical model. Schmalz (1969) has suggested a model in which thick evaporite deposits form in deep basin environments. He claims that deposition of an evaporite sequence 1200 m thick would require an initial basin depth of not less than 600 m.

Evaporite deposition is generally cyclic. The basal unit of a typical cycle is euxinic and bituminous. These beds are composed of carbonates or shale, and sometimes contain sulphide minerals. The Kupferschiefer of the Zechstein Basin is an example. Evaporation causes concentration of salts and calcium sulphate precipitates as either gypsum or anhydrite: which depends on the conditions at the time of deposition. The increase in temperature caused by depth of burial generally converts gypsum to anhydrite. Precipitation of relatively large amounts of halite follows, before the more soluble salts become concentrated and are deposited.

Examples of most stages of the cycle are present in BMR Mount Liebig No. 1. The initial euxinic stage of deposition is represented by several fragments of dolomite at 42.42 m. The dolomite is black and pyritic. Its presence as fragments within the halite demonstrates that considerable disruption of the original bedding has taken place.

The second stage is represented by anhydrite occuring in evaporite rock. This has been converted to gypsum in the upper parts of the core. Dolomite and quartz may also have been deposited during this stage. Minor amounts of mica may be either wind blown or metasomatic in origin (Carozzi, 1960).

The third stage is represented by a considerable thickness of halite. The presence of beds of impure halite is shown by fragments containing anhydrite crystals and inclusions of evaporite rock. Deposition must have been interrupted before precipitation of the more soluble potassium salts, as these are not present in major amounts in the core.

Although most stages of the cycle are present, it is difficult to relate their stratigraphic positions in the hole to a cyclic succession, as the deposit has been structurally disturbed. Décollement movement of at least 6000 metres took place on the evaporite horizon. This was followed by diapiric intrusion of halite into the overlying sequence along the Gardiner Fault. It is to be expected that the original bedding, showing cyclic deposition, has been destroyed by the accompanying brecciation and contortion. Zones up to 10 m thick in the halite contain fragments of evaporite rocks; these are probably brecciated remnants of single beds. This is the only recorded occurrence of the evaporite sequence of the Bitter Springs Formation along the length of the Gardiner Fault.

Solution of the halite by meteoric waters left a residue of anhydrite (evaporite rock) fragments above the halite, while the continuous upward movement caused more halite to be exposed to solution. By a process of solution and compensating upward movement, large amounts of halite were leached, leaving a

residue of anhydrite fragments. The size of these fragments is very variable, ranging from about 1 m across to single fine crystals. Upward movement caused brecciation of the fragments and gave them a sub-vertical orientation.

Percolating meteoric waters later converted anhydrite to gypsum and caused recrystallisation of the interstitial breccia of finer fragments. Gypsum, quartz, and dolomite may have been leached from the coarser fragments and redeposited in the breccia.

The features observed in the core can be related to this explanation for the origin of the evaporite body. The contortion and brecciation of beds in the halite is a product of strong deformation by both décollement and diapiric movement. The horizontal contact of the anhydrite and halite showed that halite was being replaced by anhydrite, giving the contact a serrated appearance. A 2-m bed in which anhydrite is present occurs above the halite. As the fragments in this bed would not have been exposed to meteoric waters for a long period, conversion to gypsum would not have taken place. Above this bed is a zone which would have been exposed to water for longer periods, and contains both gypsum and anhydrite. This is overlain by a thick bed in which all calcium sulphate is present as gypsum.

The contact of halite with the cap rock would be expected to vary in depth slightly, but would be in the order of 100 m across the length of the outcrop of gypsum. The outcrop is situated on a rise which has about 40 m relief, giving the halite-cap rock contact a depth of 60 m below the surounding plain.

There is some evidence in the cores of stages of an evaporite cycle. Halite shows that the cycle was almost completed; none of the final stage bittern salts were found, but the hole was still in halite at total depth. It also shows that an evaporitic depositional environment present throughout the Amadeus Basin in Bitter Springs time produced halite deposits over a much larger area than has been proved previously.

No potassium salts have been discovered to date. However, as the area over which evaporites were deposited is very large, sub-basins in which brines could have concentrated and precipitated the more soluble salts may have been present. The halite deposits of the Bitter Springs Formation have been sampled only at three widely scattered points. The information available is insufficient to discount the possibility that potassium salts were deposited in more restricted areas of the Bitter Springs sea.

BMR LAKE AMADEUS Nos. 3, 3A, & 3B

Drill site geology

BMR Lake Amadeus Nos. 3, 3A, and 3B were drilled near an isolated outcrop of Late Precambrian Bitter Springs Formation (Fig. 25). The outcrop is surrounded by Quaternary sand dunes, and no other rocks crop out for a distance of 8 km. It occurs at the eastern end of a northwest-trending series of gypsum outcrops of Bitter Springs Formation, which is unconformably overlain by both the Inindia Beds and the Winnall Beds in the surrounding area.

A scarp of resistant rock strikes northwest and curves towards west-northwest in the south, with a moderate but variable dip; only two dips were measured in the outcrop, 21° and 62° to the southwest. The dominant rock type is partly silicified dolomite, with several smaller isolated outcrops of gypsum on the north side of the ridge. Another less well-defined scarp with a similar strike occurs about 100 m further north.

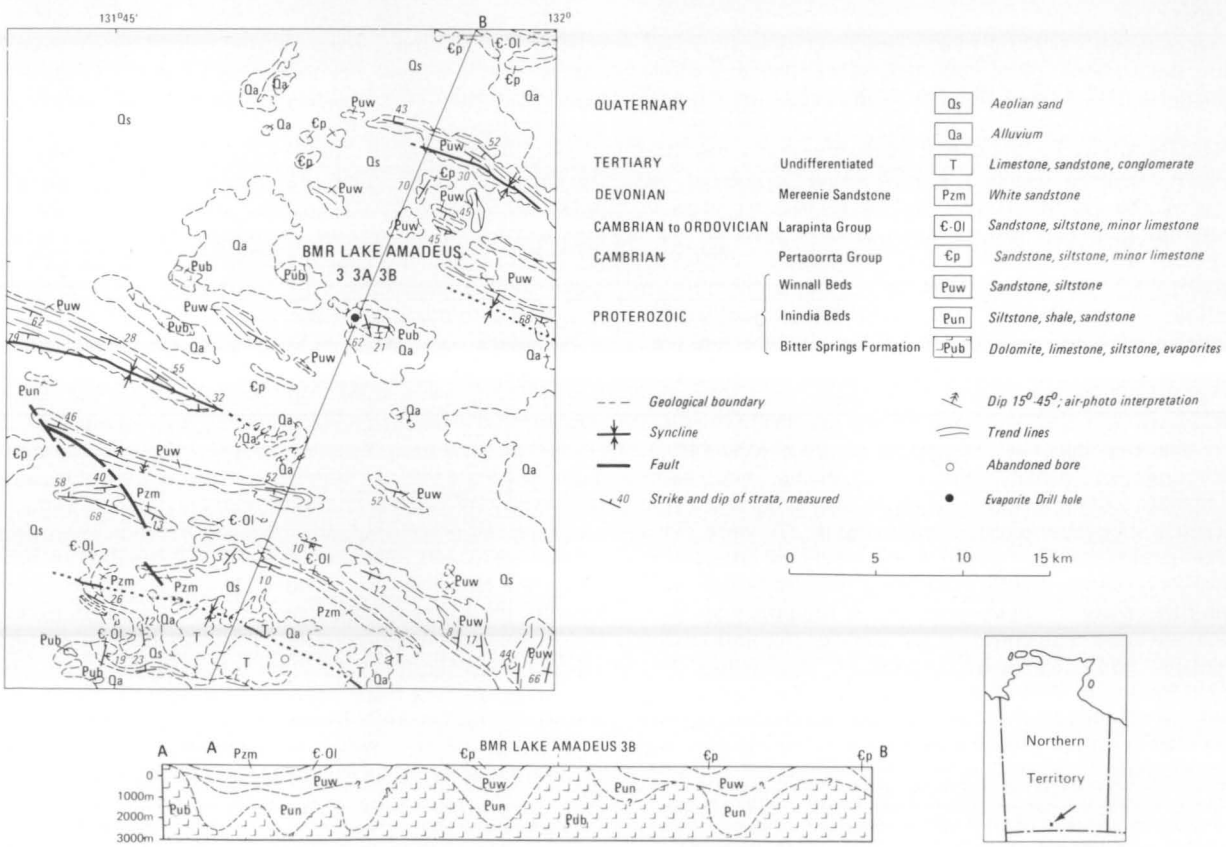

Fig. 25. Geology of the area around BMR Lake Amadeus Nos. 3, 3A, 3B.

The gypsum outcrops have the appearance of being a lenticular body of evaporites within the dolomite.

Rounded low hills of siltstone with a silcrete capping extend northwest across the northern edge of the outcrop. The siltstone and minor interbeds of sandstone dip gently northwest and appear to unconformably overlie dolomite of the Bitter Springs Formation. The siltstone is probably part of the Inindia Beds.

The gypsum outcrop near the drill holes (Fig. 26) is irregular in outline and 120 m across. The gypsum is coarsely crystalline, and contains laminae of gypsiferous dolomite up to 1 mm thick. To a depth of at least 10 cm the laminated gypsum has been softened by rainwater dissolving some crystals leaving the rock very porous. A surface crust of earthy gypsum over 15 cm thick covers the entire outcrop and in places contains single crystals up to 15 cm across. These have been corroded in parts by rainwater.

The gypsum dips west-southwest, steepening gradually from 15° at the eastern extremity of the outcrop to 70° in the western sink hole. This is not in accordance with the strikes measured elsewhere in the area, both on the ground and on aerial photographs, and may be due to contortion on a large scale. Laminae in the outcrops are contorted and in many places small overthrusts are visible. Boudinage structures are present in dolomite laminae in places. All these features are attributed to an increase in volume by hydration of anhydrite.

There are two main drainage systems on the outcrop which both terminate in large sink holes. Large V-shaped channels up to 5 m deep have cut into the outcrop. These drain by means of underground channels into the two main sink holes. The westernmost is circular in outline and about 10 m across. It is 12 m deep and drains through a small opening into a cave 5 m deep with a loose rubble floor. Several small passages can be seen in the sides; one of these must have been intersected by BMR Lake Amadeus No. 3, as the sound of drilling in this hole could be heard clearly in the cave. The easternmost sink hole is only 3 m across and 4 m deep, but drains through a small hole into a cave 2 m across and 15 m deep.

At a depth of 90 m in BMR Lake Amadeus No. 3B a flow of water of approximately 45 000 litres/hr was encountered. The water was flowing from small solution cavities in the gypsum. Water obtained at this depth contained fragments of charcoal, which were up to 2 cm across, very friable, and partly decomposed, and which appeared to have been in the water for a long time. The charcoal was probably washed into the sink holes, which are 120 m away on the surface, and transported through cavities into the zone of saturation. Some fragments were coated with a crust of gypsum. Long cylinders of gypsum were present and these are thought to have been formed by crystallisation around elongate fragments which later decomposed, leaving the gypsum crust.

Gypsum crystals with the appearance of cones with a large apical angle joined at the base were also obtained from the water. They are up to 2 mm across and were possibly caused by slow recrystallisation around an opaque nucleus in a constantly moving solution. Crystal faces can be seen on the sharp periphery. Several single crystals up to 10 mm across and which had been partly redissolved were also obtained.

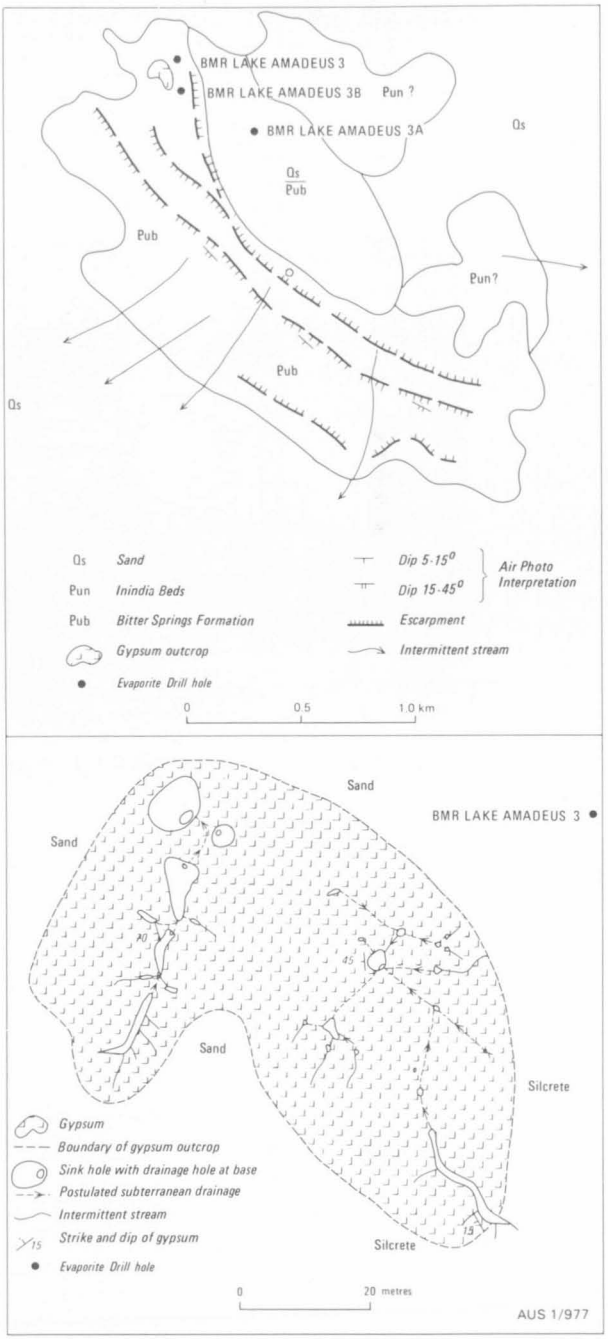

Fig. 26. Geological sketches of gypsum outcrop north of Curtin Springs, and locations of BMR Lake Amadeus Nos 3, 3A, & 3B.

Two samples of water from BMR Lake Amadeus No. 3B were analysed and the results set out in Table 8. The analyses showed a high percentage of dissolved calcium sulphate, which makes the water unfit for human consumption.

Depth to bedrock is variable: BMR Lake Amadeus No. 3 was spudded in gypsum, while No. 3A penetrated alluvium to a depth of 38.7 m, and No. 3B, situated 60 m from the gypsum outcrop, encountered 41.1 m of alluvium.

Description of rock types

The classification of rock types shown on the composite log (Plate III) was devised after a study of 17 thin sections of core from BMR Lake Amadeus No. 3B

TABLE 8. WATER ANALYSES—BMR LAKE AMADEUS No. 3B

	71.9 m	*90.5 m*
Na	935 ppm	1120 ppm
K	95 ppm	92 ppm
Ca	733 ppm	721 ppm
Mg	169 ppm	233 ppm
Fe	3.6 ppm	0.3 ppm
Cl	1520 ppm	1820 ppm
SO_4	2360 ppm	2620 ppm
NO_3	71 ppm	7 ppm
HCO_3	93 ppm	110 ppm
F	2.3 ppm	3.6 ppm
SiO_2	28 ppm	33 ppm
P_2O_5	1 ppm	1 ppm
Conductivity*	7810	8690
Total dissolved solids	6200 ppm	6920 ppm
pH	6.5	6.6
Hardness, total	2530	2760
Hardness, temporary	76	90
Hardness, permanent	2454	2670
Alkalinity	76	90

Remarks: Unsuitable for human consumption or stock use.
* micromhos/cm^2

Analyses by Northern Territory Administration Water Resources Branch.

and 9 thin sections from BMR Lake Amadeus No. 3. These were selected to cover the range of rock types and to yield as much information as possible on texture and mineralogy.

The methods used in preparation of the thin sections, mineralogical analyses. and the crystal size classification adopted, have been described earlier in the section on BMR Mount Liebig No. 1.

Anhydrite rock

Anhydrite rock occurs in the core below approximately 250 m. It grades from white to light brown. and is interlaminated with dolomite-anhydrite rock throughout. Laminae are gently folded, but the dip is generally near vertical. It is assumed that this is the true dip of sediments in the drillhole, and that anomalous dips recorded throughout the gypsum are due to later contortion.

Anhydrite rock is generally medium crystalline with some finely crystalline varieties. Crystals are euhedral to subhedral, and texture grades from equigranular to aligned-felted (Maiklem & others, 1969). Orientation of laths is parallel to thin laminae of dolomite and dolomitic anhydrite rock. Coarsely crystalline laths are associated with dolomite rock fragments at 284.66 m.

Zones of medium crystalline anhydrite cut across the finely crystalline varieties in places. Many crystals are euhedral, suggesting that the anhydrite in these zones is secondary.

Throughout the core anhydrite is altering to gypsum (Fig. 27). In the upper parts the alteration is complete, but in many places below 250 m the two minerals coexist. The alteration takes place by formation of euhedral gypsum crystals, which can be extremely coarsely crystalline. These are scattered evenly throughout the anhydrite rock, giving it a spotted appearance, or, more commonly, form along minute fractures which transgress the laminations. The thickness of the recrystallised zone varies, depending on the amount of dolomite scattered throughout the anhydrite rock. In pure anhydrite rock this zone can be up to 20 mm thick, but it is rarely over 5 mm thick in impure laminae.

It is difficult to determine whether anhydrite is primary or not. Alignment of the laths parallel to dolomitic laminae and regular lamination with only slight folding suggest that it is primary.

Dolomitic anhydrite rock

Interlaminated with anhydrite rock is dolomitic anhydrite rock. This grades from light brown to brown, and in some parts of the core below 250 m it is the dominant rock type. It is moderately hard to hard, gently folded, and dips are generally near vertical. Texture is aligned-felted, with fine anhedral dolomite crystals evenly disseminated throughout medium crystalline anhydrite. The percentage of dolomite is variable, but is generally 20–60%.

In laminae which contain high percentages of dolomite, anhydrite is finely crystalline, and a few opaque crystals are present. Fine crystals of dolomite are disseminated throughout. This rock type does not appear to recrystallise as readily as pure anhydrite.

Gypsum rock

Gypsum rock is the dominant rock type throughout much of the core. It is white, coarsely to very coarsely crystalline and moderately hard. Laminae of dolomitic gypsum rock are very common, giving a light grey appearance in parts. These laminae are commonly very contorted, and in many places the core has been strongly brecciated, and fragments with contorted laminae are present.

Texture is felted in most parts, and crystals commonly contain scattered fine anhedral dolomite and rare fine to medium anhydrite crystals (Fig. 28). Fine euhedral quartz and medium subhedral dolomite crystals occur in parts and are probably of secondary origin (Fig. 29). Traces of limonite and sparse very coarse calcite crystals are present near the surface. Some coarse gypsum crystals contain inclusions of fine

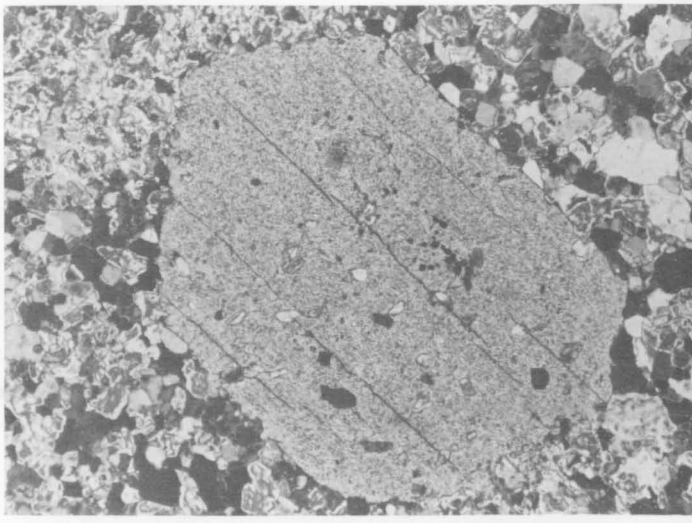

Fig. 27. Medium crystalline anhydrite (white to black), showing granular texture, being replaced by very coarse euhedral gypsum crystal (centre). Note anhydrite inclusions in gypsum; from 253.34 m. Crossed nicols, x 20. (M1195-12)

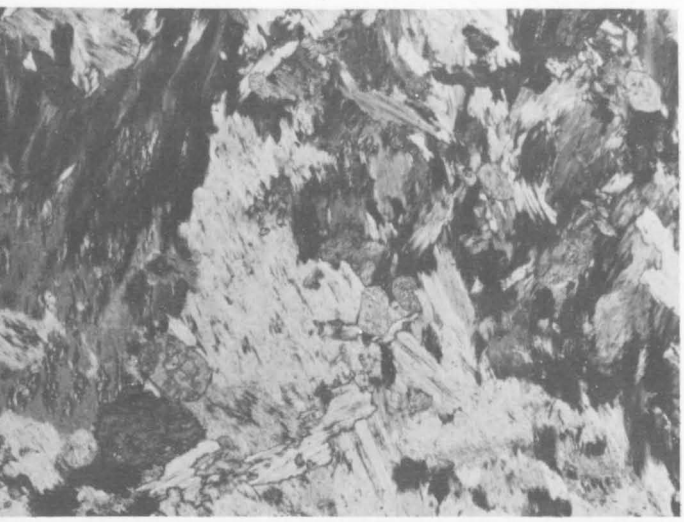

Fig. 28. Gypsum (light grey to black) showing felted texture and sparse dolomite crystals (grey rounded); from 33.91 m. Crossed nicols, x 60. (M/1195-36)

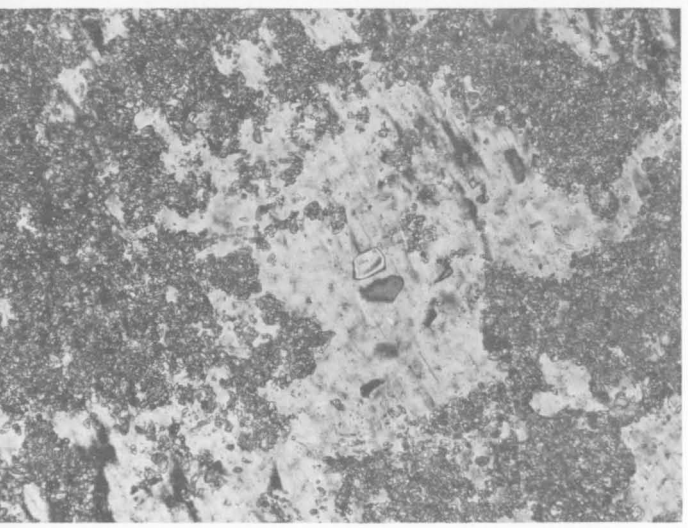

Fig. 29. Gypsum (light grey) and fine dolomite crystals (small, dark, rounded); from 303.7 m. Crossed nicols, x 60. (M/1195-2)

Fig. 30. Slabbed section of core showing contorted laminae of gypsiferous dolomite (black) and fragments of light brown tough dolomite (grey) in brecciated and contorted gypsum; from 38.31 m. x 1. (GA/4319)

acicular gypsum. These are probably the result of recrystallisation by percolating meteoric waters. Bassanite is present, but is produced by heating of the rock during preparation of thin sections.

Acicular gypsum rock

Acicular gypsum rock (satin spar) occurs in veins up to 20 mm thick in many parts of the core. It is composed of fibres of gypsum generally oriented at right angles to the fractures they fill. Where slight movement has occurred along the fractures the fibres are not perpendicular to the walls. Some fractures are filled with crystals which have grown from both walls.

Gypsiferous dolomite rock

Laminae of gypsiferous dolomite rock occur throughout the gypsum. They rarely exceed 1 mm in thickness, and are light grey, moderately hard, and often contorted (Fig. 30).

The amount of dolomite varies greatly, but is mostly more than 50%. Dolomite is anhedral, finely crystalline, and disseminated in a matrix of finely crystalline gypsum. Limonite is common, and is associated with dolomite. Sparse finely crystalline remnants of anhydrite crystals are present with dolomite in parts.

Although dolomite is predominant in these laminae, its X-ray diffraction pattern is weak, whereas chlorite and quartz show a strong pattern, although thin sections show only very minor amounts of these minerals.

The laminae probably originated as dolomitic anhydrite rock and were converted to dolomitic gypsum rock by hydration.

Black tough dolomite rock

This variety of dolomite rock occurs as beds and fragments in several zones up to 2 m thick. It grades from dark brown to black, and is very tough. Texture is equigranular with interlocking fine anhedral crystals. At 125.61 m the rock is laminated, with fine and medium crystalline laminae; these are separated in parts by traces of limonite. In several other places, as at 284.63 m, it is composed of laminated finely crystalline fragments up to 10 mm across in a matrix of finely crystalline dolomite. Gypsum is rarely present in the matrix.

Much of the dolomite rock is pure, and this is the reason for its toughness. In some places, a few fine crystals of quartz and traces of limonite are present, and in others, the fine dolomite crystals are contained within very coarse poikiloblasts of gypsum. Some dolomite rock fragments have a slight salty taste.

Light brown tough dolomite rock

This variety occurs as beds up to 1 m thick and as fragments throughout the core (Fig. 31). It grades from light brown to grey, and from moderately tough to tough. Texture in hand specimen appears to be even, but in thin section the rock is heterogeneous, consisting dominantly of finely crystalline anhedral dolomite with a varying proportion of fine to very coarsely crystalline gypsum. Minor amounts of limonite are associated with the dolomite, and sparse unaltered medium crystals of anhydrite are present.

Dolomite constitutes about 60% of the rock and is generally evenly disseminated through felted gypsum. In zones of very high dolomite concentration the texture is laminated with both crystal sizes and crystals of different mineralogy alternating.

The rock resembles siltstone in hand specimen and was given that name in field descriptions.

Fig. 31. Steeply dipping lamina of light brown tough dolomite (grey) in gypsum, showing boudinage structure. Fractures are filled with acicular gypsum from 73.51 m. x ½. (GA/4787)

Grey friable dolomite rock

This rock type occurs as regular and irregular laminae up to 5 mm across in gypsum, as matrix for gypsum fragments, and as beds up to 15 m thick. It grades from light to dark grey, and from moderately soft to soft and friable.

In occurrences as laminae and matrix it is anhedral and very finely crystalline. Texture is equigranular, and finely crystalline euhedral to subhedral quartz, anhydrite, and gypsum are commonly present. Traces of limonite, muscovite and opaques have been noted. Feldspar was recorded in X-ray diffraction analyses, but was not seen in thin sections. The amount of dolomite present is variable, but is almost always in excess of 60%.

In occurrences as thick beds, texture is brecciated, with fragments of finely to very finely crystalline dolomite rock, sparse fragments of finely crystalline evaporite rock, and coarse euhedral gypsum crystals in a matrix of very finely crystalline dolomite (Fig. 32). Dolomite rock fragments are laminated in part, owing to variations in both composition and crystal size. Fine crystals of quartz, muscovite and gypsum are present in amounts less than 20%.

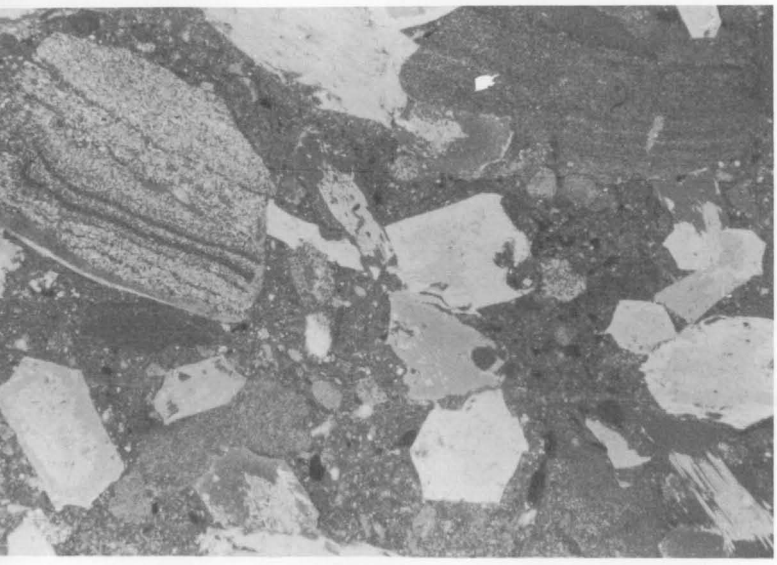

Fig. 32. Coarse euhedral gypsum crystals (white to light grey) and laminated dolomite fragments in very finely crystalline dolomite matrix, from 150.54 m. Plane polarised light, x 20. (M1195-14)

Evaporite rock fragments consist of fine crystals of euhedral to anhedral dolomite, quartz, gypsum, and limonite, with minor opaques and muscovite. Halite, chlorite, and feldspar were detected in minor amounts in the X-ray diffraction analyses, but were not noted in thin sections. The proportions in which the constituent minerals occur in evaporite rock are extremely variable.

The coarse euhedral gypsum crystals are almost all recrystallised in the centre. This may be an original feature of the crystals, but is more probably produced during processing of thin sections.

This rock resembles claystone in hand specimen and was given that name in field descriptions.

Siltstone

Siltstone occurs in the alluvium intersected in the upper 41.1 m of BMR Lake Amadeus No. 3B, and has been observed only in cuttings. It grades from white to brown and pink, is soft and friable, and is composed of silt-sized quartz grains in a white matrix. X-ray diffraction analyses demonstrate the presence of quartz, gypsum, kaolinite, and muscovite, and a trace of chlorite. Calcite is also present in some samples.

Sandy siltstone

This rock is similar to siltstone in appearance and occurrence, but contains up to 35% sand-sized quartz grains. These are well rounded and grade from colourless to brown.

Claystone

Claystone occurs in the alluvium intersected in the upper 41.1 m of BMR Lake Amadeus No. 3B, and has been observed only in cuttings. It grades from white to brown, is soft and friable, and closely resembles the matrix in siltstone. Sparse fine silt-sized quartz grains are present in parts.

Silcrete

Silcrete occurs between 33.5 m and 39.6 m in the alluvium in BMR Lake Amadeus No. 3B. It grades from light brown to brown, and is hard and tough. Texture shows medium sand-sized quartz grains in a ?siliceous matrix.

Sandstone

Sandstone is orange-brown, fine grained and well sorted. It effervesces strongly when HCl is added, and contains up to 60% coarsely crystalline gypsum in most parts. The cement contains a high proportion of limonite. The sandstone is probably a filling of solution cavities in the rock, and contains a large amount of surface detritus.

Description of core

BMR Lake Amadeus No. 3

0–48.8 m

Lithology is uniform throughout most of this core, consisting of gypsum rock with laminae of gypsiferous dolomite rock and grey friable dolomite rock. Strong contortion and brecciation have taken place throughout, and veins of acicular gypsum rock are common. In several zones throughout the core there are beds of highly calcareous orange-brown claystone, siltstone, and fine sandstone. These consist mainly of surface detritus washed into solution cavities.

At about 21 m a zone of beds and fragments of dolomite rock is present in a matrix of grey friable dolomite rock, and at 24.4 m there is a bed of soft friable dolomite rock with fragments of light grey tough calcareous dolomite rock.

BMR Lake Amadeus No. 3A

0–38.7 m

This hole penetrated unconsolidated detritus throughout, and only two cores were taken, from 13.7 m to 16.8 m and 27.4 m to 30.5 m. The upper core consists of soft white claystone with limestone fragments. The lower core consists of grey tough dolomite rock, grey soft siltstone, and white soft claystone.

BMR Lake Amadeus No. 3B

0–41.1 m

Cuttings reveal that to a depth of 41.1 m the hole penetrated siltstone and claystone of possible Tertiary age. Siltstone, sandy in parts, is the dominant rock type to 18.3 m. A core taken at 12.2 m has an even texture with very coarse secondary gypsum crystals scattered throughout. From 18.3 m to 41.1 m the rock type is claystone. A core taken at 31.3 m is evenly textured with very coarse secondary gypsum crystals throughout. Silcrete occurs between 33.5 m and 39.6 m. The cores taken in this interval have a weathered appearance.

41.1–149.4 m

Gypsum rock is dominant throughout this interval. It is strongly contorted throughout and brecciated in parts. Laminae of gypsiferous dolomite rock occur throughout, while irregular laminae, lenses, and sparse beds up to 1 m thick of grey friable dolomite rock are present. Beds and fragments of black and light brown tough dolomite rock occur in parts. Veins of acicular gypsum rock are common.

At 71.9 m a very prominent subvertical joint with limonitic clay on its surface was encountered. This may be a small fault of indeterminate displacement. A flow of water originated from the joint. Solution cavities occur between 90.2 m and 100.6 m.

149.4–164.6 m

Grey friable dolomite rock is dominant in this interval. Texture is generally even, with fragments of gypsum rock disseminated throughout. Small fragments of dolomite rock and evaporite rock are visible, and small veins of acicular gypsum rock are present in places.

164.6–250.8 m

Texture throughout this interval is heterogeneous, and the core consists dominantly of fragments of gypsum rock in a matrix of grey friable dolomite rock. Numerous beds of gypsum rock with contorted laminae of gypsiferous dolomite rock up to 3 m thick and beds of grey friable dolomite rock up to 2 m thick occur throughout. Both light brown and black tough dolomite rock are present as beds up to 2 m thick and as fragments. Veins of acicular gypsum rock are present in most parts.

250.8–305.9 m

Anhydrite rock is dominant throughout this interval, and is interbedded and interlaminated with dolomitic anhydrite rock. Dip is generally vertical, with gentle folding visible in parts.

The anhydrite-dolomitic anhydrite rock shows alteration to gypsum rock throught the interval. The alteration grades from negligible to complete, and gypsum crystals can be seen along bedding planes, fractures in the rock, and at points enclosed within massive anhydrite rock. Veins of acicular gypsum rock are commonly concordant with lamination. Beds of grey friable dolomite rock up to 2 m thick are present, and in places contain fragments of gypsum, anhydrite, and light brown tough dolomite rock.

Below 283.5 m black tough dolomite rock occurs as sparse fragments and, more commonly, as beds up to 2 m thick.

Geochemistry

BMR Lake Amadeus No. 3 (Fig. 33)

Potassium

The analyses show that no commercial deposits of this element are present. Amounts range from 300 to 1800 ppm and are similar to those obtained in gypsum in other parts of the Amadeus Basin, and in Lake Amadeus No. 3B.

Boron

Figures for boron analyses are comparatively very high, ranging from 500 to 1900 ppm. They are much higher than those from BMR Lake Amadeus No. 3B, and may indicate a concentration of boron in the near surface gypsum zones. Limonitic staining is present in some laminae in this hole, and fissures and cavities are filled with surface detritus, suggesting that some concentration of weathering products may have taken place.

BMR Lake Amadeus No. 3B (Plate IV)

Potassium

Results of potassium analyses vary from 200 to 20 000 ppm. The two samples with 20 000 ppm potassium were grey friable dolomite; the mode of occurrence of the element is not known. Feldspar was recorded in some X-ray diffraction analyses of this rock type and, may be potassium rich.

Results throughout most of the hole are similar to those of BMR Lake Amadeus No. 3, BMR Mount Liebig No. 1 and BMR Alice Springs No. 3. In the anhydrite-dolomitic anhydrite rock results are low, suggesting that potassium has been introduced in zones in which percolating meteoric water has caused recrystallisation.

Boron

Boron analyses throughout the gypsum show very high results, up to 500 ppm. These bear little relation to the lithology.

Within the anhydrite-dolomitic anhydrite rock results are low, suggesting that boron, like potassium, has been introduced by percolating meteoric water which causes recrystallisation. The sample within the anhydrite at 305.84 m (100 ppm) was composed of gypsum. Apart from this, all samples below 267 m contain less than 30 ppm boron. These results are typical of anhydrite deposits (Stewart, 1963).

Manganese

Manganese content of the core is similar to that in the caprock of BMR Mount Liebig No. 1. Amounts vary from 2 to 130 ppm and are generally low towards the base of the hole. The figures are very low for

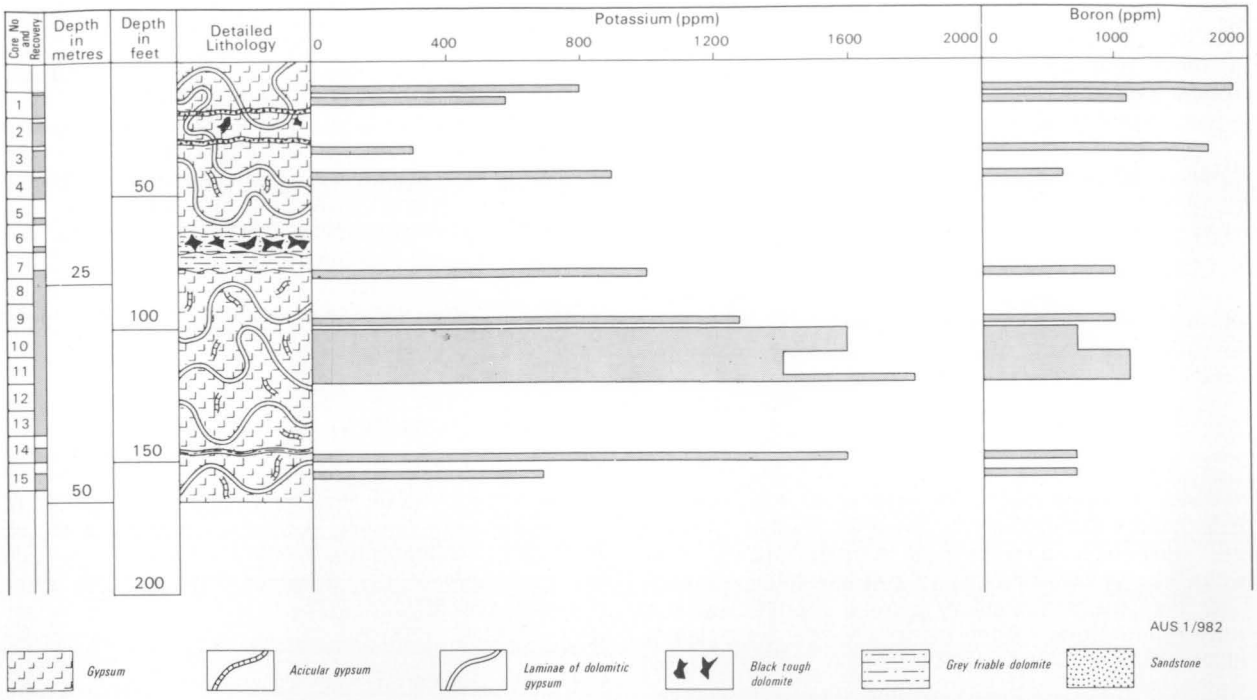

Fig. 33. Graphic log and chemical analyses, BMR Lake Amadeus No. 3.

epigenetic gypsum rock, and slightly low for epigenetic anhydrite. This may indicate that initial deposition of calcium sulphate was as anhydrite; gypsum was formed by later hydration, and retained an initially low manganese content.

Barium

Barium commonly replaces calcium in anhydrite and gypsum (Stewart, 1963). In this hole, however, it occurs mostly in grey friable dolomite. Amounts in beds of this rock type are between 70 and 300 ppm. These are comparable with high values found in salt clays in German evaporites. Amounts throughout the remainder of the core are below 30 ppm. These figures are slightly high for evaporite deposits, which contain on the average 3–10 ppm barium (Stewart, 1963).

Strontium

Strontium occurs in amounts between 20 and 600 ppm, and appears to be more abundant towards the base of the hole. Noll (1934) found that gypsum which had replaced earlier anhydrite at ordinary temperatures cannot always retain all the strontium of the anhydrite, and so celestite is formed (Stewart, 1963). This may explain the generally higher strontium values in the anhydrite. The results of the analyses obtained are as expected in gypsum rock, but below average in anhydrite rock.

Comparison of logs with core lithology (Plate III)

Spontaneous potential

Throughout most of its length the spontaneous potential curve shows minor irregularities superimposed on an irregular drift. This is to be expected in rocks with little contrast in porosities, such as those in the drill hole.

A minor deflection occurs at 91.5 m which may be related to the presence of water or cement filling cavities. The maximum deflection to the right at 122 m corresponds to a zone of very high resistivity. To a depth of 152 m the spontaneous potential curve is similar to the resistivity curve. Beds of friable dolomite produce deflections to the left. The slight deflection at 141.7 m corresponds to such a bed, while the large bed from 149.4 m to 164.6 m produces a large deflection.

The drop in resistivity below 213.4 m corresponds to a shift in the spontaneous potential curve. A friable dolomite bed occurs at 216.4 m and a 3 m core loss below 218.3 m may be due to a similar bed.

Below 229 m the curve is featureless. This is due to vertical lamination producing few sharp variations in lithology.

Resistivity

Resistivity above 139 m is high, generally above 1500 ohm-metres, and shows no deflection over the non-cored interval 90.2 m to 98.5 m, indicating that its lithology is similar to that above and below.

From this depth to 149 m the resistivity declines sharply, owing to dolomite in the gypsum. Resistivities within the bed of friable dolomite from 149 m to 165 m are relatively low, between 50 and 100 ohm-metres. It is difficult to explain why the minimum resistance in the hole occurs at 166 m within a bed of gypsum.

Interbedded gypsum, friable dolomite, and light brown tough dolomite give resistivities in the order of 150 ohm-metres between 168 m and 177 m. Similar lithology to 256 m shows resistivities around 1500 ohm-meters, with a sharp drop to less than 100 ohm-metres from 215.8 m to 223.1 m. This can only be partly explained by the presence of beds of friable dolomite in the gypsum between 213 m and 222 m. Similar beds in other parts of the core do not produce similar deflections.

Below 256 m the resistivity shows few sharp variations because of uniform lithology and vertical dip, but gradually increases in value to almost 2000 ohm-metres at the base of the hole.

Resistivity throughout most of the hole is extremely high; the two zones in which prominent deflections occur only represent a change from extremely high to very high resistivity.

Both the spontaneous potential and resistivity logs (guard log) end at 58.8 m because the upper bridle electrode was not submersed in fluid. Fluid level was at 23.8 m, as for the neutron log, and the distance from bridle electrode to zero guard log, 35 m, resulted in a cut-off level of 58.8 m for the guard log.

Gamma ray

To 244 m the gamma-ray curve is irregular with sharp peaks, and recorded values generally range from 25 to 100 API units. It is difficult to correlate the peaks with any particular rock type. Above 23.8 m the peaks are less marked, because there is no fluid present in the hole.

From 149 m to 165 m recorded values range from 75 to 150 API units in a bed of friable dolomite. This correlates with an increase in potassium content recorded by the chemical analyses over this interval. Values up to 20 000 ppm potassium were recorded. A similar zone with values between 60 and 100 API units occurs between 212.1 m and 223.7 m. Both these beds have a low resistivity.

Below 224 m recorded values are generally higher, between 60 and 120 API units. This increase is attributed to the presence of anhydrite in the core. The low values recorded at 290 m correlate with a bed of friable dolomite. This does not agree with the gamma-ray response in other dolomite beds.

Neutron

To a depth of 232 m the neutron log shows numerous fluctuations, but is essentially uniform, with values between 300 and 500 cps. An increase in recorded values to over 1000 cps occurs above 23.8 m, because there is no fluid present in the hole. There is no correlation between the fluctuations in the curve and the lithology.

From 232 m to 256 m the curve becomes smoother because the lithology is more uniform. Values gradually increase to about 600 cps, possibly as a result of increasing amounts of anhydrite in the core.

Below 256 m values fluctuate between 500 and 700 cps and probably reflect the degree to which recrystallisation of anhydrite to gypsum has taken place. The higher values are a result of a dominantly anhydritic lithology; lower values below 302 m result from the presence of gypsum.

Caliper

The caliper log shows a decrease in hole diameter from 20.3 cm to 15.2 cm at 43.6 m. This corresponds to the base of the casing. Very little caving was recorded in the hole. If it was present above 195 m it would have been filled by the cementing operations.

Hole diameter exceeds 15.2 cm only between 92.7 m and 96.3 m in the zone of solution cavities, and in several places between 146 m and 165 m in the beds of friable dolomite.

Density

Density measurements were not possible above 23.8 m, because no fluid was present in the hole. From this depth to 36.6 m densities are low, in the order of 1.9. This may be due to either the shielding effect of the casing or the lower density of alluvium, which was penetrated to a depth of 41.1 m. Anomalous values as low as 1.5 occur between 39.6 m and 53.3 m and may be related to the presence of the casing, as lithology is uniform below 42.7 m.

Densities to a depth of 244 m are generally in the range 2.1 to 2.35. These are the expected values in rock composed dominantly of gypsum (density 2.3).

A zone of slightly lower density occurs from 91.4 m to 103.6 m which may be related to either solution cavities in the rock, or cement filling cavities.

Low densities (2.05) are recorded in the beds of friable dolomite at 141.7 m, between 149.4 m and 164.6 m and from 213.7 m to 217.0 m. High densities would be expected in dolomite beds (density 2.9); the discrepancy must be due to either porosity of the dolomite or the presence of gypsum.

From 244 m densities gradually increase and from 250 m are between 2.4 and 2.6. The increase is due to the presence of anhydrite (density 2.9 to 3.0) in the core. The lower values recorded in the basal 3 m are due to the presence of gypsum.

Discussion and conclusions

The origin of evaporite deposits with respect to cyclic deposition has been discussed in the section on BMR Mount Liebig No. 1. Examples of several stages of the depositional cycle are present in BMR Lake Amadeus No. 3B.

The initial euxinic stage is represented by black tough dolomite. In some fragments cubic cavities are present. These initially contained crystals of either halite or, more probably pyrite, which have decomposed. Pyrite is an indicator of euxinic conditions.

The light brown tough dolomite and grey friable dolomite possibly represent an intermediate stage between the deposition of dolomite and calcium sulphate, as both are present in varying proportions in these rocks. The presence of mica and feldspar indicate that some detrital material was deposited at this time.

The regularly laminated texture of the anhydrite-dolomitic anhydrite rock, results of chemical analyses, and texture in thin section suggest that initial deposition of calcium sulphate was as anhydrite. To produce interlaminated anhydrite and dolomitic anhydrite, as occurs in the lower portion of the core, deposition of dolomite at irregular intervals synchronous with the deposition of anhydrite would have been necessary. The presence of dolomite may indicate that deposition in the rocks encountered in the drill hole did not progress beyond the initial part of the calcium sulphate stage. Silica was deposited either as chert, which later recrystallised, or as detrital grains, throughout all stages.

Gypsum in the core formed later by hydration of anhydrite. Recrystallisation can be seen throughout the massive anhydrite rock which occurs below 250 m. An increase in volume should occur where individual coarse gypsum crystals have formed at the expense of anhydrite. There is no evidence in the core of a volume change associated with the recrystallisation; this means that excess gypsum has been transported away from the crystals by percolating water. It is this gypsum which has recrystallised along bedding planes in fissures, forming veins of acicular gypsum.

Above 250 m, in the zone in which almost complete conversion of anhydrite has taken place, gypsum has been strongly contorted and brecciated by the increase in volume of the mass of rock. Where regular com-

Fig. 34. Vertical aerial photograph of the Goyder Pass structure. White circle indicates site of BMR Hermannsburg No. 40. For explanation of symbols see Fig. 36.

petent beds such as dolomite occur, they are subjected to tension. This is caused by the overlying and underlying beds increasing in volume (and length) and fracturing the competent bed, forming boudinage structure. The fractures formed are filled with acicular gypsum. Compressional features, such as miniature overthrusts, and small reverse faults are also present. They are caused by compressional forces produced by an increase in volume.

Laminae of dolomite present in the original anhydrite are preserved in a contorted and sometimes brecciated form in the gypsum.

It is possible that the dips measured in the area of the sinkholes were produced by large scale contortion on hydration of anhydrite, as they are not in accord with regional trends. The drilling demonstrated that laminated and bedded anhydrite occurs at depth beneath the gypsum outcrop. The anhydrite dips near vertically and is only gently folded. Inspection of aerial photographs suggests that it occurs as a lenticular body interbedded with the surrounding sediments.

There is litle indication that a salt dome is present in the area. The only evidence which could support this idea is the vertical dip of the anhydrite, which could be produced on the flanks of a dome. There is no evidence of brecciation and only slight folding of the anhydrite. This indicates that the strong deformation associated with diapiric intrusion is not present. Neither gypsum nor anhydrite has the structure of a cap rock which might be overlying a halite body.

BMR HERMANNSBURG No. 40

Drill site geology

BMR Hermannsburg No. 40 is situated at approximately 23°38.3′S, 132°27′E, about 32 km southwest of Glen Helen homestead, in the MacDonnell Ranges.

The drill hole is sited in the core of the Goyder Pass structure (Figs. 34, 35, 36), which has been described by Prichard & Quinlan (1962) as being a cross-section of a diapir with the Bitter Springs Formation constituting the mobile beds. The lensing out of the lower member of the Mereenie Sandstone against the domed Larapinta Group was given as evidence for structural growth during Mereenie Sandstone deposition, and the lack of thinning and disruption of the beds after the deposition of the basal member of the Pertnjara Group, as evidence for the age of cessation of growth of the structure. Prichard & Quinlan state that the Goyder Pass structure developed during the period of tectonism which formed the steep dips along the northern flank of the Missionary Plain syncline, although they suggest that its location was controlled by earlier tectonic effects not now apparent. McNaughton & others (1967) also considered Goyder Pass to be a diapir, but Quinlan & Forman (1968) thought that, because thrusting between two décollement horizons had been demonstrated elsewhere in the basin, it is possible that the structure was caused by thrusting upwards from the Bitter Springs Formation into a possible salt horizon within the Pertaoorrta Group.

Fig. 35. Oblique aerial photograph, looking east, of the Goyder Pass structure. (G/9578)

The closest petroleum exploration well to the Goyder Pass structure is Tyler No. 1, sited about 14 km south of BMR Hermannsburg No. 40. It reached a total depth of 3830 m and penetrated ?Devono-Carboniferous and Ordovician sediments of similar lithology and thickness to the formations exposed in the Goyder Pass structure (Huckaba & Magee, 1969).

A seismic line was surveyed by the BMR between the Gardiner Range and Goyder Pass, and many seismic surveys were conducted in the Missionary Plains area by Magellan Petroleum Corporation (Froelich & Krieg, 1969). The latter surveys presented evidence to show that the disrupted beds at Goyder Pass continue in the subsurface westwards towards the Deering fault and Carmichael structure. The thrust on the east side of the structure, appears to split into several planes between Goyder Pass and the Carmichael structure. They estimate that in places the minimum vertical displacement is about 3500 m. Thinning of the sedimentary section has also taken place on the flanks of the Carmichael structure and indicates structural growth throughout the Ordovician.

Description of drill hole (Plate V)

The well was drilled to a total depth of 91.4 m. The hole was rotary drilled and cored with air and salt-saturated drilling fluid. Coring commenced at about 4 m and a total of 18 cores was obtained to total depth. Continuous coring was attempted, but proved impracticable because of caving hole conditions. Coring was attempted over 66.6 m, and 28.7 m of core was recovered.

The drill hole penetrated about 17 m of friable, medium-grained sandstone, and 24 m of silty sandstone, and claystone, the clay and other fine-grained components increasing proportionately with depth. From 42 m to 79 m, core recovery was very poor and caving hole conditions were encountered; the core recovered consisted mostly of light grey to black unconsolidated clay with abundant light to dark grey vuggy and massive chert particles, either with pyrite filled fractures or small clusters of encrusted pyrite crystals. Some discrete aggregates of pyrite crystals occur in the clay matrix.

Below 79 m to total depth (91.4 m) no core or cuttings were recovered, with the exception of 15 cm of dark grey clay and grey pyritic and partly oolitic chert obtained over the last interval cored from 86.9 m to 91.4 m. The poor returns were caused by cavities in the sequence and resultant loss of fluid circulation.

There are several possible explanations for the origin of the sequence penetrated below 40 m, but the most

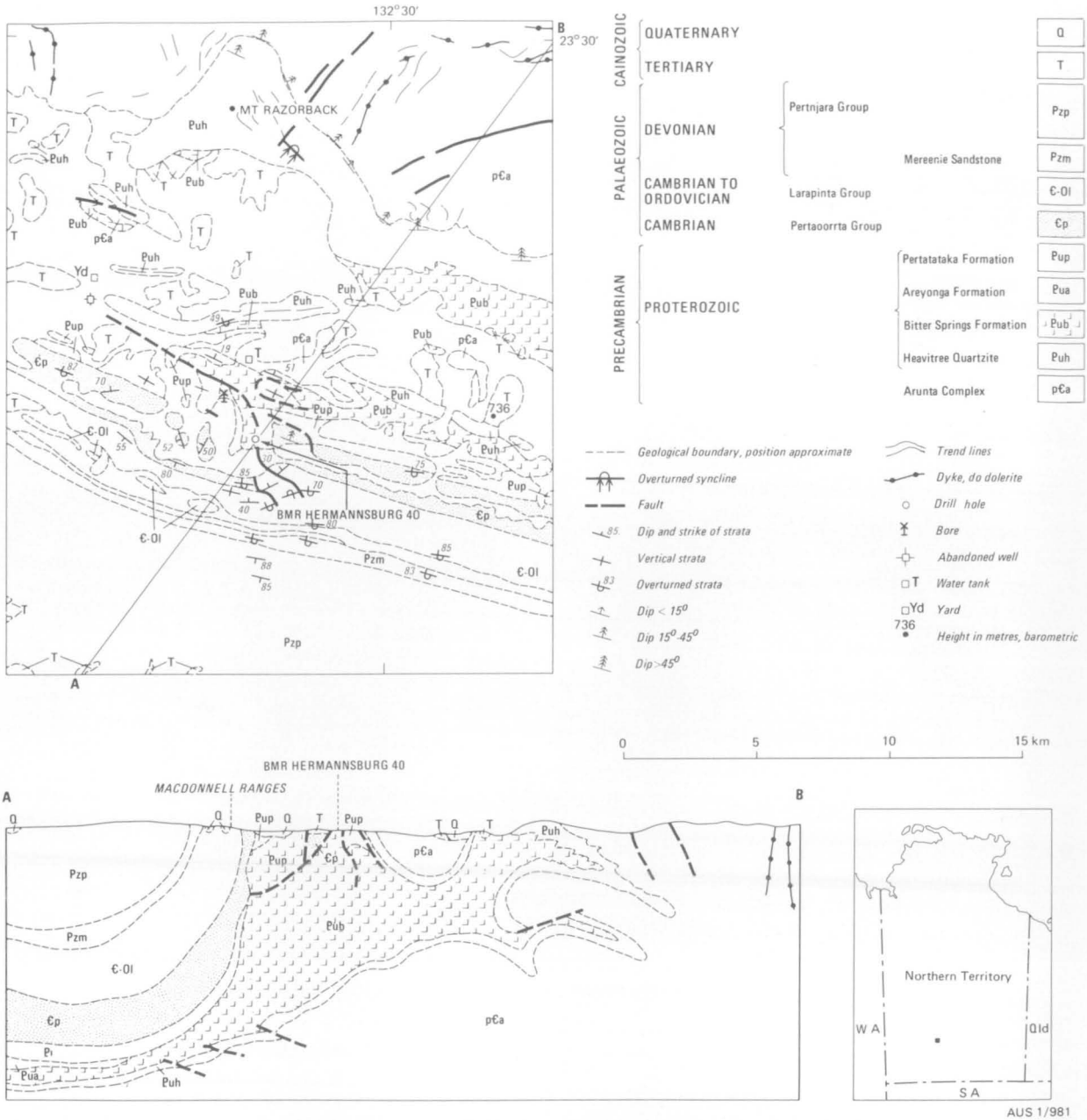

Fig. 36. Geology of the area around BMR Hermannsburg No. 40.

likely is that the chert and fine clay are residual materials filling cavities remaining after dissolution of salt from the Gillen Member of the Bitter Springs Formation.

The drill hole was abandoned at 91.4 m, because of the difficult drilling conditions and also because no evaporites had been encountered to that depth. The hole is now plugged and abandoned.

Discussion and conclusions

The gravels forming the first 3.05 m in BMR Hermannsburg No. 40 have been deposited by modern streams. Tertiary clastic rocks occupy from 3.05 m to 41.1 m. They are mainly lacustrine and fluviatile and lie unconformably on the eroded upturned edges of the folded Palaeozoic and Proterozoic rocks.

The interpretation of the age and origin of the sequence below 41.1 m is more problematic. Chert and dark shales are known in the late Precambrian Bitter Springs Formation, and pyritic sediments are also common in the formation. The possible modes of origin envisaged for this deposit are:

- Residual erosion products on bedrock composed of the Bitter Springs Formation.
- Breccia in a fault crush zone. A fault, near the drill-site, separates outcrops of the Bitter Springs Formation and the Cambrian Pertaoorrta Group.
- Residual material filling cavities remaining after dissolution of salt from the Gillen Member of the Bitter Springs Formation.

Cavities were encountered during drilling of the test hole and similar cavities occur in drill holes that have penetrated evaporites in the Bitter Springs Formation. In addition, pyritic chert and black shale are common in the evaporitic sequences of the Bitter Springs Formation, and these two facts suggest that the last mode outlined above is the more likely explanation for the origin of the deposit. However, the other two explanations cannot be entirely ruled out, and

further test drilling in the area would be necessary to prove the presence of evaporites. The area is not recommended for further shallow test drilling of evaporites as the depth of weathering is not known, and hence the top of the evaporite sequence cannot be predicted with any certainty. There are also many other localities in the Amadeus Basin where evaporites of the Bitter Springs Formation crop out and offer better targets for shallow test holes.

RECOMMENDATIONS FOR FURTHER INVESTIGATIONS

There appear to be two structural modes of occurence of evaporite minerals intersected by drilling in the Bitter Springs Formation of the Amadeus Basin. Bedded deposits were drilled by BMR Alice Springs No. 3 and BMR Lake Amadeus No. 3B, and deposits of probable diapiric origin were intersected by BMR Mount Liebig No. 1.

The chances of intersecting halite in bedded deposits where the drill is spudded in gypsum appear to be low. None was intersected in either Alice Springs No. 3 or Lake Amadeus No. 3B, although elsewhere several oil wells have penetrated halite beds at depth within the formation. Hydration of anhydrite to gypsum has taken place at depths from 100 m to over 300 m, and percolating ground water would be expected to leach halite occurring at shallower depths in most deposits. A 300-m drill hole may effectively sample only a small interval of the stratigraphic sequence, if beds are steeply dipping or incompetently folded, and if an inclined hole is drilled, the leached interval will be correspondingly thicker.

The halite intersected by the drilling is in a structure of probable diapiric origin. The outcrop over the structure is also gypsum, but the potential of these deposits is much greater than that of bedded deposits, because, in the majority of cases, halite is necessary for their formation. If a cap rock is present, halite is expected at depths generally less than 300 m. The drilling results, together with surface studies of the outcrops, have provided criteria for determination of the mineralogy of gypsum cap rocks.

A weathered surface crust of earthy gypsum with discrete crystals up to 15 cm across is common to all deposits and can be over 1 m thick. In clay pan and salt lake deposits this variety would be expected to be present at depth.

At BMR Mount Liebig No. 1 drill site, outcrops overlying the halite body are composed of brecciated cap rock. The weathered surface crust is underlain by very coarsely crystalline, massive, generally brown gypsum with an equigranular texture.

The gypsum deposits on which BMR Alice Springs No. 3 and BMR Lake Amadeus No. 3B were drilled are bedded and have quite a different appearance on the surface. They are coarsely crystalline, but have a laminated and in parts contorted texture, which is distinctive. Tracings and laminae of gypsiferous dolomite give a grey appearance to the rock.

Detailed examination of enlarged aerial photographs gave information on the relation of the gypsum body to the surrounding sediments. Diapiric movement of a halite body produces a circular or oval outcrop, which may be surrounded by one formation. A circular ridge uplifted by the halite may be preserved around the outcrop, while the gypsum may have shallow dips away from the centre. Conversely, the concordant nature of bedded deposits may be apparent on the aerial photographs and, therefore, distinguishable from diapiric bodies.

Further drill sites can be selected by using these criteria to distinguish cap rock gypsum. In cases where the bedrock gypsum is obscured by a thick weathered crust, the crust should be penetrated by either shallow drilling or trenching to determine the mode of occurrence of the underlying gypsum and allow an assessment of the nature of the deposit.

Gravity surveys over surface evaporite occurrences may provide data on the presence and extent of halite bodies, but the cost involved may be similar to that of drilling several shallow stratigraphic holes in the deposit, and the relative costs and benefits should be closely compared beforehand.

The next stage of the evaporite investigations in the Amadeus Basin should consist of reassessment of all known gypsum occurrences. Deposits which appear to be of diapiric origin should be investigated by a program of shallow drilling to a depth of about 20 m, and occurrences which appear to be underlain by cap rock should be drilled to a depth of at least 300 m to assess the intrusive core.

It is in deposits of diapiric origin that the probability of intersecting halite and associated potassium salts at relatively shallow depths is greatest; in addition, most of the worlds native sulphur deposits occur in the cap rock of salt domes.

ARCKARINGA BASIN

Evidence for the presence of evaporites in the Arckaringa Basin comes from interpretation of surface structures and from the results of drilling for oil and minerals.

At Mount Toondina, near the centre of the Arckaringa Basin, an inlier of strongly dislocated Lower Permian and Upper Jurassic sediments occurs in an area of slightly tilted Lower Cretaceous rocks (Fig. 37). An isolated small positive gravity anomaly coincides approximately with the inlier, and a small, relatively low, reversal corresponds with the centre of the structure. Seismic surveys have shown that apart from this disturbed area the sedimentary sequence in the basin is only mildly deformed.

The structure at Mount Toondina has been explained by Freytag (1965) as probably being caused by the elevation of blocks of Permian and Jurassic sediments above a piercement with a core of incompetent rocks of unknown age and composition. Although the structure is dissimilar to diapirs in the Flinders, and Peake and Denison Ranges (Coats, 1964), sediments of Willouran age which are considered to contribute the breccia core complexes of the diapirs crop out only 50 km to the east of Mount Toondina. The Mount Toondina piercement is younger than Early Cretaceous and there is some evidence for Quaternary movement. Numerous mound springs scattered in and around Mount Toondina owe their development to the formation of the structure.

By comparing features of the Mount Toondina structure with those of Gosses Bluff, Youles (1976) concluded that the piercement at Mount Toondina was caused by impact of an extra-terrestrial body. His main evidence is that the highly disturbed older sedi-

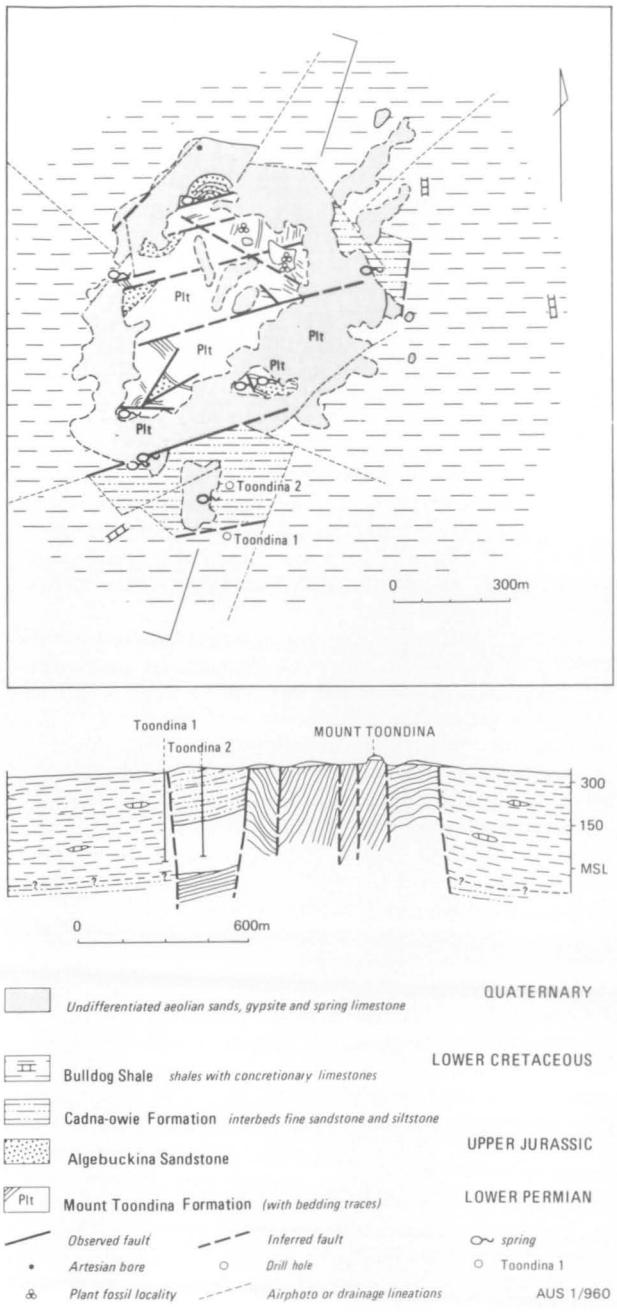

Fig. 37. Geology of the Mount Toondina structure (after Freytag, 1965).

ments of the structure have a fault-bounded polygonal outline and are surrounded by sub-horizontal younger sediments, and that the structure contains welded rocks with high-temperature minerals. He also cites geophysical and fracture patterns, and kink bands and parallel planar features in quartz grains. Wopfner (1977), however, argues that as diapiric intrusion can satisfactorily explain Gosses Bluff, so can it also explain the Mount Toondina structure. The contorted core, which here consists of coal-bearing sediments, is, according to Wopfner, a common feature of diapiric structures throughout the world, as is the polygonal outline with sub-tangential shear or fault planes. The high temperature minerals are described by Wopfner as occurring in a usually vesicular slag, which can be explained by internal in situ combustion of a coal seam. Thus he concludes that all the evidence points to a diapiric origin for Mount Toondina, and suggests that the diapirism resulted from incompent behaviour of Devonian evaporites beneath the Permian under the influence of an interference stress field.

Over 100 m of halite (573-690 m) was intersected in Wilkinson No. 1 well, drilled by the South Australia Department of Mines in the Tallaringa Trough of the Arckaringa Basin (Fig. 38), immediately west of the Karari Fault, near the northwest margin of the Gawler Platform. The halite occurs in the ?Cambrian Observatory Hill Beds, which, originally, were almost certainly deposited in the Officer Basin. The Beds may be a correlative of the Early Cambrian Chandler Limestone of the Amadeus Basin.

Occidental Minerals Special Mining Lease (329) was taken up after the discovery of Devonian evaporites in the South Australia Department of Mines Cootanoorina No. 1 well (Figs. 39, 40) (Wopfner & Allchurch, 1967; Allchurch & others, 1973), about 53 km south-southwest of Oodnadatta and about 5 km south of Mount Toondina. Devonian rocks (identified by palynology) penetrated in this well proved to be a prominent and widespread seismic reflector previously recorded in reconnaissance geophysical studies. These studies indicated that Devonian rocks are widespread in the subsurface within the Arckaringa Basin and the Boorthanna Trough. The Devonian cores from the Cootanoorina well consist of alternations of black shale and anhydrite, probably deposited in a restricted environment. The anhydrite is commonly pink and occurs in pods.

Holmes (1970) considered that if, in the Devonian, a connection to the open seas lay to the north or west, then the southerly parts of the Arckaringa Basin and the Boorthanna Trough would be the most prospective for accumulations of bittern salts. Geophysical surveys have suggested a southerly tongue of Devonian sediments and, at the northern end of an elongate trough, a lip which would inhibit the flow of brines. The Boorthanna Trough is a narrow half-graben which formed at the time (Devono-Carboniferous) of the Alice Springs Orogeny. By contrast, the sequence in the Adelaide Geosyncline was folded much earlier (by Ordovician movements, possibly equivalent to the Rodingan Movement in the Amadeus Basin), and the Flinders Ranges diapirs presumably ceased movement at or soon after this event.

On the basis of the interpretation of Holmes (1970), Boorthanna No. 1 (Holmes & Rayment, 1970) was drilled by Occidental Minerals 111 km south-southeast of Cootanoorina No. 1, to a total depth of 1225.6 m. No identifiable Devonian rocks were encountered, and Precambrian metavolcanics were intersected at 1158.2 m.

The sequence penetrated in the Boorthanna No. 1 well is:

Age	*Formation*	*Interval*
Early Cretaceous (Neocomian to Aptian)	Cadna-Owie Formation	0–46 m
Early Permian (Artinskian to Kungurian?)	Mount Toondina Beds	46–643 m
Carboniferous to Early Permian (Sakmarian)	Unit One Beds	643–863 m
	Unit Two? Beds (Lake Phillipson Beds?)	863–1158 m
Precambrian	Metavolcanic sequence	1158–1226 m

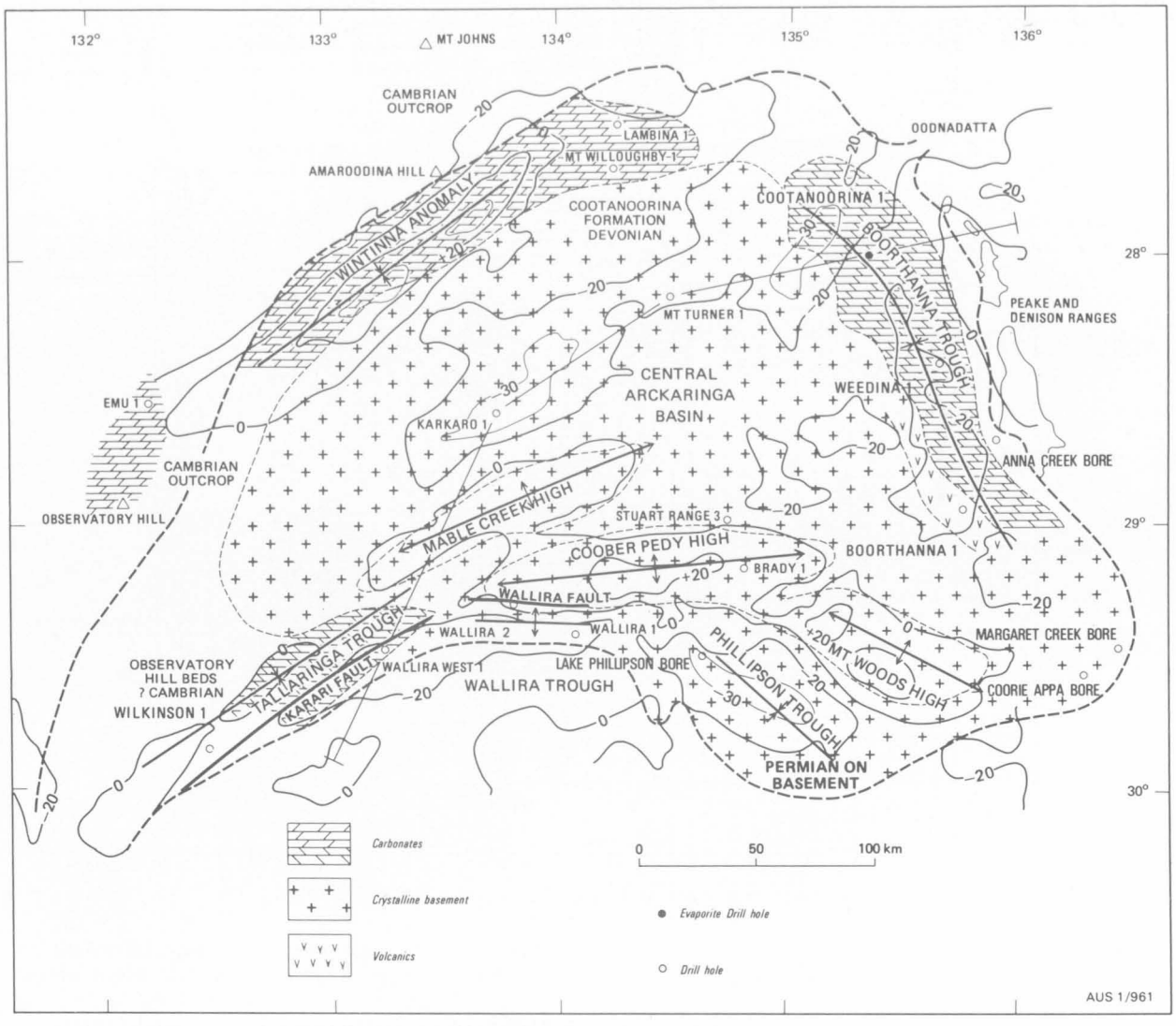

Fig. 38. Geology and structure of pre-Permian depositional structure, Arckaringa Basin (after Townsend, 1976).

The absence of Devonian rocks suggests that deposition may not have extended into the southern part of the Boorthanna Trough or was confined to the eastern side of the trough at this latitude.

Weedina No. 1 (28°28′31″S, 135°39′20″E) sited on the Warrangarrana structure in the northern section of the Boorthanna Trough was drilled by Pexa Oil N.L. It reached a total depth of 1625 m and penetrated 800–900 m of dolomite, dolomitic sandstone, and shale of probable Devonian age. A few minor anhydrite occurrences were noted. The dolomite in Weedina No. 1 is believed to have originated as an algal mat facies in an intertidal zone. The dolomitic beds occur in the interval 726.3–1624.3 m and are probably Devonian, but no fossils have been found. The small amount of anhydrite in the sequence commonly occurs in pods. Quartzite at total depth is possibly Ordovician.

BONAPARTE GULF BASIN

Until 1971, the evidence for evaporites in the Bonaparte Gulf Basin mainly revolved around interpretation of the origin of several anomalous structures on seismic cross-sections (Fig. 41). Only when Sandpiper No. 1 and Pelican Island No. 1 wells were drilled was the presence of evaporites in the basin established. Before that, Smith (1966), reporting a combined gravity and seismic survey in the Timor Sea/Joseph Bonaparte Gulf area by the Bureau of Mineral Resources in 1965, noted 'a few minor disturbances which appear as if they may be caused by intrusive material'. Several intrusive features were described by Arco and Australian Aquitaine (Arco, 1966) from the Sahul Shelf, and others were reported after further marine seismic surveys (Arco, 1967, 1969; Australian Aquitaine, 1968a, 1969; Jones, 1969). By 1973 fourteen diapiric intrusives had been mapped.

Generally, the surveys showed very strong discontinuities in the sedimentary sequence. But, except for the intrusive features, over large areas the beds are undisturbed or only mildly tilted. The distribution of intrusions is shown in Figures 42 and 43. The intrusions have remarkably straight sides, and the sedimentary beds continue uninterrupted but domed across their tops and, lower down, end abruptly against the vertical walls. The tops of the domes are covered by about 1200 m of sediment.

Intrusions in the southern Sahul Shelf are not randomly spread, but are found in zones thought to be fault-controlled Palaeozoic Sub-basin margins. They

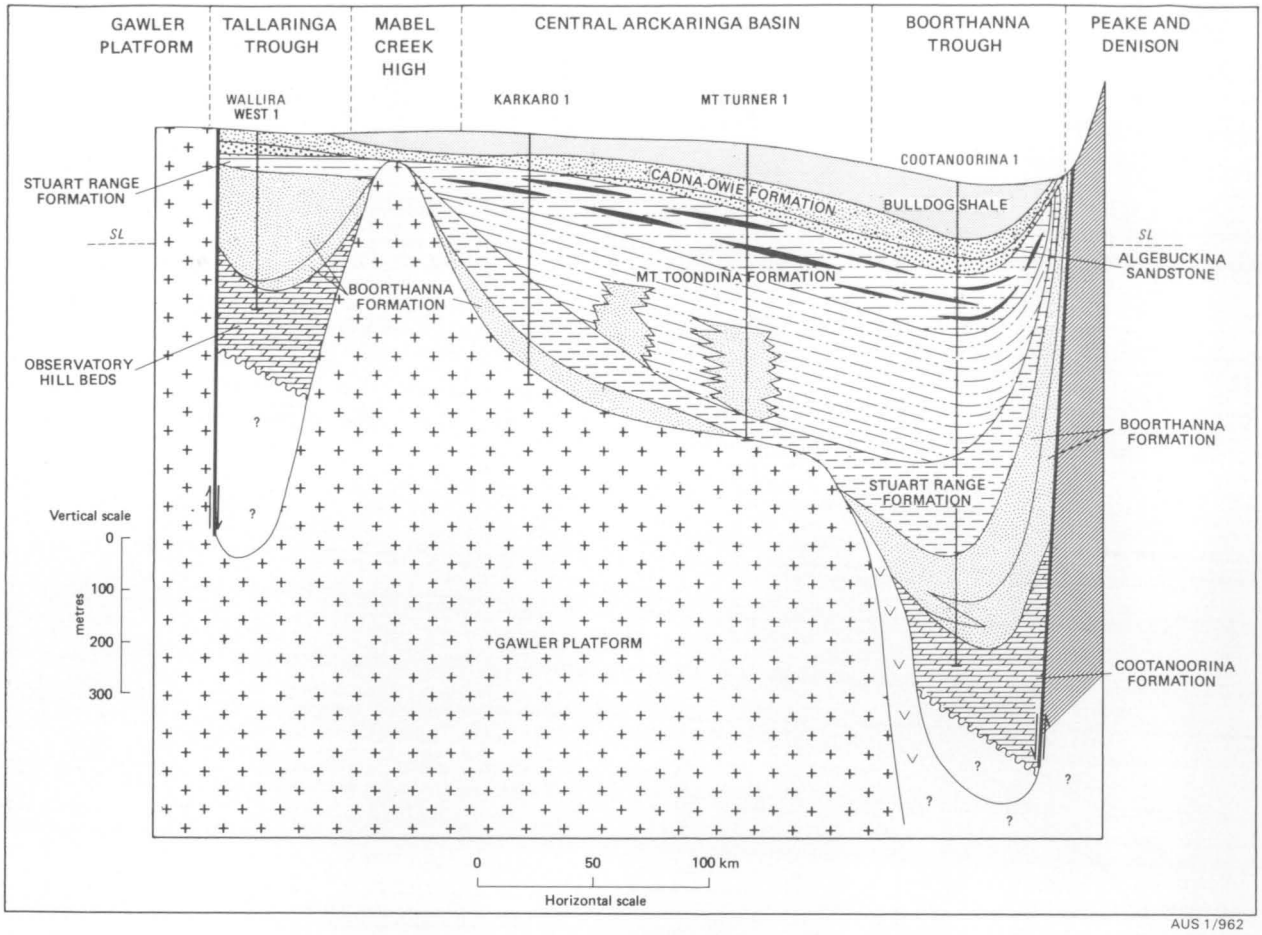

Fig. 39. Cross-section of the Arckaringa Basin (after Townsend, 1976).

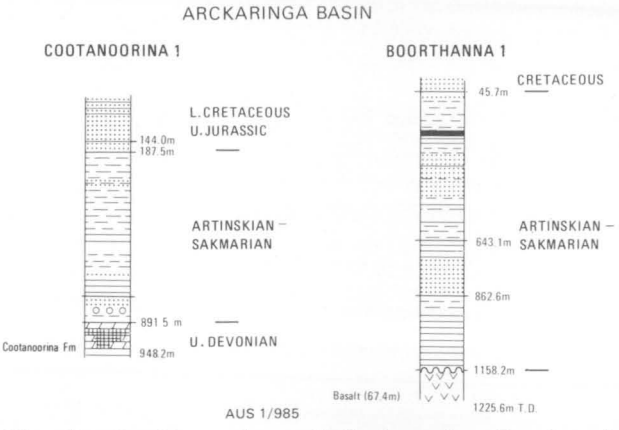

Fig. 40. Graphic sections of Cootanoorina No. 1 and Boorthanna No. 1 wells, Arckaringa Basin. For reference to symbols see Fig. 4.

show negative magnetic anomalies of up to 1 nT. The structures compare with those caused by salt diapirs in Germany and Gabon (Caye, 1968).

Australian Aquitaine had suggested, on the seismic evidence, that the intrusive bodies were salt domes, and in 1971, when Sandpiper No. 1 was drilled, that interpretation was proved correct. Sandpiper No. 1 (Fig. 44) intersected a cap-rock zone of disturbed sediments 809 m thick (944–1753 m) and reached total depth after penetrating 139 m of halite (1753–1892 m) (Arco, 1972a). The cap rock is considered to be Upper Devonian to Lower Carboniferous and the underlying halite, Upper Devonian (Fammenian). The cap rock is about the same age as the Ningbing Limestone of the onshore Bonaparte Gulf Basin. Movement of the diapir is thought to have ceased at least before the deposition of the Cretaceous-Jurassic Petrel Formation.

Pelican Island No. 1 was drilled by Arco Australia Ltd to a total depth of 1981.2 m, and the interval 1791.3–1981.2 m consisted of massive halite. No conventional cores were attempted in the halite sequence, but sidewall cores were obtained at 1890 m and 1966 m. The first recovered 3 cm, and the deeper 2 cm, of light grey transparent to translucent fractured halite. The sediments above the salt are identified as the Lower Carboniferous Bonaparte Beds; so the halite could also be Lower Carboniferous, but is more likely to be Devonian or older.

Recent papers describing the regional geological setting of the Bonaparte Gulf Basin include those of Laws & Brown (1976) and Laws & Kraus (1974). Crist & Hobday (1973) suggested that salt in the offshore Bonaparte Gulf Basin has migrated laterally in the basin towards boundary faults and movement has taken place at several times from Late Permian to Holocene. Edgerley & Crist (1974) concluded that the salt emplacement began with subsidence of an area between the Kimberley and Darwin Blocks, and formation of a shallow marine basin, bordered to the west and south by tilted fault blocks or terraces, intermediate in depth between platform and basin. The basin was restricted in area and depth and salt was deposited on the terraces and in the central basin. Further subsidence in Frasnian and Fammenian times permitted reef growth on the platform margins. Salt creeping over the

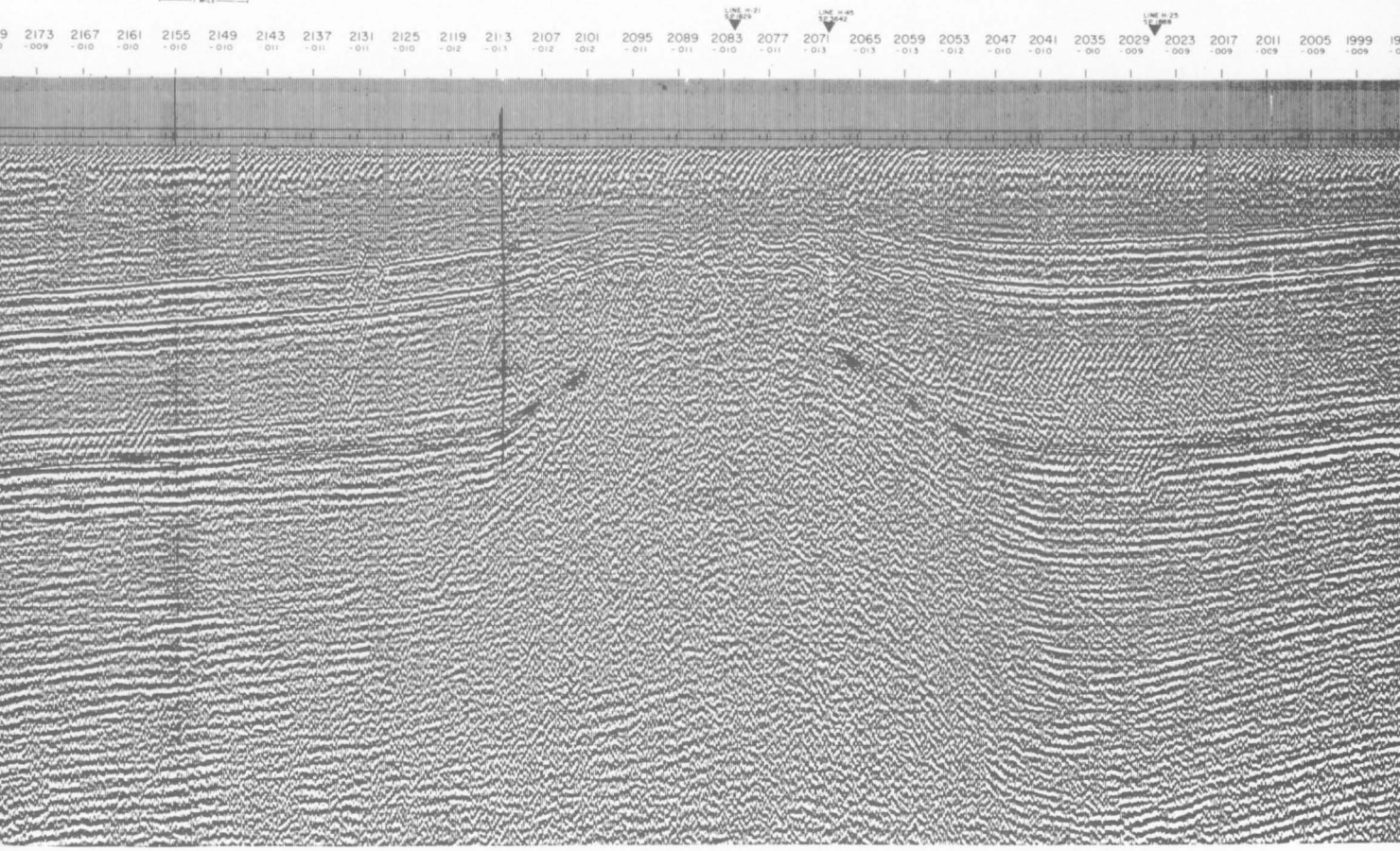

Fig. 41. Seismic cross-section of intrusive body, offshore Bonaparte Gulf Basin (Australian Aquitaine Petroleum Hyland seismic survey, line H22).

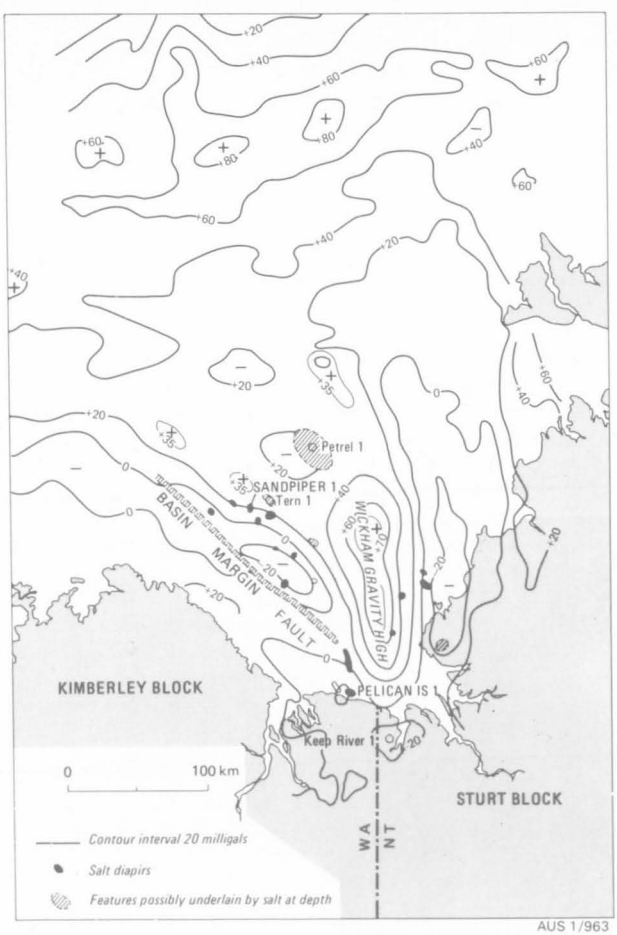

Fig. 42. Bouguer anomalies, salt diapirs, and probable salt-controlled structures, Bonaparte Gulf Basin (from Crist & Hobday, 1973)

Lacrosse Terrace rose up against the faulted basin margin, and in the deep parts of the basin salt ridges may have started to form by creep. The weight of Carboniferous sediments, thickened toward the central graben by epeirogenic movements, caused salt to flow on the Lacrosse Terrace and in the deep basin, forming sinks and ridges parallel to the western margin of the

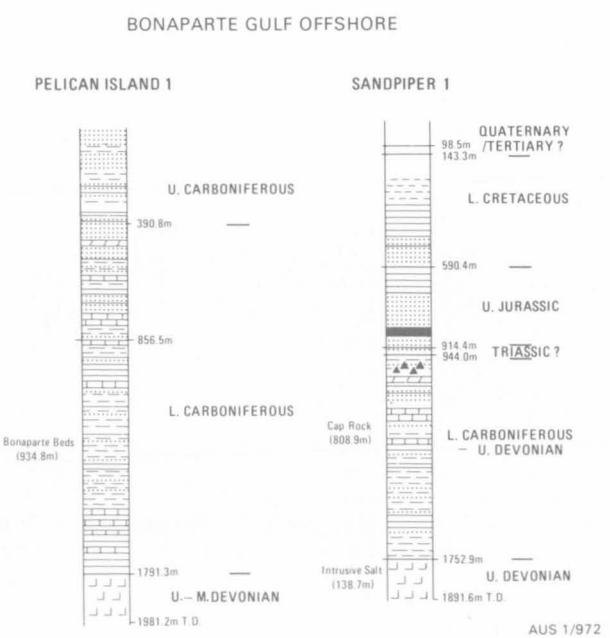

Fig. 44. Graphic sections of Pelican Island No. 1 and Sandpiper No. 1 wells, offshore Bonaparte Gulf Basin. For reference to symbols see Fig. 4.

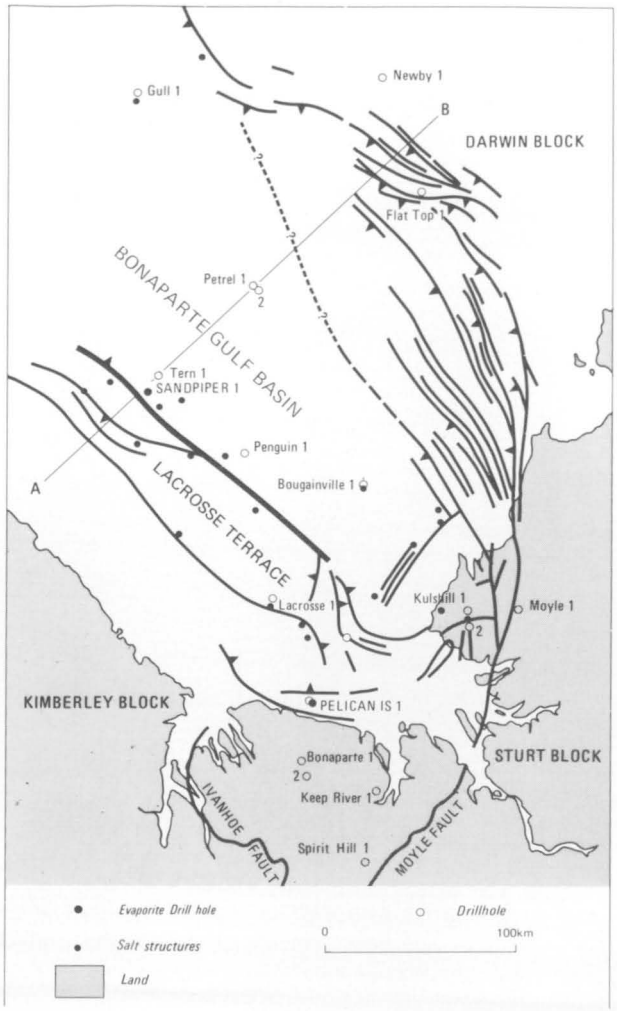

central graben. Locally, salt rose along the side of fault blocks. In the Permian and Triassic the salt ridges continued to grow, and salt moved laterally in the centre of the basin. Late Triassic-Early Jurassic tectonism caused rapid diapirism of salt into sediments along the Lacrosse Terrace hinge zone. Salt on the southern terrace rose only slowly, and may have pierced Lower Permian sediments. Repeated cycles of uplift, erosion and deposition resulted in a number of unconformities in the Jurassic, Cretaceous, and Tertiary sediments. Salt may have been injected into the diapirs and salt structures at a late stage to cause uplift of these beds.

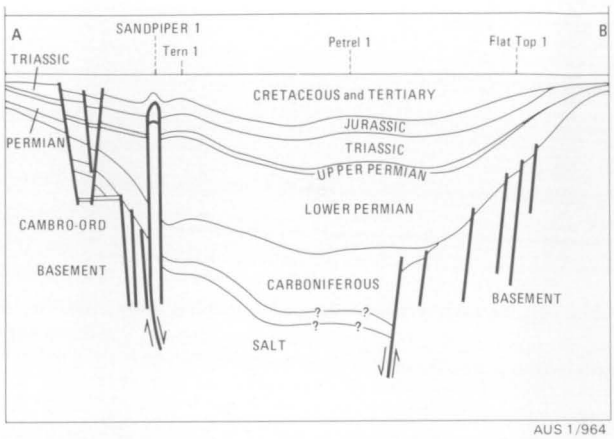

Fig. 43. Geological structure, Southeast Bonaparte Gulf Basin (from Edgerley & Crist, 1974).

CANNING BASIN

There are no surface exposures of bedded evaporites in the Canning Basin, but evaporites of probable Devonian age have been intersected in eight petroleum exploration wells. Most of the evaporites occur in the Carribuddy Formation, which underlies an area of about 210 000 km^2 in the Canning Basin, although evaporites are not present everywhere in the formation (Fig. 45).

The thickest sequence of evaporites (740 m) was penetrated in McLarty No. 1 well (Fig. 46); other major evaporite sequences were intersected in Kidson No. 1 (526 m), and Willara No. 1 (about 280 m). Evaporite sections penetrated in Parda No. 1 and Wilson Cliffs No. 1 were poorly developed, and only the top of the Carribuddy Formation was penetrated in Sahara No. 1. The bottom hole core (1060.7–1066.8 m) in Munda No. 1 well contains halite. Sections of the Carribuddy Formation have been penetrated in other wells, such as Kemp Field No. 1 and Matches Springs No. 1, but lack any noticeable thicknesses of salt.

Other evaporites have been intersected in Frome Rocks No. 1 (530 m) and Blackstone No. 1, but the origin and age of those in Frome Rocks No. 1 are unknown, and those in Blackstone No. 1, whose presence was inferred from increased salinity of drilling fluids, could only perhaps be correlated with the Carribuddy Formation. Minor evaporites have been noted in the Devonian reef complex on the Lennard Shelf (Playford & Lowry, 1966).

The Fitzroy Graben (Trough) and the Broome Platform continue essentially uninterrupted into the northeast Canning Basin (Fig. 47). The equivalent of the Broome Platform, the Crossland Platform, appears to extend to the southeast and eventually terminates near marginal Precambrian outcrops in the Webb 1:250 000 Sheet area. In the southeast extension of the Fitzroy Graben, the Gregory Sub-basin, the sediments are up to 9 000 m thick. There is a major unconformity in the sequence, and Permian rocks rest unconformably on the eroded Carboniferous sediments. In Lake Betty No. 1 and Point Moody No. 1 wells the Permian Grant Formation overlies Carboniferous sequences about 900 m and 466 m thick, respectively. The Point Moody well was still in Lower Carboniferous at total depth, so an appreciably thicker Carboniferous section may be present in this area. Gravity and magnetotelluric surveys in this area suggest the presence of salt (Australian Aquitane Petroleum, 1968b).

After the discovery of evaporites in Frome Rocks No. 1 WAPET was granted Temporary Reserve 1691-H to prospect for evaporites and associated minerals over a large part of the Jurgurra Terrace and the southern part of the Fitzroy Graben (Lehmann, 1969).

A detailed gravity survey, together with a reinterpretation of previous geophysical data and later seismic work outlined the extent of the Frome Rocks salt dome and indicated other possible salt-cored structures.

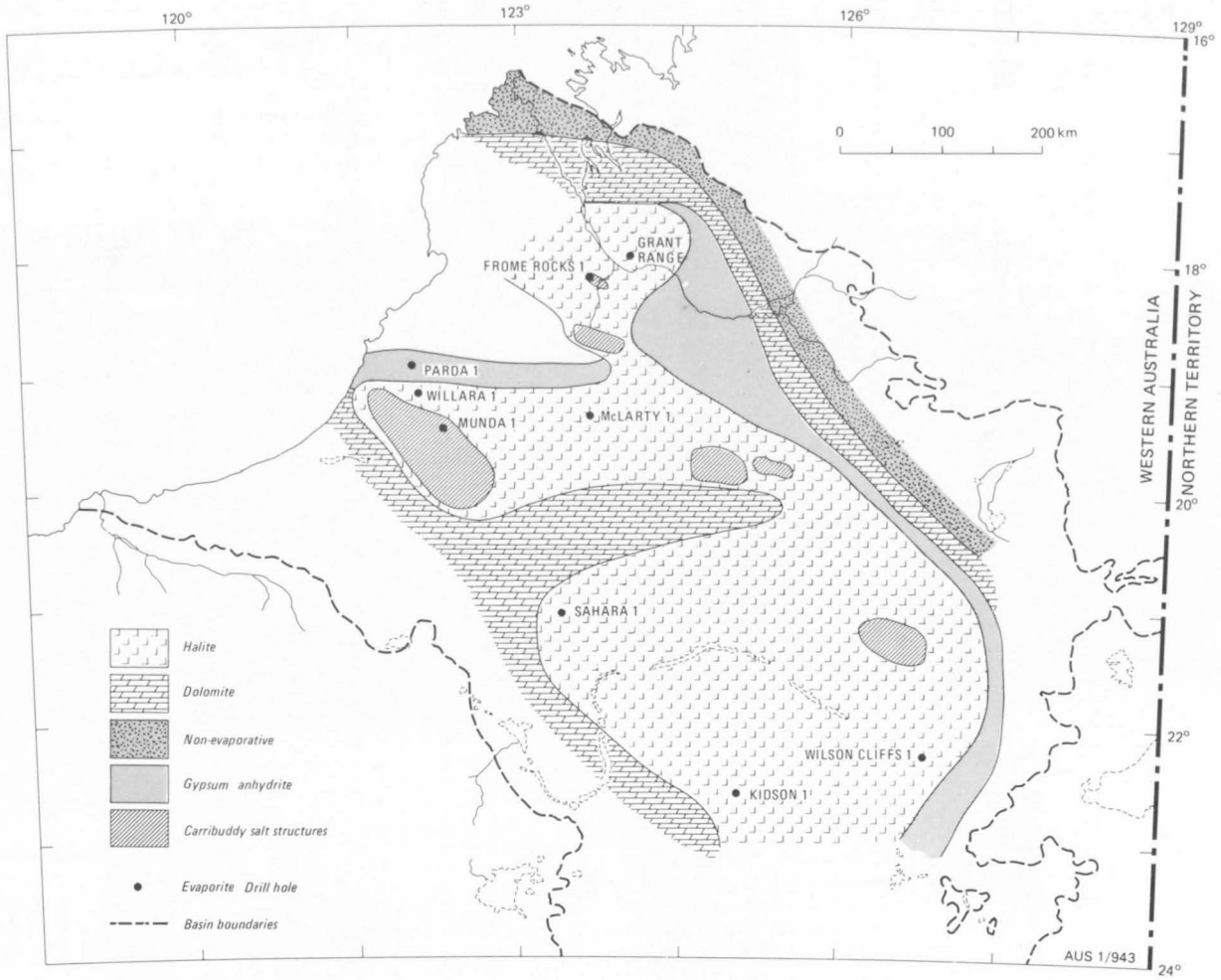

Fig. 45. Maximum extent of evaporite minerals in the Carribuddy Formation, Canning Basin.

No salt-induced structures were detected by a similar program in the Barlee area of the western part of the Fitzroy Graben.

Doran Core Hole No. 1 was drilled on the crest of the most prominent geophysical anomalies, about 16 km west of the Frome Rocks No. 1. No evaporites were encountered to total depth of 763 m.

Carribuddy Formation

The Carribuddy Formation is thickest in the centre of the Kidson Sub-basin (Figs. 48, 49) and the pre-Permian sequence there is (slightly modified from Koop, 1966, and Creevey, 1971):

TOP	—Mellinjerie Limestone	— Frasnian to ?Givetian (probably basal Frasnian)
	Tandalgoo Red Beds	— Gedinnian
	Carribuddy Formation	— ?Devonian
	Nita Formation	— Llanvirnian to Llandeilian
	Goldwyer Formation	— Llanvirnian to ?Llandeilian
	Willara Formation	—Arenigian
BASE—	Nambeet Formation	— Tremadocian ? to Arenigian

There are no marked lateral variations within the evaporite sequence, although it seems that some regional facies changes to carbonate and sulphate sequences are present. Some changes may have been removed during erosion of the sequence below the Permian unconformity. In early interpretations, the distinct increase in carbonate (dolomite) content was assigned to the lower part of the Carribuddy Formation, and was called the Nita 'Facies'. This has since been defined as the Nita Formation, which, on the evidence of conodont faunas found in several wells, is Llanvirnian to Llandeilian.

Glover (1973) analysed the halite-bearing cores from the Carribuddy Formation, and concluded that the low bromine content was in accord with the absence of potassium salts. The halite is colourless to red-brown, the latter perhaps caused by precipitation of ferric hydrate, a precursor of hematite, from percolating oxygenated water, which dissolved and reprecipitated the halite. The bromine content is generally greater in the red-brown halite than in the colourless, suggesting that the colourless variety was not dissolved and reprecipitated. In addition, Glover concludes that the diagenetic sequence in the halite of the formation is halite, dolomite and anhydrite, quartz, and hematite pigment (Fig. 50). Colour patterns in the halite veins indicate that the minerals have not moved significantly since pre-Middle Devonian times. Most pigment in the redbeds with halite has probably formed in place by diagenesis, but some could have been transported to the basin.

Age of the Carribuddy Formation

There are no published reports of any internal evidence for the age of the Carribuddy Formation, although McTavish (personal communication) states

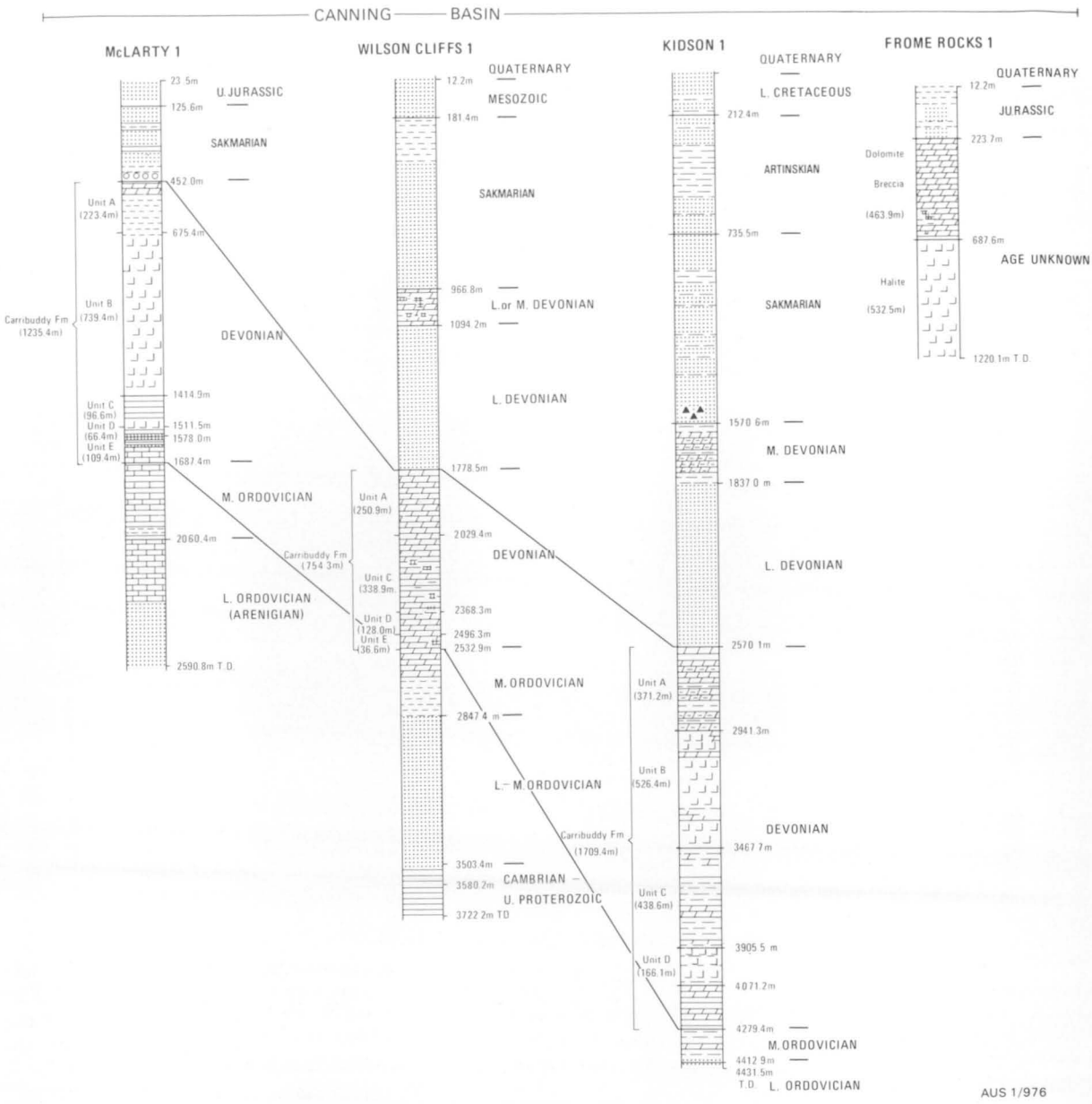

Fig. 46. Graphic sections of wells penetrating evaporites in the Canning Basin. For reference to symbols see Fig. 4.

that palynomorphs, conodonts, ostracods, foraminifera, and fish scales have been recorded and discussed in reports by WAPET and TOTAL, and he favours a Devonian age. More specifically, McTavish indicated that there were possible Lower Devonian fish scales about 60 m from the top of the formation in the upper part of the Carribuddy Formation penetrated in Kemp Field No. 1 well.

Potassium-argon determinations on clays from the Mellinjerie Limestone (core no. 2), Tandalgoo Red Beds (core nos. 3–7), and Carribuddy Formation (core nos. 8–10) in cores from Wilson Cliffs No. 1 well gave an Early Devonian age (K. J. Creevey, personal communication).

The Tandalgoo Red Beds, that commonly overlie the Carribuddy Formation, contain probably aeolian sands, and rare agnathid and acanthian fish scales with Early Devonian affinities have been described from beds between 1353.0 m and 1345.5 m in Wilson Cliffs No. 1 well (Gross, 1971). The specimens appear to be abraded and could have been reworked. This implies that the lower part of the Tandalgoo Red Beds or the Carribuddy Formation could be Early Devonian.

If the Carribuddy Formation is older than Early Devonian, it could be correlated with the Dirk Hartog Formation of the Carnarvon Basin, a view favoured by some oil company geologists. Others favour correlating the Tandalgoo Red Beds with the Dirk Hartog Formation (Playford & Cope, 1971), though, from the evidence of the fish scales and a recent discovery of Devonian spores in the Upper Tandalgoo Red Beds (K. J. Creevey, personal communication), this correlation does not appear to be valid.

Similarities between the Tandalgoo Red Beds and the Mereenie Sandstone of the Amadeus Basin suggest that the evaporites may be Ordovician, because there is ample evidence of evaporitic conditions in the pre-Mereenie Cambro-Ordovician Larapinta Group.

Other evidence supporting a Devonian age for the Carribuddy Formation is: Lower Devonian, Middle

Fig. 46 continues on next page.

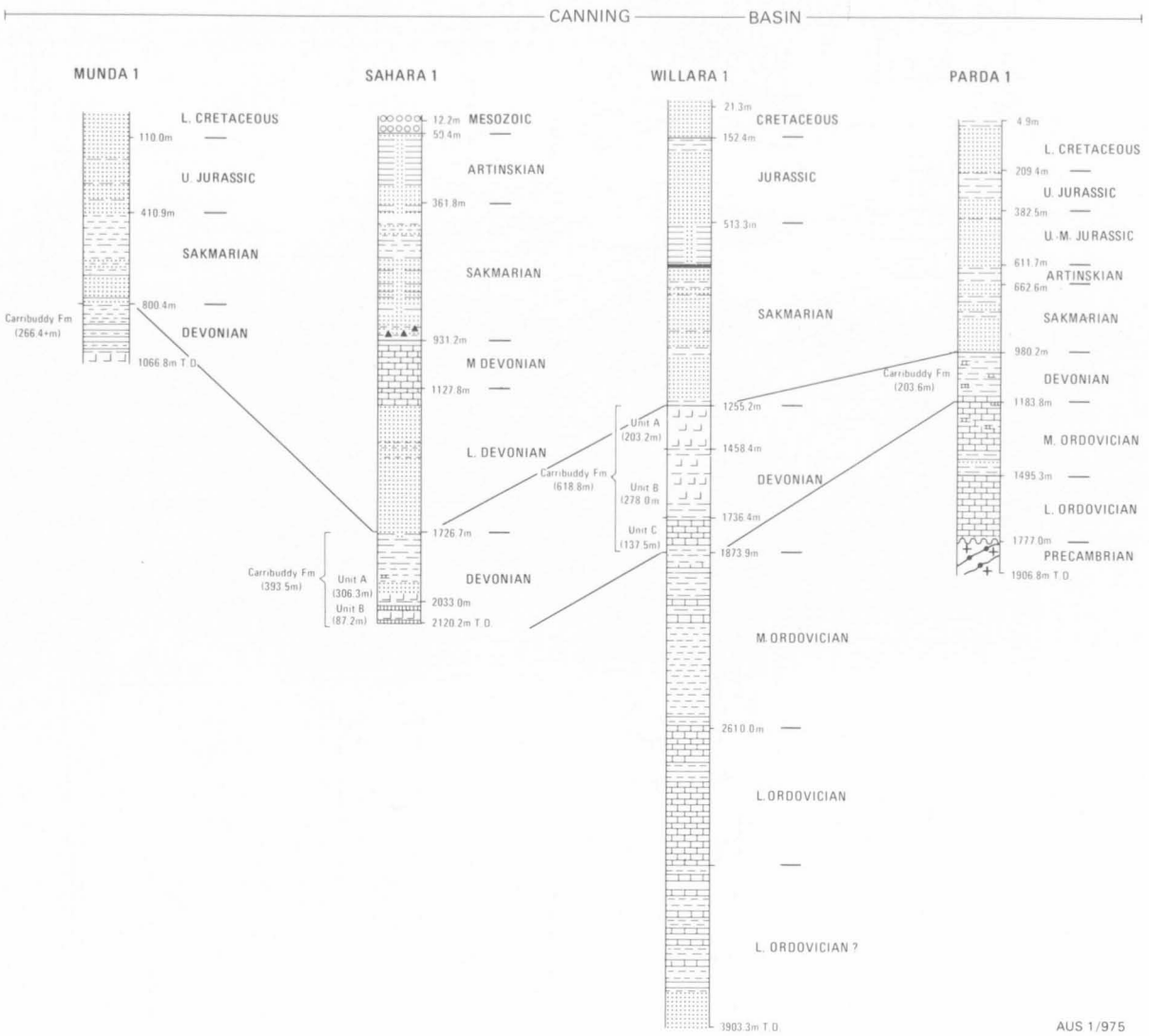

Devonian and/or Upper Devonian spores and pollen, and a conodont related to an Ordovician morphotype, in Contention Heights No. 1 (Burne, *in* Gorter & others, 1979); poorly preserved Endothyrid foraminifera in ?Devonian cores no. 17 (3742.1–3744.5 m) and no. 18 (3864.3–3867.4 m) in Kidson No. 1 (Burne, *in* Gorter & others, 1979); sparse Devonian spores in Parda No. 1 (Burne, *in* Gorter & others, 1979); and Devonian microflora in core no. 5 (1741.6–1743.5 m) of Willara No. 1 (McTavish, unpublished report for WAPET).

In Parda No. 1, Willara No. 1, and McLarty No. 1 wells the Carribuddy Formation is overlain unconformably by Lower Permian sediments.

Thus, the age of the Carribuddy Formation is between Early Ordovician and Early Devonian, and the bulk of evidence appears to favour the Devonian.

Salt structures

Structures in the Canning Basin that have been related to the evaporite sequences in the Carribuddy Formation have been interpreted from seismic interval velocities. The distribution of salt in the Carribuddy Formation, as shown by seismic surveys, suggests the presence of solution features. These are thought to have formed before or during the Permian, as Permian sediments appear to thicken off the residual salt. In this way salt solution structures may form anomalous zones that indicate closures (Fig. 51). For example, Willara No. 1 is not on a structure, but may be on a salt remnant; probable salt anticlines and collapse structures formed by salt leaching are present on the Broome Arch. Similar features in the North Sea have been described by Lohmann (1972), in south-western Ontario by Grieve (1955), and in the English Zechstein by D. B. Smith (1972).

The thickness of the Carribuddy Formation is commonly modified by salt solution in the region of fracture zones. For example, in the Munro area the Carribuddy Formation is dissolved over an old fracture system in the underlying Goldwyer Formation.

The beds in the Kidson Sub-basin are only gently folded, and because of this there has probably been little movement in the salt members. Most structures probably formed by compaction, although interpretation of recent seismic surveys (Angove & Douglass, 1972) has suggested that diapirism has caused overturning at shallow levels. On some lines, the seismic cross-section has been likened to those across salt domes in the North Sea. The extent of piercement is uncertain, but appears to be limited to deeper levels; in the section above the piercement zone there appears to be arching of the sediments, suggesting upward displacement. The preponderance of multi-cycle events deep in the section is consistent with diapirism.

In the southeast of Morris 1:250 000 Sheet area, a probable salt anticline occurs in the lower part of the

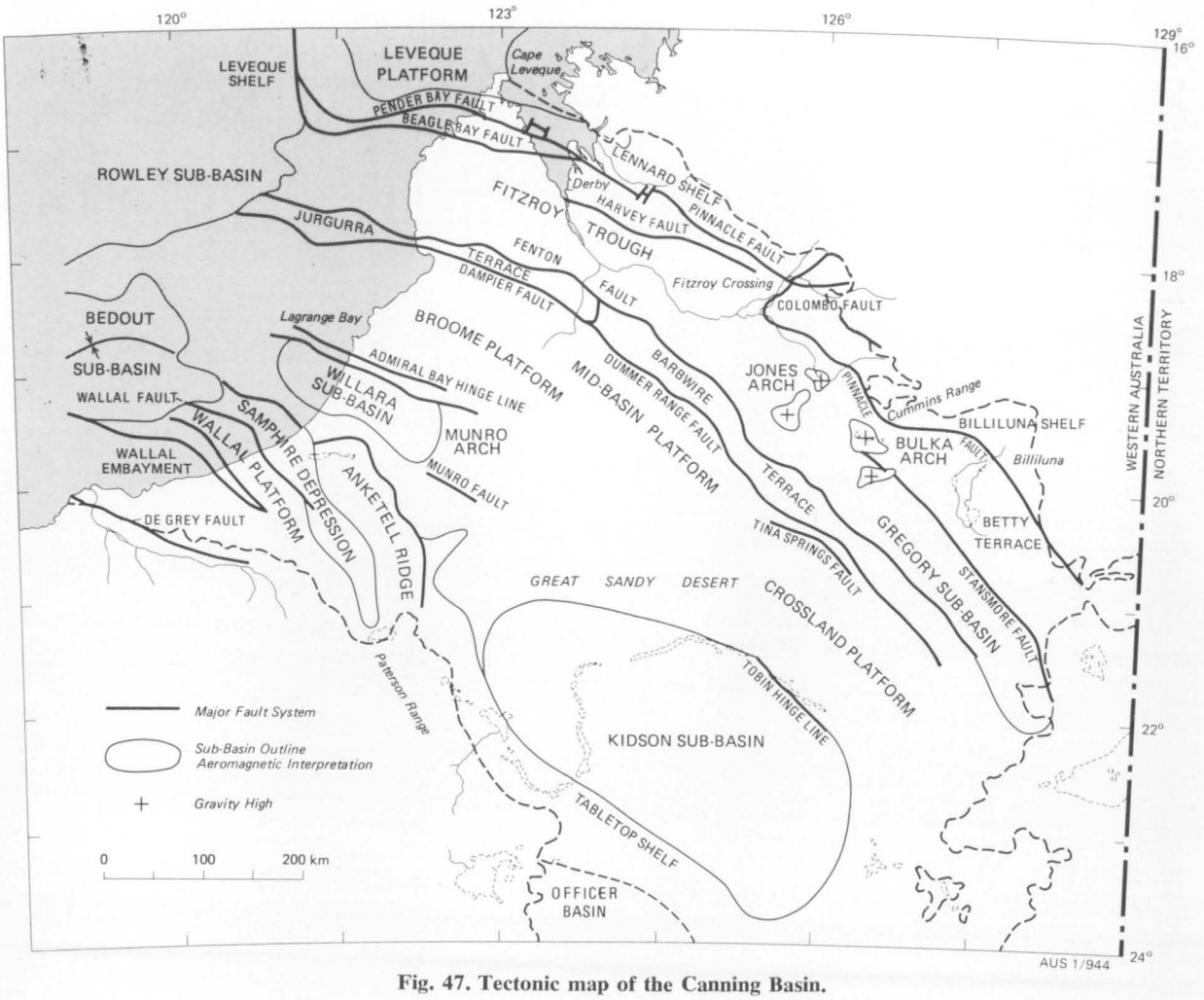

Fig. 47. Tectonic map of the Canning Basin.

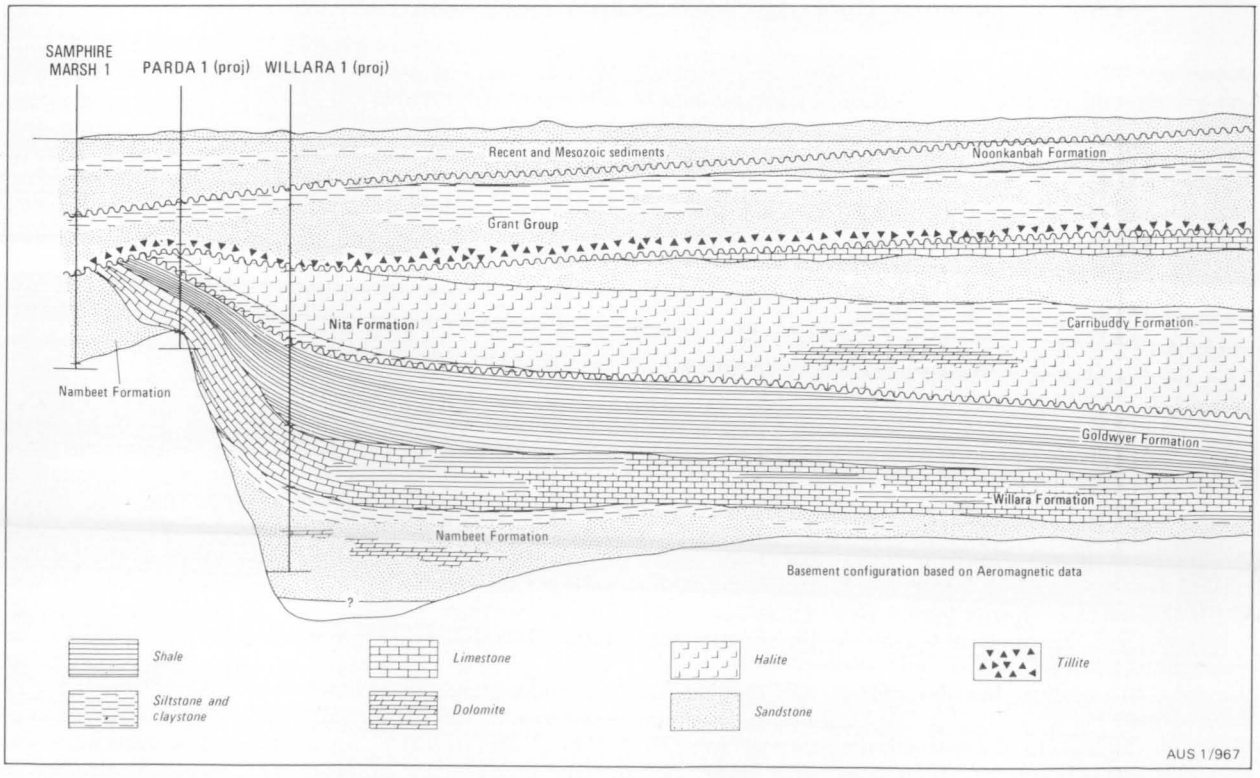

Fig. 49. Cross-section of the Kidson Sub-basin, Canning Basin.

Fig. 49 continues on next page.

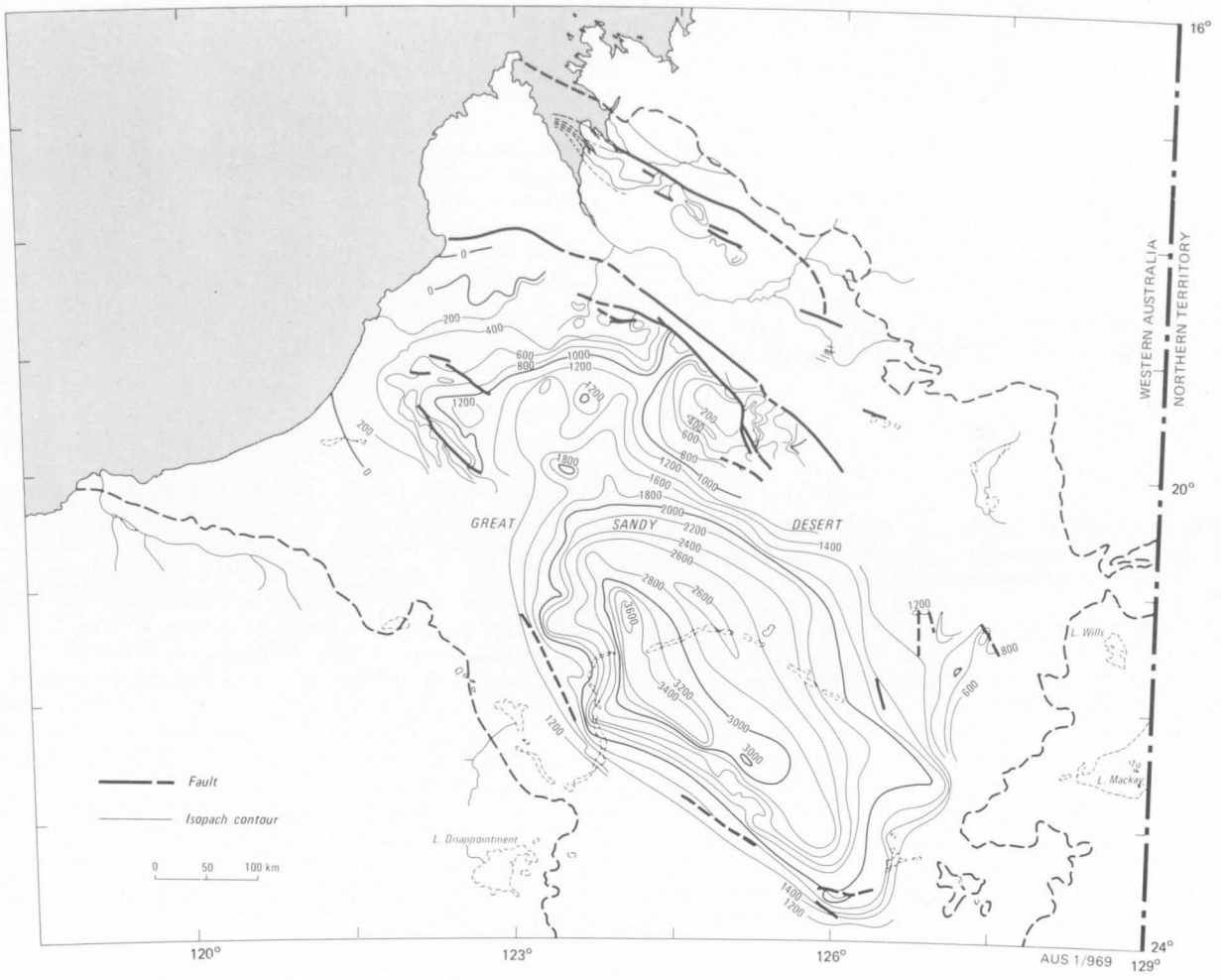

Fig. 48. Isopach map of the Carribuddy Formation, Canning Basin.

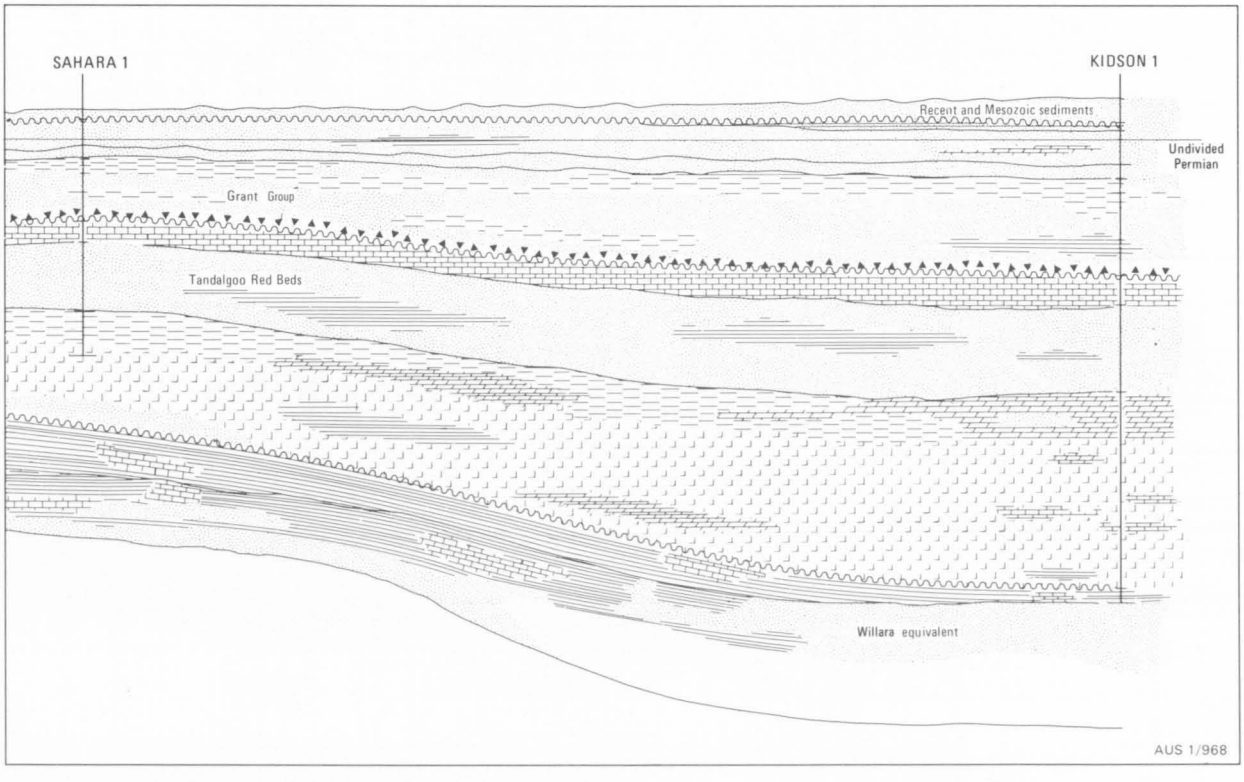

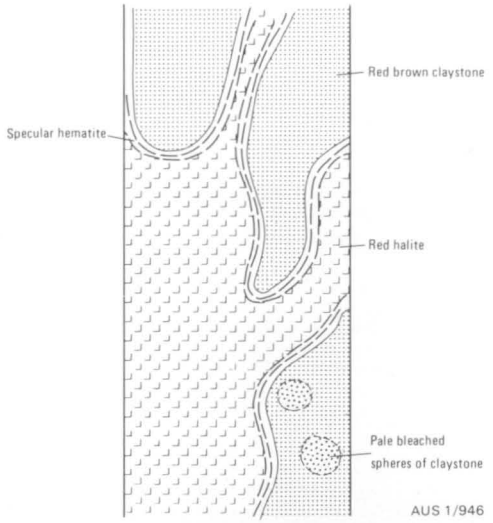

Fig. 50. Sketch of part of core no. 19, Kidson No. 1 well. Secondary red salt encasing hematite-sheathed fragments of red-brown claystone.

sedimentary sequence, which may be Proterozoic. Movements are apparent in the intervals late Precambrian to near top Goldwyer Formation, and near top Carribuddy Formation to base Permian unconformity, and a quiescent period in the interval of the Carribuddy Formation. The structural style fits well with salt tectonics, with broad deformation on the late Precambrian level, narrower on top upper Proterozoic and near top Goldwyer Formation, and the final phase on a near-surface fault (Pinchon, 1973).

On the Barbwire Terrace a probable salt anticline occurs immediately north of the Dummer Range Fault, and on the Jurgurra Terrace a fault-bounded anticline may be related to the Frome Rocks structure, which lies 20 km further west. In the Willara Sub-basin salt anticlines are interpreted along the Munro Fault, where salt migration was associated with renewed movements along the fault. Emplacement probably took place no later than the Upper Triassic, because Early Jurassic sediments are not folded by the structures.

Several domes have been indicated by seismic and gravity surveys, such as at Logue and Doran. Gravity maxima over the crests of the domes suggest that they are probably not the result of salt intrusion. A core hole drilled on the Doran structure to 2699.7 m terminated in Fammenian siltstone and shale.

In the Fitzroy Graben the sediments are more strongly folded and faulted; at least one salt dome, Frome Rocks, has been discovered, next to the graben on the Jurgurra Terrace.

In Frome Rocks No. 1 well 530 m of evaporites was intersected. About 460 m of dolomite is underlain by halite. The dolomite is thought to be a cap rock on the salt, but its composition is unusual, as cap rocks mostly consist of limestone and anhydrite or gypsum. The origin of the salt in Frome Rocks No. 1 well is not certain. Some geologists consider that the dome may have resulted from tectonic movements, because other wells drilled on similar anomalies failed to intersect salt. In early interpretations the salt was shown intruded along the Fenton Fault and probably originating in beds in the deeper parts of the Fitzroy Graben. Later workers considered that this picture is probably not correct and that there is no clear evidence of intrusion along the fault. The Matches Spring well was expected to intersect a thick sequence of marine shales and dolomites of the Carribuddy Formation, but

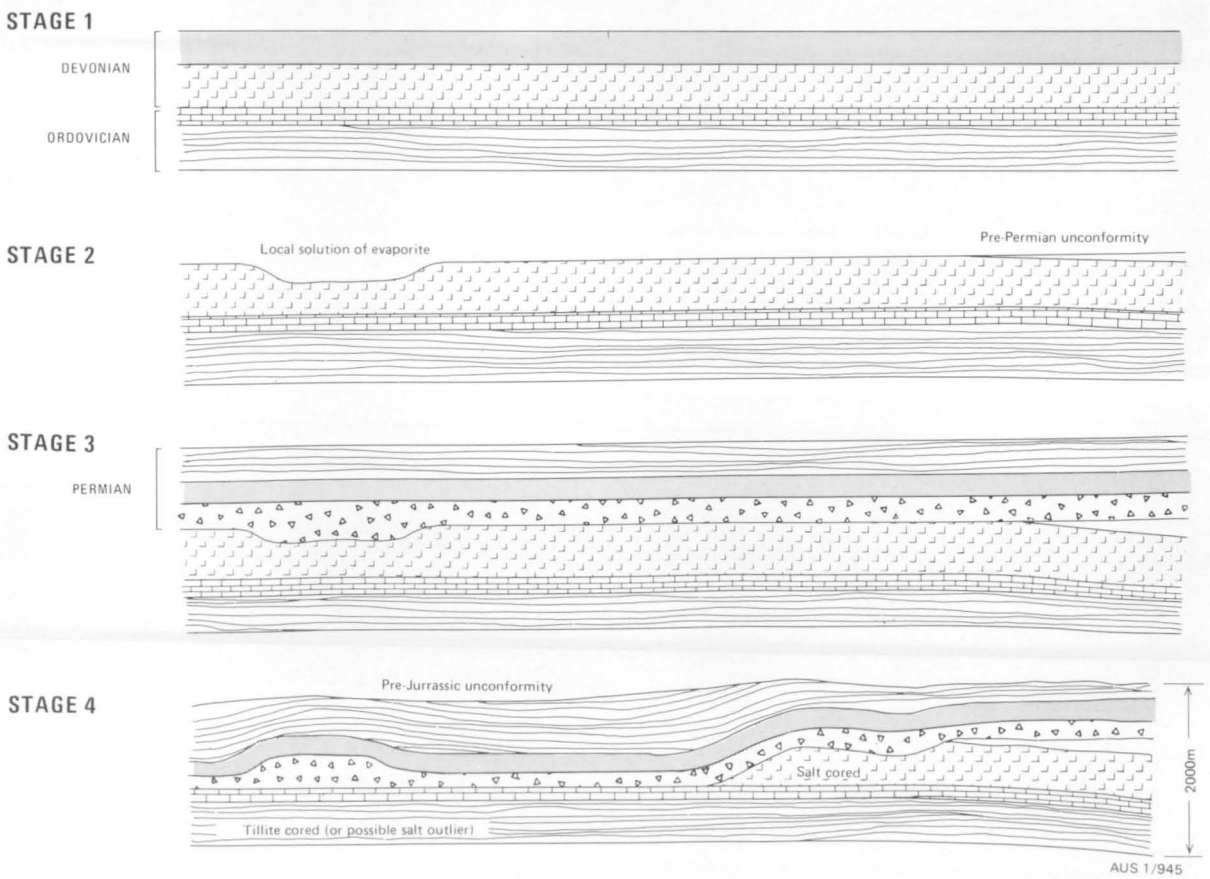

Fig. 51. Sequence of salt solution and sedimentation, Canning Basin (from Munda No. 1 well completion report).

only 180–200 m was penetrated. Either faulting or thinning of the units must be invoked to explain the reduced section: but if the formation is thinning, then it appears unlikely that the Carribuddy Formation is the source of the Frome Rocks salt.

Besides the evidence from Frome Rocks No. 1 for the presence of evaporites in the Fitzroy Graben, there are other indications of thick salt beds and their continuation into the northeast part of the Canning Basin. On the north side of the Fitzroy Graben, Blackstone No. 1 well penetrated red siltstone with evaporites, of Givetian age, overlying an Ordovician sequence. The evaporites were indicated by a marked increase in salinity of the drilling fluid. In Blackstone No. 1 well completion report it is stated that the 'Blackstone Formation' (sic; amended to Poulton Formation) contained traces of salt. It is likely that this red bed sequence contains crystalline halite. Although no halite was seen in cuttings or cores, as this part of the well was drilled using aerated water as the drilling fluid, the salinity of the water rose from 6800 ppm NaCl at 1852 m to 48 000 ppm NaCl at 2226 m. Such an increase in salinity while penetrating an essentially tight formation can only be attributed to solution of rock salt. This siltstone with evidence of evaporites in the succession, has been named the Poulton Formation, and indicates environmental similarities with the Kidson Sub-basin. The Poulton Formation is probably best correlated with the Carribuddy Formation.

Palaeogeography

The Kidson Sub-basin and Fitzroy Graben were apparently connected until Carboniferous time, but Carboniferous sediments were deposited only in the Fitzroy Graben. Earlier in the Palaeozoic, during the period of salt deposition, the Broome Platform, although acting as a partial barrier, may not have been sufficiently pronounced to completely sever connections between the two basins, and channels probably existed across the swell. From the middle Devonian to Permian the source of sediments lay partly on the Broome Platform.

Burne (*in* Gorter & others, 1979) recognises three phases in the history of the Devonian of the Canning Basin. A pre-evaporite phase is represented by a hiatus of 40 m.y., during which time the land surface was gradually and evenly lowered. The succeeding evaporite phase saw halite deposited and localised in the centre of the basin with a progression outwards through sulphates and dolomites and, finally, non-evaporitic sediments in the north. The evaporite minerals—halite, dolomite, anhydrite and barite—together with the low initial bromine content of the halite indicate that the evaporites did not arise from total desiccation of the original brine. Diagenetic changes in the halite indicate that during deposition the environment was subject to lowering of groundwater salinity and local oxidising sub-surface conditions.

In the post-evaporative red-bed phase the marginal clastics migrated across the basin, forming extensive sand sheets with aeolianite dunes and some fluvial channels. An arid desert environment is inferred, and the unit probably represents an extension of the Mereenie Sandstone from the Amadeus Basin.

The model of evaporite deposition proposed is a deep water desiccating basin as proposed by Hsü (1971). This model envisages—

- A deflating pediment covered by a marine incursion.
- Isolation of the basin from the ocean.
- Successive desiccations and inundations.
- Constant brine dilution by runoff.
- Formation of sabkha supratidal flats on margins bared by desiccation with pore water reactions producing some of the diagenetic modifications.

Discussion and conclusions

No potentially economic minerals are known in the evaporite deposits and it is unlikely that the halite could be exploited, as the top of the shallowest deposits occurs at a depth of about 700 m, at Frome Rocks. If the Kidson Sub-basin was a more or less symmetrical basin with the bittern salts concentrated in the residual brines, it would seem logical to expect the more soluble salts of the evaporite sequence to be preserved in or near the geographical centre of the basin. The geography of the mid-Palaezoic basin may have been such that slight irregularities of the basin floor would allow concentration of the more soluble salts in small ponds, situated in depressions, or in smaller satellite basins, separated from the open sea by the main evaporite basin, in a similar manner to that proposed by Goldsmith (1966, 1969). If these beds were of sufficient thickness and lateral extent they could possibly be located and outlined by seismic surveys.

CARNARVON BASIN

Evaporites were first reported in the Gascoyne Subbasin from a WAPET deep test well, Dirk Hartog No. 17B, drilled in 1957 on Dirk Hartog Island in Shark Bay (Fig. 52). Anhydrite occurs in the Dirk Hartog Formation, a predominantly dolomitic sequence, first named the Dirk Hartog Limestone by McWhae & others (1958) and amended by Henderson & Shannon (1966). The formation, which is known only from drill holes is Late Silurian (Öpik *in* Glenister & Glenister, 1957; Philip, 1969).

Only Tertiary rocks crop out close to Shark Bay, but cross-sections by Condon (1965) suggest the presence of over 6000 m of sedimentary section, consisting primarily of Ordovician Tumblagooda Sandstone overlying Precambrian granulitic rocks and overlain by Dirk Hartog Formation, possible Devonian rocks, Lower Permian, and thin Cretaceous and Tertiary rocks.

Geary (1970) described Pendock No. 1 well, an offshore well which reached a total depth of 2501 m and bottomed in the Upper Silurian Dirk Hartog Formation (Fig. 53). Anhydrite occurs mainly in the upper cryptocrystalline dolomite.

Yaringa No. 1 well (TD 2288.4 m), drilled by Continental Oil Co. of Australia, discovered 36.2 m of salt in eight beds in the Dirk Hartog Formation. Until Yaringa No. 1 was drilled, there was no evidence of halite in the Dirk Hartog Formation.

Exploration of the Dirk Hartog Formation for potash deposits, the first exploratory drilling specifically for evaporites, was undertaken on a farm-out arrangement to Magellan Petroleum (N.T.) Pty Ltd from Continental Oil Co. of Australia Ltd and Australian Sun Oil Co. Ltd. Two exploratory holes were drilled: Hamelin Pool No. 1 (TD 1595.3 m) and No. 2 (TD 1219.2 m). In Hamelin Pool No. 1 seven beds,

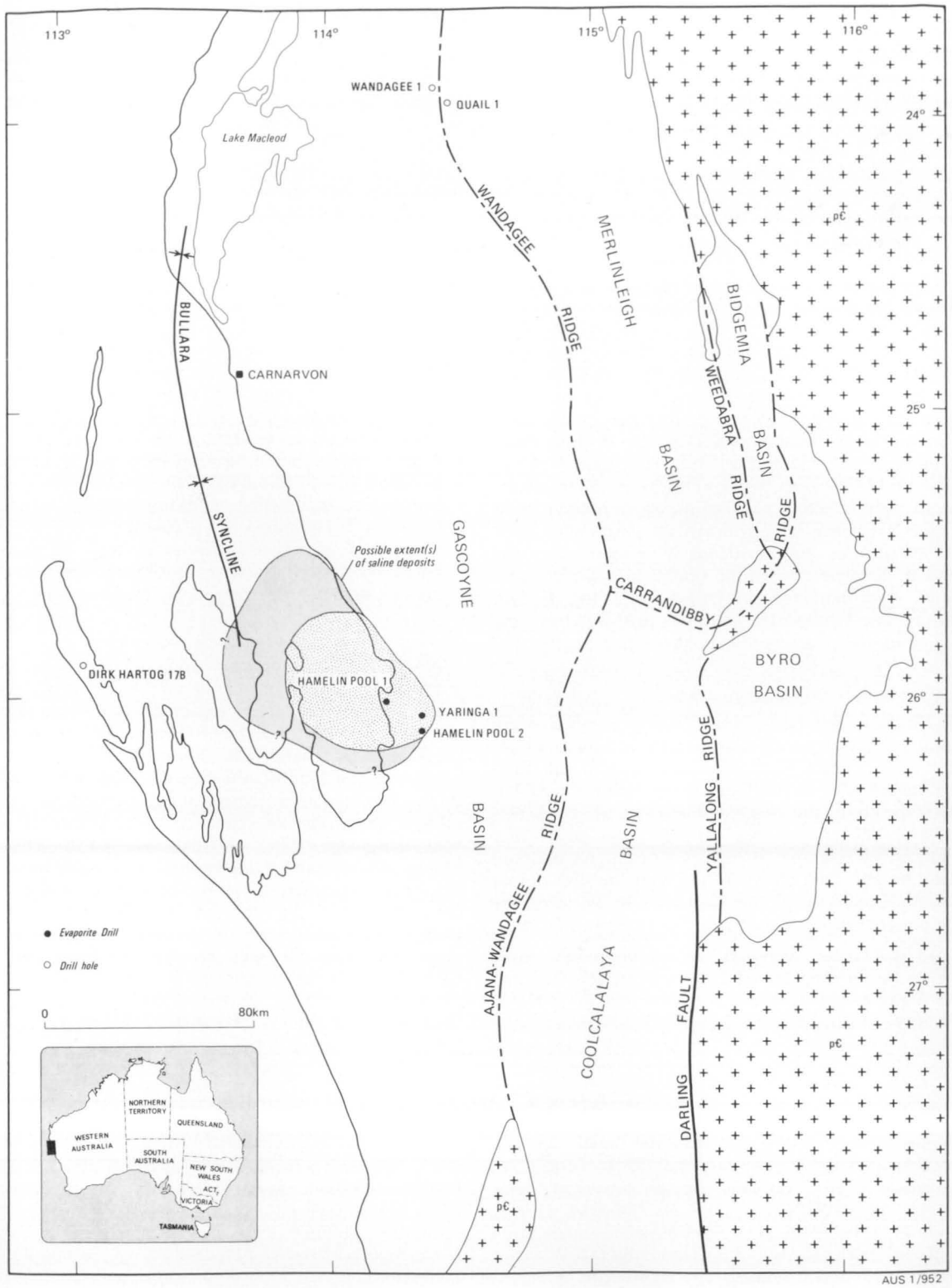

Fig. 52. Location of wells, and known and possible extent of evaporites, Carnarvon Basin.

totalling 22.9 m of salt, were recognised, and in Hamelin Pool No. 2, 5.2 m of salt is distributed over three beds of varying thickness. The thinning of salt beds in Hamelin Pool No. 2 suggests that the well site is near the southeast edge of the saline deposits. In Hamelin Pool No. 1 the upper salt beds are not present, either because of erosion or non-deposition, but the remaining beds are about the same thickness. Pendery (1970) suggests that the evaporites may thicken to the northwest or north from the Yaringa location. However, the evaporite sequence is apparently undetectable by geophysical methods and may be relatively thin throughout the area. The correlation of the salt beds between the wells is shown in Figure 54.

Analyses of the Dirk Hartog evaporites show that salt bed 2, present only in Yaringa No. 1, is the most prospective for possible bittern salt deposition, in that bromine values are high (up to 330 ppm) and the

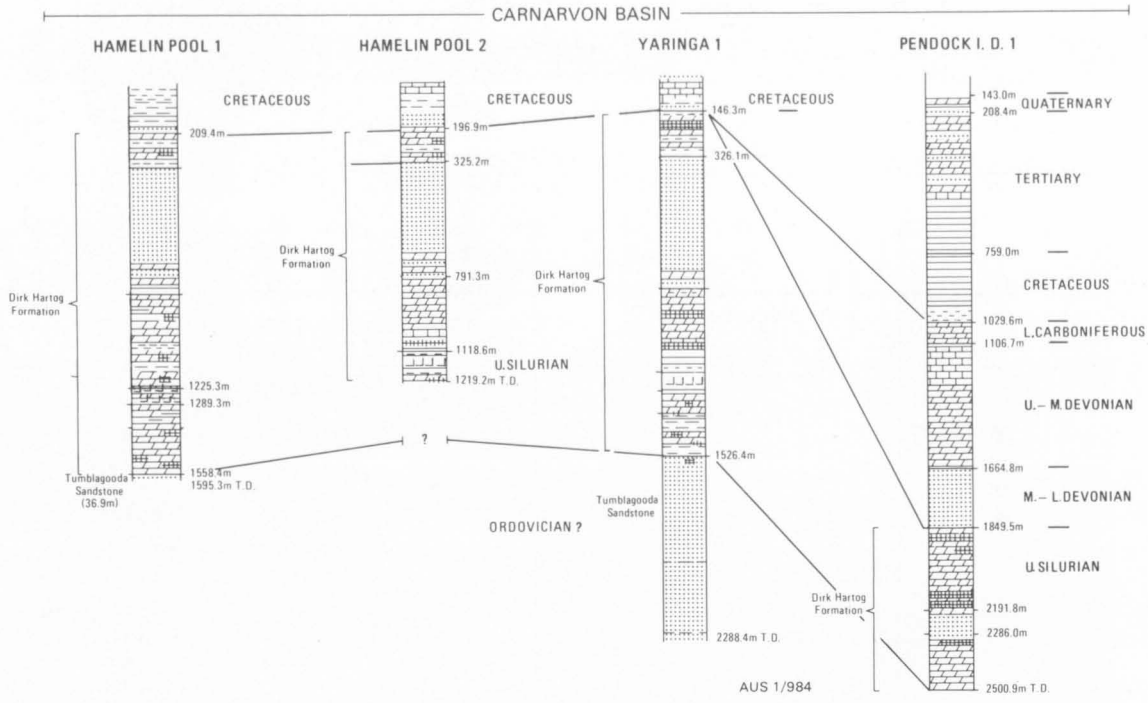

Fig. 53. Graphic sections of wells (excluding Dirk Hartog No. 17B) penetrating evaporites in the Carnarvon Basin. For reference to symbols see Fig. 4.

bed is relatively thick. Salt beds 3 and 4 may also be of interest, as they too have high bromine values and would appear to be more persistent laterally. Sylvite is reported in small amounts in the halite (GSWA, 1975).

In some parts of the Carnarvon Basin, local doming of formations may be related to diapirism (Sturmfels, 1952). Domes occur in Permian sediments near Hill Springs on the west side of the Kennedy Range, and small circular structures are present near the Lyndon River. However, it has been pointed out that derivation of thick evaporites would be most unusual from the thick glacial Permian rocks of the Lyons Group, which underlies the area, and the source may lie in the older Palaeozoic sequence. The Artinskian rocks may neither have had a thick interbedded evaporite sequence nor have been buried sufficiently deep to allow piercement structures to develop. Noakes (1972) states that salt domes inland from Shark Bay were explored for potash, but results were not encouraging. Other geologists consider that the domes are essentially tectonic features associated with major zones of faulting, and are unlikely to have a diapiric origin. The circular features near the Lyndon River are thought by some workers to be synclinal drags.

Evaporitic gypsum occurs in ou crops of the Artinskian Bulgadoo Shale and Wandagee Formation, and brine occurs in bores drilled in the Wandagee Formation on the Lyons River Station. Condon (1967, 1968), mentions the occurrence of evaporitic material in the Quinnanie Shale, the Madeline Formation, and in the Bulgadoo Shale, all of which are Artinskian.

Dirk Hartog Formation

The Dirk Hartog Formation is not exposed at the surface, but is known in the subsurface from Shark Bay to Marrilla No. 1 well. It is 671.1 m thick (855.3–1526.4 m) in Yaringa No. 1 well (Henderson & Shannon, 1966), and in the type section in Dirk Hartog No. 17B, where the formation was first described, it is 739.1 m thick (665.4–1404.5 m). Playford & others (GSWA, 1975) now include in the Dirk Hartog Formation the unknown 146–855 m in Yaringa No. 1, which makes the total of 1380.1 m in this well the greatest known thickness of Dirk Hartog Formation.

The age of the Dirk Hartog Formation was first determined as Late Silurian on the basis of poorly preserved megafossils (Öpik *in* Glenister & Glenister, 1957). Philip (1969) has since described conodont faunas from the upper part of the formation which he considers indicate a middle and late Ludlovian age.

The top of the formation is an erosion surface farther north in the Carnarvon-Minilya area, where it is unconformably overlain by Devonian rocks. Salt is not known in Pendock I.D. No. 1, Quail No. 1, and Wandagee No. 1 wells (Fig. 52), which penetrate the formation in the north, but anhydrite is common and has been reported also in Dirk Hartog No. 17B. The Wandagee No. 1 and Quail No. 1 sequences in the Dirk Hartog Formation are somewhat similar, though Quail No. 1 is outside the Gascoyne area in the adjacent Merlinleigh Basin; the two basins were not separated (by faulting) until the Late Jurassic.

The Yaringa Evaporite Member of the Dirk Hartog Formation is known mainly from the Gascoyne Subbasin. Its type section is 1195–1271 m in Yaringa No. 1 well, and it corresponds to 'Unit B' of Henderson & Shannon (1966).

The Tumblagooda Sandstone occurs beneath the Dirk Hartog Formation in Dirk Hartog No. 17B. It is a fluvial deposit shed primarily from the Darling Fault area, although it is known in Wandagee No. 1, considerably farther north. It contains high-salt brines, is up to 3000 m thick in outcrop, mostly red, and grades upwards into the Dirk Hartog Formation, which suggests that the Tumblagooda Sandstone too may be

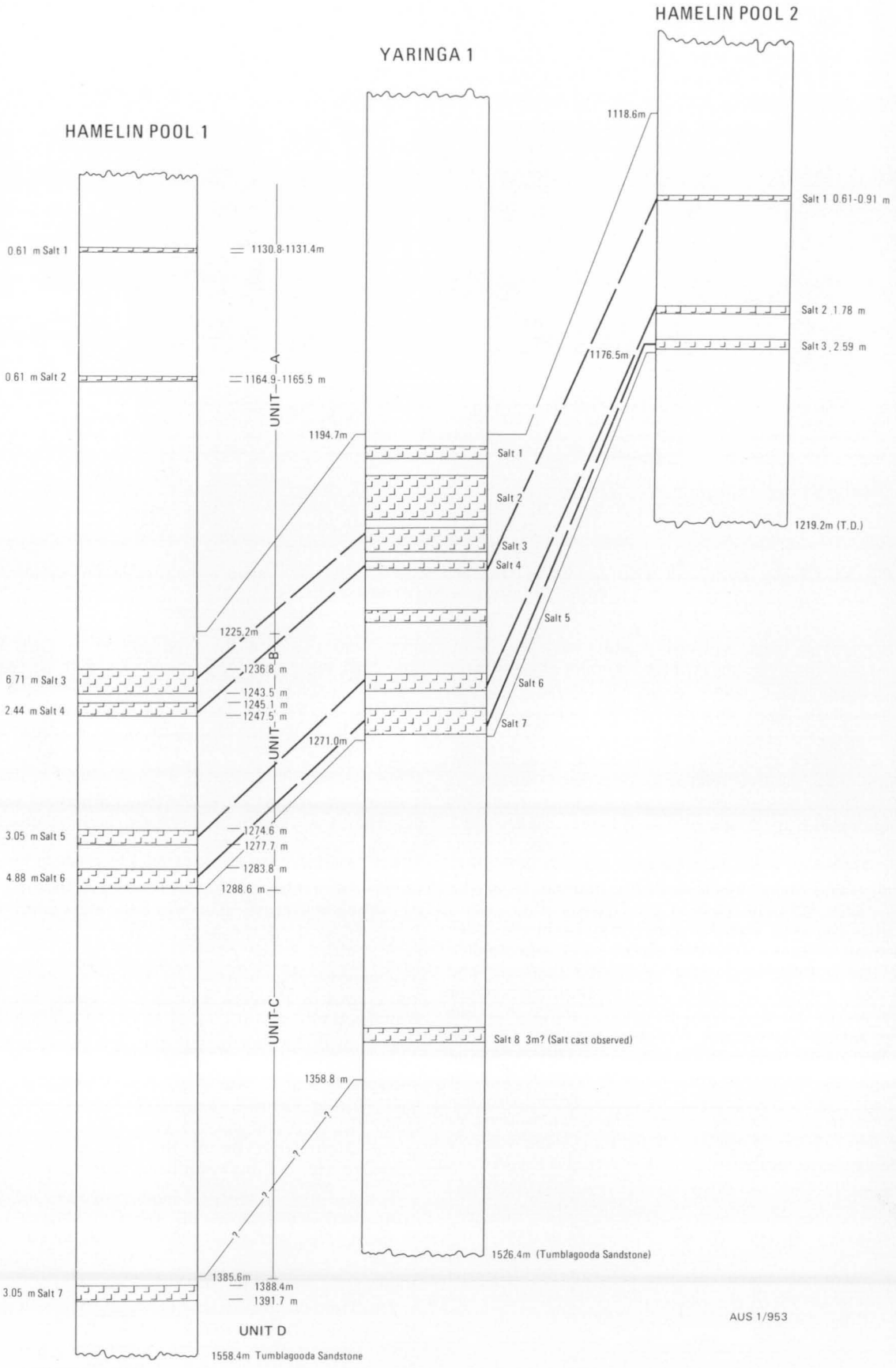

Fig. 54. Correlation of salt beds between wells in the Dirk Hartog Formation, Carnarvon Basin (after Pendery & others, 1969).

Silurian. The sandstone in Quail No. 1 and Wandagee No. 1 sections beneath the Dirk Hartog Formation is lithologically similar to the Tumblagooda Sandstone.

The Middle to Upper Devonian Point Maud Formation shows a reefoid development in Pendock I.D. No. 1. In addition to the Silurian evaporites, minor Devonian evaporites are present in the Gneudna Formation in Yaringa No. 1, and these may have important palaeogeographic implications.

It has been suggested by some geologists that very thick evaporites could be present in the Rough Range area, and may be situated on the basin side of a reef, but no evidence in support of this claim has been cited.

The sequences penetrated in Yaringa No. 1 and Hamelin Pool Nos. 1 and 2 are shown in Table 9 below, which has been taken from Hamelin Pool No. 2 well completion report.

TABLE 9. SEQUENCES PENETRATED IN YARINGA No. 1 AND HAMELIN POOL Nos. 1 AND 2

Formation		*Hamelin Pool No. 1*	*Yaringa No. 1*	*Hamelin Pool No. 2*
Surface deposits				8.8 m
Toolonga Calcilutite (Senonian)		132.6+m	64.9 m	55.5 m
Alinga Formation (Albian-Cenomanian)		51.8 m	50.9 m	61.0 m
Birdrong Formation (Aptian)		20.4 m	25.0 m	66.8 m
Unknown A (?)		136.2 m	179.8 m	128.3 m
Unknown B (?)		506.6 m	529.1 m	466.0 m
Dirk Hartog A	Late Silurian	373.1 m	339.5 m	327.4 m
Dirk Hartog B		64.0 m	76.2 m	59.4 m
Dirk Hartog C		96.3 m	88.4 m	41.1+m
Dirk Hartog D		172.8 m	167.6 m	—
Tumblagooda Sandstone (Ordovician)		36.9 m	762.0 m	—
TD		1595.3 m	2288.4 m	1219.2 m

OFFICER BASIN

Outcrops of evaporites in the Officer Basin were first discovered in the centre of the Woolnough Hills in 1956, during geological reconnaissance mapping of the southern Canning Basin by BMR. The occurrence was recognised as possibly constituting the core of a salt dome (Veevers & Wells, 1959, 1960) and, subsequently, Leslie (1961) made a regional geological investigation of the Gibson Desert area in the Officer Basin and further observations in the Woolnough Hills. Wells (1963) reported the occurrence of other diapiric structures, the Madley diapirs, some with exposed cores of evaporites, arranged in an arc a few kilometres southwest of the Woolnough Hills. Wilson (1967) considered that at least twelve domes are present along this southwest-trending line, which he called the Madley diapiric trend. The best exposed diapirs occur in a central zone. They all have cores of Proterozoic rocks and rims of Permian and Mesozoic strata.

The Woolnough Hills and Madley diapirs occur in a northwestern lobe of the Officer Basin (Fig. 55); geophysical surveys show that this part of the basin contains at least 4500 m and perhaps as much as 7500 m of sediment and is separated from the Kidson Sub-basin to the north by a buried basement ridge. The Woolnough Hills are on the southwest flank of the ridge.

The age and history of movements of the intrusive evaporitic cores are not known with certainty, but the latest movements of the diapirs probably continued into mid-Tertiary times. It was generally considered that the evaporites were Precambrian, because of similarities between the overlying stromatolitic dolomite and the Precambrian dolomites in neighbouring basins, notably the Bitter Springs Formation of the Amadeus Basin. Reinterpretation of seismic work for Hunt Oil Co. has suggested that there are two levels of evaporites, ?Cambrian and Precambrian. The probable younger evaporite sequence has been called the Babbagoola Beds (defined from Yowalga No. 2 well); the presumed older sequence, called the Browne Beds, was defined by Lowry & others (1972) in Browne No. 1 well, where it forms the intrusive core of the Browne diapir (Fig. 56). Evaporites lithologically similar are exposed in the diapiric cores of some domes along the Madley diapirs and in the Woolnough Hills diapir. Interpretation of the seismic cross-section through Browne No. 2 well suggests that the evaporitic sequence may be part of the Babbagoola Beds. The assumed age of both the Browne and Babbagoola Beds depends on isotopic age determinations carried out on volcanic rocks in the sequence.

The Table Hill Volcanics (described by Talbot & Clarke, 1917, and named by Peers, 1969) are interbedded in the succession and are thought to lie stratigraphically above both evaporite sequences (Jackson & van de Graaff, in preparation). Compston (1974) has calculated their age using an initial $^{87}Sr/^{86}Sr$ ratio calculated from apparently unaltered primary pyroxenes, combined with the Rb–Sr model ages for total rock samples. He concludes that the Rb–Sr data are best interpreted as signifying an original extrusion of the basalts at 575 ∓ 40 m.y.

The dolomite at the Woolnough Hills is interbedded with thinly bedded siltstone with moulds of halite, and unconformably overlain, in turn, by Permian fluvioglacial deposits and Cretaceous sediments. Poorly exposed lateritised Lower Cretaceous lutite crops out in the distal parts of the dome and in neighbouring outcrops. The geological succession in the Madley diapirs is somewhat similar (Wells, 1963; Wilson, 1967).

The evaporites cropping out at the Woolnough Hills and Madley consist mainly of secondary friable gypsum in contact with scattered blocks of brecciated dolomite. A few fresh exposures of tightly folded and in part brecciated gypsum are exposed in sink holes at the Woolnough Hills and in some of the Madley diapirs.

Other less well-defined domes are present in the Madley and Warri Sheet areas. They include poorly defined domes in Permian and Mesozoic rocks at Lake Cohen, in Cretaceous rocks at the eastern end of the Young Range, and another in Permian, Mesozoic, and Cretaceous rocks near the Iragana Fault (Wells, 1963).

Several closely spaced, doubly plunging anticlines and synclines lie in a northwest-trending zone between Lake Breaden and the Baker Range. A seismic cross-

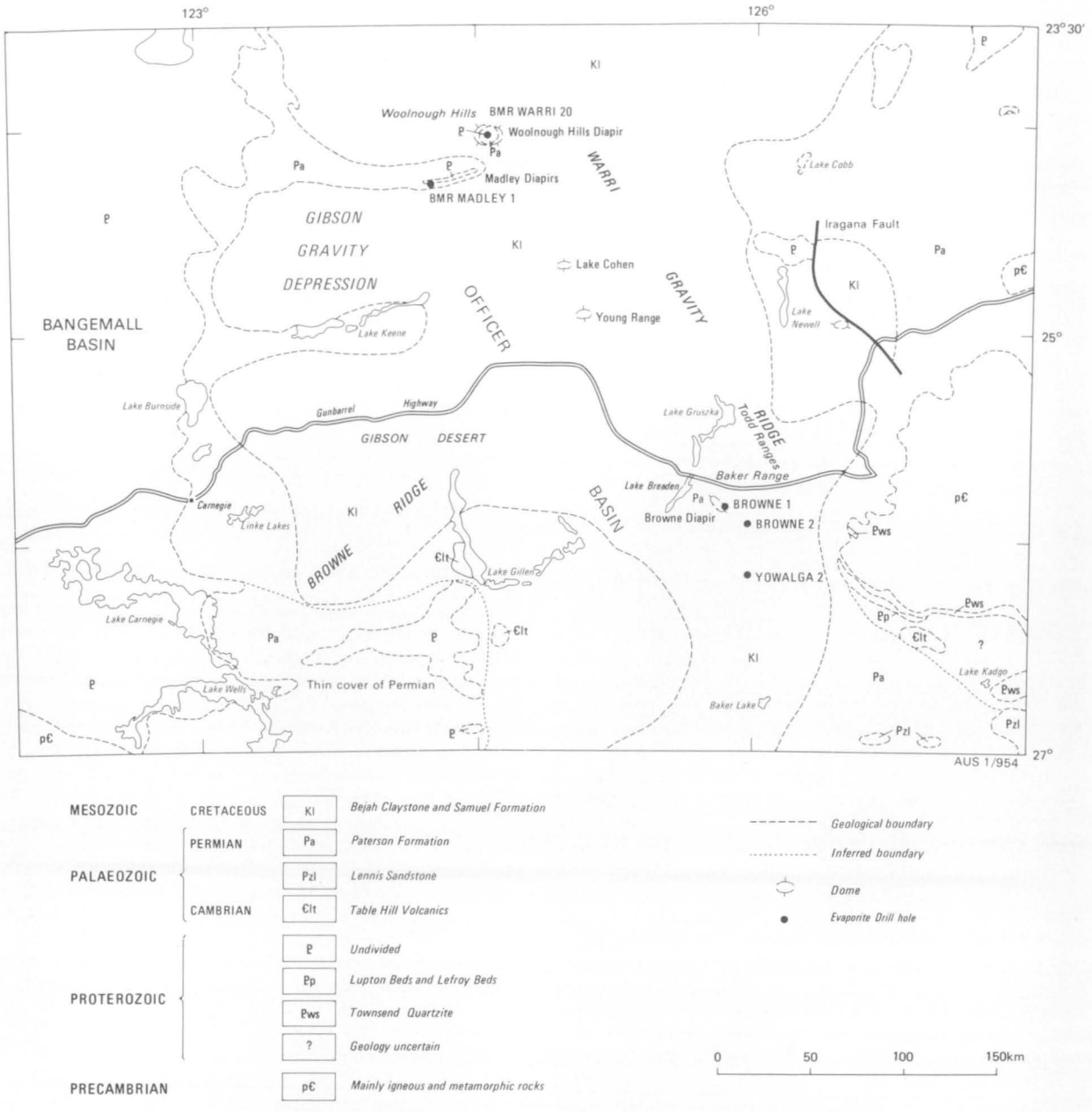

Fig. 55. Diapirs, and wells penetrating evaporites, northwestern Officer Basin.

section (Jackson, 1966b, fig. 23) indicated the presence of a diapiric core underlying the fold zone, and the structure has been termed the Browne diapir (Figs. 57, 58). Evaporitic sequences were subsequently penetrated in Browne Nos. 1 and 2 wells (Jackson, 1966b). Hunt Oil Co. seismic lines 12D and 12E (Hunt Oil Co., 1966) show possible diapiric masses which may trend parallel to the Browne diapir axis.

Seismic-record sections in Turpie (1967) show possible diapirs along the Gunbarrel Highway—one is a possible continuation of the Browne diapir trend, and the other occurs a few kilometres farther west.

Thin evaporite beds were intersected in two shallow stratigraphic test holes and a petroleum exploration well drilled by Hunt–Placid Oil Co. (Jackson, 1966a). In Yowalga No. 2 well, evaporites occur in Unit B of the Babbagoola Beds, which lie unconformably beneath the Table Hill Volcanics (Fig. 59). Microfossils from samples of grey shale from Yowalga No. 2 suggest an early Cambrian age (M. D. Muir, BMR, personal communication, 1978). The succession penetrated in the well is given in Table 10.

Unit A of the Babbagoola Beds consists of interbedded fine to very coarse-grained sandstone and dark red-brown micaceous shale. Anhydrite occurs in these rocks as fractures and joint fillings. Unit B consists of silicified anhydritic dolomite with gypsum and anhydrite veins and fracture fillings. Unit C is interbedded siltstone and shale.

Evaporites were encountered in the Browne Beds sequence of uncertain age (?Proterozoic) in the Hunt/Placid Browne Nos. 1 and 2 shallow stratigraphic holes, drilled on the Browne diapir between Lake Breaden and the Todd Range, in the Browne Sheet area (Jackson, 1966a). The sequences penetrated in the two wells are given in Table 11.

In Browne No. 1 the evaporites occur in the Browne Beds (132.6–386.8 m) in a sequence consisting of 152 m of limestone, gypsum, and shale, overlying 101 m of gypsum banded with varying amounts of

Fig. 56. Vertical aerial photograph of the northern part of the Browne diapir, Officer Basin.

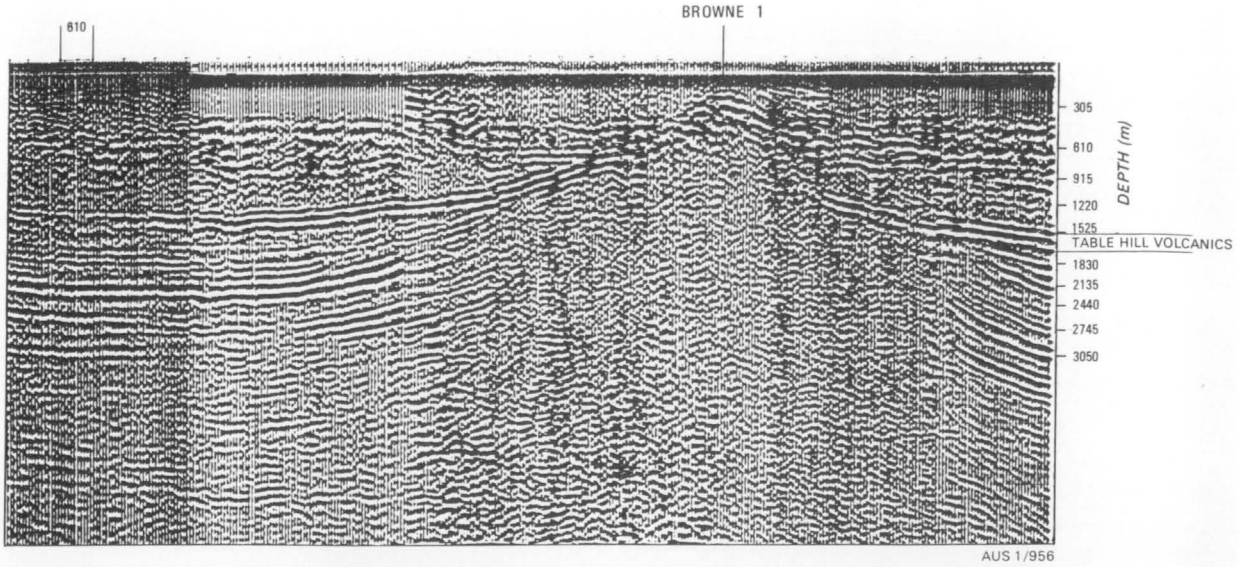

Fig. 57. Seismic cross-section of the Browne diapir, Officer Basin (after Jackson, 1966b).

TABLE 10. SUCCESSION PENETRATED IN YOWALGA No. 2 WELL.

Age	*Formation*	*Thickness*	
Cainozoic	laterite		3.7 m
Early Cretaceous	Samuel Formation		86.9 m
	unconformity		
Permian (Sakmarian)	Paterson Formation (Yowalga Sandstone of Jackson, 1966a)		312.4 m
	unconformity		
Early Palaeozoic	Lennis Sandstone		321.6 m
	unconformity		
Early Cambrian	Table Hill Volcanics		117.3 m
	unconformity		
?Cambrian	Babbagoola Beds		
	Unit A	41.1 m	
	Unit B	6.1 m	143.5 m
	Unit C	96.3 m	
		TD	989.4 m

TABLE 11. SEQUENCES PENTRATED IN BROWNE Nos. 1 & 2 WELLS.

Age	*Formation**	*Thickness* *Browne No. 1*	*Browne No. 2***
Early Cretaceous	Samuel Fm.	84.4 m	140.2 m
Early Permian	Paterson Formation ("Yowalga Sandstone" of Jackson, 1966a)	48.2 m	121.9 m
Proterozoic	Browne Beds	254.2 m	30.5 m
		TD 386.8 m	292.6 m

* The formation names used informally by Jackson (1966a), have been changed to conform with those proposed by Lowry and other (1972) and Peers & Trendall (1968).

** It has been suggested on the basis of interpretation of seismic reflection sections in the Browne diapir-Yowalga No. 2 area, that the sequence in Browne No. 2 may be Babbagoola Beds.

ary fracture fillings. Minor shows of hydrocarbons were encountered in both wells in the Browne Beds. These have particular significance for the formation of sulphur, especially as sulphate is common in the evaporitic sequence.

In the northeastern part of the Officer Basin, in South Australia, about 350 km east-southeast of the Browne diapir area, a Palaeozoic sequence about 2800 m thick unconformably overlies Proterozoic sediments on the south side of the Musgrave and Mann Ranges. The Devonian sandstones in outcrop pass into shale/dolomite sequences basinwards, but the westerly extent of this sequence is unknown. The Cambrian sediments in outcrop are predominantly marginal arkosic sandstone, but some anhydrite has been reported interbedded in Cambrian sediments in Emu No. 1 well (Krieg, 1969).

Continental Birksgate No. 1 well in the eastern Officer Basin penetrated about 500 m of Lower Palaeozoic sediments and over 1200 m of unnamed siltstone, black and grey waxy shale. In Browne No. 2 they occur over the interval 262.1–292.6 m in a sequence consisting of 26 m of limestone and a little shale, overlying 4.5 m of gypsum with lath-like crystals and shale partings. The evaporite minerals are anhydrite, gypsum, and halite; they occur as thin beds or as second-sandstone, and some limestone of presumed late Precambrian age. Anhydrite constitutes up to 10 percent of a small interval in the siltstone and limestone.

South Australia Department of Mines and Energy drill hole Byilkaoora No. 1 penetrated an ?Early Cambrian sequence including 224 m of claystone, dolomitic and calcareous claystone, siltstone, dolomite, and limestone. A variety of evaporite minerals, including trona and shortite, throughout much of the sequence has been replaced by calcite pseudomorphs. The pseudomorphs occur as subspherical feathery rosettes and cuniform crystals and crystal aggregates embedded in clayey and cherty carbonates (Benbow & Pitt, 1979). The evaporite sequence in Byilkaoora No. 1 is probably equivalent to the halite-bearing sequence in Wilkinson No. 1 (Arckaringa Basin), which is probably Cambrian (Muir *in* Gatehouse, 1979) and correlated with the Observatory Hill Beds (Pitt & others, 1980).

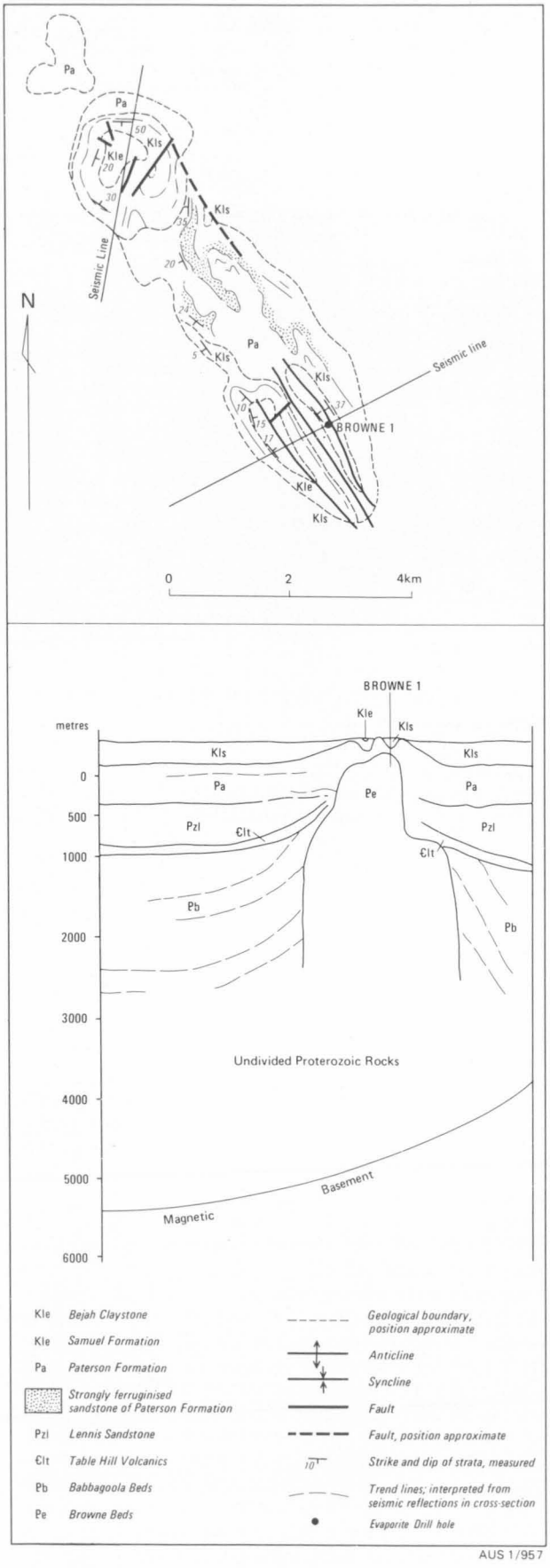

Fig. 58. Geological sketch map and section of the Browne diapir, Officer Basin.

Mack & Herrmann (1965) described a sequence of 8500 m of late Precambrian to ?Cambrian sediments in the Runton-Carnegie area. The sequence is divided into two major units by an angular unconformity. The lower unit consists of sandstone, shale, carbonate rocks, and evaporites, and the upper, sandstone, shale, and evaporites. The evaporites consist mostly of gypsum, but are poorly exposed. Mack & Herrmann (1965) correlated the sequence, which is now thought to be part of the Bangemall Basin, with the Carnegie Sandstone–Maurice Formation interval in the western part of the Amadeus Basin. But whatever its age, it has been used as evidence of widespread evaporitic sedimentation. Because the sequence occurs in areas near salt lakes, some doubt has been expressed as to whether the evaporites are actually interbedded with the sediments. The occurrence of evaporites is not described by later workers (Crowe & Chin, 1979).

In 1972, BMR drilled several shallow stratigraphic holes in the Woolnough Hills and Madley diapirs. BMR Warri Nos. 1, 2, and 4 to 19 were drilled in the Woolnough Hill diapir to determine the extent of gypsum cap rock under thin alluvial deposits, and were used to select a site for a deeper test hole, BMR Warri No. 20. BMR Warri No. 3 was drilled about 12 km southeast of Woolnough Hills. BMR Madley No. 1 was drilled in the core of Madley diapir no. 6. Details of the holes, which proved that the intrusive beds are halite, are given below (from Wells & Kennewell, 1974).

BMR WARRI Nos. 1–20

Drill site geology

The Woolnough Hills diapir is a near-circular structure consisting of a central core of evaporites surrounded by beds of dolomite and shale dipping radially outwards from the core at between 70° and 40° (Figs. 60, 61). These rocks are probably Proterozoic, and are unconformably overlain by the Lower Permian Paterson Formation, which dips radially outwards from the core at between 60° and 5°.

The central core was shown by the drilling to consist of anhydrite, and dolomite, to about 200 m, and halite below that depth. Recrystallisation and movement along cleavage planes has occurred in the past during upward movement of the body, and considerable brecciation of beds of anhydrite, dolomite, and quartzite has resulted.

Upward movement of the salt body into zones of percolating groundwater has resulted in solution of halite to leave a residual cap rock of fragments initially contained within the diapiric core. This cap rock is about 200 m thick on the northwest part of the core. Anhydrite fragments are common in the lower part, and gypsum fragments in the upper part. A crust of 'earthy' gypsum up to 0.5 m thick covers parts of the core. Large blocks of Proterozoic dolomite and quartzite and Permian sandstone up to hundreds of metres in diameter are present on top of the cap rock. These formed from the breakup of beds by the upward moving halite, and were left as a residue on the surface when the evaporite minerals weathered.

Sink holes have developed in the gypsum, particularly in creek beds on the south part of the core. Several large flat-lying areas, particularly in the beds of ill-defined creeks, are covered with alluvium washed from the surrounding sediments.

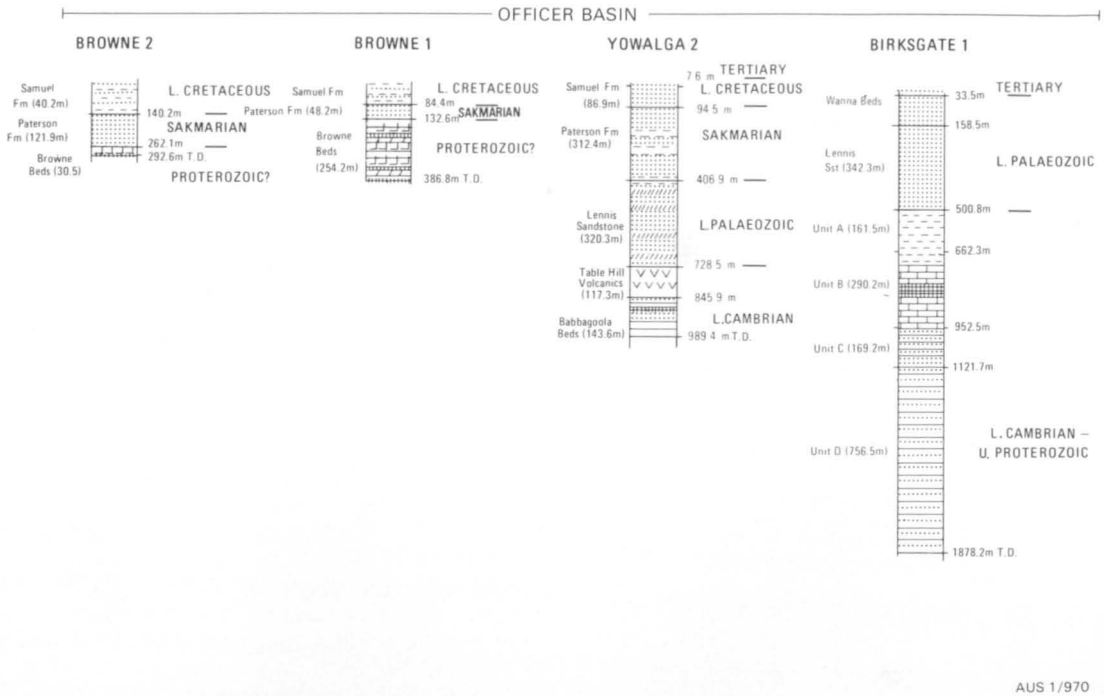

Fig. 59. Graphic sections of petroleum exploration wells penetrating evaporites in the Officer Basin. For reference to symbols see Fig. 4.

In several places around the edge of the evaporitic core, siltstone and stromatolitic dolomite of probable Proterozoic age are present. The extent and precise sequence in these rocks is uncertain, as they crop out in only a few places. Alluvium and soil containing pebbles, cobbles, and boulders of dolomite and quartzite cover large areas, and give the impression that the area is underlain by the presumed Proterozoic sediments. In the northwest of the structure, where shallow drilling was carried out, this is not the case; the boulders are either erratics from Permian diamictite or fragments from within the gypsum cap rock left as residuals by weathering. In the northeast and southwest, however, the dolomite and siltstone appear to form continuous beds which dip radially outwards from the core with slightly steeper dips than the Permian sediments. Whether the dolomite and siltstone are present around most of the gypsum core is uncertain. Their contact with the core has not been observed, and it may be either faulted or unconformable.

The Proterozoic rocks are surrounded by the Lower Permian Paterson Formation, which dips radially outwards from the core with dips in the range 5° and 60°. The two main rock types are a conglomerate of sparse pebbles, cobbles, and boulders in a silty clay matrix (interpreted as a tillite), and a coarse-grained quartz sandstone, which is subangular, well sorted, and of uncertain depositional environment, but also interpreted as tillite. The conglomerate occurs towards the base of the sequence, and the sandstone is dominant towards the top. 350 m of sediments is exposed on the western side of the diapir. The sediments are commonly cemented by hematite and goethite, formed during a period of intense weathering in the Tertiary. Where the Paterson Formation was intersected by shallow drilling in the northeast of the diapir, gypsum veins up to 2 cm across and crystals up to 5 mm across are present; these are probably derived from the gypsum cap rock and precipitated from water percolating in fractures. These crystals can give rise to secondary gypsum in the soil overlying the Paterson Formation, making detection of the exact limits of the gypsum outcrop difficult. The nature of the contact between the Paterson Formation and Proterozoic rocks is uncertain; it may be either unconformable or faulted.

Outcrops of Paterson Formation in the northeast show two diverging trends on aerial photographs, suggesting a local unconformity within the Permian sequence. No differences in lithology are apparent on the ground, and no dips can be measured, owing to poor outcrop.

In the same general area, but farther to the northeast, very weathered silty sediments are exposed on an isolated hill. These may represent the Lower Cretaceous Samuel Formation, which crops out several kilometres to the east. The relationship between these sediments and those of the underlying Paterson Formation is unknown.

Intense weathering during a period of wetter climate in the Tertiary caused a laterite soil profile to develop on a gently undulating surface. The upper zone (the 'ironstone crust') of the profile is present on rises around the diapir. The middle, mottled zone is developed in probable Samuel Formation in the northeast part of the structure, and the lower, weathered zone is represented by the ferruginised sediments of the Paterson Formation. This soil profile is not present in the centre of the diapir. As continuous upward movement is usual in diapirs, it is likely that uplift and erosion have taken place since development of the laterite profile.

A fault of unknown displacement on the southern side of the structure within the Paterson Formation is marked by conglomerate faulted against sandstone. Several other small faults are present in the southwest part of the structure, and a zone of faulting is apparent in the southeast, although outcrop is too poor to enable enumeration of the faults.

Gravity contours show two minima to the northeast and southwest of the structure. These have been in-

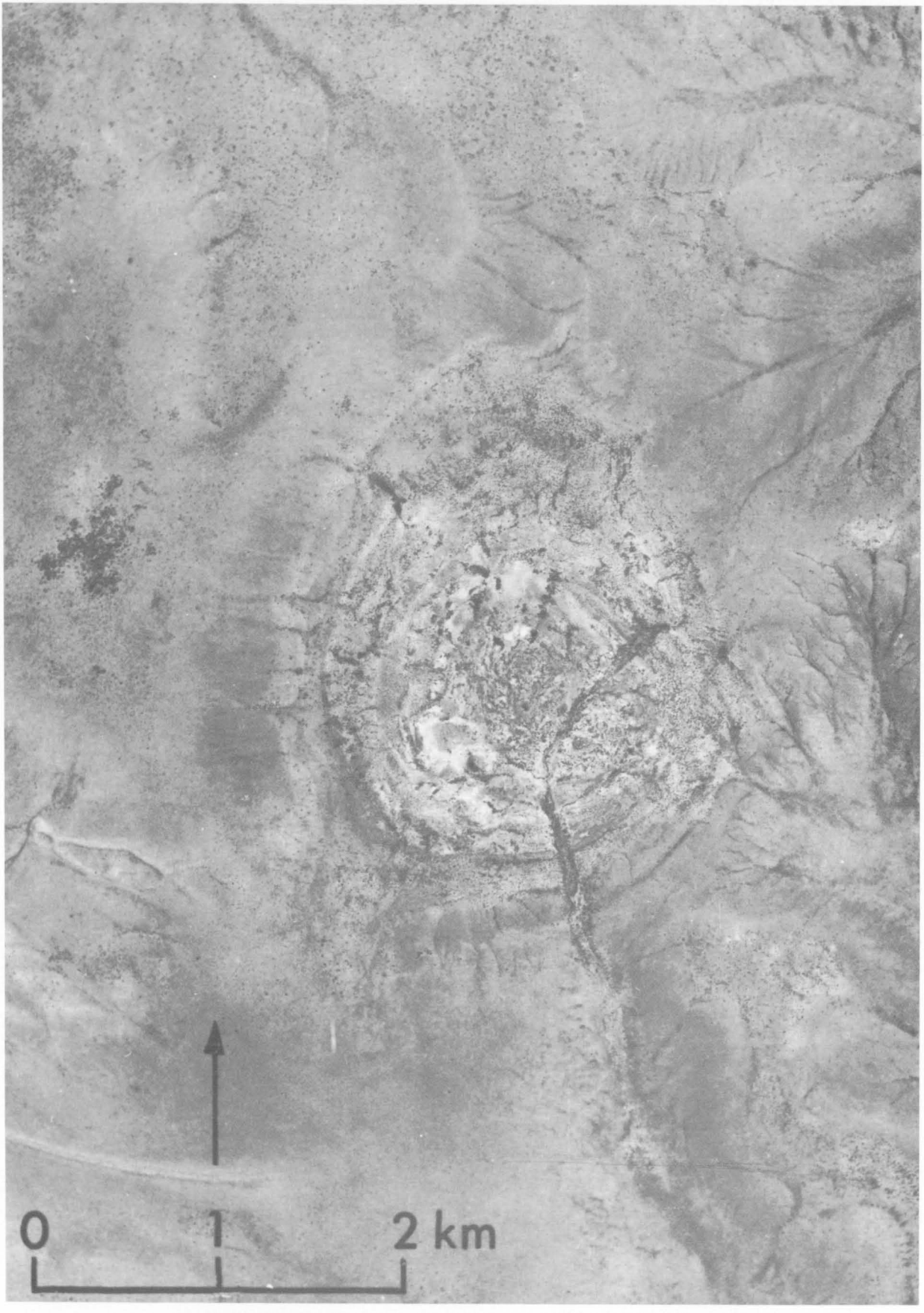

Fig. 60. Vertical aerial photograph of the Woolnough Hills diapir, Officer Basin.

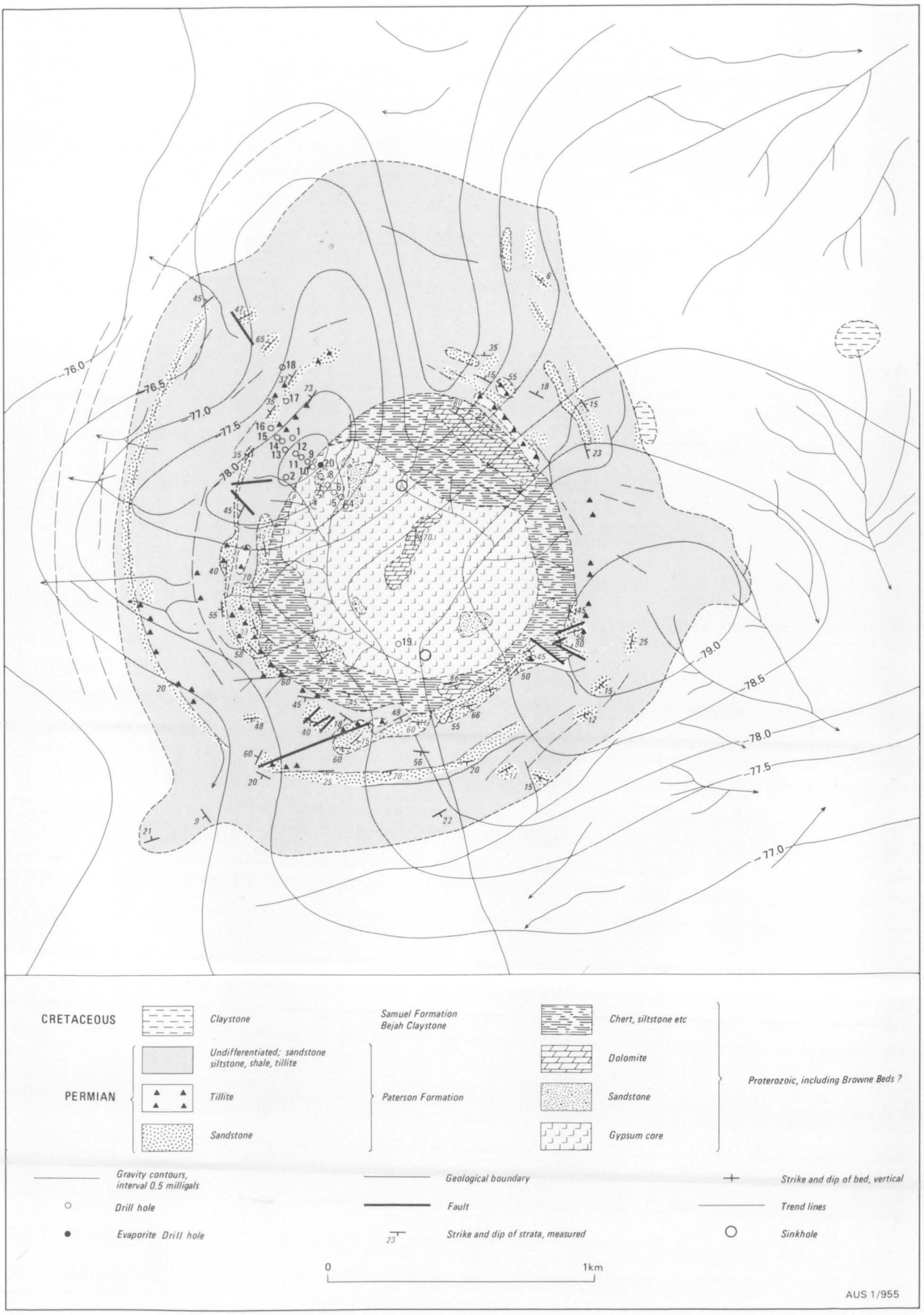

Fig. 61. Geology and Bouguer gravity anomalies of the Woolnough Hills diapir, Officer Basin.

terpreted as caused by bodies of evaporite minerals. The evaporite body, therefore, is possibly much larger than is apparent from surface mapping, and the present structure may be a small part of a larger one concealed beneath the Permian and Cretaceous sediments.

The gravity values obtained over the structure are, in general, consistent with a salt dome model, with halite (density 2.1) in a body 1000 m in diameter and 5000 m high intruding rocks of density 2.3 in an area where the total thickness of sediments is about 7000 m and the assumed basement density 2.5–2.6 (Wells, 1973).

Because of insufficient reliable surface and subsurface information it is difficult to construct a meaningful cross-section of the structure.

Description of rock types

The classification of rock types in the drill cores is similar to that used by Wells & Kennewell (1972). Following common practice, a rock composed dominantly of a single mineral has been referred to by the name of that mineral; 'rock' has been used after the mineral name when reference is made to an aggregate of crystals composed dominantly of one mineral.

A graphic presentation of rock types penetrated in BMR Warri No. 20 is shown in Plate VI. The description below and on Plate VI were compiled after a study of twenty thin sections selected to cover the range of rock types and to yield as much information as possible on texture and mineralogy. The minerals in sixteen samples were identified by X-ray diffraction analysis to aid description of the thin sections.

Most rock types are friable and all slides were impregnated with resin to prevent the sample disintegrating during preparation of thin sections. Samples taken above 200 m were prepared in water to prevent formation of bassanite ($2CaSO_4.H_2O$) from gypsum ($CaSO_4.2H_2O$) by heating during grinding of the slide. Samples taken below 200 m were prepared in kerosene to avoid dissolving halite.

There are very few detrital minerals present and most minerals in the cores originated either as primary chemical precipitates or as products of recrystallisation. Therefore, a crystal size classification for recrystallised carbonates suggested by Folk (1964) has been adopted; extremely coarsely crystalline, >4 mm; very coarsely crystalline, 1.00–4.00 mm; coarsely crystalline, 0.25–1.00 mm; medium crystalline, 0.0625–0.25 mm; finely crystalline, 0.0156–0.0625 mm; very fine crystalline, 0.0039–0.0156 mm; aphanocrystalline, <0.0039 mm.

It is not known whether the dolomite and quartz in the core have an evaporitic origin or not. For the purposes of this report they are discussed with the evaporite minerals.

Gypsum rock

Gypsum rock is dominant in the upper 161 m of the core and occurs as several varieties. The most common, referred to as gypsum in the core descriptions, is white to grey, with a granular texture and generally coarsely crystalline. It occurs interlaminated with other rock types as fragments and as massive beds (or possibly fragments) up to several metres across. Microscopic examination shows that the composition ranges from almost pure gypsum to gypsum with about 15 percent quartz and dolomite crystals and traces of anhydrite, ?limonite, and clay. These minerals are enclosed within coarse gypsum crystals.

Acicular gypsum rock

Acicular gypsum rock is present above 62 m and in all the shallow holes drilled in gypsum. It is generally pure and white, consisting of needle-like crystals of gypsum oriented at right angles to fractures which they fill.

Brown gypsum rock

Brown gypsum rock is rare, and fills small fractures. The vein filling consists of a single crystal, and the brown is imparted by small quantities of ?limonite and clay. It cannot be distinguished from gypsum rock in thin section.

Gypsum crystals rock

Gypsum crystals rock is referred to in several parts of the core descriptions, particularly between 26 m and 40 m. It consists of euhedral crystals, generally pure and colourless, which have grown together to form an interlocking meshwork of crystals up to several centimetres across.

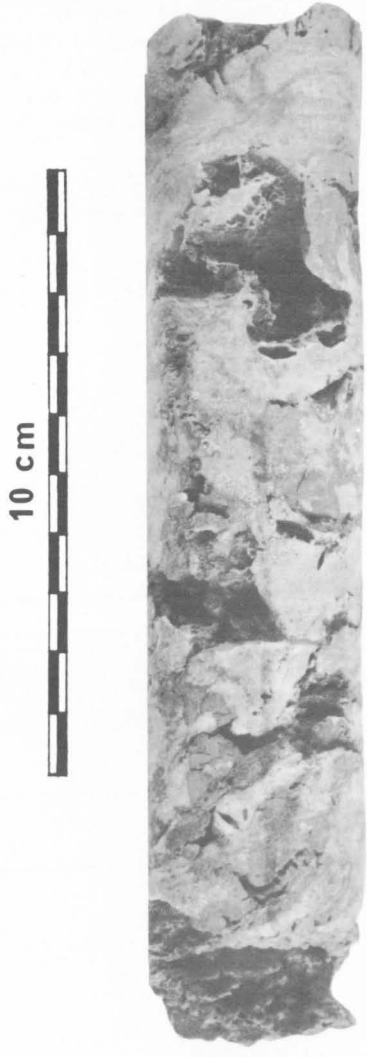

Fig. 62. Core from about 205 m in BMR Warri No. 20, consisting mainly of brecciated anhydrite, with vugs where halite has washed out. (GA/935)

Dolomitic gypsum rock

Dolomitic gypsum rock occurs above 161 m as fragments up to several centimetres thick, and interlaminated with gypsum rock and grey friable dolomite rock in beds several metres thick. It is moderately soft and generally light to dark grey. Composition is variable, but generally coarse gypsum crystals enclose 15–50 percent dolomite and quartz crystals with minor anhydrite, ?limonite, and clay.

Anhydrite rock

Anhydrite rock occurs in significant amounts only at depths greater than 161 m (Fig. 62). It is white to light brown when exposed on the side of core, but on freshly broken surfaces it is clear with a slight black or blue colour and a shiny micaceous appearance, owing to its perfect cleavage. Texture is commonly even and it occurs as beds or fragments up to several metres across. Anhydrite rock may also be interlaminated with grey friable dolomite rock or dolomitic anhydrite rock. Traces of ?limonite or ?clay are present in some specimens.

Dolomitic anhydrite rock

Dolomitic anhydrite rock occurs as fragments and beds up to several metres across, and may also be interlaminated with anhydrite rock, gypsum rock and grey friable dolomite rock. It is commonly finely crystalline, light brown to light grey, and moderately hard. Anhydrite is the dominant mineral, with about 15–50 percent finely crystalline dolomite and coarsely crystalline quartz, and traces of chlorite, ?clay, and ?limonite.

TABLE 12. WATER ANALYSIS, BMR WARRI No. 3*

Cations	*mg/l*	*me/l*
Ca	59	2.9
Mg	74	6.1
Na	590	25.5
K	76	1.9
Fe	0.26	—
Anions		
CO_3	—	—
HCO_3	175	2.9
SO_4	485	10.1
Cl	790	22.3
F	1.2	—
NO_3	40	0.7
PO_4	0.1	—

Totals and balance

Cations me/l 36.4 — Anions me/l 36.0

diff :0.4 sum :72.4 % $\frac{\text{diff} \times 100}{\text{sum}}$:0.55

Derived and other data

Conductivity (E.C.) μS/cm at 25°C:	3400
Total dissolved solids calculated (HCO_3=CO_3):	2201 mg/l
Total hardness as $CaCO_3$:	450 mg/l
Carbonate hardness as $CaCO_3$:	145 mg/l
Non-carbonate hardness as $CaCO_3$:	305 mg/l
Total alkalinity as $CaCO_3$:	145 mg/l
Silica (SiO_2):	51 mg/l
Reaction –pH	7.2
Sodium to total cations ratio:	70.0%

* Sample No: 73880151
AMDEL Report No: AN3528/73

TABLE 13. ANALYSIS OF CORES, BMR WARRI No. 20

	Sample No., depth, & rock type		
	73880152 27.85 m Gypsum	73880153 187.85 m Anhydrite	73880154 203.80 m Halite
SiO_2	14.9%	26.2%	1.85%
Al_2O_3	3.50	2.45	0.63
Total Fe as Fe_2O_3	1.19	0.87	0.27
CaO	24.4	25.5	2.20
MgO	3.80	4.50	0.60
Na_2O	0.06	0.27	—
Na	—	—	35.2
K_2O	1.07	1.01	0.15
TiO_2	0.19	0.16	0.01
H_2O^+(over 105°C)	2.30	0.92	1.32
H_2O^-(at 105°C)	12.9	0.12	0.14
H_2O^- (at 44°C)	0.14	0.10	—
CO_2	4.30	7.95	0.85
MnO	0.01	0.02	0.01
P_2O_5	0.05	0.08	0.02
SrO	0.035	0.058	0.007
Cl	0.04	0.31	54.3
F	0.05	0.055	0.02
SO_3	31.3	29.7	2.45
S (as sulphide and elemental)	0.2	0.25	—

Reference: AMDEL Report 3528/73.

Grey friable dolomite rock

Grey friable dolomite rock has been recorded to depths of 202 m in the caprock of the diapir. It is generally soft, friable, and light to dark grey. Beds up to several metres thick are present at shallow depth, but below 25 m occurrences are as matrix for fragments of other rock types and laminae in fragments of other rock types. Composition is very variable, but finely crystalline dolomite is usually in excess of 50 percent. Gypsum or anhydrite are usually a major component, with gypsum common towards the surface and anhydrite towards the base of the cap rock. Quartz may also be a major component, as coarse, commonly euhedral crystals. Minor amounts of chlorite, limonite and clay are present, particularly towards the base of the cap rock.

Dolomitic chert

Dolomitic chert was recorded near the surface in BMR Warri No. 8. It is brown, hard and faintly laminated. It is composed dominantly of quartz with dolomite, small amounts of ?limonite and ?clay, and traces of anhydrite.

Anhydritic chert

A single fragment of anhydritic chert was intersected by drilling in the halite zone. It is light brown and tough. The hand specimen has the appearance of a fine sandstone, as it contains fine grains of anhydrite rock. The anhydritic chert consists of finely crystalline quartz and anhydrite in almost equal proportions with a granular texture.

Halite rock

Halite rock was encountered in drilling at depths of about 203 m (Fig. 63). Traces of halite are present several metres above 203 m. It is extremely coarsely

crystalline, colourless to pale orange and contains numerous fragments of anhydrite rock and dolomitic anhydrite rock. Finely crystalline anhydrite and quartz are scattered throughout the halite crystals. Traces of deliquescent magnesium salts are present (Table 13 and Plate VI).

Description of core

BMR Warri No. 1

0–4.6 m *Sandstone,* white, fine-grained, poorly sorted, rounded to angular, silty, hard.

BMR Warri No. 2

0–9.1 m *Claystone,* yellow to chocolate brown, slightly silty in parts, moderately soft.

BMR Warri No. 3

0–21.3 m *Sandstone,* white, fine-grained, contains a few quartz granules, slightly calcareous; and *claystone,* white, silty, hard, probably chalcedonic and highly weathered.

21.3–24.4 m *Claystone,* red in upper and yellow in lower parts, moderately hard.

24.4–29.3 m *Sandstone,* white, fine-grained, and *claystone,* white, silty, hard; interbedded with *claystone,* yellow and red, moderately hard.

29.3–30.5 m *Sandstone,* white, fine-grained, and *claystone,* white, silty, hard; bed contains numerous cavities up to 100 m across.

30.5–33.5 m *Granule conglomerate,* soft, poorly consolidated, well sorted with little matrix, contains granules of quartz, limonitic siltsone and sandstone, and weathered chalcedonic claystone.

Note: The hole was damp below 12 m, and between 16 m and 17 m a flow of brackish water of about 500 l/hr was encountered, presumably from a permeable bed. In the interval 23.9 m to 30.5 m a flow of water at the rate of about 2000 l/hr was obtained from cavities up to 100 mm across in the sandstone and claystone. At 30.5 m a large flow of about 5000 l/hr was obtained from a poorly consolidated gravel bringing total flow from the hole to 7500 l/hr. For a detailed analysis of the water see Table 12.

BMR Warri No. 4

0–3.65 m. 60% *grey friable dolomite;* 30% *angular gypsum;* 10% *dolomitic gypsum.* Fragments of dolomitic gypsum and veins of acicular gypsum in matrix of grey friable dolomite.

BMR Warri No. 5

0–3.65 m. 90% *brown gypsum;* 10% *acicular gypsum.* Veins of acicular gypsum in matrix of brown gypsum.

BMR Warri No. 6

0–3.65 m. 90% *gypsum;* 10% *claystone.* Gypsum with solution cavities throughout infilled with claystone.

BMR Warri No. 7

0–3.65 m. 50% *brown gypsum;* 40% *gypsum;* 10% *claystone.* Fragments of brown gypsum in gypsum with solution cavities infilled with claystone.

BMR Warri No. 8

0–3.35 m 50% *gypsum crystals;* 50% *claystone;* gypsum crystals up to 10 mm across in matrix of claystone.

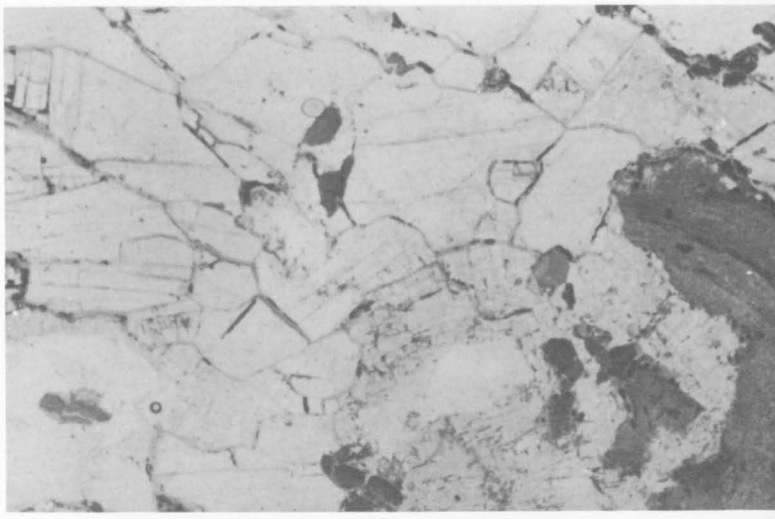

Fig. 63. Crystalline halite with included anhydrite fragment on right; from 203.8 m. Plane polarised light, x 17.

BMR Warri No. 9

0–3.95 m 60% *gypsum;* 30% *dolomitic gypsum;* 10% *brown gypsum;* interlaminated gypsum, brown gypsum, and dolomitic gypsum.

BMR Warri No. 10

0–3.55 m. *Gypsiferous sandstone,* dark brown, fine-grained, silty, very porous, contains white, fine to coarse grains of gypsum, limonitic cement, and some small solution cavities; probably leached.

BMR Warri No. 11

0–3.35 m. *Siltstone,* dark brown, contains a large proportion of limonite, very hard, rare sand grains, sparse fine mica grains.

BMR Warri No. 12

0–3.35 m. *Siltstone,* brown, contains clay, numerous sand and rare granule-size grains, and rare gypsum crystals up to 2 mm across; probably tillite.

BMR Warri No. 13

0–3.35 m. *Sandstone,* white, fine-grained, moderately sorted, angular to rounded, moderately hard; similar to sandstone in BMR Warri No. 1.

BMR Warri No. 14

0–3.35 m. *Siltstone,* grey, soft, clayey, contains abundant fine to coarse sand grains, angular to rounded; contains several veins of acicular gypsum up to 20 mm across; and rare fine crystals of gypsum; probably tillite.

BMR Warri No. 15

0–3.25 m. *Siltstone,* light brown, very clayey, contains a few rounded fine sand grains and sparse coarse grains of gypsum, moderately soft; probably tillite.

BMR Warri No. 16

0–3.65 m. *Sandstone,* white, fine to coarse-grained, angular to rounded, silty, contains angular lithic fragments up to 10 mm across; probably tillite.

BMR Warri No. 17

0–3.65 m. *Siltstone,* light grey, clayey, contains abundant fine to medium sand grains and lithic fragments up to 10 mm across; probably tillite.

BMR Warri No. 18

0–3.65 m. *Siltstone,* light grey, clayey, hard, contains few fine angular to rounded sand grains, rare lithic fragments and few gypsum crystals to 5 mm across; probably tillite.

BMR Warri No. 19

0–4.25 m. *90% gypsum; 5% claystone; 5% gypsum crystals.* Gypsum with rare solution cavities filled with claystone and gypsum crystals.

BMR Warri No. 20

0–123.35 m.

This interval is composed of gypsum cap rock. The cores are heterogeneous, but gypsum is the dominant rock type, occurring as fragments, laminae, and beds throughout, and acicular veins towards the top. Grey friable dolomite is present, as a matrix, although several beds occur towards the top of the interval, and laminae are present in some rock fragments. Gypsiferous dolomite is also present, generally as laminae in rock fragments, but also as fragments and beds. Traces of dolomitic anhydrite and anhydrite occur as discontinuous laminae almost completely converted to gypsum. Between 26 m and 40 m, euhedral gypsum crystals form an interlocking meshwork with a matrix of grey friable dolomite. Between 106 m and 120 m, the core is composed almost entirely of gypsum, with only traces of grey friable dolomite.

123.35–160.73 m.

This interval is the transition zone between gypsum-rich and anhydrite-rich cap rock, and contains almost all the rock types described. In most cores dolomitic anhydrite with rare anhydrite is being converted to gypsum and the texture is one of replacement; the conversion is evident along planes of weakness in the rock, such as laminations and joints. The rock types generally occur as thick beds, but in places they are fragmented with a matrix of grey friable dolomite. Fragments of gypsiferous dolomite and veins of acicular gypsum are also present.

160.73–203.00 m.

Anhydrite-rich cap rock composed of anhydrite, anhydritic dolomite, and grey friable dolomite is present in this interval. The anhydrite and anhydritic dolomite are generally interlaminated, and occur as beds several metres thick and as fragments in a matrix of grey friable dolomite. In some fragments and beds dolomitic anhydrite is recrystallising to anhydrite, leaving a residue of grey friable dolomite which fills lamination planes and forms thin layers around areas of recrystallised anhydrite.

203.00 m–206.65 m.

This interval is the transition zone between anhydrite cap rock and the halite core of the diapir. Fragments and beds of anhydrite up to a metre thick, which contain irregular patches and veins of halite, are embedded in a halite matrix.

206.65 m–265.48 m.

Halite is the dominant mineral throughout this interval, although there was very little recovery of rock salt in the cores, most of the mineral having been dissolved in the drilling mud. A few insoluble fragments of anhydrite, dolomitic anhydrite, and anhydritic chert were recovered. The halite constitutes the intrusive core of the diapiric structure.

Geochemistry

Analyses for trace elements in the cap rock, carried out on cores from BMR Warri No. 20 by emission spectroscopy, showed that many elements are present in trace amounts (Plate VI). Halite samples from the transition zone between the cap rock and halite core were analysed by wet chemical methods for potassium, bromine, magnesium, and iodine, as well as trace elements. Samples of drilling mud taken at 3-m intervals while the halite core was being drilled were analysed by emission spectroscopy for potassium and sodium in an attempt to assess whether beds of potassium salts were being penetrated (see Plate VI).

Close examination of the analyses of the cap rock shows that two or more elements vary sympathetically. An attempt was made to relate groups of elements to specific rock types, but no correlation could be found. It is concluded that the elements of a group are probably contained within one mineral, and that the concentration of the individual elements of a group is therefore dependent on the concentration of that mineral in rocks of the cap rock. No correlation could be found between the easily distinguished dominant minerals, and the groups of elements.

The groups consist of: K, B, Rb; Mn, Fe, ?Ni, ?Cr; V, Ti. Be, Ir, Os, Th, Cs were not detected. Ba, Co, and Sr do not fall within groups. Only the elements of possible economic significance are considered below.

Potassium

Analyses throughout the cap rock show that less than 5000 ppm (0.5%) potassium is present. Concentrations of potassium do not appear to be related to specific rock types. Feldspar was detected in some X-ray diffraction analyses and this is probably the source of potassium.

In the transition zone between the cap rock and the halite core, values are less than 3300 ppm (0.33%). As some percolating rainwater would penetrate this zone, most potassium salts, being more soluble than halite, have probably been leached.

No direct potassium analyses are available for the halite core. Because all halite penetrated by the bit was being dissolved, samples of the drilling mud were obtained at 3 m intervals and analysed for sodium and potassium. It was anticipated that any interbeds of potassium salts would be detected. The results of the analyses are inconclusive, however, because the mud coming from the hole contained halite from both the mud pit and the formation being drilled. It is estimated that about equal amounts of dissolved sodium came from each source. The concentration of sodium in the mud pit constantly varied, however, as water was lost in the hole, and more halite crystals were added to the mud pit. The amount of potassium in the salt dissolved in the mud pit is also unknown.

The analyses show an average K/Na ratio of 0.015. The only conclusion that can be drawn is that no thick beds of potassium are present.

Magnesium

Magnesium analyses were conducted on 13 halite samples from the transitional zone between the cap rock and the halite core. The results ranged from 0.005 percent to 0.61 percent with an average value of 0.056 percent, indicating that no economic deposits are present in the transitional zone.

Iodine

In all except one analysis, less than 15 ppm of iodine occurs, indicating that no economic deposits are present in the transitional zone.

Bromine

Bromine concentration ranges from 20 to 90 ppm in the transitional zone from cap rock into halite. Bromine replaces chlorine in the crystal lattice of halite, and its concentration increases as evaporation of the water goes to completion. The values recorded in the halite are about the same as those in the anhydrite zone in the Stassfurt evaporites (Stewart, 1963). This would suggest that the halite sampled was from an early stage of the evaporite cycle.

Lithium

The lithium concentrations throughout the core are low compared with those in BMR Madley No. 1. Lithium is most abundant in a red dololutite in that well, but this rock type is not present in Warri No. 20.

Whole-rock analyses

Three specimens of core were analysed for major constituents (Table 6) to obtain a more accurate estimate of the abundance of individual minerals and to provide more precise figures on which to gauge the semi-quantitative analyses. The cores are heterogenous and the analyses are not, therefore, representative averages of the cap rocks and halite penetrated.

Specimen 73880152 (27.85 m), from the gypsum cap rock, contained about 66% gypsum, 15% quartz, 11% dolomite, and 8% clay, feldspar, and limonite.

Specimen 73880153 (187.85 m), from the anhydrite cap rock, contained about 50% anhydrite, 26% quartz, 19% dolomite, and 5% clay, feldspar, and limonite.

Specimen 73880154 (203.80 m), from the halite zone, contained about 89% halite, 5% anhydrite, 2% quartz, 2% dolomite, and 2% clay, feldspar and limonite.

Comparison of logs with core lithology

Wireline logs were run in the hole ten days after completion. It was found that the hole had collapsed to 110 m, the depth at which water had been encountered during drilling.

Spontaneous potential

The spontaneous potential log is almost featureless. Although a variety of rock types is present over the interval logged, the brecciated texture and consequent rapid changes of type over small distances would be expected to give the same result as a homogeneous rock type.

Several fluctuations at the base of the log may be due to zones of porosity or cement filling these zones.

Resistivity

The resistivity log is also featureless, probably owing to the uniform gross composition of the core.

Discussion and conclusions

Origin of Deposit

The classical concept of evaporite deposition, and one that has been substantiated by detailed study of several major deposits of the world, prescribes a cyclic sequence of precipitated salts, resulting from a steadily increasing concentration of salts, ideally in an evaporating enclosed or partly enclosed basin. A review of evaporite cycles in epicontinental marine environments is included in Duff & others (1967).

The cycle usually commences with a basal bituminous and possibly also sulphide-rich shale, followed by carbonate rocks, then anhydrite and gypsum, and halite. The last stage of the cycle involves precipitation of the most soluble bittern salts, such as those of potassium and magnesium. In practice these cycles may be interrupted several times by the commencement of new cycles and, as well, the relative proportions of evaporites within each cycle may vary considerably.

It is not known whether the last bittern stage of the evaporite cycle was reached in the deposits at Woolnough Hills. Several other rock types present in the core and cap rock at Woolnough Hills may belong to other parts of a cyclic deposit, but because of the highly disturbed nature of the cap rock and sediments in the immediate vicinity, they cannot be successfully reassembled into stratigraphic order. That they do belong to an evaporite cycle is suggested by the presence of halite moulds in several of the rock types.

Paragenesis of rock types

Of the rock types described, probably only halite, dolomitic anhydrite, and anhydritic chert were present in the original deposit. In the lower part of the cap rock it is evident that dolomitic anhydrite is recrystallising along laminae, joints, and irregular bodies, forming coarsely crystalline anhydrite, which is relatively pure. The dolomite which is present in the original rock appears to have been concentrated in layers several millimetres thick around the irregular bodies of anhydrite, and in joints and laminae throughout the dolomitic anhydrite. Where the concentration is high, it forms grey friable dolomite containing anhydrite.

The action of water percolating through the evaporites and forming a cap rock of residual matter after the halite was leached out is a major factor in the formation of the rock types. In the basal part of the cap rock this groundwater dissolves halite in the transition zone, leaving a residue of dolomite, anhydrite, and quartz. Anhydritic grey friable dolomite also forms and fills the spaces between fragments of other rock types. In the middle part of the cap rock, where more percolating water is available, anhydrite absorbs water into its crystal structure to form gypsum. In the anhydrite/gypsum transition zone gypsum is present along lamination planes and joints and as irregular bodies. In the upper parts of the cap rock the transition is complete and only gypsum is present. The hydration of anhydrite to gypsum increases its volume by about 50 percent, causing contortion of beds and fragments.

As no gypsum has been recorded within the halite, and none in the lower parts of the cap rock, calcium sulphate must be present within the halite as anhydrite. If this is so, all the gypsum-bearing rock types encountered in BMR Warri No. 20 must have originated by hydration of anhydrite in the upper part of the cap rock. Dolomitic anhydrite would recrystallise to form either dolomitic gypsum or gypsum crystals. In the latter case, the residual dolomite would form a matrix of grey friable dolomite containing gypsum. Grey friable dolomite containing anhydrite would also recrystallise to form its gypsum-bearing equivalent. Anhydrite was reconstituted to gypsum by hydration and accompanying recrystallisation. In the near-surface cap rock, gypsum has been leached and redeposited along joints and lamination planes.

Economic potential

BMR Warri No. 20 was drilled to determine the mineralogy of the evaporite core in the Woolnough Hills diapir to evaluate the economic mineral potential of the evaporite deposits. The identification of the intrusive core as halite considerably enhances the potential of the sequence. The undisturbed mother salt beds must be at least 500 m thick, and where potash is present in an evaporitic sequence, it is nearly always associated with the halite. However, analyses of cores from the anhydrite/halite transition zone indicate that potassium is present only in trace amounts. This is to be expected as the halite has been slightly affected by percolating water, which would preferentially leach any potassium salts, because of their higher solubility. The composition of the drilling muds is subject to many variable factors and the analyses are considered to be of very limited use. It suggests however, that no thick beds of potassium salts are present in the interval penetrated; otherwise a significant increase would have been detected in the drilling fluid.

The sulphur potential is difficult to predict, but the abundance of sulphate fulfils the first prerequisite for sulphur formation. There are other, as yet unknown, factors which may militate against its formation in this region. No native sulphur was encountered in the drill samples, although the hole was drilled into the apparent edge of the core, where the cap rock is commonly thickest and, hence, the chances of intersecting native sulphur are greater. It is probable that very little native sulphur is present within the cap rock. However, less than 100 m halite was penetrated by the drilling and the core of the diapir is about 1000 m across. The possibility of discovering potassium salts and sulphur by further drilling cannot be discounted.

GEOLOGY OF THE MADLEY DIAPIRS

The diapirs of the Madley Sheet area are regularly spaced in a latitudinal trend. There are six well-defined domes, which have rocks of probable Adelaidean age exposed in their cores, and in three the cap rocks to the evaporites are exposed (Figs. 64–68).

Madley diapir no. 1

The most easterly dome, Madley diapir no. 1, is a small structure about 1100 m long and 600 m wide, almost completely surrounded by red sand dunes. Outcrop of bedrock is sparse, and most of what is interpreted as the intrusive core is covered by numerous low mounds of secondary gypsum on an otherwise flat surface of dark brown earth. There are no obvious sink holes in the gypsum. The dark earth is commonly dotted with small irregular fragments of white and some black chert, which are derived from a few scattered limestone and dolomite blocks, 2–3 m across and rising up to 1 m above the otherwise flat floor of the core.

The main prominences in the dome are composed of limestone, dolomite, and limestone breccia and obviously originated as blocks rafted on the mobile evaporites. The limestone is grey, dark-grey, red, yellow, and black, fine and medium-grained, and is partly replaced by chert. The rock is mostly thin-bedded with interbedded fine and medium laminae, and in places shows limonite pseudomorphs after ?pyrite. Some irregular patches of secondary gypsum are present close

Fig. 64. Air-photo mosaic of the Madley diapiric trend, Officer Basin.

to the top of the limestone hills, adding further weight to the argument that those blocks were once completely surrounded by gypsum. The largest outcrop of limestone occurs near the northern margin of the core, and here the structure appears to be a south-plunging anticline with beds dipping 50–70°.

Some low mounds of pisolitic ironstone occur on the southern flanks of the dome, together with travertine, which has incorporated numerous pisolites, undoubtedly from the ironstone.

Madley diapir no. 2

Madley diapir no. 2, 3100 m long and 1500 m wide, is the largest of the group (Madley diapir no. 1 has the smallest surface expression, although, obviously, most of the flanking sediments are obscured). The core of diapir no. 2 consists of sandstone, of presumed Late Precambrian age, which is well sorted, medium to fine-grained, medium bedded, friable and clean, white on a fresh surface, and orange-brown weathered. The beds dip about 45° to the south. There is no sign of carbonate rocks, gypsum, or any other evaporites which are commonly associated with the intrusive cores of the diapirs.

On the north side of the dome Permian and Cretaceous beds are poorly exposed and unconformably overlie the Proterozoic sandstone. The Permian rocks are poorly sorted, pebbly and bouldery, massive siltstone, white siltstone, and poorly sorted, ferruginised sandstone. Scattered erratics of weathered schist and quartzite, up to 50 cm across, are present in the siltstone. These rocks are overlain by cream and yellow siltstone, which has a hackly fracture, is poorly bedded, and poorly exposed. The siltstone is succeeded by beds of ferruginised, poorly sorted, granule conglomeratic sandstone, with lateritic sandstone forming the distal outcrops on the north flank. The siltstone and ferruginous sandstones were regarded as part of the Cretaceous sequence by Wilson (1964), but later workers (Kennewell, 1974) have suggested that they are all part of the Paterson Formation.

Madley diapir no. 3

Diapir no. 3 is about 1500 m long and 800 m wide, with a central core mostly obscured by debris of dark grey, black, and ochre-coloured rubble of chert and silcrete. There is one outcrop of dolomite at the eastern end of the dome which shows small cross-laminae and beds selectively replaced by chert. There are also several small outcrops of dolomite in the northwest which are now replaced by black and grey chert with a few remnant dolomite laminae. Many of these outcrops show strong brecciation. One or two outcrops of poorly sorted silicified sandstone occur on the north side of the dome, and these rocks and a similar silcrete-capped sandstone in the prominent hill at the western end of the structure are probably Permian in age.

Madley diapir no. 4

Diapir no. 4, approximately 1200 m by 800 m, was not visited, but descriptions by other workers indicate that the core is Proterozoic sandstone of similar composition to that present in diapir no. 2. The sandstone beds also dip south at about 20°. There is no gypsum core or blocks of dolomite and limestone. The rocks of the flanking sediments are mostly Permian arenites.

Madley diapir no. 5

Madley diapir no. 5 is the best exposed of the six diapirs and measures about 2500 m long by 1000 m wide. The central part of the dome is poorly exposed, and unweathered gypsum crops out only in the basal part of several sink holes present in the beds of some of the small water-courses. The largest sink hole observed is about 9 m deep and 3 m across at the entrance and shows coarsely crystalline secondary deposits at the surface. The base was not examined, but the exposures are obviously less-weathered gypsum. The secondary deposits are more evident in the western part of the core.

The grey and minor black limestone floaters are predominantly fine to medium-grained, thin-bedded, and mostly steeply dipping. Accompanying chert floaters, which are replacements of limestone, are almost invariably black. Brecciated textures are best displayed by many of the chert boulders, with the angular chert fragments etched into relief. The best exposures of limestone are in the eastern part of the structure. In one of these exposures, the steeply dipping beds strike west-northwest, normal to the strike of the rim rocks.

The rim rocks of the structure are mostly sandstone, which is poorly sorted and bedded, and strongly silicified in places. The silcrete crust on the sandstone breaks into large angular blocks. Fragments of grey thin-bedded friable siltstone occur in areas of the sandstone outcrop, but could not be placed readily in the sequence. The unweathered rock that commonly crops out at the base of the more prominent flanking scarps is a poorly sorted, massive, fawn to white, sandy siltstone, which, by virtue of its closely spaced jointing, breaks into irregular blocks. Crumbly and friable deposits of earthy gypsum are also common at the base of several of the westerly sandstone scarps. It is yellow, red, and ochre coloured, and includes some large clear selenite crystals. It is not certain whether the gypsum is derived from weathering of shales or derived from the intrusive gypsum, which seems a more likely explanation. Claystone crops out on the north rim of the dome and resembles the Cretaceous sediments.

The sediments on the north and south flanks show steep dips up to 70°, but are much shallower on the east and west flanks. The southern flank of the dome is truncated by a fault which post-dates the Permian rocks. The beds are, in places, slightly overturned next to the fault zone.

BMR MADLEY No. 1

Drill site geology

BMR Madley no. 1 evaporite test hole was drilled in the core of the most westerly dome in the group of six diapirs. The linear arrangement of the diapirs is probably controlled by a major fault, which is readily apparent along the southern margin of diapir no. 6. In addition, the close jointing, banding, and incipient brecciation apparent in the rim rocks on the south flank suggest the proximity of a fault.

Diapir no. 6 was chosen as the well site, firstly, because evaporites were exposed at the surface, and, secondly, because it was the farthest removed in the group from the previous drill site at Woolnough Hills, and, hence, would be more likely to penetrate a different sequence.

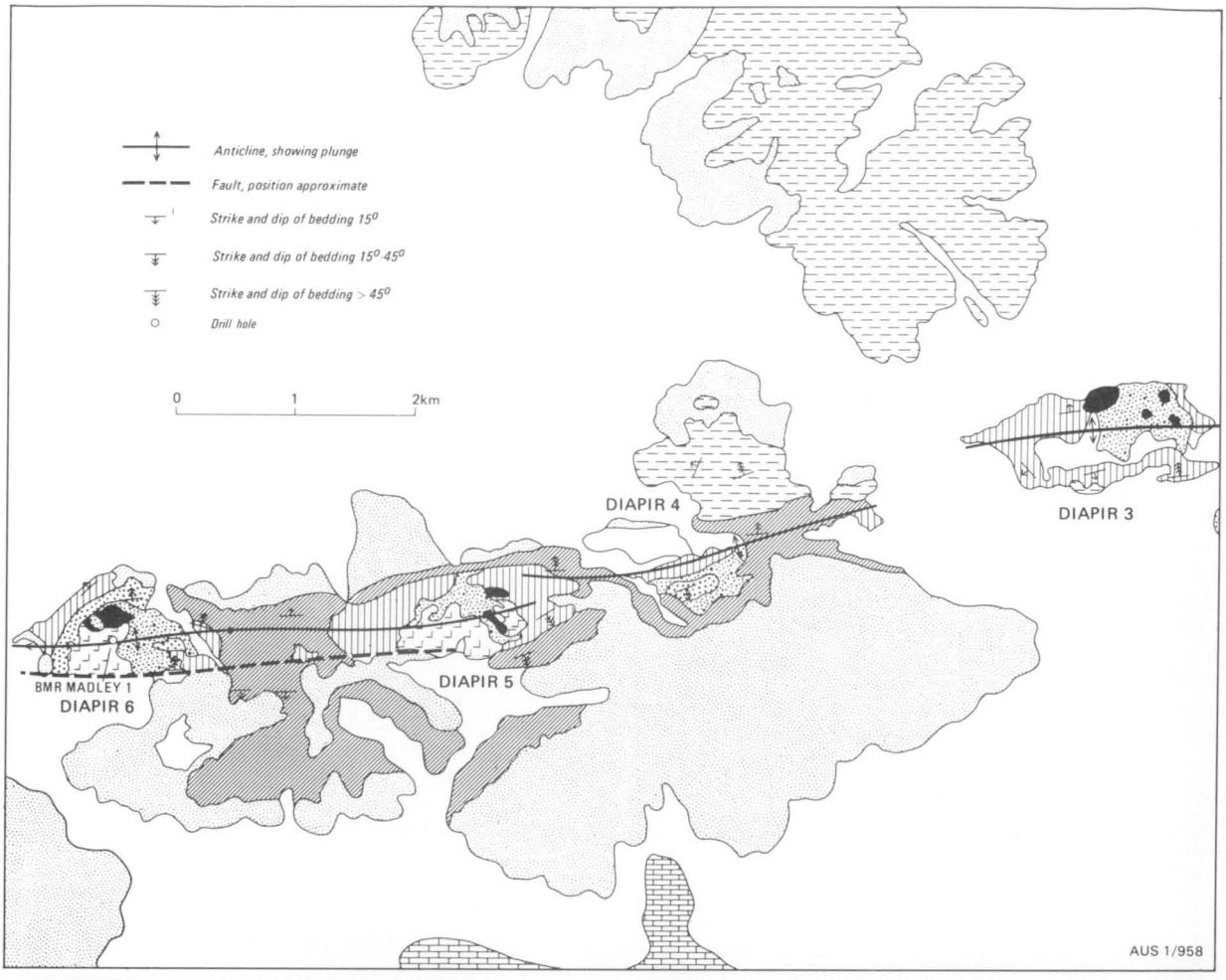

Fig. 65. Geological map of the Madley diapirs, Officer Basin (after Wilson, 1967).

Fig. 66. Vertical aerial photograph of Madley diapirs nos. 5 and 6, Officer Basin. (G/5472)

Fig. 65 continues on next page.

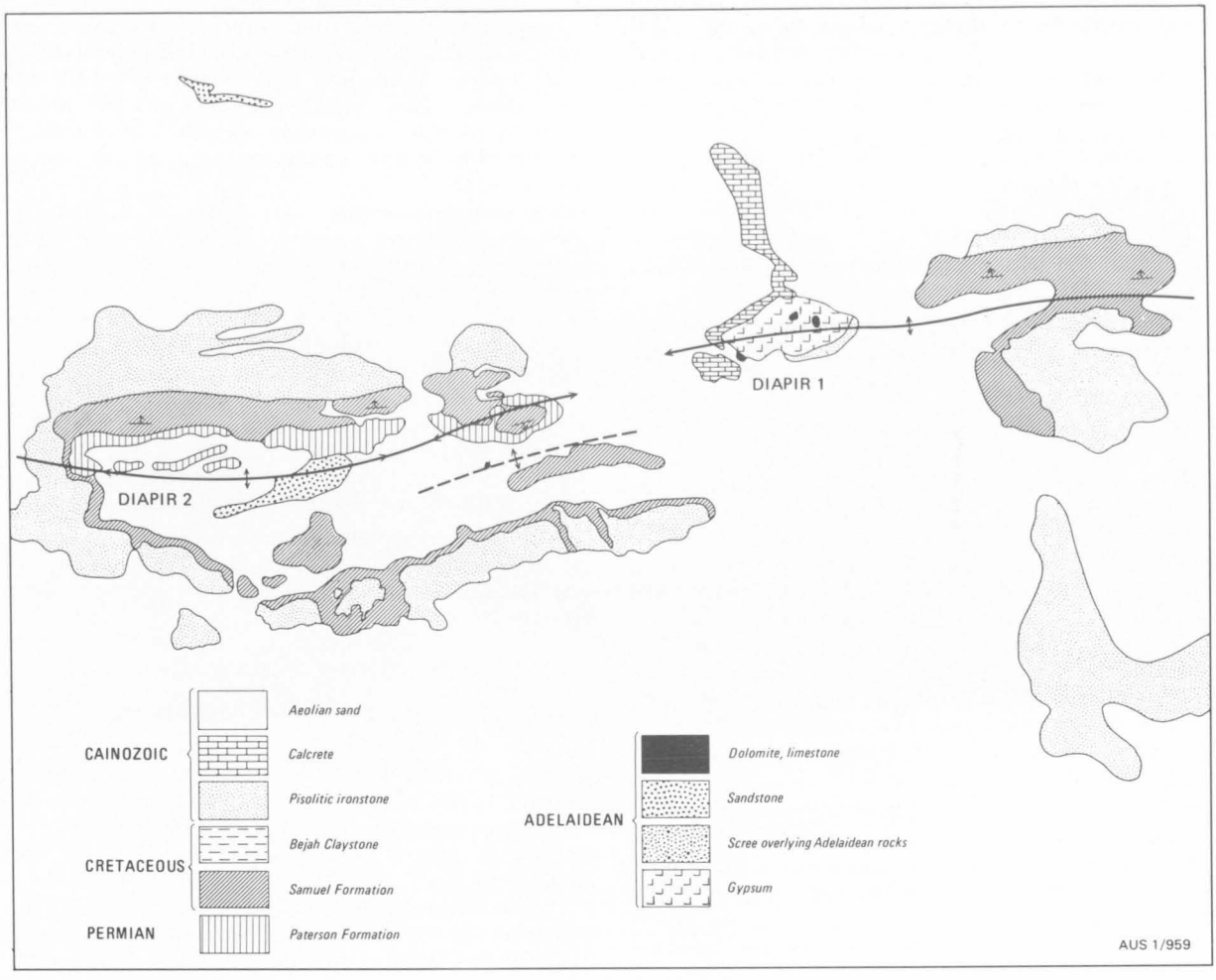

Fig. 67. Oblique aerial photograph of the Madley diapiric trend, viewed from the west. Diapir no. 5 in middle distance. (GA/9094)

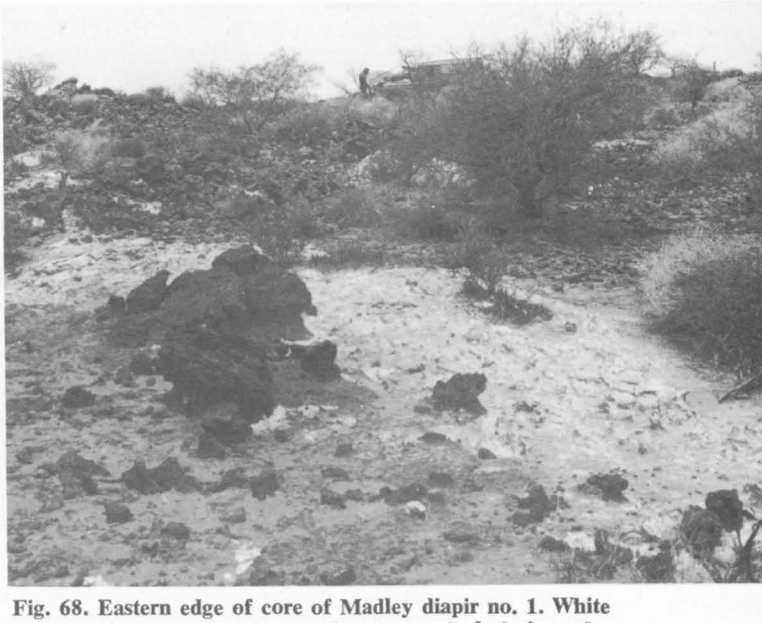

Fig. 68. Eastern edge of core of Madley diapir no. 1. White weathered gypsum in depressed areas and dark irregular blocks of resistant dolomite formerly enclosed in gypsum and now accentuated by weathering. (M1434-27)

The evaporites in the sparse outcrop of the diapir core consist of weathered earthy or rock gypsum, together with some secondary selenite. The evaporite is mostly obscured by rubble, the larger fragments in which consist of banded chalcedony, ironstone, silcrete, and silicified sandstone. The outcrops of evaporite occur in low mounds in the central core area and at the base of the low scarps of sandstone which surround the core. Several detritus-filled sink holes are present on the east side of the core, but no fresh gypsum breccia is exposed.

There are a few scattered small pinnacles of dolomite and limestone in the central core, and some larger outcrops on the northwest side. The dolomite is thin to medium bedded, pink and grey to reddish, weathers yellow-brown, and is medium and fine-grained. Much of the dolomite is brecciated, and has a porous leached appearance. Some of the dolomite beds are oolitic and pelletal. The outcrops of carbonate rocks on the west side of the diapir appear to be mostly limestone, which is thin bedded, grey, in part brecciated, and interbedded with black chert. Many of the outcrops are covered by small patches of secondary limonite crusts. The beds in the limestone here mostly dip steeply to the west. A prominent outcrop of dolomite about 20 m south-west of the drillsite is about 12 m long and 1–2 m high, and the thin and medium beds dip about 45° southwest. The attitude of the scattered blocks of the core would be expected to be quite random.

The rocks of the diapir rim consist almost exclusively of arenites, chiefly sublitharenite (Pettijohn & others, 1972) and they are commonly capped by a thick crust of silcrete, particularly those in the topographically higher exposures.

In several outcrops, the finer-grained arenites overlie the intrusive gypsum. An intrusive contact is suggested, because nowhere are the arenites shown to be in stratigraphic sequence with gypsum, and in other diapirs thick ?Proterozoic rocks commonly intervene between the gypsum and identical arenites. This contact was seen on the southwest and northern flanks of the dome and in the prominent hill about 250 m east of the drillsite. The siltstone is poorly bedded, white (some is yellow and mauve), sandy, and irregularly jointed. In other places the contact is obscured by pink and fawn travertinous limestone, which contains cemented ironstone pisolites. The siltstone is overlain by friable, clean, thick-bedded to massive, well-sorted medium-grained sandstone, which forms the more prominent ridges in the area. The weathered surface of the sediments is commonly strongly silicified and dark brown.

The intrusive core and the overlying sediments so far described are most probably Proterozoic. The beds are similar lithologically to the Browne Beds in Browne Nos. 1 and 2 wells, which are probably Adelaidean. The Babbagoola Beds, the only other known partly evaporitic formation in the Officer Basin, are probably Cambrian. The carbonate beds and remnant blocks in the core of Woolnough Hills, which are probably coeval with those in the Madley diapirs, contain columnar and mound-shaped stromatolites which are superficially similar to those described by Preiss (1972) from the Precambrian of the Adelaide Geosyncline.

Fossil microbiota are preserved in black cherts within undulose stratiform stromatolites from Madley diapir no. 1. The specimens occur in a large block of dolomite within the central gypsum core. The microbiota resemble several other Precambrian assemblages and preservationally are very similar to those of the Bitter Springs Formation (M. Walter, personal communication). The stratiform nature of the Madley cherty stromatolites combined with the composition of the microflora indicates an upper intertidal environment of deposition.

The sediments on the outer flanks of the dome are poorly exposed and consist of coarse to very coarse, ferruginised, poorly sorted and bedded sandstone with a mixed matrix of medium-grained sand, silt, and clay. The sandstone is also commonly strongly silicified and breaks into large irregular blocks. There are a few interbeds of yellow, poorly bedded siltstone. The finer-grained rocks are commonly obscured by patches of travertine. These sediments of the outer flank are lithologically similar to Permian rocks of the Paterson Formation mapped elsewhere in the Madley diapirs and Officer Basin.

With a few exceptions the rim rocks dip away from the diapir core mostly at 10–15°. The beds steepen near the southern margin, and on the southwest flank dips are 20–35°.

Description of rock types

Classification of textures and rock types

Unless the sedimentary rocks have been subjected to close petrographic scrutiny, only general descriptive rock terms are used. However, for those rocks that have been examined in detail, the classifications of Pettijohn & others (1972) and Folk (1959) have been used for arenites and carbonate rocks, respectively.

The classification of Pettijohn & others uses a basic triangular system with feldspar, quartz, and rock fragments constituting the end members, and the percentage of matrix forming the fourth or secondary variable. This secondary criterion distinguishes arenites or sands with less than 15 percent matrix, and wackes or sands with more than 15 percent matrix. Arenites with no more than 5 percent of either feldspar or rock particles are called quartz arenite. Those with 25 percent or more feldspar which also exceeds the content of rock fragments are called arkosic arenite. Conversely those with 25 percent or more rock fragments which also exceeds the content of feldspar are called lithic arenites. Sublitharenite and subarkose are transitional types between quartz arenite and lithic arenite or arkosic arenite, respectively. The greywackes are divided into feldspathic greywacke or lithic greywacke depending on the composition of the dominant rock particle. Quartzwacke contains 5 percent or less feldspar and rock fragments. The character of the cement can be added as a prefix to the rock name.

The carbonate rocks encountered in the well section are mostly microcrystalline, and some thin beds contain abundant terrigenous material. However, the bulk of the finely crystalline dolomite probably consists of allochemical components. Using Folk's grainsize scale the carbonates mostly fall into the medium dololutite division.

The classification used for crystal size of recrystallized carbonates is that of Folk (1964).

Mostly, the colours of the rocks are described in general terms. To give a more precise idea of the meaning of these terms, they have been coded with reference to the Geological Society of America rock-colour chart. The common terms used and the equivalent colour-chart codings are as follows: red-

brown dololutite—pale red 5R 6/2, 10R 6/2; chocolate-brown dololutite—greyish red 10R 4/2; green dololutite—light greenish grey 5 G/Y 8/1, 5G 8/1; red-brown dolarenite—pale red 10R 6/2.

The cores were first analysed by X-ray diffraction, and, subsequently, numerous thin sections were studied in detail.

Mineral and rock composition

A graphic presentation of rock types penetrated in BMR Madley No. 1 is shown in Plate VII.

Dolomite is the most common mineral in the drill cores recovered from the cap rock of Madley diapir no. 6, and dololutite the most abundant rock type. The other common minerals in order of abundance are quartz, anhydrite, gypsum, and muscovite. Minor minerals include feldspar, chlorite, and hematite. The dololutite is commonly thinly bedded to laminated, mostly chocolate-brown, with subordinate brown, green, and pale brown varieties. The brown is aparently caused by hematite and the lighter coloured varieties contain a large proportion of anhydrite or gypsum (Fig. 69). The dolomite and quartz grains in the dololutite are medium crystalline, generally around 0.02 mm, except where recrystallisation has affected the rocks and dolomite rhombs and euhedral quartz are present.

The chocolate-brown and green fragments have essentially the same composition, except that the proportion of quartz and reddish chlorite (clay) is slightly higher and the grains slightly coarser in the chocolate-brown fragments. Fine-grained mica flakes and opaque minerals are common to both types.

Coarser-grained anhydritic lithic arenite is present in thin interbeds at several levels (Fig. 70), mainly in the deeper parts of the sequence. The rock consists of anhydritic and feldspathic arenite with rounded to well-rounded grains of quartz, feldspar, chert, and quartzite. Quartz 'shards' are present in some of these rocks, and some of the chert shows boxwork-like and corroded textures, suggesting that some of the grains may be derived from volcanic rocks. Some of the grains of ?chalcedonic clay and quartz showing resorbed textures are possibly derived from the alteration of acid lavas, other grains showing a granophyric texture are most probably derived from granitic rocks, and the rounded chert grains, from a silicified oolitic dolomite.

Very fine-grained quartz occurs in the dololutite, and in places where it is recrystallised shows a well-developed euhedral hexagonal crystal outline.

Gypsum is common in the near-surface layers. It was found in core 1 (45.1 m) and occurs together with anhydrite in cores 2 and 4 (154.05 and 158.88 m), but only anhydrite occurs in cores below. Gypsum and anhydrite are common in the dololutites, where a Fontainebleau texture, with dispersed dolomite and quartz grains in an optically continuous gypsum groundmass, is commonly formed by recrystallisation. Coarse euhedral anhydrite is also present in recrystallised zones. Most of the vein anhydrite appears to be concentrated in the upper parts of the core. Muscovite is generally present as fine flakes in the dololutite, and is only rarely found as coarser crystals. Biotite was only found in one core section. Gypsum becomes the predominant mineral over certain intervals of the core, notably from about 48-49 m (95%), 52-55 m (70%), and 56–61 m (50–70%).

The opaque minerals appear to be invariably composed of hematite. X-ray diffraction analyses showed

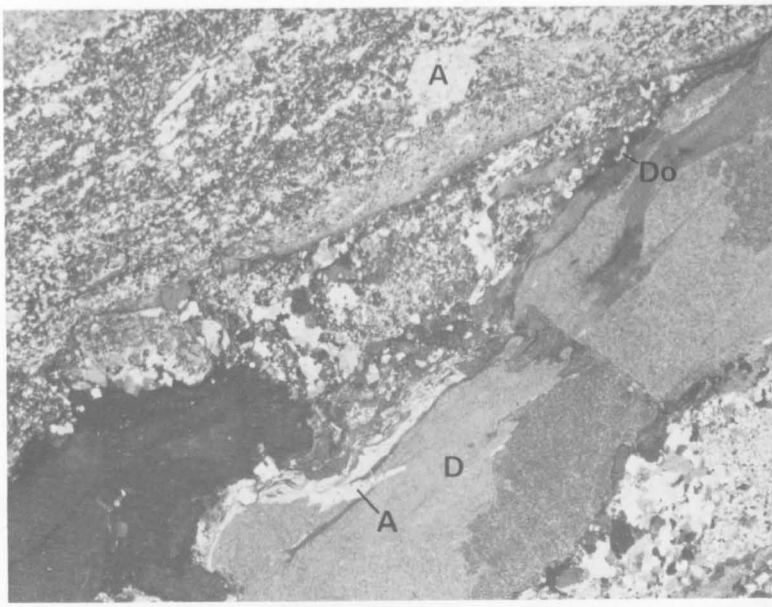

Fig. 69. Dololutite (D) fragments in a matrix of recrystallised anhydrite. Fine-grained dololutite with dolomite, anhydrite, and quartz, in a matrix of predominantly anhydrite (A) and subordinate dolomite (Do) and fine-grained quartz. Dark area in lower left consists of dolomite, quartz, and anhydrite coloured by limonite; from 200.7 m. Crossed nicols, x 5. (GA/8720)

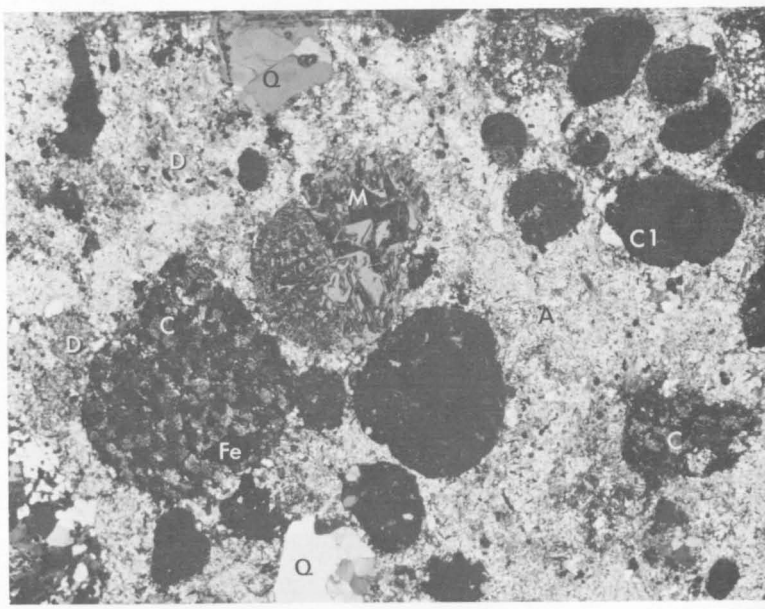

Fig. 70. Anhydritic lithic arenite. A—anhydrite, D—anhydritic dolomite, M—microperthitic feldspar, Q—quartz, C—chert and hematite, Fe—mainly hematite, Cl—?chlorite; from 185.4 m. Crossed nicols, x 20. (GA/9354)

that chlorite and feldspar are present, but these were not easily recognised in the thin sections, except that feldspar grains showing granophyric intergrowths with quartz were easily recognised.

Rock and mineral textures

The cap rock is brecciated or tightly folded. Some parts of the core are made up of steeply inclined thin-bedded anhydritic dololutite, and the core does not reveal whether these intervals are part of much larger breccia fragments or constitute part of a tightly folded

sequence. It seems more likely from the overall texture that they constitute parts of much larger fragments. The brecciated rocks are less likely to be in the form of layered zones of restricted thickness. Well-preserved slickensided surfaces are evident in parts of the core, for example at 202.25 m.

The brecciation and tight folding have caused certain mineral components to remobilise and many recrystallisation textures have resulted (Fig. 71). The matrix of the fragments is composed mainly of euhedral anhydrite with subordinate dolomite rhombs and hexagonal quartz. Anhydrite in fibrous form commonly cuts the dololutite. The gypsum and anhydrite in parts of the dololutite are also partly recrystallised and commonly form stellate clusters or Fontainebleau texture. The recrystallisation has produced some textures that resemble those of replacements.

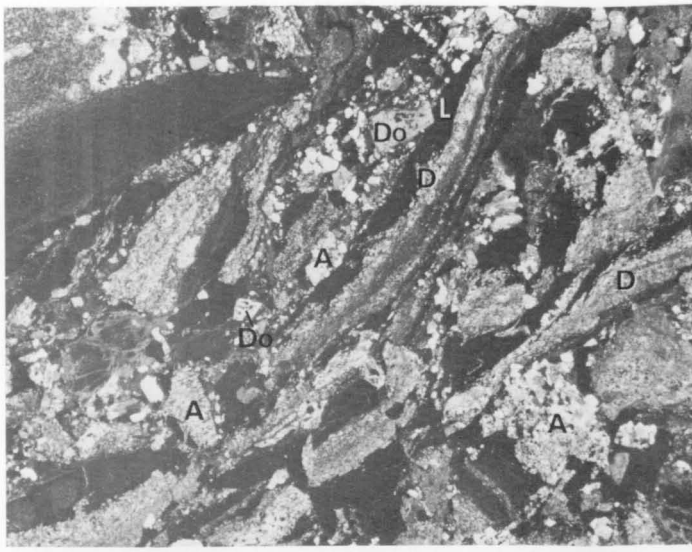

Fig. 71. Brecciated limonitic dololutite (L), and recrystallised anhydritic dololutite (D) in matrix of recrystallised anhydrite (A) and dolomite (Do); from 165.0 m. Crossed nicols, x 6. (GA/8732)

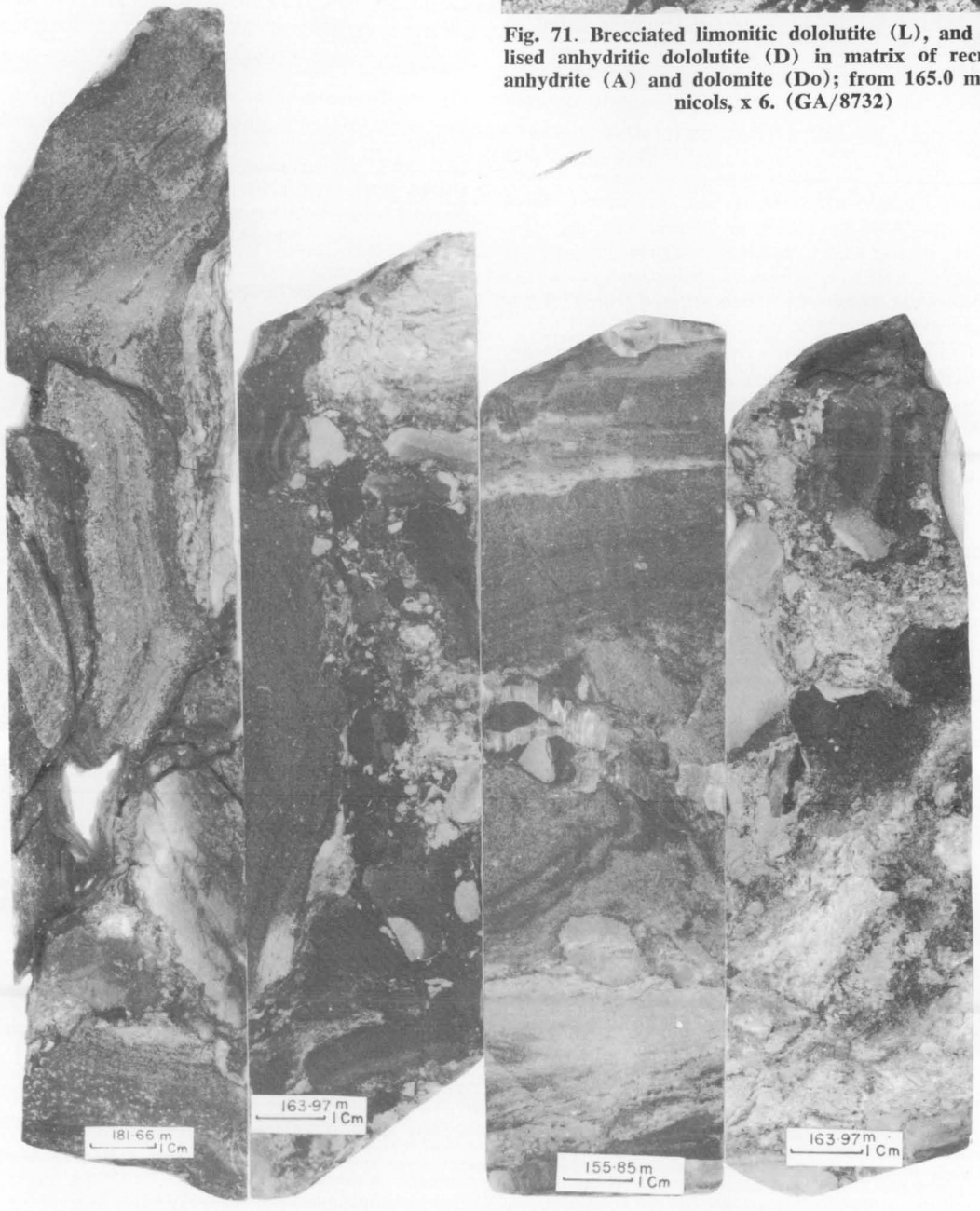

Fig. 72. Textures displayed in polished cores from the cap rock in BMR Madley No. 1.

Origin of deposits

The pre-diapiric sequence interpreted from the cap-rock zone is an interbedded assemblage of silty dololutite, anhydritic dololutite, feldspathic arenite and gypsum/anhydrite with saline interbeds. This evaporitic sequence and the predicted underlying halite mass are probably Precambrian, and may be equivalent to the Browne or Babbagoola Beds—the only sequences in the Officer Basin that show any affinities with sediments deposited in an evaporitic environment. The Babbagoola Beds occur only in Yowalga No. 2 well, and consist of interbedded sandstone, shale, siltstone, and dolomite. The dolomite is anhydritic, and anhydrite and gypsum fill fractures and thin veins in the sediments. The Browne Beds consist of inter-bedded dolomitic limestone, calcareous shale, anhydrite, and halite.

As a result of diapirism the beds of the sequence have been mechanically disrupted, and breccias and tight folding produced (Fig. 72). Cores up to one metre long, showing non-brecciated, but steeply inclined, beds are probably sections through large blocks. The cap-rock zone is undoubtedly a breccia with a large variation in breccia fragment sizes, and some zones of megabreccia are indicated by these core sections.

Recrystallisation effects are also common, and the matrix of the breccia is composed of mostly euhedral anhydrite and, less commonly, euhedral quartz and dolomite rhombs. The anhydrite or gypsum was partly remobilised into vein deposits, which intrude the dololutites and matrix. The gypsum and anhydrite of the dololutites were partly recrystallised to give Fontainebleau-like textures. Gypsum was converted to anhydrite after burial, and the reverse process in the near surface layers was caused by subsequent diapirism and exhumation.

TABLE 14. CHEMICAL ANALYSES, BMR MADLEY No. 1

	Sample No. & depth	
	7388–0155 (43.9 m)	7388–0156 (203.5 m)
SiO_2	23.3	21.1
Al_2O_3	4.95	4.35
Total Fe as Fe_2O_3	2.55	2.25
CaO	20.2	23.4
MgO	7.90	9.20
Na_2O	0.05	0.53
K_2O	1.20	1.30
TiO_2	0.37	0.29
H_2O^+(over 105°C)	2.40	1.71
H_2O^-(at 105°C)	7.90	0.39
H_2O^-(at 44°C)	0.20	0.20
CO_2	11.4	14.0
MnO	0.03	0.03
P_2O_5	0.07	0.07
SrO	0.018	0.057
Cl	0.02	0.59
F	0.06	0.015
SO_3	17.6	20.7
S (as sulphide and elemental)	0.1	0.1

Note: For samples containing significant $CaSO_4.2H_2O$ it is normal to determine moisture at 44°C only.

Geochemistry

Quantitative analyses for major components were carried out on two samples of core from BMR Madley No. 1 (Table 14): core no. 1 (sample taken at 43.9 m) and core no. 21 (sample taken at 203.5 m). The major components of the breccia, dolomite, quartz, and gypsum/anhydrite, account for most of the CaO, MgO, CO_2, SiO_2, and SO_4 content. Halite content increases downhole and accounts for the increase in sodium and chlorine values obtained from the deeper sample. The potassium and small portions of the silica and alumina can be accounted for in the muscovite and potash feldspar (perthite). A small proportion of magnesium, iron, aluminium, and silica would be taken up by the chlorite, and the major part of the iron content is accounted for by the hematite grains.

The water component of the core decreases with depth, mainly because of the conversion of anhydrite to gypsum at shallower levels. Some water is bound in the lattices of muscovite and chlorite.

The minor elements determined in the rocks include small quantities of titanium, manganese, phosphorus, strontium, fluorine, and sulphur. Titanium and manganese are probably associated with the iron-bearing minerals in the sediments, and the phosphorus and strontium with the gypsum/anhydrite. Sulphur probably occurs mainly in the form of sulphide, chiefly pyrite.

Semi-quantitative spectrographic analyses were carried out for 16 elements on 21 samples, and 3 other elements were determined by wet chemical methods (Plate VII). 15 of the determinations were carried out on cuttings samples, and the remaining 6 were samples of core.

The results found for the element concentrations were compared and the following groups were tabulated comparing similar concentrations and vertical variations.

High concentrations; generally above 500 ppm, and show no depth zonation: titanium, potassium, iron. *Low concentration*; values generally in range 0–500 ppm, and show no vertical zonation: cobalt, beryllium, nickel, caesium, manganese, vanadium, barium, rubidium. *Low concentrations*; generally in range 0–500 ppm, and show an increase with depth: strontium, sodium, boron. *Low concentrations*; generally in range 0–500 ppm, and show decreasing values with depth: chromium. *Absent from core*: iridium, osmium, thorium.

In the following chemical notes, the detection limit in ppm, if any, for the particular method of determination is shown in brackets after each element heading. Most of the information on trace element concentrations in overseas evaporite deposits that have been used for comparative purposes has been obtained from Stewart (1963).

Manganese (10)

Manganese values are fairly consistent at about 80–100 ppm through the core, and show no obvious trend with depth. These values are similar to those obtained from the cap-rock zone in BMR Mount Liebig No. 1 well. Insignificant concentrations are present in the underlying halite zone in this well. Similar values were also recorded in BMR Warri No. 20 well. Average values of 120 ppm manganese in 80 anhydrite rocks were reported by Kropachev (Stewart, 1963).

Cobalt (5)

Values for cobalt are generally around 5 ppm and do not show any vertical zonation. No comparative

figures for cobalt in cap rocks are readily available, except in BMR Warri No. 20, where the element was mostly not detected.

Chromium (20)

Values are low and fairly consistent through the core, although a marginal decrease with depth is noticeable. Similar values were found in BMR Warri No. 20. Published chromium concentrations show that it is absent from halite and bittern salts (Stewart, 1963), but clays in the evaporite sequences usually contain much larger amounts than the evaporites.

Beryllium (1)

Beryllium values are low and show no significant trend. In BMR Warri No. 20 beryllium was mostly not detected.

Iridium (2), Osmium (10), & Thorium (100)

Iridium, osmium, and thorium are absent at the detection limits given, and no other information is available on concentrations in evaporites. They were not detected in BMR Warri No. 20.

Nickel (5)

Low nickel values are evident, and show no trend. Values are marginally higher in BMR Warri No. 20 and show a very slight increase in the lower half of the cap-rock zone.

Vanadium (10)

Except for one sample at about 110 m with 400 ppm, vanadium values are 80 ppm and below. Similar values were found in BMR Warri No. 20, with 80 ppm the highest. Kropachev reported no vanadium in 9 anhydrite rocks (Stewart, 1963).

Titanium (100)

Titanium values are fairly consistent through the well section at about 1000 ppm, with a few samples showing concentrations up to 2500 ppm. No comparative figures are available.

Barium (50)

Barium concentrations are generally around 200 ppm. Similar values were apparent in the cap-rock zone in BMR Mount Liebig No. 1 (Wells & Kennewell, 1972) and, with only two or three exceptions, practically no barium occurs in the halite zone. Values in BMR Warri No. 20 are likewise remarkably consistent at about 200 ppm. This pattern follows the one generally experienced in salt domes. Stewart (1963) reported that barium replaces calcium in anhydrite and gypsum, but is usually much less abundant in halite rock. Von Engelhardt found 210 ppm barium in salt-clay; 1–3 ppm in anhydrite rock and anhydrite-halite rock; 3–10 ppm in gypsum, polyhalite and some halite, carnallite, and sylvite; and 10 ppm in clear halite, in German evaporites (Stewart, 1963).

Strontium (10)

Strontium values show an increase with depth, from 10–20 ppm near the surface to about 200–500 ppm at deeper levels. There is a sharp increase in values below 150 metres. Like barium, strontium replaces the calcite in sulphate and carbonates. In BMR Mount Liebig No. 1, strontium is fairly consistent in the cap-rock zone (generally 100–200 ppm), but more erratic in the halite and, whereas it is mostly absent, there are a few values of 600–800 ppm, generally where gypsum interbeds occur in the halite. In BMR Warri No. 20 a similar pattern is evident, with a sharp increase in values from an average of about 100 ppm to 300 ppm in the lowest 30 metres of cap rock.

The SrO figures that Stewart (1963) cites (after Noll, 1934) are highest in anhydrite rock: 0.17–0.69%; 0.003–0.13% in gypsum rock; 0.12% in polyhalite rock; and 0.00002–0.0002% in sylvite and carnallite. Noll (1934) found that the gypsum that has replaced earlier anhydrite rock cannot retain all the strontium from the original anhydrite. This may give an indication of the origin of anhydrite deposits, and enable a distinction between primary anhydrite with high strontium concentration and anhydrite which has replaced primary gypsum.

Potassium (5)

Potassium values down to 60 m range from 300 to 10 000 ppm. Below 60 m values are 10 000 ppm or above, the upper detection limit lying at around this figure. Quantitative K_2O values were obtained on two samples of core (Table 14). No soluble potassium minerals are evident in the core and the potassium probably is in muscovite and potash feldspar, particularly in the lithic arenite sequences. Potassium values in BMR Warri No. 20 are lower and show no trend.

TABLE 15. LITHIUM AND POTASSIUM ANALYSES OF SELECTED ROCK TYPES IN CORES FROM BMR MADLEY No. 1

Sample No.	*Depth (m)*	*K%*	*Li ppm*	*Rock type*
7488 0001	185.4	1.43	105	Green dololutite
7488 0002	189.9	1.78	48	Lithic arenite
7488 0003	199.9	1.43	84	Green dololutite
7488 0004	154.6	1.39	68	Red dololutite
7488 0005	155.3	0.63	32	Gypsiferous dololutite
7488 0006	155.5	1.31	60	Green dololutite
7488 0007	156.1	0.36	20	Acicular gypsum
7488 0008	158.0	2.25	140	Red dololutite
7488 0009	158.5	1.13	56	Green dololutite
7488 0010	182.4	0.55	28	Anhydritic dololutite
7488 0011	185.1	2.40	140	Red friable dololutite
7488 0012	202.25	0.86	40	Anhydrite
7488 0014	203.40	1.50	110	Red dololutite

All the samples that showed potassium values in excess of 10 000 ppm by semi-quantitative analyses were re-analysed by wet chemical methods; the highest value obtained was 2.05% K in cuttings from 129.54–137.06 m, and with one exception all the values are above 1 percent. Selected samples of various rock types from the cap rock were analysed for potassium and lithium (Table 15). The results show an obvious correlation between rock type and element concentration; the highest potassium values occur in the red friable dololutite, red dololutite, and lithic arenite; intermediate values in the green dololutite; and lowest in gypsiferous dololutite, acicular gypsum, anhydritic dololutite, and anhydrite. This confirms the assumption that the potassium is derived mainly from feldspars.

Caesium (30)

Caesium values are mostly at or below detection limits and show no obvious variation with depth. Caesium was not detected in BMR Warri No. 20.

Rubidium (10)

Values are mostly about 100 ppm and show no obvious trends. Values range from below 10 ppm up to 150 ppm in BMR Warri No. 20, with a random scatter of values within these limits in the core.

Sodium

Sodium content increases gradually with depth, and values are around 0.02 percent near the surface to about 0.5 percent near total depth. A sample of red and green dololutite breccia from the core at 202.35 m gave an analysis of 1.08 percent NaCl and a water insoluble content of 76.3 percent.

Halite could not be detected in thin sections and some of the sodium may be derived from the feldspar. The gradual increase in sodium values with depth is no doubt related to diapirism and leaching of soluble salts as the cap rock migrated through surface water zones. Three core analyses in BMR Warri No. 20 show a similar increase in Na values with depth, and in the halite below the cap rock, sodium content is 35.2 percent, which is close to the value for pure halite (39.4 percent).

Boron

The boron concentration increases marginally downhole, although the rate varies considerably and is somewhat erratic. Boron enrichment generally occurs in clays of evaporite sequences, which probably explains the slight increase in boron values with depth, and bears a direct relation to the increase in halite content. Boron values in BMR Warri No. 20 show no trend and range from about 20 to 250 ppm. The boron and potassium concentrations are very similar in BMR Warri No. 20 and BMR Mount Liebig No. 1 holes. Boron values in the cap rock of BMR Mount Liebig No. 1 are generally around 10 ppm down to about 20 m depth and from 10–100 ppm below this (Wells & Kennewell, 1972). Boron values in the halite were below 100 ppm, but could not be more accurately determined, because of interference from sodium.

Generally the values are comparable to those that are quoted for overseas evaporite occurrences. The higher values of around 600 ppm (Stewart, 1963) are found in salt clays.

Iron

The iron content is remarkably constant and shows no vertical zonation. The iron is mainly present as hematite, which gives the coloration to the dololutites. The iron content of readily soluble evaporite sequences is generally lost; what remains is mostly in the range 2–70 ppm. Iron in BMR Warri No. 20 is high in the near-surface samples (30 000 ppm at about 5 m), and varies from 1–10 000 ppm with no obvious trend in the remainder of the cap rock.

In BMR Mount Liebig No. 1 the highest iron content occurs in the cap rock from about 50–150 m (just below 3 percent). Concentrations in the halite are low and show no trend.

Lithium

Lithium values fall in the range 20 to 140 ppm with no particular trend with depth, although the higher values occur mostly in samples from below 150 m. With few exceptions the values are closely aligned to the variation in potassium content. Selected rock types were analysed for potassium and lithium and the results are given in Table 15. The highest lithium values were found in the red dololutite and red friable dololutite; intermediate values in the green dololutite; and low values in lithic arenite, anhydrite, gypsiferous dololutite, anhydritic dololutite, and acicular gypsum. The most notable exception to the parallel values with potassium is a sample of lithic arenite which contains 1.78% K, but only 48 ppm lithium.

A comparison of vertical variation in trace element concentrations in the well shows that several groupings of elements are present. These show similar trends although the concentrations are several orders of magnitude apart. The six groups are: beryllium, nickel, chromium, cobalt; boron, strontium, barium; caesium, potassium, sodium, lithium; rubidium, titanium, vanadium; iridium, osmium, thorium; iron, manganese. The similar geochemistry of many of these elements would explain their parallel concentration changes.

Discussion and conclusions

The secondary gypsum and dolomite float present in the cores of the Permian and Cretaceous domes of the Madley diapiric trend were described by previous authors to be part of an evaporitic sequence of unknown age and thickness. The gypsum was considered to be the more insoluble part of the evaporite deposit, and the dolomite to be part of the overlying or interbedded sequence. It was postulated that halite probably constituted the intrusive core of the dome.

The exploratory driling did not conclusively confirm the presence of the intrusive halite, but the increase in halite content in the predominantly dololutite core with depth is strong evidence for the presence of soluble evaporites beneath the dolomite and gypsum.

The dololutite and gypsum rock in the cap rock were originally part of a bedded evaporite sequence, presumably stratigraphically above and partly interbedded with a thick halite zone. The more soluble constituents were dissolved and removed as the salt plug advanced through the overlying strata and eventually encountered groundwater. The more insoluble beds now constitute the residue and make up the cap rock.

Paragenesis of rock types

As they were transported ahead of the rising salt mass, the rocks were tightly folded, brecciated, and recrystallised. Otherwise, most of the chocolate-brown and green dololutites underwent little internal change, although some have been recrystallised. Some of the dololutite fragments and intervals encountered in the core are little changed, whereas other parts have been recrystallised. Recrystallisation of the fragments has produced a mosaic of coarse crystals or stellate crystals of anhydrite or gypsum, so that the framework of the rock is changed, the grains becoming completely surrounded by monocrystalline anhydrite or gypsum, and the individual grains and crystals in most places being entirely dispersed.

The groundmass of the brecciated zone consists mainly of recrystallised anhydrite and a little dolomite and quartz. The anhydrite/gypsum has been remobilised to form veins, with acicular and euhedral crystals cutting both matrix and fragments. The long axes of the crystals are generally normal to the vein walls.

The change to recrystallised dololutite appears to be gradational, and, in places where the process has affected most of the components of the rock, the proportion of gypsum/anhydrite is high, but euhedral dolomite and quartz are also present. It appears most

likely that the remobilising of the gypsum/anhydrite has caused the originally anhydritic dololutite to recrystallise and disaggregate, with some recrystallisation of the other rock components, but very little effect on non-anhydritic dololutite. Where extensive recrystallisation has taken place, the boundary between fragments and matrix cannot be readily distinguished.

Economic potential

No minerals of immediate economic interest, including sulphur, potash, calcium sulphate, trona, calcium bicarbonate, or any other evaporite minerals were intersected; and, indeed, from the insignificant amount of exploration of the diapirs to date, it is unlikely that any deposits, even if they existed, would have been found. The odds are sharply against any economic deposit being discovered in one drill hole which only recovered 20 percent of core over the total depth, and did not penetrate the cap rock to sample the core material.

The necessary prerequisities for formation of potash deposits are a large marine sedimentary basin with thick halite deposits, and a relatively undisturbed history of sedimentation in a barred basin in which evaporation can proceed to or near completion. The first prerequisite is satisfied at least in the northern part of the Officer Basin. Widespread diapiric structures and surface and drill-hole intersections of evaporites attest to the thickness and wide distribution of the deposits. A minimum thickness of the salt source bed of the order of 300–400 m is required for the development of diapirs. The depth to the mother salt, as established from known examples in diapir areas, varies, but is generally in the range 3000 to 9000 m. However, there appears to be no minimum depth of burial to separate deformable from competent salt beds. Whether or not evaporation proceeded as far as the stage of bittern salt deposition cannot be gauged, although the estimated large thickness of salt present increases the probability that it did.

Sulphur deposits commonly form in the cap-rock zone of salt domes by bacterial reduction of sulphate to hydrogen sulphide and thence to sulphur. Thode & others (1954), Jones & others (1956), and Feely & Kulp (1957) suggested that oxygen of ground water oxidised the H_2S, which would limit the depth at which deposits of native sulphur could form. The Madley diapirs contain abundant sulphate in the form of gypsum and anhydrite; traces of hydrocarbons which could provide the energy source, have been reported in drillholes that penetrated evaporite sequences of the basin. Stratigraphic test holes at the Browne diapir produced small quantities of hydrocarbons from the Browne Beds.

No elemental sulphur was found in the cores through the cap rock of the Madley Dome, and it would be surprising if any sulphur deposits were discovered as a result of drilling only one hole.

Extensive deposits of calcium sulphate and halite are present, but remoteness from markets makes them uneconomic at the moment, and probably into the forseeable future as well.

MINOR OCCURRENCES OF EVAPORITES

ARGO ABYSSAL PLAIN

The presence of diapirs in the Argo Abyssal Plain, in the eastern Indian Ocean off northwestern Australia, has been indicated by Cook & others (1978). The structures, which occur in water depths of 4400–5800 m over a wide area of the plain and adjacent areas, range in width from about 200 m to 1 km or more, and in vertical extent from 200 m to 700 m. There are three main types:

- Diapirs indicated by decreased seismic reflectivity, localised arching of the flanking and overlying sediment, and a sea bottom topography. These include the largest structures, but are rare.
- Diapirs as above, but without topographic expression. These are more common than the first group.
- Columns indicated solely by decreased seismic reflectivity. These are the smallest structures and the most widespread, but the least convincing as diapirs.

There is insufficient evidence at present to determine if the diapirs have cores of mud or salt. An acoustically transparent layer, drilled at DSDP Site 261, (Veevers & others, 1974) which appears to be the diapiric unit is a Late Jurassic-Cretaceous clay, with montmorillonite the dominant clay mineral. However, the clay has an average bulk density of 1.69 compared with 1.56 for the overlying layer, so it could not rise by buoyancy effects alone. Many deep-sea diapirs are thought to have salt cores, and young rift oceans are commonly sites of large-scale evaporite deposition at low latitudes. The low Jurassic palaeolatitude and its possible location near a spillway from the open Tethys to the north would favour the Argo Abyssal Plain as a site for formation of evaporites.

Palaeozoic salt is known on the West Australia margin and Pliocene or possibly Miocene salt is inferred to be present in the Timor Trough area (Veevers & others, 1974).

BANCANNIA TROUGH

The main area of interest for evaporites in New South Wales is in western New South Wales, where up to 4500 m of Devonian sediments are present. Minor evaporitic intersections and redbed sequences have been reported by Planet Exploration in their wells Bancannia North No. 1, Bancannia South No. 1, and Jupiter No. 1 in the Broken Hill area. A Late Devonian age for these sediments has been determined from collections of fish fossils.

BROWSE BASIN

Substantial patches and veins filled with anhydrite have been reported in core no. 2 (1895.8–1897.4 m) from Rob Roy No. 1 well in the offshore Browse Basin. The anhydrite occurs in a Sakmarian sandstone. A graphic section of Rob Roy No. 1 is shown in Figure 73.

CAPRICORN EMBAYMENT

Anhydrite occurs over two main intervals, probably Early Tertiary and Mesozoic in age, in Aquarius No. 1 well situated in the Capricorn Embayment (Fig. 74). The Early Tertiary sequence comprises interbedded calcareous claystone and finely crystalline to granular anhydrite in the interval 1453.9–1472.18 m, and minor anhydrite interbeds and inclusions of fine crystalline anhydrite in quartzose sandstone from 1472.18–1536.19 m.

Minor anhydrite occurs in a dark reddish brown claystone of ?Mesozoic age, over the interval 2069.59–2185.42 m; a core in this interval contained a 10-cm band of dense cryptocrystalline anhydrite.

The extent of the anhydrite zones is not known, although the equivalent ?Early Tertiary interval in the Capricorn 1A well does not contain anhydrite.

DALY RIVER BASIN

Thin anhydrite beds occur in the Cambrian of the Daly River Basin. They are of small extent and only a few centimetres thick.

EROMANGA BASIN

Some gypsum has been found in the Lower Cretaceous Rolling Downs Group and other Mesozoic rocks of the Eromanga Basin, but the deposits are thin (less than 5 cm thick) and there is little indication that any substantial thicknesses are present.

Evaporites, including gypsum, were deposited in Cainozoic depressions in the Eromanga Basin and were penetrated in the BMR Barrolka No. 1 and BMR Canterbury No. 3 stratigraphic drill holes. The Cainozoic sediments are over 100 m thick, and the evaporites were possibly the result of seasonal evaporation of floodwaters during the Tertiary and Quaternary (Senior, 1970).

Halite has been recorded from the Hutton Sandstone of the Eromanga Basin in Queensland (Wells, 1971). The salt occurs in a white siltstone exposed at the back of a large cave situated in the Canaga Creek area near Jandowae (26°38′S, 157°03′E) on the Chinchilla Sheet area. The salt is most probably secondary in origin.

GEORGINA BASIN

Evaporative conditions were probably widespread across the shallow water carbonate shelf of the Georgina Basin throughout the Early Cambrian to Early Ordovician. Pseudomorphs after gypsum, halite, and probably anhydrite are common throughout the Arrinthrunga Formation (Upper Cambrian), and one occurence of bedded gypsum, 10 cm thick, now replaced by silica, is known (pers. comm., J. Kennard) in the Ninmaroo Formation (Upper Cambrian-Lower Ordovician). Pseudomorphs of gypsum are similarly widespread, and trace amounts (<0.1%) of barite, celestite, anhydrite, and possibly gypsum have been identified in approximately 10 percent of all petrographic samples collected (pers. comm., B. Radke). Crude estimates of lost sulphates average about 30 percent (rarely, up to 80 percent) in the rock.

Evaporative conditions are also indicated in the Middle Cambrian Mail Change Limestone (pers. comm., P. Southgate) and probably the Selwyn Range Limestone (Öpik, 1961) and Mungerebar Limestone (pers. comm., R. Henderson).

A silicified dissolution collapse breccia occurs at the contact between the Beetle Creek Formation and the Thorntonia Limestone (both Middle Cambrian) (R. A. Henderson & P. N. Southgate, ANU, personal communication, 1980). The breccia contains siliceous pseudomorphs after nodular and bedded anhydrite, and sheeted, hopper, and chevron halite. The breccia has a patchy discontinuous distribution, up to 2 m thick, but, as indicated by the brecciation and folding of the overlying stratigraphic units, a substantial thickness of evaporites has probably been dissolved.

Probable further evaporite horizons are indicated by other brecciated levels above the Beetle Creek Formation-Thorntonia Limestone contact. For example, the Beetle Creek Formation is brecciated south of Duchess and at Lady Annie, and the overlying Inca Formation is severely contorted at some localities.

A minor occurrence of gypsum has been recorded in the Frewena No. 1 bore (19°22′00″S, 135°30′00″E)

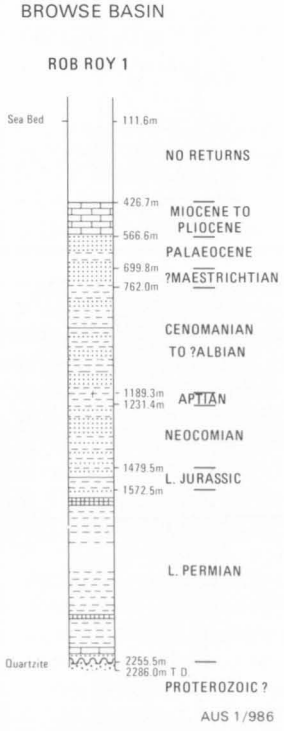

Fig. 73. Graphic section of Rob Roy No. 1 well, Browse Basin. For reference to symbols see Fig. 4.

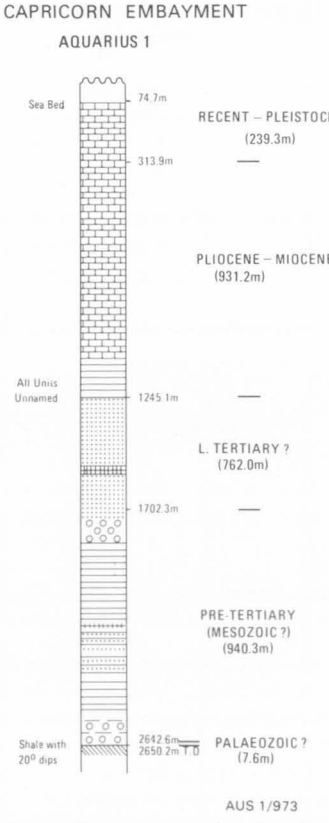

Fig. 74. Graphic section of Aquarius No. 1 well, Capricorn Embayment. For reference to symbols see Fig. 4.

from the Middle Cambrian Wonarah Beds. The age of the beds has been determined from fossils collected from outcrops. In subsurface the beds consist of carbonate rocks with minor siltstone and sandstone. The Barkley Oil Co. Pty. Ltd. (Pemberton & Webb, 1965; *in* K. G. Smith, 1972) recorded limestone and dolomite with some red and purple shale to 149 m in Frewena No. 1, and dolomite from 149–312 m (T.D.). Gypsum is abundant in the interval 110–149 m and also in the upper half of the dolomite interval.

Anhydrite has been reported from drill holes penetrating the Central Mount Stuart Beds in the Alcoota area of central Australia, and gypsum reported to be of secondary origin has been described from the Grant Bluff Formation by K. G. Smith (1964).

NGALIA BASIN

In outcrop the Treuer Member of the basal Vaughan Springs Quartzite in the Ngalia Basin consists of interbedded white siltstone and thin-bedded grey silicified sandstone, in part glauconitic, up to 1370 m thick. It may contain interbedded evaporites at depth and a powdery effloresence is commonly present on the outcrops of siltstone. Coarsely crystalline selenite commonly occurs as a surface crust, notably near Eva Springs and on the north side of the Hann Range, near the Stuart Highway.

SYDNEY BASIN

The exotic evaporite mineral dawnsonite was detected in eight wells in the central and northern part of the basin (Nicholas & Ozimic, 1970). It occurs in marine beds and coal measures, and in the lower part of the Narrabeen Group in Kurrajong Heights No. 1 well. Dawsonite has also been described from the Greta Coal Measures at Muswellbrook (Loughnan & See, 1967), in the Berry Formation in the western part of the basin, and in the Singleton Coal Measures (Loughnan, 1967; Loughnan & Goldbery, 1972).

WISO BASIN

Minor deposits of gypsum occur in vugs in siltstone and dolomite of the Middle Cambrian Merrina Beds, in shallow stratigraphic drill holes in the Wiso Basin (Milligan & others, 1966).

EVAPORITES IN ARCHAEAN TO MID-PROTEROZOIC ROCKS

Evidence for the widespread occurrence of large volumes of sulphate evaporites and subordinate halitic evaporites in the Archaean to mid-Proterozoic has been documented recently from several widely separated areas. Previously, it had been supposed that such deposits were insignificant before about 1000 m.y. ago, and it indicates that hypotheses of atmosphere-hydrosphere evolution (Cloud, 1976) may have to be revised.

The oldest documented occurrences in Australia are those from the North Pole deposit in the Pilbara Block of Western Australia. Archaean bedded barite and minor sulphide minerals lie in a 30-m thick fossiliferous sequence of laminated chert, silicified arenite, and conglomerate, between slightly metamorphosed mafic and ultramafic volcanics of the Warrawoona Group (Hickman, 1973). Their age is about 3400 m.y., and textures and structures imply that the bedded barite and chert have replaced an original evaporitic gypsum-carbonate sequence. The barite beds contain sub-radiating crystals that strongly resemble growth structures of evaporite deposits. The barite is pseudomorphing gypsum; eroded crystal tops and sediment drapes and fills between crystals suggest synsedimentary formation. Textures indicate peritidal deposition of chert precursors, early lithification of precursor gypsum and probably early baritisation and silicification of carbonates. (Dunlop, 1976, 1978; Lambert, 1978; Lambert & others, 1978). Lambert suggests that the sulphate may have originated through oxidation of sulphur by microorganisms and may not necessarily mean the presence of significant amounts of free oxygen in the hydrosphere or the stable existence of oxygen in the contemporaneous atmosphere.

The Archaean Black Flag Beds (older than 2675 ± 35 m.y.) at Kalgoorlie, Western Australia, contain ankerite pseudomorphs after gypsum and possibly also after anhydrite (Golding & Walter, 1979) and indicate the presence of hypersaline brines during deposition or diagenesis. The deposit may have extended for several kilometres, and conditions for sulphate accumulation may have existed for a long time.

Early Proterozoic carbonates of the Pine Creek Geosyncline contain abundant evidence of pseudomorphs after evaporites (Crick & Muir, 1979). Coarsely crystalline carbonates pseudomorph evaporites in the Celia Dolomite, Coomalie Dolomite, Cahill Formation, and, to a lesser extent, in the Koolpin Formation. The sediments are older than about 1870 m.y. and probably younger than about 2000 m.y. Magnesite, dolomite, or chert pseudomorph gypsum, anhydrite, and halite. Relicts of calcium sulphate, probably anhydrite, occur as inclusions in the carbonate pseudomorphs. Abundant cubic crystal pseudomorphs in some magnesite beds contain inclusions of sodium chloride, and scapolite, a metamorphic mineral indicator of hypersalinity, has been recorded from several localities. The crystal forms in the shallow marine to supratidal carbonates are similar to gypsum diagenetically emplaced in a sabkha environment.

Sediments that fall roughly in the age range 1400–1600 m.y. in the McArthur Basin and Mt. Isa area show abundant evidence of widespread evaporite deposition. They were reported from the McArthur Basin in the 1960s (J. W. Smith, 1964; Plumb & Rhodes, 1964; Cotton, 1965), and have been described by Walker & others (1977), and Muir (1979). Extensive sulphate evaporite relics in the McArthur Group comprise carbonate pseudomorphs after anhydrite and gypsum, chert pseudomorphs—including cauliflower chert nodules—after anhydrite nodules, halite casts, and traces of unaltered sulphate minerals. Circular carbonate pseudomorphs in the McArthur Group, thought to be dolomite pseudomorphs after aragonite, have a similar morphology to gypsum forming in modern brine pools. The pseudomorphs are most abundant in the Mallapunyah Formation and Amelia Dolomite (Muir, 1979). Ephemeral salt crusts were probably the origin of the halite pseudomorphs. Halite and sulphate pseudomorphs do not occur together, probably because halite was removed during surface flooding. The sediments were deposited in a regressive/transgressive cycle with frequent oscillations, and the evaporite relics are known over an area of 5000 km² in the Batten Trough and compose up to 40 percent of

some sections. The textures indicate that these sediments were deposited in a marginal sabkha environment, and some probably in a lacustrine environment.

Evidence of evaporitic conditions in sediments of the Mount Isa area have been documented by Derrick & Sweet (1979), Walter (1978), and McClay & Carlile (1978). Iron oxide pseudomorphs after gypsum occur in the Overhang Jaspilite (~1740–1780 m.y.), and abundant scapolite in the Corella Formation probably indicates evaporite conditions.

Several formations in the McNamara Group in the Mount Isa area contain pseudomorphs after evaporites (Walter, 1978). Pseudomorphs after gypsum crystals occur in the Torpedo Creek Quartzite, Paradise Creek Formation (~1670 m.y.), and Esperanza Formation, and discoidal cauliflower cherts which are replacements of anhydrite nodules occur in the Lady Loretta and Paradise Creek Formations.

Pseudomorphed sulphate evaporites occur in the silica-dolomite sequence (McClay & Carlile, 1978) which interfingers with the Urquhart Shale of the Mount Isa Group. Early diagenetic gypsum and anhydrite have been replaced by quartz, dolomite, calcite, and pyrrhotite, and rare minute anhydrite relics have been identified in some dolomite pseudomorphs after gypsum.

Beds of cherty material from the orebody at the Mount Isa Mine are pseudomorphous after enterolithic beds of anhydrite (Muir, 1980). They are not like the cauliflower chert of the McArthur Group, which indicates a sabkha environment, but are more like a nodular anhydrite described by Dean & others (1975) from varve-like basinal deposits.

Large halite casts several centimetres across are present in the Kennedy Siltstone of the Mount Isa Group.

RECENT EVAPORITES OF CONTINENTAL AREAS

There are numerous thin deposits of evaporites (chiefly halite and gypsum) in playa lakes scattered across the continent, and groundwaters rich in dissolved salts are common in Australia, particularly in the desert areas of central and Western Australia. In the southern part of the Northern Territory, for example, brines from some water bores contain up to 100 000 ppm total dissolved salts and many bores contain about 30 000 ppm. Salt springs are also common throughout the more arid areas of Australia. Very few lakes in Australia contain concentrations of anything other than halite and gypsum: numerous analyses of evaporites from large lakes in South Australia have failed to indicate any significant concentration of bittern salts. However, when climate and provenance are considered, perhaps this is not surprising. Sodium carbonate, for example, is a product of humid weathering, especially of volcanic rocks, and sodium sulphate is produced chiefly by erosion of igneous rocks or from sediments deposited in a continental environment. Similarly, borates are mostly derived from weathering of igneous rocks and from hot springs, and nitrates originate by oxidation of organic matter in the presence of potassium and sodium salts, or from volcanic sources.

Two minor surface occurrences of trona (sodium carbonate) have been reported in Australia: at Lake Mueller, 25 km northeast of Aramac in Queensland, a 12-mm crust of trona occurs over an area of several thousand square metres; and at Hillside Station in the northwest of Western Australia there is an occurrence of a mixture of halite, trona, and thenardite ($NaSO_4$) as an efflorescence.

South Australia

Short accounts of South Australian surface occurrences of evaporites are given in Parkin (1969) and brief resumés of salt and gypsum occurrences and production in the State are given in the Mineral Information Series issued by the South Australia Department of Mines and Energy.

Probably most of the near-coastal salt lakes in South Australia had marine connections at one time or another. One of the most notable is Lake MacDonnell, which contains the largest gypsum deposits in Australia, reaching a thickness of 8–10 m. The deposits occur just above sea level, and it has been estimated that they contain 500 million tonnes of practically pure rock gypsum.

The large inland lakes north of Spencer Gulf have had no marine connections. Lake Torrens, for example, contains mainly gypsiferous clays and the magnesium content is much lower than sea water. The surface of Lake Torrens is 34.1 m above sea level and it is normally a dry salina. It has been the site of accumulation of some 300 m of lacustrine sediments since Eocene time. The succession consists of Eocene carbonaceous mudstone, sand, and siltstone, a ?Miocene dolomite-mudstone sequence, and Quaternary red-brown siltstone, clay, gypsum, sand, and mud. The brines enclosed by the lake sediments are chloride waters without useful concentrations of salts other than sodium chloride.

In Lake Eyre the deposits are thinner: modern lake sediments in the Lake Eyre Basin are only 4.5 m thick in the deflated lake floor. They overlie a 30–45-m dolomite sequence of the Tertiary Etadunna Formation, which crops out to the east of Lake Eyre and is underlain by a lacustrine sequence of carbonaceous sand, silt, and clay to the total depth of boring, 299.6 m. Sedimentation appears to have been continuous from the Cretaceous Winton Formation into the Lower Tertiary. The salt crust in the lake may reach 50 cm, and trace element analyses have shown that strontium and barium values are higher in areas where the evaporites begin to form. Structurally, the lake has formed in a synclinal sink, and horsts of Middle Tertiary age occur on the east side of the basin. Radiocarbon dates indicate that it took 20 000 years for the lake floor to deflate to a level of 18 m below sea level. Tilting of the present lake surface suggests that the region is tectonically active: it is certainly seismically active.

The presence of nodular gypsum and sulphur in the southeastern part of Lake Eyre has been described by Bonython & King (1956), and their origin discussed by Baas-Becking & Kaplan (1956). The source bed is an early Holocene clay lying between Pleistocene and late Holocene sediments. The nodules consist of a shell of coarsely crystalline gypsum around a core partly filled by gypsum and the remainder consisting of over 90 percent sulphur as orthorhombic crystals, with traces of selenium and arsenic. The relative abundances of sulphur isotopes suggest an organic origin, with the

gypsum crust formed by bacterial oxidation of the core sulphur. The known sulphur occurrence occupies an area of about 0.4 ha and the sulphur content of the bed is only about one percent. C^{14} determinations on a composite sulphur sample showed an age of 20 000 years.

Lake Eyre was investigated by Bonython (1956) and Johns & Ludbrook (1963), and a similar report on Lakes Torrens and Gairdner was given by Johns (1968). The geomorphology and stratigraphic record of Lake Eyre North have been described by King (1956).

Western Australia

Lake Macleod is an elongate depression covering an area of 2900 km^2, 65–145 km north of Carnarvon. The lake is an arm of the sea that has been progressively isolated during the Holocene by beach and dune ridges of the Gascoyne delta. It is probably recharged by sea water through a 3–15-km barrier of calcified Pleistocene aeolianites. The lake bed lies about 3 m below sea level, and the water table is 15–25 cm deep. The surface is underlain by a layered evaporite sequence—halite, gypsum, bassanite, sylvite, calcite, aragonite, and dolomite—which is up to 15 m thick at the lake centre and overlies Pleistocene and Recent marine and terrigenous sediments. Large hopper crystals of halite are common in the clay sediments in parts of the lake. The deposits are probably mainly related to past hydrologic systems. The sequence, established by excavation in a part of the lake, is given in Table 16.

TABLE 16. SEDIMENTARY SEQUENCE IN LAKE MACLEOD, W.A.

TOP		
Gypsite member	2.5 m	elastic, bedded and cross-bedded, slumps and drag folds in graben-like structures
	0.2 m	red-brown clay layer at base interpreted as storm/sheet flood deposit
Halite member	1.1 m	columnar halite; massive halite with grey laminae with silt, organic matter, and gypsum
Carbonate member	0.5 m	skeletal packstone and grainstone
	0.03 m	basal sheet
UNCONFORMITY		
Pleistocene Depuch/? Dampier Fm.		red clayey quartz sand

Fossil sea water brines trapped within the formations are a major influence on the diagenetic phenomena observed in the gypsum and halite deposits of Lake McLeod. A typical analysis of the brine is: Mg—1.14%, K—0.34%, Na—8.36%, Cl—15.44%, SO_4—1.52%, Br—0.06%, H_2O—73.14%.

Queensland

In Queensland, Lake Buchanan, a salt lake of roughly 150 km^2, about 160 km south-southwest of Charters Towers is a site of seasonal salt formation. This is worked intermittently during the dry winter months to provide salt for local agricultural use.

In the far Western Division a number of lakes have a high salt content. Several lakes in the Mulligan River —Eyre Creek area, in the southwestern corner, are reported to contain extensive deposits of salt. One of the largest, Kalidawarry Waterhole, is 19 km long and 90 m wide. It is reported to have, in places, 1.2 m of salt partly buried beneath alluvium. Highly concentrated brine was located at a depth of 3 m in an excavation near Lake Machattie, 130 km north-northeast of Birdsville.

Underground brines occur in Pleistocene beds at the mouth of the Fitzroy River in Queensland, and are known over a wide area centred on Casuarina Island. Brines occur in separate beds, and concentration increases in each with depth.

COMMERCIAL EXPLOITATION OF EVAPORITES

Salt is harvested either by scraping it from the surface of natural salt lakes or by solar evaporation of sea water or other brines in artificial ponds.

In 1978*, almost six million tonnes of salt was produced in Australia. Nearly five million tonnes of this came from Western Australia and most of it was exported. The main areas of production in Western Australia are Dampier and Port Hedland—about 2.7 million tonnes by crystallisation from sea water, and Lake Macleod—about one million tonnes by harvesting from the salt lake surface. About 120 000 tonnes was harvested from Lake Lefroy, and about 18 000 and 6000 tonnes from Lake Deborah near Koolyanobbing and Pink Lake near Esperance, respectively.

In Queensland most salt (about 140 000 tonnes) was produced at Bajool, about 30 km south of Rockhampton, from a mixture of sea water and brine pumped from an underground aquifer. About 9000 tonnes was produced at Bowen, entirely from sea water. The Bowen salt is used locally, mainly for tanning hides. The rest of Queensland's production is used to make sodium hydroxide.

About 75 percent of Victoria's production of about 107 000 tonnes comes from sea water at Port Phillip Bay and Corio Bay, and the remainder from brine at Lake Tyrell.

South Australia produced about 680 000 tonnes of salt in 1978. Most of this (about 500 000 tonnes) was from Dry Creek by solar evaporation of sea water, with lesser amounts being harvested from Lake MacDonnell, Lake Bumbunga, Price, and Whyalla.

Australian production of gypsum in 1978 totalled nearly 940 000 tonnes. Of this, nearly 70 per cent was produced in South Australia, mainly from Kangaroo Island, but with Lake MacDonnell another important source. Western Australia produced about 170 000 tonnes, just over half of this coming from Shark Bay. The other half came from deposits near Southern Cross, and at Lake Grace, Lake Cowcowing, and Lake Brown. Victoria's production of about 107 000 tonnes came from deposits at Millewa, Nowing, and Hattah, near Mildura. In New South Wales, deposits near Bourke and Cobar produced about 18 000 tonnes of gypsum during 1978.

* Information for this chapter has been taken from the Australian Mineral Industry Annual Review 1978 (in press).

RECOMMENDATIONS FOR FURTHER STUDY

Further work in the investigation of Australian evaporite deposits could be divided into several stages:

1. Additional geological investigations of surface evaporite occurrences and palaeogeographic studies of evaporite sequences in the more prospective basins.

Geological mapping should be confined to the Officer and Amadeus Basins, where diapirs are known and there are surface occurrences of evaporites. Lithofacies studies to determine the palaeogeography of an evaporite deposit would necessarily be limited in other basins to a study of well sections. Detailed mapping of the Bitter Springs Formation in the Amadeus Basin could form part of this program, but would pose special problems because of the complexity of incompetent folding in the formation.

2. Stratigraphic drilling of surface or near-surface occurrences and shallow pattern drilling of diapir cores: geochemical studies of the evaporite cores, particularly bromine analysis, which gives an indication of the stage the evaporite cycle has reached.

The Officer and Amadeus Basins offer several targets for shallow stratigraphic drilling. The Woolnough, Madley, and Browne diapirs are prime targets in the Officer Basin and some preliminary shallow test drilling has already been attempted. Many other possible diapiric structures in the basin have been outlined by air photo-interpretation. There are several outcrops of evaporites in the Amadeus Basin, but the cap rock gypsum should first be located by mapping and drilled, because that is more likely to signify evaporite mineralisation at shallow depth.

In South Australia, the most interesting target for exploration is the Mount Toondina Structure. The composition of the intrusive core is unknown, and could probably be established by shallow drilling.

3. Geophysical investigations: detailed gravity and seismic traverses of known diapirs, and other areas to solve specific problems.

Geophysical studies can be used to solve specific problems in some basins: for example, the precise minimum depth to the top of the evaporites in the Adavale Basin may be determined by detailed gravity and seismic surveys. Similarly, a detailed gravity survey of the Lake Amadeus area in the Amadeus Basin has been suggested as a method of determining the distribution of low density evaporites, which were postulated to underlie the salt lake belt. However, it would probably be more expedient to establish, by shallow stratigraphic drilling, that evaporites do in fact extend into the southern part of the basin.

Of fundamental importance is the detailed geophysical study of known diapiric structures to establish the attitude, depth, source, and dimensions of the mostly buried or largely concealed evaporite bodies. These investigations could in many areas indicate the age and origin of the intrusive material.

4. Further drilling to detail targets outlined by geophysical surveys and ground mapping.

Most of the evaporite basins are being explored for petroleum and during the course of this exploration a basin is normally investigated by seismic surveys. These surveys may indicate shallow diapiric structures, areas where salt-bearing formations approach ground level or areas of sedimentary cover where saline beds are buried at shallow depth. These types of deposits would present accessible drilling targets.

REFERENCES

ALLCHURCH, P. D., WOPFNER, H., HARRIS, W. K., & MCGOWRAN, B., 1973—South Australian Department of Mines Cootanoorina No. 1 well. *Geological Survey of South Australia Report of Investigations* 40.

ANGOVE, R. V., & DOUGLASS, J. L., 1972—Hickey Hills seismic survey. *Bureau of Mineral Resources, Australia, Petroleum Search Subsidy Acts File* 72/2761 (unpublished).

ARCO, 1966—Sahul Shelf marine seismic survey, sparker method. May-November 1966. *Bureau of Mineral Resources, Australia, Petroleum Search Subsidy Acts File* 66/11088 (unpublished).

ARCO, 1967—Lesueur seismic survey, sparker method. *Bureau of Mineral Resources, Australia, Petroleum Search Subsidy Acts File* 67/11165 (unpublished).

ARCO, 1969—Londonderry Rise seismic survey, final report. *Bureau of Mineral Resources, Australia, Petroleum Search Subsidy Acts File* 68/3024 (unpublished).

AUSTRALIAN AQUITAINE PETROLEUM, 1968a—Hyland seismic survey OP2-OP84, N.T. Interpretation report. *Bureau of Mineral Resources, Australia, Petroleum Search Subsidy Acts File* 67/11181 (unpublished).

AUSTRALIAN AQUITAINE PETROLEUM, 1968b—Terry Range magnetotelluric survey. final report. *Bureau of Mineral Resources, Australia, Petroleum Search Subsidy Acts File* 68/3016 (unpublished).

AUSTRALIAN AQUITAINE PETROLEUM, 1969—Keep River No. 1, OP 162 Northern Territory, well completion report. *Bureau of Mineral Resources, Australia, Petroleum Search Subsidy Acts File* 68/2029 (unpublished).

BAAS-BECKING, L. G. M., & KAPLAN, I. R., 1956—The microbiological origin of the sulphur nodules of Lake Eyre. *Transactions of the Royal Society of South Australia,* 79, 52-65.

BARNES, L. C., 1969—Exploration of the Mount Coffin diapir, northern Flinders Ranges. *South Australia Department of Mines, Mineral Resources Review,* 131, 62-83.

BARNES, L. C., 1970—Geological investigation of the Burra crush zone. *South Australia Department of Mines, Mineral Resources Review* 132, 7-35.

BENBOW, M. C., & PITT, G. M., 1979—Byilkaoora No. 1 well completion report. Report No. 1 of the Officer Basin Study Group. *Geological Survey of South Australia, Report Book* 79/115 (unpublished).

BINKS, P. J., 1971—The geology of the Orroroo 1:250 000 map area. *Geological Survey of South Australia, Report of Investigations* 36.

BONYTHON, C. W., & KING, D., 1956—The occurrence of native sulphur at Lake Eyre. *Transactions of the Royal Society of South Australia,* 79, 121-30.

BORCHERT, H., & MUIR, R. O., 1964—SALT DEPOSITS: The origin, metamorphism and deformation of evaporites. *Van Nostrand, London.*

BURNS, K. L., STEPHANSSON, O., & WHITE, A. J. R., 1977—The Flinders Ranges breccias of South Australia—diapirs or decollement? *Journal of the Geological Society, London,* 134, 363-84.

CAROZZI, A. V., 1960—MICROSCOPIC SEDIMENTARY PETROGRAPHY. *Wiley, New York.*

CAYE, J. P., 1968—The Timor Sea-Sahul Shelf area. *The APEA Journal,* 8(2), 35-41.

CLOUD, P. E., 1976—Beginnings of biospheric evolution and their biochemical consequences. *Paleobiology,* 2(4), 351-87.

CLOUD, P. E., 1976—Major features of crustal evolution. *Transactions of the Geological Society of South Africa,* Annexure to Volume 79.

COATS, R. P., 1964—The geology and mineralization of the Blinman Dome Diapir. *Geological Survey of South Australia, Report of Investigations,* 26.

COATS, R. P., 1965—Diapirism in the Adelaide Geosyncline. *The APEA Journal,* 5, 98-102.

COATS, R. P., 1973—Copley, South Australia, 1:250 000 Geological Series. *Geological Survey of South Australia, Explanatory Notes* SH/54-9.

COMPSTON, W., 1974—The Table Hill Volcanics of the Officer Basin—Precambrian or Palaeozoic? *Journal of the Geological Society of Australia,* 21(4), 403-11.

CONDON, M. A., 1965—The geology of the Carnarvon Basin, Western Australia. Part 1—Pre-Permian stratigraphy. *Bureau of Mineral Resources, Australia, Bulletin* 77.

CONDON, M. A., 1967—The geology of the Carnarvon Basin, Western Australia. Part 2—Permian stratigraphy. *Bureau of Mineral Resources, Australia, Bulletin* 77.

CONDON, M. A., 1968—The geology of the Carnarvon Basin, Western Australia. Part 3—Post-Permian stratigraphy; structure; economic geology. *Bureau of Mineral Resources, Australia, Bulletin* 77.

COOK, P. J., VEEVERS, J. J., HEIRTZLER, J. R., & CAMERON, P. J., 1978—The sediments of the Argo Abyssal Plain and adjacent areas, northeast Indian Ocean. *BMR Journal of Australian Geology & Geophysics,* 3(2), 113-24.

COTTON, R. E., 1965—H.Y.C. lead-zinc-silver ore deposit, MacArthur River. *In* MCANDREW, J.—Geology of Australian Ore Deposits. *Eighth Commonwealth Mining and Metallurgical Congress Publications,* 1, 197-200.

CREEVEY, K. J., 1971—Recent information and prospects in the Kidson Sub-basin. *The APEA Journal,* 11, 53-8.

CRICK, I. H., & MUIR, M. D., 1979—Evaporites and uranium mineralisation in the Pine Creek Geosyncline. *International Uranium Symposium on the Pine Creek Geosyncline, N.T., Australia. Extended Abstracts,* 30-33.

CRIST, R. P., & HOBDAY, M., 1973—Diapiric features of the offshore Bonaparte Gulf Basin, Northwest Australian Shelf. *Australian Society of Exploration Geophysicists, Bulletin* 4(1), 43-66.

CROWE, R. W. A., & CHIN, R. J., 1979—Runton, Western Australia—1:250 000 Geological Series. *Bureau of Mineral Resources, Australia, Explanatory Notes* SF/51-15.

DALGARNO, C. R., & JOHNSON, J. E., 1968—Diapiric structures and late Precambrian-early Cambrian sedimentation in Flinders Ranges, South Australia. *In* BRAUNSTEIN, J., & O'BRIEN, G. D. (editors), Diapirs and Diapirism. *American Association of Petroleum Geologists, Memoir,* 8, 301-14.

DEAN, W. E., DAVIES, G. R., & ANDERSON, R. Y., 1975—Sedimentological significance of nodular and laminated anhydrite. *Geology,* 3, 367-72.

DEER, W. A., HOWIE, R. A., & ZUSSMAN, J., 1962—ROCK-FORMING MINERALS. 5. NON-SILICATES. *Longmans, London.*

DERRICK, G. M., & SWEET, I. P., 1979—Mount Isa-Lawn Hill Project. *In* Geological Branch Summary of Activities 1978. *Bureau of Mineral Resources, Australia, Report* 212; *BMR Microform* MF81.

DUFF, P. MCL. D., HALLAM, A., & WALTON, E. K., 1967—CYCLIC SEDIMENTATION. Developments in Sedimentology 10. *Elsevier, Amsterdam.*

DUNLOP, J. S. R., 1976—The geology and mineralization of part of the North Pole barite deposits. Pilbara region, Western Australia. *B.Sc. Honours Thesis, University of Western Australia* (unpublished).

DUNLOP, J. S. R., 1978—Shallow water sedimentation at North Pole, Pilbara Block, Western Australia. *In* GLOVER, J. E., & GROVES, D. I. (editors)—Archaean cherty metasediments: their sedimentology, micropalaeontology, biochemistry, and significance to mineralisation. *University of Western Australia, Special Publication* 2, 30-38.

EDGERLEY, D. W., & CRIST, R. P., 1974—Salt and diapiric anomalies in the southeast Bonaparte Gulf Basin. *The APEA Journal,* 14(1), 85-94.

FEELY, H. W., & KULP, J. L., 1957—Origin of Gulf Coast salt-dome sulphur deposits. *Bulletin of the American Association of Petroleum Geologists,* 41(8), 1802-53.

FOLK, R. L., 1959—Practical petrographic classification of limestone. *Bulletin of the American Association of Petroleum Geologists,* 43(1), 1-38.

FOLK, R. L., 1964—THE PETROLOGY OF SEDIMENTARY ROCKS. *Hemphills, Austin.*

FREYTAG, I. B., 1965—Mount Toondina Beds—Permian sediments in a probable piercement structure. *Transactions of the Royal Society of South Australia,* 89, 61-76.

FRIEDMAN, G. M., 1972—Significance of Red Sea in problem of evaporites and basinal limestones. *Bulletin of the American Association of Petroleum Geologists,* 56, 1072-86.

FROELICH, A. J., & KRIEG, E. A., 1969—Geophysical-geologic study of northern Amadeus Trough, Australia. *Bulletin of the American Association of Petroleum Geologists,* 53, 1978-2004.

GALLOWAY, M. C., 1970—Adavale, Queensland—1:250 000 Geological Series. *Bureau of Mineral Resources, Australia, Explanatory Notes* SG/55-5.

GATEHOUSE, C. G., 1979—Well completion report, Wilkinson No. 1. *Fossil Fuels Division, Geological Survey of South Australia, Report Book* 79/88 (unpublished).

GEARY, J. K., 1970—Offshore exploration of the southern Carnarvon Basin. *The APEA Journal,* 10(2), 9-15.

GLENISTER, B. F., & GLENISTER, A. T., 1957—Discovery of Silurian strata from Western Australia. *Australian Journal of Science,* 20, 115-6.

GLOVER, J. E., 1973—Petrology of the halite-bearing Carribuddy Formation, Canning Basin, Western Australia. *Journal of the Geological Society of Australia,* 20(3), 343-59.

GOLDING, L. Y., & WALTER, M. R., 1979—Evidence of evaporite minerals in the Archaean Black Flag Beds, Kalgoorlie, Western Australia. *BMR Journal of Australian Geology & Geophysics,* 4(1), 67-72.

GOLDMAN, M. I., 1952—Deformation, metamorphism, and mineralization in gypsum-anhydrite cap rock, Sulphur Salt Dome, Louisiana. *Geological Society of America, Memoir* 50.

GOLDSMITH, L. H., 1966—Some fundamentals of potash geology as a guide to exploration. *Society of Professional Well Log Analysts, 7th Annual Logging Symposium, Transaction O,* 13 pp.

GOLDSMITH, L. H., 1969—Concentration of potash salts in saline basins. *Bulletin of the American Association of Petroleum Geologists,* 53(4), 790-97.

GORTER, J. D., RASIDI, J. S., TUCKER, D. H., BURNE, R. V., PASSMORE, V. L., WALES, D. W., & FORMAN, D. J., 1979—Petroleum geology of the Canning Basin. *Bureau of Mineral Resources, Australia, Record* 1979/32 (unpublished).

GRAHMANN, W., 1920—Ulser Barytocolestin und das Verhaltnis von Anhydrit zu Colestin und Baryt. *Neues Jahrbuch für Mineralogie, Geologie und Paläontologie,* 1, 1-23.

GRIEVE, R. O., 1955—Leaching (?) of Silurian salt beds in southwestern Ontario as evidenced in wells drilled for oil and gas. *Transactions of the Canadian Institute of Mining and Metallurgy,* 55, 10-16.

GROSS, W., 1971—Unterdevonische Thelodontier—und Acanthodier-schuppen aus Westaustralien. *Paläontologische Zeitschrift,* 45(3/4), 97-106.

G.S.W.A., 1975—Geology of Western Australia. *Geological Survey of Western Australia, Memoir* 2.

HENDERSON, S. W., & SHANNON, P. H., 1966—Yaringa No. 1 well, West Australia stratigraphic drilling project. *Bureau of Mineral Resources, Australia, Petroleum Search Subsidy Acts File* 66/4215 (unpublished).

HICKMAN, A. H., 1973—The North Pole barite deposits, Pilbara goldfield. *Geological Survey of Western Australia, Annual Report,* 1972, 57-60.

HOLMES, D. A., 1970—South Australian potash project (612), special mining lease 329. *Occidental Minerals Corporation of Australia* (unpublished).

HOLMES, D. A., & RAYMENT, P., 1970—Well completion report, OxyMin Boorthanna No. 1, South Australia potash project. *Occidental Minerals Corporation of Australia* (unpublished).

HUCKABA, W. A., & MAGEE, R. A., 1969—Tyler No. 1, Northern Territory, final well report. *Bureau of Mineral Resources, Australia, Petroleum Search Subsidy Acts File* 68/2031 (unpublished).

HUNT OIL CO., 1966—Yowalga seismic survey, Western Australia. *Bureau of Mineral Resources, Australia, Petroleum Search Subsidy Acts File* 65/4579 (unpublished).

JACKSON, M. J., & VAN DE GRAAFF, W. J. E. (in preparation)—Geology of the Officer Basin in Western Australia. *Bureau of Mineral Resources, Australia, Bulletin* 206.

JACKSON, P. R., 1966a—Well completion report, No. 2 Yowalga, Officer Basin, Western Australia. *Bureau of Mineral Resources, Australia, Petroleum Search Subsidy Acts File* 66/4191.

JACKSON, P. R., 1966b—Geology and review of exploration, Officer Basin, Western Australia. *Hunt Oil Company Report* (unpublished).

JOHNS, R. K., 1968—Investigations of Lakes Torrens and Gairdner. *Geological Survey of South Australia, Report of Investigations,* 31.

JOHNS, R. K., 1969—Exploration for copper in the Oraparinna and Enorama diapirs. *South Australia Department of Mines, Mineral Resources Review* 131, 104-14.

JOHNS, R. K., & LUDBROOK, N. H., 1963—Investigations of Lake Eyre. *Geological Survey of South Australia, Report of Investigations,* 24.

JONES, B. F., 1969—Timor Sea gravity, magnetic, and seismic survey, 1967. *Bureau of Mineral Resources, Australia, Record* 1969/40 (unpublished).

JONES, G. E., STARKEY, R. L., FEELY, H. W., & KULP, J. L., 1956—Biological origin of native sulphur in salt domes of Texas and Louisiana. *Science,* 123, 1124-5.

KASTNER, M., 1971—Authigenic feldspars in carbonate rocks. *American Mineralogist,* 56, 1403-42.

KEEVERS, R. E., 1968—Marine basinal evaporite deposits in Australia. *Confidential report for Mines Exploration Pty Ltd* (unpublished).

KENNEWELL, P. J., 1975—Madley, Western Australia—1:250 000 Geological Series. *Bureau of Mineral Resources, Australia, Explanatory Notes* SG/51-3.

KING, D., 1956—The Quaternary stratigraphic record at Lake Eyre North and the evolution of existing topographic forms. *Transactions of the Royal Society of South Australia,* 79, 93-103.

KOOP, W. J., 1966—Recent contributions to Palaeozoic geology in the south Canning Basin, Western Australia. *The APEA Journal,* 6, 105-9.

KRIEG, C., 1969—Geological developments in the eastern Officer Basin of South Australia. *The APEA Journal,* 9(2), 8-13.

LANGSFORD, N. R., 1969—Mineral exploration of the Windowarta diapir. *South Australia Department of Mines, Mineral Resources Review* 131, 77-9.

LAMBERT, I. B., 1978—Sulphur-isotope investigations of Archaean mineralisation and some implications concerning geochemical evolution. *In* GLOVER, J. E., & GROVES, D. I. (editors)—Archaean cherty metasediments: their sedimentology, micropalaeontology, biochemistry, and significance to mineralisation. *University of Western Australia, Special Publication* 2, 45-56.

LAMBERT, I. B., DONNELLY, T. H., DUNLOP, J. S. R., & GROVES, D. I., 1978—Stable isotope studies of early Archaean evaporitic sulphates at North Pole, Western Australia, and possible equivalents at Barberton, South Africa. *Nature,* 276, 808-11.

LAWS, R. A., & BROWN, R. S., 1976—Bonaparte Gulf Basin —southeastern part. *In* LESLIE, R. B., EVANS, H. J., & KNIGHT, C. L., ECONOMIC GEOLOGY OF AUSTRALIA AND PAPUA NEW GUINEA. 3. PETROLEUM. *Australasian Institute of Mining and Metallurgy, Monograph* 7, 200-8.

LAWS, R. A., & KRAUS, G. P., 1974—The regional geology of the Bonaparte Gulf-Timor Sea area. *The APEA Journal,* 14(1), 77-84.

LEHMANN, P. R., 1969—Temporary reserve 1691 H (evaporites), Canning Basin, W.A. final report. *West Australian Petroleum Pty Ltd* (unpublished).

LESLIE, R. B., 1961—Geology of the Gibson Desert area, Western Australia. *Frome-Broken Hill Company Report* 3000-G-38 (unpublished).

LOHMANN, H. H., 1972—Salt dissolution in subsurface of British North Sea as interpreted from seismograms. *Bulletin of the American Association of Petroleum Geologists,* 56(3), 472-9.

LOUGHNAN, F. C., 1967—Some aspects of coal measure sedimentation in the Sydney Basin. *2nd Symposium on Advances in the Study of the Sydney Basin, Newcastle University,* 13-14.

LOUGHNAN, F. C., & GOLDBERY, R., 1972—Problems with the genesis of dawsonite in the Sydney Basin, N.S.W. *Geological Society of Australia, Specialist Groups Meeting, Canberra, 1972, Abstracts,* D29-32.

LOUGHNAN, F. C., & SEE, G. T., 1967—Dawsonite in the Greta Coal Measures at Muswellbrook, N.S.W. *American Mineralogist,* 52, 7-8.

LOWRY, D. C., JACKSON, M. J., VAN DE GRAAFF, W. J. E., & KENNEWELL, P. J., 1972—Preliminary results of geological mapping in the Officer Basin, Western Australia, 1971. *Geological Survey of Western Australia, Annual Report,* 1971, 50-56.

MCCLAY, K. R., & CARLILE, D. G., 1978—Mid-Proterozoic sulphate evaporites at Mount Isa Mine, Queensland, Australia. *Nature,* 274, 240-1.

MACK, J. E., & HERMANN, F. A., 1965—Reconnaissance geological survey of the Alliance Gibson Desert Block PE 205H, 206H, 207H, Western Australia. *Union Oil Development Corporation,* G.R. 18 (unpublished).

MCKIRDY, D. M., 1977—The diagenesis of microbial organic matter: a geochemical classification and its use in evaluating the hydrocarbon-generating potential of Proterozoic and Lower Palaeozoic sediments, Amadeus Basin, central Australia. *Ph.D. thesis, Australian National University, Canberra* (unpublished).

MCNAMARA, M., 1965—The lower greenschist facies in the Scottish Highlands. *Geologiska föreningens i Stockholm förhandlingar,* 87, 347-89.

MCNAUGHTON, D. A., QUINLAN, T., HOPKINS, R. M., & WELLS, A. T., 1968—Evolution of salt anticlines and salt domes in the Amadeus Basin, central Australia. *Geological Society of America, Special Paper* 80, 157-82.

MCWHAE, J. R. H., PLAYFORD, P. E., LINDNER, A. W., GLENISTER, B. R., & BALME, B. E., 1958—The stratigraphy of Western Australia. *Journal of the Geological Society of Australia,* 4(2).

MAIKLEM, W. R., BEDOUT, D. G., & GLAISTER, R. P., 1969 —Classification of anhydrite—a practical approach. *Bulletin of Canadian Petroleum Geology,* 17, 234-46.

MARATHON, 1967—West Blackall seismic survey, Authority to Prospect 83P, Queensland. *Bureau of Mineral Resources, Australia, Petroleum Search Subsidy Acts File* 66/11113 (unpublished).

MILLIGAN, E. N., SMITH, K. G., NICHOLS, R. A. H., DOUTCH, H. F., 1966—Geology of the Wiso Basin, Northern Territory. *Bureau of Mineral Resources, Australia, Record* 1966/47 (unpublished).

MOSS, F. J., 1964—Gosses Bluff seismic survey, Amadeus Basin, Northern Territory, 1962. *Bureau of Mineral Resources, Australia, Record* 1964/66 (unpublished).

MUFFLER, L. J. P., & WHITE, D. E., 1969—Active metamorphism of Upper Cenozoic sediments in the Salton Sea geothermal field and the Salton Trough, southeastern California. *Bulletin of the Geological Society of America,* 80, 157-82.

MUIR, M. D., 1979—A sabkha model for the deposition of part of the Proterozoic McArthur Group of the Northern Territory, and its implications for mineralisation. *BMR Journal of Australian Geology & Geophysics,* 4(2), 149-62.

MUIR, M. D., 1980—Petrological report on cherty material from the 1100 orebody, Mt Isa mine. *Bureau of Mineral Resources, Australia, Professional Opinion Geol.* 80:001 (unpublished).

NICHOLAS, E., & OZIMIC, S., 1970—Dawsonite in Sydney Basin wells. *Bureau of Mineral Resources, Australia, Record* 1970/7 (unpublished).

NOAKES, L. C., 1972—Mineral resources of Australia. *Bureau of Mineral Resources, Australia, Record* 1972/12 (unpublished).

NOLL, W., 1934—Geochemie des Strontiums; mit Bemerkungen zur Geochemie des Bariums. *Chemie der Erde,* 8, 507-600.

OCHSENIUS, C., 1877—Die Bildung der Steinsalzlager und ihrer Mutterlangensalze. *Pfeffer, Halle.*

OCHSENIUS, C., 1888—On the formation of rock-salt beds and mother-liquor salts. *Proceedings of the Academy of Natural Sciences of Philadelphia,* 181-7.

PARKIN, L. W., 1969— HANDBOOK OF SOUTH AUSTRALIAN GEOLOGY. *Geological Survey of South Australia, Adelaide.*

PATEN, R. J., 1977—The Adavale Basin, Queensland: *Proceedings of symposium, Petroleum in Queensland: a stocktake for the future. November 1977. Petroleum Exploration Society of Australia, Queensland Branch, Brisbane.*

PEERS, R., 1969—A comparison of some volcanic rocks of uncertain age in the Warburton Range area. *Geological Survey of Western Australia, Annual Report,* 1968, 57-61.

PEERS, R., & TRENDALL, A. F., 1968—Precambrian rocks encountered during drilling in the main Phanerozoic sedimentary basins of Western Australia. *Geological Survey of Western Australia, Annual Report,* 1967, 69-77.

PEMBERTON, R. L., & WEBB, E. A., 1965—Frewena No. 1 well completion report. *Barkley Oil Company Pty Ltd* (unpublished).

PENDERY, E. C., 1970—Final completion report, temporary reserves 4186H and 4187H, Western Australia. *Confidential report for Magellan Petroleum (Australia) Ltd* (unpublished).

PENDERY, E. C., CAMPBELL, M. D., FARMER, R. T., & MCDANIEL, K. W., 1969—Well completion report, Hamelin Pool No. 2, and summary report—potash potential—Carnarvon Basin, temporary reserves 4186H and 4187H, Western Australia. *Magellan Petroleum Pty Ltd* (unpublished).

PETERSON, M. N. A., & VON DER BORCH, C. C., 1965— Chert: modern inorganic deposition in a carbonate-precipitating locality. *Science,* 149, 1501-3.

PETTIJOHN, F. J., 1957—SEDIMENTARY ROCKS. *Harper & Row, New York.*

PETTIJOHN, F. J., POTTER, P. E., & SIEVER, R., 1972— SAND AND SANDSTONE. *Springer-Verlag, Berlin.*

PHILIP, G. M., 1969—Silurian conodonts from the Dirk Hartog Formation, Western Australia. *Proceedings of the Royal Society of Victoria,* 82, 287-97.

PINCHON, D., 1973—Australian Aquitaine Petroleum Pty Ltd, Hickey Hills (EP20) interpretation. *Bureau of Mineral Resources, Australia, Petroleum Search Subsidy Acts File* 72/2761 (unpublished).

PITT, G. M., BENBOW, M. C., & YOUNGS, B. C., 1980—A review of recent geological work in the Officer Basin, South Australia. *The APEA Journal,* 20(1), 209-20.

PLAYFORD, P. E., & COPE, R. N., 1971—The Phanerozoic stratigraphy of Western Australia: a correlation chart in two parts. *Geological Survey of Western Australia, Annual Report,* 1970, 32-3.

PLAYFORD, P. E., & LOWRY, D. C., 1966—Devonian reef complexes of the Canning Basin, Western Australia. *Geological Survey of Western Australia, Bulletin* 118.

PLUMB, K. A., & RHODES, J. M., 1964—Wallhallow, Northern Territory — 1:250 000 Geological Series. *Bureau of Mineral Resources, Australia, Explanatory Notes* SE/53-7.

PREISS, W. V., 1972—Proterozoic stromatolites: succession, correlations, and problems. *In* JONES, J. B., & MCGOWRAN, B. (editors)—Stratigraphic problems of the later Precambrian and Early Cambrian. *University of Adelaide Centre for Precambrian Research, Special Paper* 1, 53-62.

PRICHARD, C. E., & QUINLAN, T., 1962—The geology of the southern half of the Hermannsburg 1:250 000 Sheet. *Bureau of Mineral Resources, Australia, Report* 61.

QUINLAN, T., & FORMAN, D. J., 1968—Hermannsburg, Northern Territory—1:250 000 Geological Series. *Bureau of Mineral Resources, Australia, Explanatory Notes* SF/53-13.

RICHTER-BERNBURG, G., 1972—Saline deposits in Germany: a review and general introduction to the excursions. *In* RICHTER-BERNBURG, G. (editor)—Geology of Saline Deposits. *Proceedings of Hanover Symposium, UNESCO, Earth Sciences,* 7, 275-87.

SCHMALZ, R. F., 1969—Deep water evaporite deposition: a genetic model. *Bulletin of the American Association of Petroleum Geologists,* 53(4), 798-823.

SENIOR, B. R., 1970—Barrolka, Queensland—1:250 000 Geological Series. *Bureau of Mineral Resources, Australia, Explanatory Notes* SG/54-11.

SLANIS, A. A., & NETZEL, R. K., 1967—Geological review of Authorities to Prospect 109P and 125P, Queensland, Australia. *Geological Survey of Queensland, Open File Report* (unpublished).

SMITH, D. B., 1972—Foundered strata, collapse-breccias and subsidence features of the English Zechstein. *In* RICHTER-BERNBURG, G. (editor)—Geology of Saline Deposits. *Proceedings of Hanover Symposium, UNESCO, Earth Sciences,* 7, 255-69.

SMITH, E. R., 1966—Timor Sea/Joseph Bonaparte Gulf marine gravity and seismic 'spark array' survey, northwest Australia, 1965. *Bureau of Mineral Resources, Australia, Record* 1966/72 (unpublished).

SMITH, J. W., 1964—Bauhinia Downs, Northern Territory —1:250 000 Geological Series. *Bureau of Mineral Resources, Australia, Explanatory Notes* SE/53-3.

SMITH, K. G., 1964—Progress report on the geology of the Huckitta 1:250 000 Sheet, Northern Territory. *Bureau of Mineral Resources, Australia, Report* 67.

SMITH, K. G., 1972—Stratigraphy of the Georgina Basin. *Bureau of Mineral Resources, Australia, Bulletin* 111.

STEWART, A. J., 1974—Petrographic and geochemical study of the Ringwood evaporite deposit. *Bureau of Mineral Resources, Australia, Record* 1974/145 (unpublished).

STEWART, F. H., 1949—The petrology of the evaporites of the Eskdale No. 2 boring, east Yorkshire. I. The lower evaporite bed. *Mineralogical Magazine,* 28, 621-75.

STEWART, F. H., 1963—Marine evaporites. *United States Geological Survey, Professional Paper* 440Y.

STURMFELS, E. K., 1952—Report on investigation of evaporites in the Northwest Basin, W.A., during May, June, and July, 1951. *Australian Mining & Smelting Ltd.* (unpublished).

TALBOT, H. W. B., & CLARKE, E. DE C., 1917—A geological reconnaissance of the country between Laverton and the South Australian border. *Geological Survey of Western Australia, Bulletin* 75.

TALLIS, N. C., & FJELSTUL, C. R., 1966—The Lake Dartmouth seismic survey, 1965. *Bureau of Mineral Resources, Australia, Petroleum Search Subsidy Acts File* 65/11005 (unpublished).

TANNER, J. J., 1968—Devonian of the Adavale Basin, Queensland. *In* OSWALD, D. H. (editor)—*International Symposium on the Devonian System, Calgary 1967,* 2, 111-6.

THODE, H. G., WANLESS, R. K., WALLOUCH, R., 1954—The origin of native sulphur deposits from isotope fractionation studies. *Geochimica et Cosmochimica Acta,* 5, 286-98.

TOWNSEND, I. J., 1976—Stratigraphic drilling in the Arckaringa Basin, 1969-1971. *Geological Survey of South Australia, Report of Investigations,* 45.

TURPIE, A., 1967—Giles-Carnegie seismic survey, Western Australia, 1961-1962. *Bureau of Mineral Resources, Australia, Record* 1967/123 (unpublished).

VEEVERS, J. J., & WELLS, A. T., 1959—Probable salt dome at Woolnough Hills, Canning Basin, Western Australia. *Australian Journal of Science* 21(6), 193-4.

VEEVERS, J. J., & WELLS, A. T., 1960—Probable salt dome at Woolnough Hills, Canning Basin, Western Australia. *Bureau of Mineral Resources, Australia, Report* 38, 97-112.

VEEVERS, J. J., HEIRTZLER, J. R., & OTHERS, 1974—Initial reports of the Deep Sea Drilling Project, 27. *US Government Printing Office, Washington.*

WALKER, R. N., MUIR, M. D., DIVER, W. L., WILLIAMS, N., & WILKINS, N., 1977—Evidence of major sulphate evaporite deposits in the Proterozoic McArthur Group, Northern Territory, Australia. *Nature,* 265, 526-9.

WALTER, M. R., 1978—Report on an examination of sedimentary rocks in the Mt Isa district. *Bureau of Mineral Resources, Australia, Professional Opinion,* Geol. 78:016 (unpublished).

WATTS, T. R., GAUSDEN, J., & HEISLER, H. H., 1966—Stansbury West No. 1 well completion report. *Bureau of Mineral Resources, Australia, Petroleum Search Subsidy Acts File* 66/4204 (unpublished).

WEBB, B. P., 1960—Diapiric structures in the Flinders Ranges, South Australia. *Australian Journal of Science,* 22(9), 390-1.

WEBB, B. P., 1961—The geological structure of the Blinman Dome. *Transactions of the Royal Society of South Australia,* 85, 1-6.

WELLS, A. T., 1963—Reconnaissance geology by helicopter in the Gibson Desert, Western Australia. *Bureau of Mineral Resources, Australia, Record* 1963/59 (unpublished).

WELLS, A. T., 1973—Evaporites in Australia. *Bureau of Mineral Resources, Australia, Record* 1973/170 (unpublished).

WELLS, A. T., & KENNEWELL, P. J., 1972—Evaporite drilling in the Amadeus Basin: Goyder Pass, Gardiner Range and Lake Amadeus, Northern Territory. *Bureau of Mineral Resources, Australia, Record* 1972/36 (unpublished).

WELLS, A. T., & KENNEWELL, P. J., 1974—Evaporite exploration in the Officer Basin, Western Australia, at the Woolnough Hills and Madley Diapirs. *Bureau of Mineral Resources, Australia, Record* 1974/194 (unpublished).

WELLS, A. T., FORMAN, D. J., RANFORD, L. C., & COOK, P. J., 1970—Geology of the Amadeus Basin, central Australia. *Bureau of Mineral Resources, Australia, Bulletin* 100.

WELLS, B. E., 1971—An occurrence of common salt near Jandowae. *Queensland Government Mining Journal,* 72, 369.

WHELAN, J. A., 1972—Ochsenius bar theory of saline deposition supported by quantitative data, Great Salt Lake, Utah. *24th International Geological Congress,* Section 10, 296-303.

WILSON, R. B., 1964—The geology of permits to explore Nos. 205H, 206H, and 207H, Western Australia. *Confidential report to Alliance Petroleum Australia, N.L.* (unpublished).

WILSON, R. B., 1967—Woolnough Hills and Madley diapiric structures, Gibson Desert, W.A. *The APEA Journal,* 7(2), 94-102.

WOPFNER, H., 1977—Mount Toondina—?diapir or astrobleme. *Geological Survey of South Australia, Quarterly Geological Notes,* 62, 21-4.

WOPFNER, H., & ALLCHURCH, P. D., 1967—Devonian sediments enhance petroleum potential of Arckaringa Subbasin. *Australasian Oil & Gas Journal,* 14(3), 18-32.

YOULES, I. P., 1976—Mount Toondina impact structure. *Geological Survey of South Australia, Quarterly Geological Notes,* 60, 10-11.

ZEN, E-AN, 1959—Clay mineral-carbonate relations in sedimentary rocks. *American Journal of Science,* 257, 29-43.

R79/360(1) Cat. No. 80 0706 9

INDEX

Page numbers in bold type indicate a section heading.

COMPOSITE LOG

OPERATOR: BUREAU OF MINERAL RESOURCES

NAME AND NUMBER: BMR MOUNT LIEBIG No.1.

STATE: NORTHERN TERRITORY. 1:250,000 SHEET: MOUNT LIEBIG SF 52-16. BASIN: AMADEUS. WELL STATUS: PLUGGED AND ABANDONED

PLATE
SUPPLIED BY THE AUSTRALIAN GOVERNMENT PUBLISHING SERVICE UNDER THE FREE ISSUE SCHEME TO AUSTRALIAN UNIVERSITY LIBRARIES

DRILLING DATA

LOCATION: Lat 23°52'30"S., Long 131°56'E
ELEVATION: Ground level 817m (2680') approx
DATE SPUDDED: 4-8-70
DATE DRILLING STOPPED: 11-9-71
DATE RIG OFF: 15-9-71
TOTAL DEPTH: driller 305.87m (1003'6")
mibolog 303.89m (997'), 303.51m (996')
HOLE SIZE: DIAMETER FROM TO
25.4cm (9 7/8") 0m (0') 42.98m (141')
15.8cm (6 1/4") 42.98m (141') 305.87m (1003'6")
CASING:

DIA	WT	GR	DEPTH	CMT	CMT'D TO
20.3cm (8")	32.3Kg/m (21.7lb/ft)	W/bore	42.98m (141')	22sx	28m (90')

CEMENT PLUGS: SURFACE
PERFORATIONS: NIL
DRILLED BY: BUREAU OF MINERAL RESOURCES
WELL HEAD FITTINGS: none
CEMENTED BY: driller
LOGGED BY: mibolog
DRILLING METHOD: air rotary
LITHOLOGY BY: P.J. Kennewell
DRILLING DATA BY: J.M. Henry

LOG DATA

LOG TYPE	SPONTANEOUS POT		RESISTIVITY		GAMMA RAY		NEUTRON		CALIPER		DENSITY	
DATE	5-9-70		5-9-70		5-9-70		5-9-70		5-9-70		5-9-70	
RUN No	1/1		1/1		1/1		1/1		1/1		1/1	
DEPTH-DRILLER	305.87m		305.87m		305.87m		305.87m		305.87m		305.87m	
DEPTH-LOGGER	303.89m		303.89m		303.89m		303.89m		303.51m		303.51m	
BTM LOG INTERVAL	303.51m		303.51m		303.51m		303.51m		303.21m		303.21m	
TOP LOG INTERVAL	92.06m		92.06m		0m		0m		92.06m		92.06m	
CASING-DRILLER	20.3cm at 42.98m		20.3cm at 42.98m		20.3cm at 42.98m		20.3cm at 42.98m		20.3cm at 42.98m		20.3cm at 42.98m	
CASING-LOGGER	42.06m		42.06m		42.06m		42.06m		42.06m		42.06m	
BIT SIZE	15.3cm		15.3cm		15.3cm		15.3cm		15.3cm		15.3cm	
TYPE FLUID IN HOLE	SALT WATER and BENTONITE		SALT WATER and BENTONITE		SALT WATER and BENTONITE		SALT WATER and BENTONITE		SALT WATER and BENTONITE		SALT WATER and BENTONITE	
DENS / VISC	N.A.	N.A.	N.A.	N.A.	N.A.	N.A.	N.A.	N.A.	N.A.	N.A.	N.A.	N.A.
PH / FLUID LOSS	N.A.	N.A.	N.A.	N.A.	N.A.	N.A.	N.A.	N.A.	N.A.	N.A.	N.A.	N.A.
SOURCE OF SAMPLE	—		—		—		—		—		—	
Rm at MEAS TEMP	0.04 at 92°F		0.04 at 92°F		0.04 at 92°F		0.04 at 92°F		0.04 at 92°F		0.04 at 92°F	
Rmf at MEAS TEMP	N.A.		N.A.		N.A.		N.A.		N.A.		N.A.	
Rmc at MEAS TEMP	N.A.		N.A.		N.A.		N.A.		N.A.		N.A.	
SOURCE Rmf Rmc	N.A.	N.A.	N.A.	N.A.	N.A.	N.A.	N.A.	N.A.	N.A.	N.A.	N.A.	N.A.
Rm at BHT	N.A.		N.A.		N.A.		N.A.		N.A.		N.A.	
TIME SINCE CIRC	approx. 10 hrs.		approx. 10 hrs.		approx. 10 hrs.		approx. 10 hrs.		approx. 10 hrs.		approx. 10 hrs.	
MAX. REC TEMP	N.A.		N.A.		N.A.		N.A.		N.A.		N.A.	
EQUIP LOCATION	T10I	PER	T10I	PER	T10I	PER	T10I	PER	T10I	PER	T10I	PER
INSTRUMENTS SURFACE	EL-GL1		EL-GL1		GO-RMM-204		GO-RMM-204		GO-RMM-204		GO-RMM-204	
INSTRUM. DOWN HOLE	EL-GLS		EL-GLS		GRN1"		GRN1"		FDC 1 11/16-Ce		FDC 1 11/16-Ce	
TOOL POSITION	FREE		FREE		FREE		FREE		FREE		FREE	
RECORDED BY	CRAMFORD											
WITNESSED BY	KENNEWELL											

LITHOLOGICAL REFERENCE

Gypsum; Halite; Evaporite Rock (medium crystalline); Evaporite Rock (finely crystalline); Recrystallised Evaporite Breccia; Dolomite

Py — pyritic

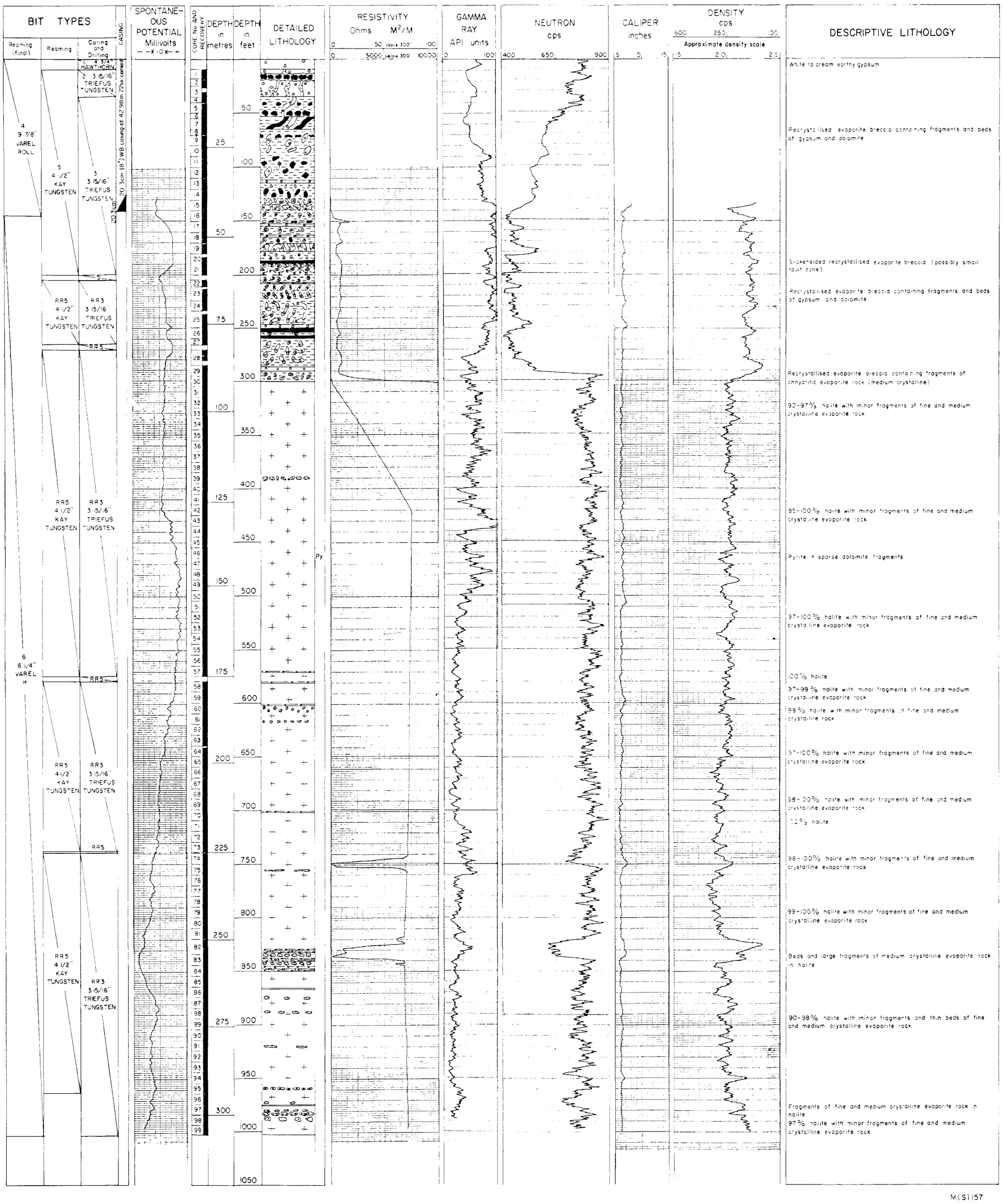

DESCRIPTIVE LITHOLOGY

White to cream earthy gypsum

Recrystallised evaporite breccia containing fragments and beds of gypsum and dolomite

Slickensided recrystallised evaporite breccia (possibly small fault zone)

Recrystallised evaporite breccia containing fragments and beds of gypsum and dolomite

Recrystallised evaporite breccia containing fragments of anhydritic evaporite rock (medium crystalline)

90-97% halite with minor fragments of fine and medium crystalline evaporite rock

85-100% halite with minor fragments of fine and medium crystalline evaporite rock

Pyrite in sparse dolomite fragments

97-100% halite with minor fragments of fine and medium crystalline evaporite rock

100% halite

97-99% halite with minor fragments of fine and medium crystalline evaporite rock

98% halite with minor fragments of fine and medium crystalline rock

97-100% halite with minor fragments of fine and medium crystalline evaporite rock

98-100% halite with minor fragments of fine and medium crystalline evaporite rock

100% halite

98-100% halite with minor fragments of fine and medium crystalline evaporite rock

99-100% halite with minor fragments of fine and medium crystalline evaporite rock

Beds and large fragments of medium crystalline evaporite rock in halite

90-98% halite with minor fragments and thin beds of fine and medium crystalline evaporite rock

Fragments of fine and medium crystalline evaporite rock in halite
97% halite with minor fragments of fine and medium crystalline evaporite rock

M(S)1157

PLATE II

RESULTS OF CHEMICAL ANALYSES – BMR MOUNT LIEBIG No 1

Analyses by Emission Spectroscopy (K, B, Sr, Mn, Ba, Fe) and Wet Chemical Methods (Br)

⊕ Not present in detectable amounts

*6 Average of 6 analyses

LITHOLOGICAL REFERENCE

Gypsum | Halite | Evaporite rock (medium crystalline) | Evaporite rock (finely crystalline) | Recrystallised evaporite breccia | Dolomite

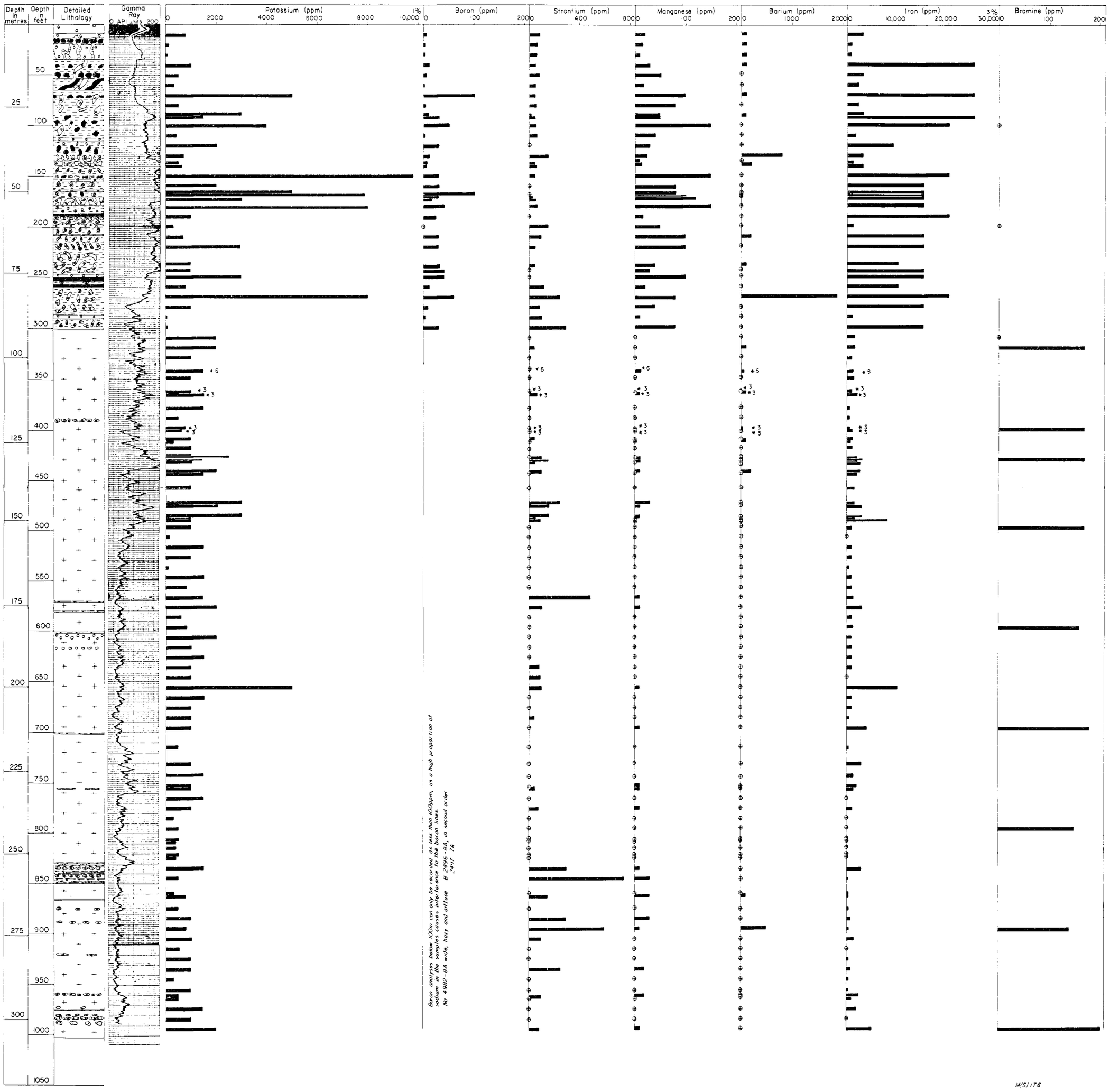

Boron analyses below 100m can only be recorded as less than 100ppm, as a high proportion of sodium in the samples causes interference to the boron lines.

No 4982 - 8A wide, hazy and diffuse B 2496 - 8A, in second order 2417 7A

M/S/ 176

COMPOSITE LOG

PLATE III

OPERATOR: BUREAU OF MINERAL RESOURCES

NAME AND NUMBER: BMR LAKE AMADEUS No. 3B.

STATE: NORTHERN TERRITORY. 1:250,000 SHEET: LAKE AMADEUS SG 52-4. BASIN: AMADEUS. WELL STATUS: PLUGGED AND ABANDONED

DRILLING DATA

LOCATION: Lat. 24°46'36"S Long. 131°53'24"E
ELEVATION: Ground level 512 m (1690') approx.
DATE SPUDDED: 8-10-70
DATE DRILLING STOPPED: 4-12-70
DATE RIG OFF: 7-12-71
TOTAL DEPTH: driller: 305·86m (1003'6")
mibolog: 305·41m (1002')
HOLE SIZE: DIAMETER FROM TO
25·3cm (9⅞") 0m (0') 45·72m (150')
14·0cm (5½") 45·72m (150') 305·86m (1003'6")
CASING:

DIA.	WT.	GR.	DEPTH	CMT.	CMT'D TO
20·3cm (8")	32·3Kg/m (21·7lb/ft)	W/bore	45·72m (144')	N.A.	surface

CEMENT PLUGS SURFACE
PERFORATIONS: NIL
DRILLED BY: BUREAU OF MINERAL RESOURCES
WELL HEAD FITTINGS: none
CEMENTED BY: driller
LOGGED BY: mibolog
DRILLING METHOD: air rotary
LITHOLOGY BY: P.J. Kennewell
DRILLING DATA BY: J.M. Henry

LOG DATA

LOG TYPE	SPONTANEOUS POT.	RESIST VITY	GAMMA RAY	NEUTRON	CALIPER	DENSITY
DATE	7·12·70	7·12·70	7·12·70	7·12·70	7·12·70	7·12·70
RUN No.	1/1	1/1	1/1	1/1	1/1	1/1
DEPTH - DRILLER	305·86m	305·86m	305·86m	305·86m	305·86m	305·86m
DEPTH - LOGGER	305·41m	305·41m	305·41m	305·41m	305·41m	305·41m
BTM. LOG INTERVAL	304·80m	304·80m	305·10m	305·10m	304·80m	304·80m
TOP LOG INTERVAL	59·64m	59·64m	0m	0m	44·49m	44·49m
CASING - DRILLER	20·3cm at 43·59m	20·3cm at 43·59m	20·3cm at 43·59m	20·3cm at 43·59m	20·3cm at 43·59m	20·3cm at 43·59m
CASING - LOGGER	44·49m	44·49m	44·49m	44·49m	44·49m	44·49m
BIT SIZE	14·0cm	14·0cm	14·0cm	14·0cm	14·0cm	14·0cm
TYPE FLUID IN HOLE	SALT WATER and BENTONITE	SALT WATER and BENTONITE	SALT WATER and BENTONITE	SALT WATER and BENTONITE	SALT WATER and BENTONITE	SALT WATER and BENTONITE
DENS. / VISC.	N.A. / N.A.	N.A. / N.A.	N.A. / N.A.	N.A. / N.A.	N.A. / N.A.	N.A. / N.A.
PH / FLUID LOSS	N.A. / N.A.	N.A. / N.A.	N.A. / N.A.	N.A. / N.A.	N.A. / N.A.	N.A. / N.A.
SOURCE OF SAMPLE	—	—	—	—	—	—
Rm at MEAS. TEMP.	0·03 at 84°F	0·03 at 84°F	0·03 at 84°F	0·03 at 84°F	0·03 at 84°F	0·03 at 84°F
Rmf at MEAS. TEMP.	N.A.	N.A.	N.A.	N.A.	N.A.	N.A.
Rmc at MEAS. TEMP.	N.A.	N.A.	N.A.	N.A.	N.A.	N.A.
SOURCE Rmf Rmc	N.A. / N.A.	N.A. / N.A.	N.A. / N.A.	N.A. / N.A.	N.A. / N.A.	N.A. / N.A.
Rm at B.H.T.	N.A.	N.A.	N.A.	N.A.	N.A.	N.A.
TIME SINCE CIRC.	1 Day	1 Day	1 Day	1 Day	1 Day	1 Day
MAX. REC. TEMP.	N.A.	N.A.	N.A.	N.A.	N.A.	N.A.
EQUIP. LOCATION	T101 / PER	T101 / PER	T101 / PER	T101 / PER	T101 / PER	T101 / PER
INSTRUMENTS SURFACE	LM464	LM464	RMM 204	RMM 204	RMM 204	RMM 204
INSTRUM. DOWN HOLE	LS-235	LS-235	GRN 1"	GRN 1"	FDC-1 11/16 - Cs	FDC-1 11/16 - Cs
TOOL POSITION	FREE					
RECORDED BY	CRAWFORD					
WITNESSED BY	KENNEWELL					

LITHOLOGICAL REFERENCE

Gypsum; Acicular Gypsum; Anhydrite; Dolomitic Anhydrite; Laminae of Dolomitic Anhydrite; Black tough Dolomite; Light brown tough Dolomite; Grey friable Dolomite; Laminae of Gypsiferous Dolomite; Siltstone; Sandy Siltstone; Claystone; Silcrete

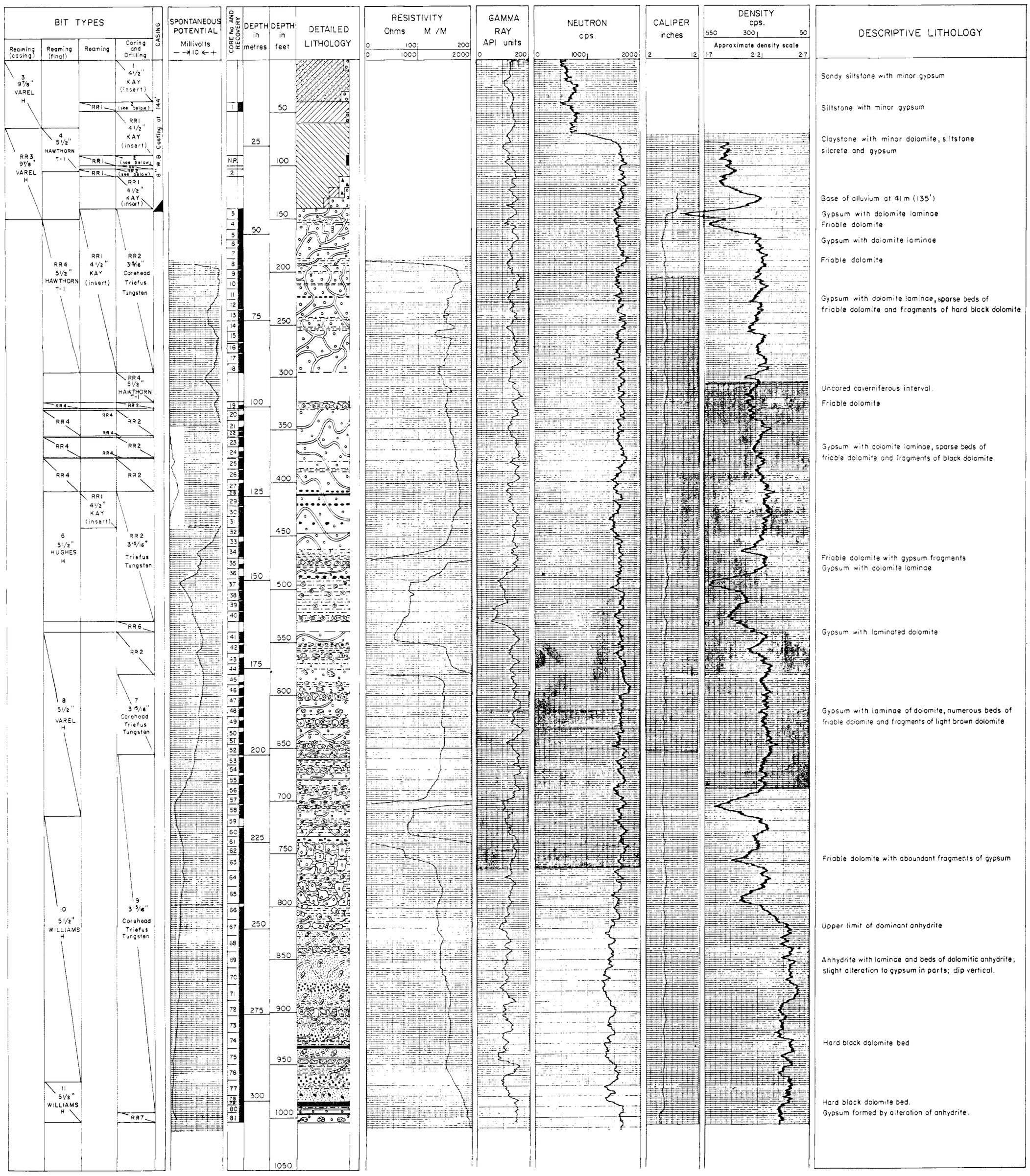

M(S)158

RESULTS OF CHEMICAL ANALYSES – BMR LAKE AMADEUS No. 3B

Analyses by Emission Spectroscopy

PLATE IV

⊕ Not present in detectable amounts

LITHOLOGICAL REFERENCE

Gypsum
Acicular gypsum
Anhydrite
Dolomitic anhydrite
Laminae of dolomitic anhydrite
Black tough dolomite
Light brown tough dolomite
Grey friable dolomite
Laminae of gypsiferous dolomite
Siltstone
Sandy siltstone
Claystone
Silcrete

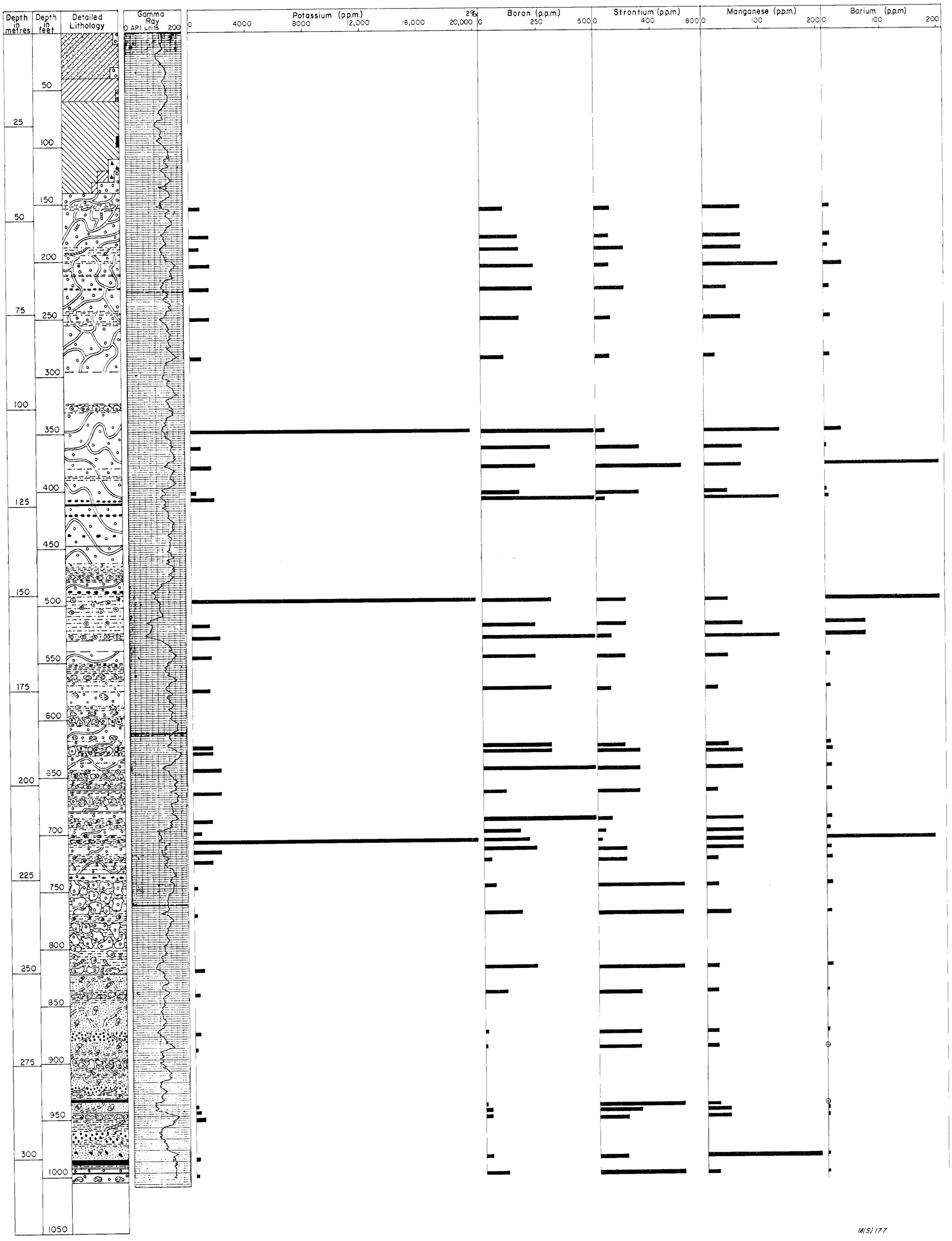

M(S) 177

COMPOSITE LOG

PLATE V

OPERATOR: BUREAU OF MINERAL RESOURCES

NAME AND NUMBER: BMR HERMANNSBURG No 40

STATE: NORTHERN TERRITORY 1:250,000 SHEET: HERMANNSBURG SF/53–13 BASIN: AMADEUS
WELL STATUS: PLUGGED AND ABANDONED

DRILLING DATA

LOCATION: Lat 23° 38·3 S Long 132° 27'E, Grid reference 562·055 (110,000 yards)
ELEVATION: Ground level about 698 metres (2290 feet)
DATE SPUDDED: 18·7·70
DATE DRILLING CEASED: 27·7·70
DATE RIG OFF: 28·7·70
TOTAL DEPTH: 91·4 metres (300 feet)

HOLE SIZE:	DIAMETER:	FROM	TO
	14"	0'	13'
	5½"	13'	277'
	3 15/16"	277'	300'

CASING	DIAMETER	WT	GR	DEPTH	CMT	CMT'D TO
	30·5cm(12")	48·06lb/ft 11·5kg/m	W/Bore	3·05m(10')	8 bags	Surface to 7·62m (25')

CEMENT PLUGS: SURFACE TO 7·62m (25')
PERFORATIONS: NIL
DRILLED BY: BUREAU OF MINERAL RESOURCES
WELL HEAD FITTINGS: none
CEMENTED BY: driller
LOGGING: none
DRILLING METHOD: rotary air and mud
LITHOLOGY BY: A.T. Wells
DRILLING DATA: BY J.M. Henry

LITHOLOGICAL REFERENCE

Conglomerate — *Coarse grained sandstone* — *Medium or fine grained sandstone* — *Siltstone* — *Claystone* — *Chert fragments, pyritic in part*

c gr	*coarse grained*	*gl*	*glauconitic*
m gr	*medium grained*	*py*	*pyritic*
f gr	*fine grained*	*fe*	*ferruginons*
		si	*silicified*

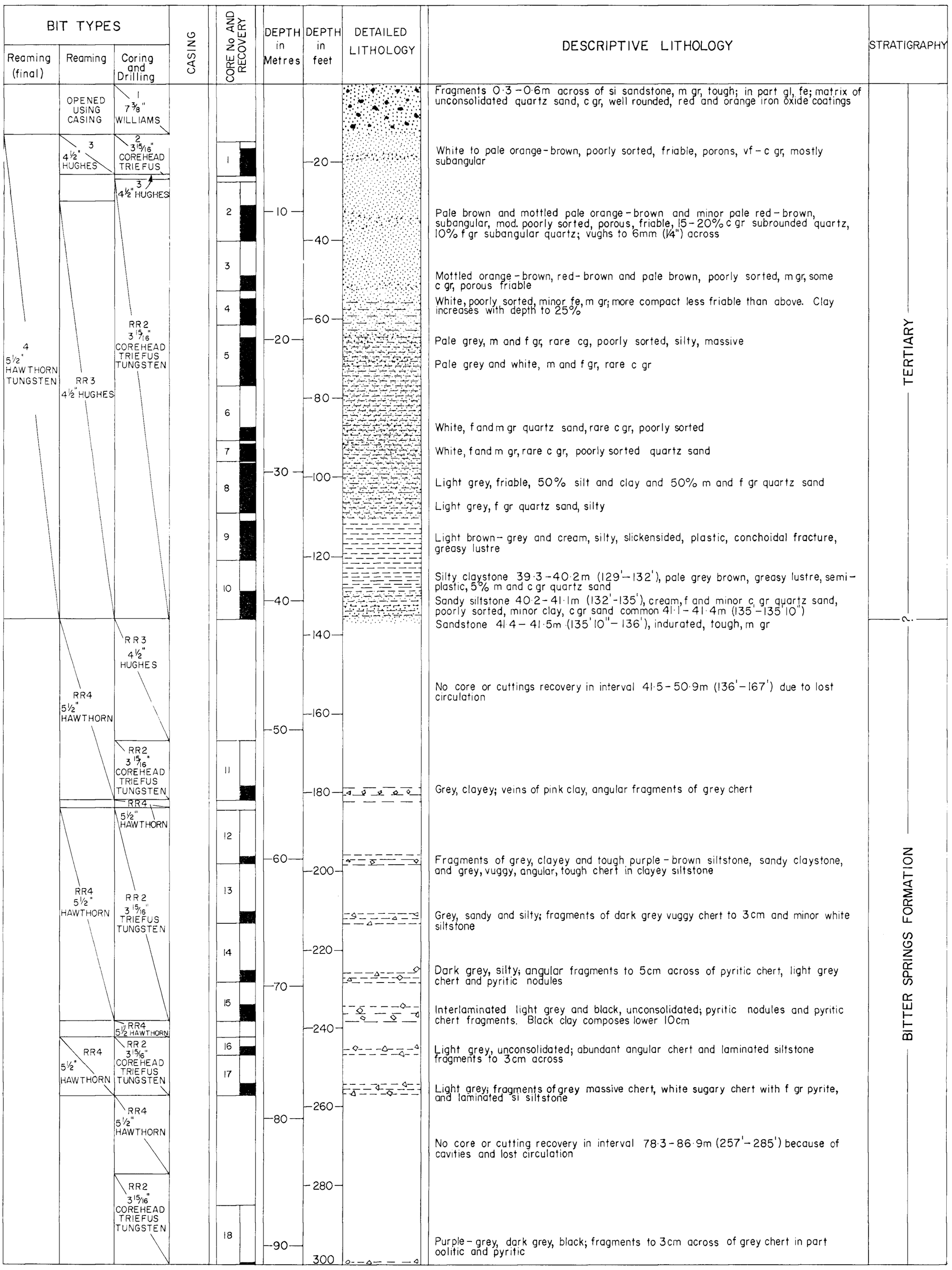

M(S) 175

RESULTS OF CHEMICAL ANALYSES – BMR WARRI No 20

PLATE VI

Analyses by Emission Spectroscopy (K, Na, Sr, Mn, Ba, Co, Cr, Be, Ir, Ni, Os, Th, V, Ti, Cs, Rb) and Wet Chemical Methods (B, Fe, Mg, Br, I)

All results in ppm

Detection limits in brackets

*13 Average of 13 analyses (for details see Table V)

● Not present in detectable amounts

LITHOLOGICAL REFERENCE

Gypsum; Acicular Gypsum; Anhydrite; Dolomitic Anhydrite; Gypsum crystals; Grey Friable Dolomite; Dolomitic Gypsum; Laminae of Dolomitic Gypsum; Halite

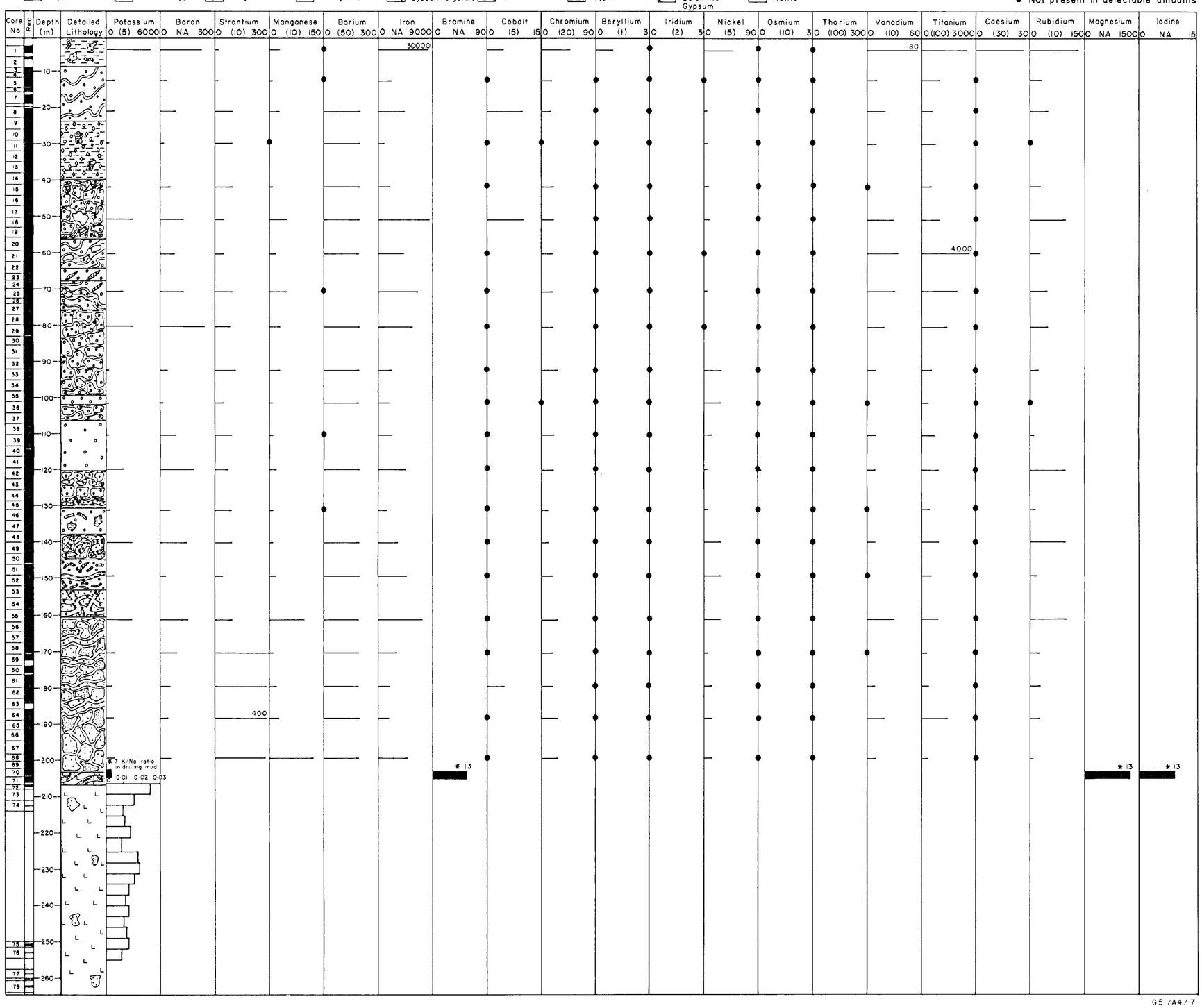

G51/A4/7

RESULTS OF CHEMICAL ANALYSES - BMR MADLEY No1

PLATE VII

Analyses by Emission Spectroscopy (K, Sr, Li, Mn, Ba, Co, Cr, Be, Ir, Ni, Os, Th, V, Ti, Cs, Rb) and Wet Chemical Methods (Na, B, Fe)

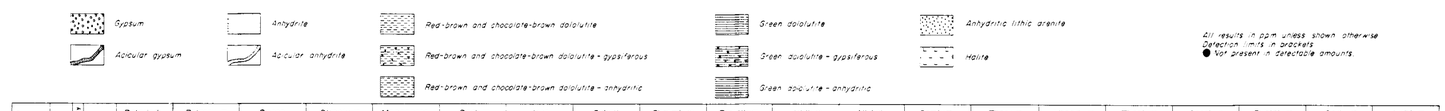

All results in ppm unless shown otherwise
Detection limits in brackets
● Not present in detectable amounts.

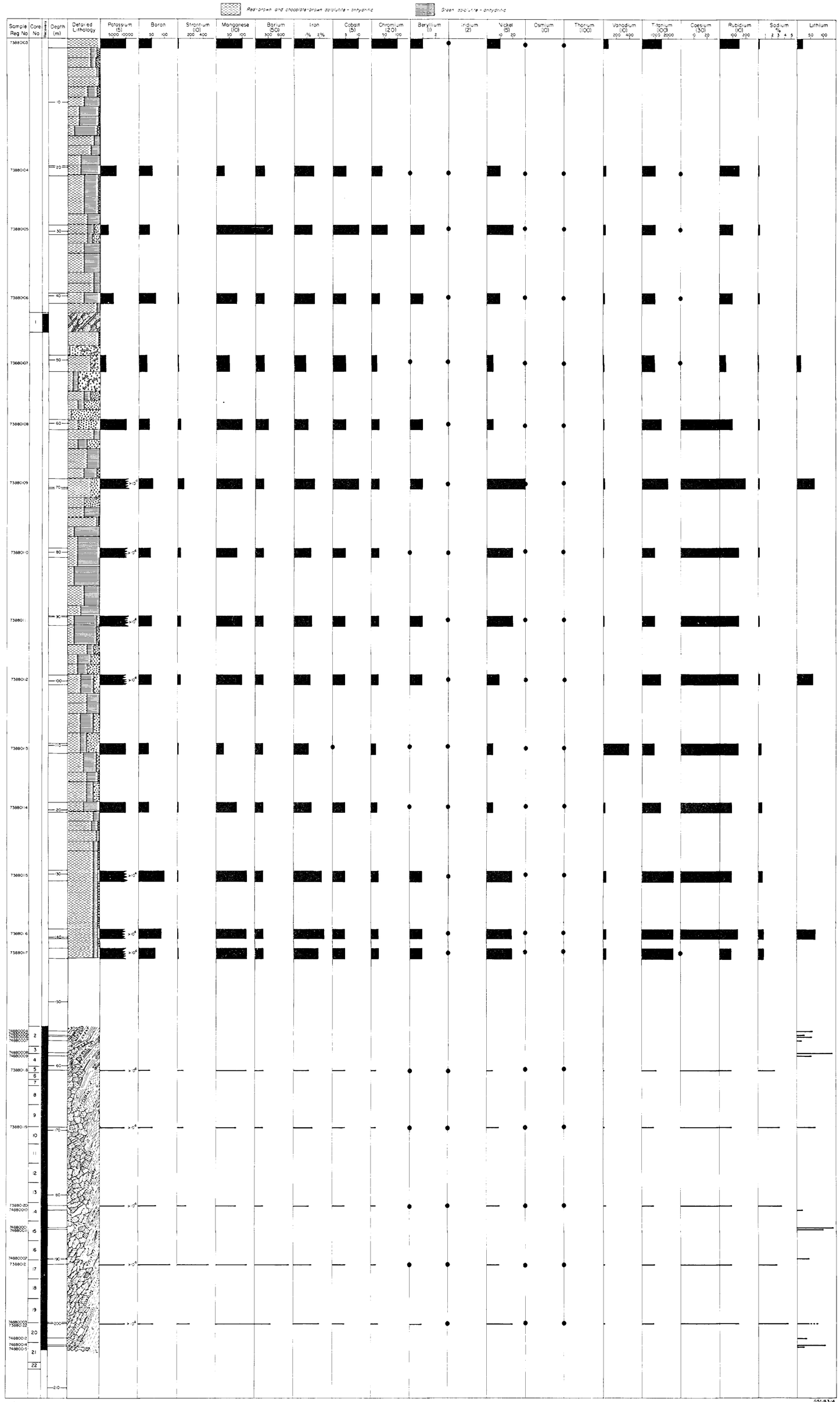

G51/A3/4